# The application and potential toxicity of innovative antifouling coatings for coral reef restoration

A dissertation by
**Lisa K. Röpke**

A dissertation by Lisa K. Röpke submitted in partial fulfilment of the requirements for obtaining a Doctoral Degree in Science (Dr. rer. nat.) at the University of Bremen, Faculty of Biology and Chemistry

The present work of this thesis was conducted from April 2019 to November 2023 at the Leibniz Centre for Tropical Marine Research (ZMT) in Bremen, Germany, and the Australian Institute of Marine Science (AIMS) in Townsville, Australia.

Reviewers: Dr. Andreas Kunzmann, Leibniz Centre for Tropical Marine Research (ZMT), Bremen, Germany

Dr. Andrew Negri, Australian Institute of Marine Science (AIMS), Townsville, Australia

Examiners: Prof. Dr. Tilmann Harder, University of Bremen, Bremen, Germany

Prof. Dr. Claudio Richter, Alfred-Wegener-Institute (AWI), Bremerhaven, Germany

Additional thesis committee members:

M.Sc. Beatrice Brix da Costa (Ph.D. candidate, University of Bremen)

Arne Heydtmann (Bachelor of Science student, University of Bremen)

Date of PhD Colloquium:

17th of November 2023

Funding for the PhD candidate and research project was provided by the Federal Ministry for Economic Affairs and Climate Action (BMWK)—ZIM programme, the University of Bremen, the Bremen International Graduate School for Marine Sciences (GLOMAR), the German Foundation Marine Conservation (DSM), the Australian Institute of Marine Science (AIMS), the Reef Restoration and Adaptation Program (RRAP), and the Kellner & Stoll foundation in Bremen.








Bremen International Graduate School
for Marine Sciences

***"Das Leben der Korallen gehört überhaupt zu den größten Wundern, die das an Wunderdingen so überreiche Meer nur zu bieten vermag."***

*"Coral life is one of the greatest marvels that the sea, so rich in marvelous things, can only offer"*
(google translator)

Zitat von Raoul Heinrich Francé aus *Korallenwelt. Der siebente Erdteil.* Kosmos, Gesellschaft der Naturfreunde, Franckh'sche Verlagshandlung, Stuttgart 1930


*

*** Selbst entworfenes Logo der eingetragenen Wortmarke „meerherz®" für das Kunstnebengewerbe der Autorin dieser Arbeit während der Zeit Ihrer Promotion durch die Inspiration Ihrer Doktorarbeit.**

* Self-designed logo of the registered wordmark "meerherz®" (seaheart) for the art sideline business of the author of this work during the time of her doctorate through the inspiration of her doctoral thesis.

# Table of Contents

# Summary

As more tropical reefs worldwide undergo climate- and eutrophication-driven phase-shifts from coral- to fleshy algal-dominated cover, interactions between fouling organisms and corals become more pronounced and frequent. Competition with benthic algae is recognized as a key threat to coral settlement and the survival and growth of coral recruits and the success of adult corals, reducing overall survival for coral reef replenishment and supply for restoration programs. The application of antifouling (AF) coatings on settlement surfaces for coral larvae may enhance the viability and profitability of sexually propagated corals by improving the survival and growth of coral spat that make it through critical early life stages.

In this context, three innovative AF coatings with potential low toxicity were developed and tested for their (1) efficacy to inhibit fouling, (2) potential toxicity towards coral spat, and (3) ability to improve coral spat survival and growth. A series of interconnected experiments was conducted at the Australian Institute of Marine Science (AIMS) in natural filtered seawater in large outdoor flow-through aquaria, as well as indoors in different temperature-controlled rooms of the National Sea Simulator (SeaSim).

In ***Chapter 2***, two of the three tested coatings (antiadhesive, encapsulated dichlorooctylisothiazolinone: DCOIT) were found to effectively inhibit algal growth (crustose coralline algae (CCA), green and brown algae) on coral settlement plugs ("coral plugs"), with no detrimental effects of the 37-day old pre-conditioned coatings on *Acropora tenuis* coral larvae during settlement. Furthermore, an adapted protocol for fouling analysis from photo monitorings was developed with the machine-learning Trainable Weka Segmentation (TWS) plugin in the Fiji distribution of the image processing program ImageJ.

In ***Chapter 3***, survival of *Acropora millepora* coral spat after 69 days on non-conditioned coral plugs was higher on the uncoated areas of the partially-coated plugs in the DCOIT treatment as compared to the Control plugs without any coating, suggesting that inhibited algal growth by the coating could have created beneficial effects on the corals' survival.

In ***Chapter 4***, *Acropora millepora* coral larval swimming behavior (velocity and activity) was investigated for the first time with an automatic and quantitative measurement software EthoVision XT (Noldus Information Technology), and differences between swimming behavior on top of the coatings became evident. Tracking of swimming behavior with this setup and software was identified as a precise and reliable method for assessing potential non-lethal responses to AF coatings. The manual for the utilization of this software with coral larvae is included in this study.

The chapters presented in this thesis provide a valuable contribution to the development of innovative and sensitive techniques to assess the ability of AF coatings to reduce competition from biofouling and increase coral survival to size-escape levels.

# Zusammenfassung

Mit zunehmender Klimaerwärmung und Eutrophierung der Meere entwickeln sich weltweit immer mehr tropische Riffe von korallendominierten zu algenbedeckten Ökosystemen. Infolgedessen nehmen die Wechselwirkungen zwischen Fouling-Organismen und Korallen weiter zu. Der Wettbewerb mit benthischen Algen wird als eine wesentliche Bedrohung für die Ansiedlung von Korallen, sowie das Überleben und Wachstum von juvenilen Korallen als auch das Überleben adulter Korallen beobachtet und eingeschätzt. Damit einhergehend verringert sich die Gesamtüberlebensrate von Riffen, die sich nicht mehr natürlich fortpflanzen und von anthropogenen verursachten Störungsereignissen erholen können. Mithilfe der Anwendung von Antifouling (AF)- Beschichtungen auf Ansiedlungsflächen für Korallenlarven kann die Lebensfähigkeit und die Rentabilität sexuell vermehrter Korallen verbessert werden, indem das Überleben und das Wachstum von juvenilen Korallen während ihrer kritischen frühen Lebensphase unterstützt werden.

In diesem Zusammenhang wurden drei innovative AF-Beschichtungen mit potenziell geringer Toxizität entwickelt und auf ihre (1) Wirksamkeit bei der Reduzierung von Fouling-Bewuchs, (2) potenzielle Toxizität gegenüber juvenilen Korallen und (3) Eignung für weitere Tests und Anwendungen im Rahmen von Riff-Restaurierungsmaßnahmen getestet. Eine Reihe zusammenhängender Experimente wurde am Australian Institute of Marine Science (AIMS) durchgeführt, sowohl in natürlich gefilterten Meerwasserbecken in großen Freiland-Aquarien, als auch in verschiedenen temperaturgesteuerten Räumen des National Sea Simulator (SeaSim).

In ***Kapitel 2*** wurden zwei der drei getesteten Beschichtungen (antiadhäsiv und ummanteltes Dichlorooctylisothiazolinon: DCOIT) als effektive Inhibitoren gegen das Algenwachstum (krustose koralline Algen, Grün- und Braunalgen) auf Ansiedlungssubstraten für Korallen („coral plugs“) identifiziert. Dabei ergaben sich keine nachteiligen Auswirkungen auf die Korallenlarven der Art *Acropora tenuis* während ihrer Ansiedlung auf den zuvor in gefiltertem Meerwasser vorkonditionierten Beschichtungen. Darüber hinaus wurde ein angepasstes Protokoll zur Fouling-Bewuchsanalyse aus Fotomonitorings entwickelt, bei dem das maschinenlernende Trainable Weka Segmentation (TWS) Plugin in der Fiji-Distribution des Bildverarbeitungsprogramms ImageJ verwendet wurde.

In ***Kapitel 3*** zeigte sich ein höheres Überleben von *Acropora millepora* Korallensiedlern nach 69 Tagen - auf zuvor nicht in gefiltertem Meerwasser vorkonditionierten Beschichtungen - auf den unbeschichteten Flächen der partiell-beschichteten Ansiedlungssubstrate, als im Vergleich zu den komplett unbeschichteten Kontroll-Substraten. Dieses Ergebnis legt nahe, dass das unterdrückte Algenwachstum durch die DCOIT Beschichtung positive Auswirkungen auf das Überleben der Korallen gehabt haben könnte.

In ***Kapitel 4*** wurde erstmals das Schwimmverhalten (Geschwindigkeit und Aktivität) von Korallenlarven der Art *Acropora millepora* mit einer automatischen und quantitativen Software EthoVision XT (Noldus Information Technology) untersucht. Hierbei konnten Unterschiede im Schwimmverhalten auf den jeweiligen Beschichtungen festgestellt werden.

Das Tracking des Schwimmverhaltens mit dem dargestellten experimentellen Aufbau in ***Kapitel 4*** und der Software konnte als zuverlässige und praktikable Methode zur Untersuchung möglicher nichtletaler Reaktionen auf die AF-Beschichtungen identifiziert werden. Eine Anleitung zur Nutzung dieser Software mit Korallenlarven ist in dieser Dissertation enthalten.

Die in dieser Thesis präsentierten Kapitel leisten einen wertvollen Beitrag zur Entwicklung innovativer und sensibler Techniken zur Bewertung der Fähigkeit von AF-Beschichtungen, den Wettbewerb zwischen Korallen und Fouling-Organismen zu reduzieren. Die Chancen und Limitierungen der Studie stellen dar, wie das Überleben von Korallen auf ein Maß erhöht werden könnte, um dem oftmals für juvenile Korallen nachteiligen Konkurrenzkampf mit Algen um Raum und Licht zu entkommen.

# Acknowledgements

Towards the end of my PhD journey, I would like to take the opportunity to express my gratitude to the people, who shared their input and supported me along the way.

First and foremost, I would like to thank my **family**, **my parents Kirsten and Andreas**, for always supporting me unconditionally just for who I am, and your open ears and offered help at all times. You give me so much strength, so I can thrive where I choose to be. Thank you. To **my brother and sister**, **Lars and Marie**, I would like to say how lucky and blessed I feel to have you in my life. I know we will always watch out for each other and learn so much from each other.

It feels like forever while I am writing these words, but it is definitely about time to thank **my partner**, **Jenny**, who has seen me in so many shapes, good and bad, throughout the last years. You are the reason why I pulled through this PhD journey, as you made me feel at home in Bremen, Husum, Australia, and everywhere. Thank you, and also your parents, **Tina and Wolly**, for being supportive and providing me with fresh food from the market. These tomatoes and mangos really make a difference.

To my deceased grandparents, **Horst**, **Irene**, and **Robert**, and my still vertical grandmother **Erika**, I am sending out big hugs and love. Thank you for what you gave my parents on the way, and thank you for loving and humorous memories, and values that persist to exist through us. Thank you, to the rest of my big family (incl. my marine auntie **Cati**), for believing in me and supporting me in one way or another.

I would like to thank my **colleagues**, for their supervision and company. Thank you, Dr. **Andreas Kunzmann**, for strengthening many of my professional skills (incl. project proposal writing) and giving me freedom to pursue my research interests. Thank you for your time and efforts in supporting my career path throughout the last years at ZMT. Also, thank you for taking care of my expenses for the G31 medicals for scientific diving and supporting my interests to pursue a scientific diving career, incl. the course "5th International PhD-student course in Documentation Techniques for Scientific Divers" at the Lovén centre of the University of Gothenburg in Kristineberg, Sweden. I can only recommend this course to any other scientific divers.

Dr. **Andrew Negri**, or as everybody likes to say, **Negs**, I cannot express how grateful I am to have met you, as you opened the window to the professional research world of corals to me. Collaborating with you at AIMS and the SeaSim facilities has made me gain so many new insights and perspectives into our passion for coral reefs. Thank you for your trust in David and myself, and for your great and steady advice along the way. Also, thank you for organizing funds provided by the **Reef Restoration and Adaptation Program**.

**David**, to you as a companion and talented co-author, I would like to say thank you for bearing with me throughout busy fieldwork days in Australia and analysis days in Germany. Your company and support in Australia meant a lot to me, especially on those days when my

ankle was swollen from taking steps the wrong way, or the day, I hit a kangaroo and my grandmother Irene died and I could not attend her funeral. I am deeply thankful to you for your support with statistics and your tolerance for answering the same-same questions again and again.

Dr. **Carly Randall**, for your contributions to meetings at AIMS, ideas for statistical analyses, and accurate revisions of the manuscripts, I would like to thank you very deeply. I am happy we got to see each other at the ICRS 2022 in Bremen and hope our ways will cross again in one way or another in the future.

To our project partner Dr. **Ulrich Soltmann**, I would like to say thank you for introducing me to the world of inorganic coatings and their abiotic characteristics. Although it sometimes was hard to follow your professional knowledge on the phone, I am glad we successfully developed these plugs with coatings together. I see a lot of potential in your expertise and work, and I feel honored to know you as a very open-minded solution-finding person for innovative ideas. My greetings and a thank you also goes out to **Beate** and **Burkhard** (AquaCare), for cheering me up on the phone at the beginning of our project.

I would like to thank **Constanze**, **Silvia, José**, **Sebastian,** and **Christian**, for your technical support in the biolab, MAREE, geolab, and workshops at ZMT. With your trust and support, we together accomplished things for the very first time which turned out well. Believe in your skills. Thank you for your practical hands. I would also like to thank **Andrea** and **Susanne**, for your public relations and event support requests concerning coral reefs. It has always been a treat to get these important topics out with your support.

At AIMS, I would like to thank **Florita**, **Peter**, and **Michael**, for their technical guidance and support in the lab, workshops, and with the software EthoVision XT. Your practical support and advice are priceless.

I would also like to thank the **staff at the National Sea Simulator at AIMS**, for assistance with experimental setups and field collections. I'd like to acknowledge the **Bindal People** as the Traditional Owners where this work took place. I pay my respects to their Elders past, present and emerging and I acknowledge their continuing spiritual connection to their land and sea country.

Another big thank you goes out to my other **friends**. **Fee**, **Carolina**, and **Mareike**, thank you for cheering me up, hearing my (sometimes weird) thoughts, and offering help in situations, where I would've been alone (sick in bed with Covid for instance). I know I can count on you and I am not alone with my thoughts. Thank you.

Finally, I would like to say thank you to my dear (former) colleagues **Lara, Sofia, Mayli, Pia L.**, **Paula**, **Nina**, and **Carolin**, who have become friends throughout the past six years. Thank you for your open ears, even if you sometimes had wished for shorter or longer conversations. I appreciate your openness for not only scientific, but daily and life topics, even if they only occur sporadically as we are all so busy and spread around the globe.

Another thank you goes out to my **neighbors** in Bremen, **Anne** and **Robert**. You have motivated and supported me to get this work done by taking care of my mail when I could not be there, and dancing in your kitchen for me to watch so I could do the same. Thank you.

Last but certainly not least, I would like to thank the **funding partners**, without whom this work would not have been possible. In this respect, I would like to acknowledge the financial support granted by the **BMWK** (Federal Ministry for Economic Affairs and Climate Action – ZIM programme) for our project "AUV Water". For both financial and educational benefits, I am particularly thankful to the graduate school **GLOMAR**, for improving my professional skills in workshops and courses, and supporting my research stay in Australia. Also, I would like to thank the **University of Bremen**, for the financial support of my research stay in Australia funded by the programme "Impulse für Forschungsvorhaben". Moreover, I would like to thank the foundation **Deutsche Stiftung Meeresschutz** for granting me financial support for a second research stay at AIMS, which could not take place due to travel restrictions during the pandemic. Thank you, for accepting to redesignate the funds to pay a few months' salary for my colleague, David. I would also like to thank Rita Kellner-Stoll and the foundation "**Kellner & Stoll Stiftung für Klima und Umwelt**", for financial support to attend the Reef Futures conference 2022 in Key Largo, Florida, and spreading the word about my research topic. Last but not least, I would like to thank the **ZMT**, for accepting to refund my expenses for the participation at the ICRS 2022 in Bremen.

I would also like to give special credits to the **members of my PhD committee**, namely Prof. Dr. Tilmann Harder, Prof. Dr. Claudio Richter, Bea Brix da Costa and Arne Heydtmann, for being available on short notice and supporting me in finalizing my journey.

# List of Figures

## Supplementary Figures

# List of Tables



## Supplementary Tables

# Chapter 1: Introduction

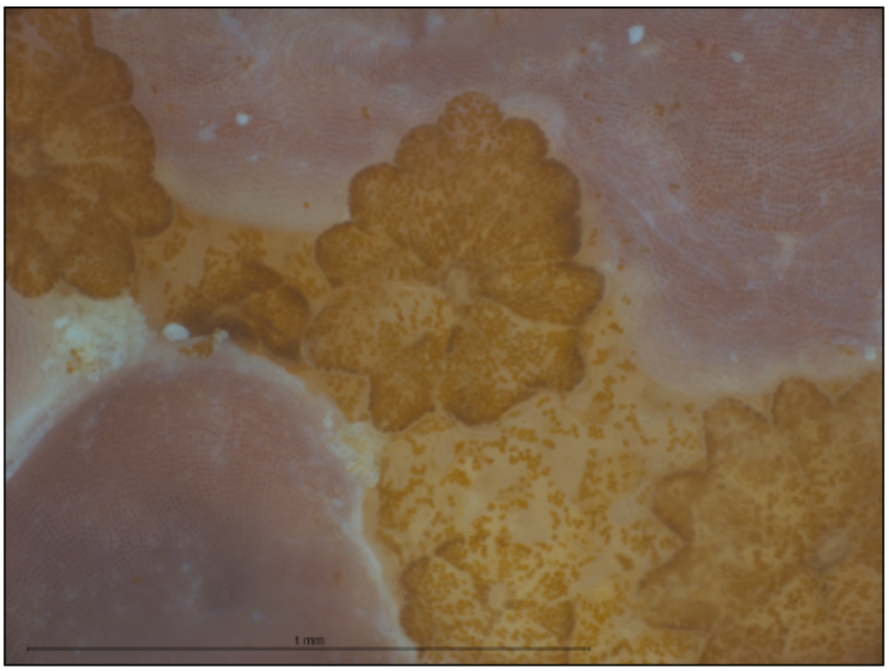

## 1.1 Biofouling, a natural process driven by various factors

Biological fouling processes, especially in the aquatic and marine environments, are natural and dynamic processes which favor ecosystem balance, contributing to nutrient and pollutant recycling, pathogen control, and the competition between pro- and eukaryotic organisms and/or populations for space and nutrition (Müller et al., 2013; Sivadon et al., 2019). In this regard, biofilms are considered critical niches for microbial life in aquatic ecosystems harboring and providing suitable conditions for most aquatic microbes (Weitere et al., 2018).

The successive process of biological fouling or biofouling can be subdivided into different stages of age and growth (**Figure 1.1**; Wahl, 1989; Abarzua and Jakubowski, 1995; Fitridge et al., 2012; Kirschner and Brennan, 2012). Any surface immersed in water is prone to the immediate accumulation of organic carbon molecules (Davey and O'Toole, 2000). The latter's composition depends on the ions, glycoproteins, and humic/fulvic acids, which are available directly in and on the submerged surface (Chambers et al., 2006). The adsorption of molecules is enforced by electrostatic interactions and Van der Waal's forces. The organic carbon source creates a nutritional base for the subsequent settlement of prokaryotes, such as bacteria, and unicellular eukaryotes. The bacterial colonization is further influenced by their biological properties such as their surface motility and surface structures, i.e., pili production. Nutrient availability, seawater chemistry, temperature, and exposure time further determine the settlement process (Rittschof, 2000). Contact and colonization between microorganisms and the surface is further promoted by the movement of water through Brownian motion, sedimentation and convective transport (Chambers et al., 2006). The developing biofilm is a cohabitation of multicellular complexes surrounded by an extracellular matrix or extracellular polymeric substance (EPS), sticking cells together and preventing hostile attacks (Wesseling, 2015). In this process, the resulting EPS is generated by the microbes themselves (Hall-Stoodley and Stoodley, 2009) and consists of bacteria in stationary phase, polysaccharides, proteins, and extracellular DNA (Branda et al., 2005). The primary microbial colonization can be discriminated into the following steps: 1. flagella and type IV pili are used for the initial surface-attachment (O'Toole and Kolter, 1998), 2. type IV pili are responsible for moving on surfaces, leading to microcolonization, 3. reduction of flagella, 4. a self-produced matrix stabilizes the 3D-structure of the biofilm (Hentzer et al., 2001).

After the primary colonization/adsorption of microorganisms, e.g., bacteria and diatoms, the "soft macrofouling" composed of visible algae and invertebrates follows (**Figure 1.1**, **Figure 1.2**; Chaudhury et al., 2005), and finally, the overgrowth by shelled invertebrates, e.g., barnacles and tube worms, termed "hard macro-fouling" defines the last stage of biofouling. Nonetheless, specific attention should be paid to the bacterial fouling, considered as the so called "Achilles heel", due to its severe economic and environmental adverse effects (Kalia, 2018) caused by

the ability of bacteria to rapidly and effectively multiply with their adhesive surface appendages (capsule, fimbria, fibrillae, flagella, outer membranes; Hori and Matsumoto, 2010).

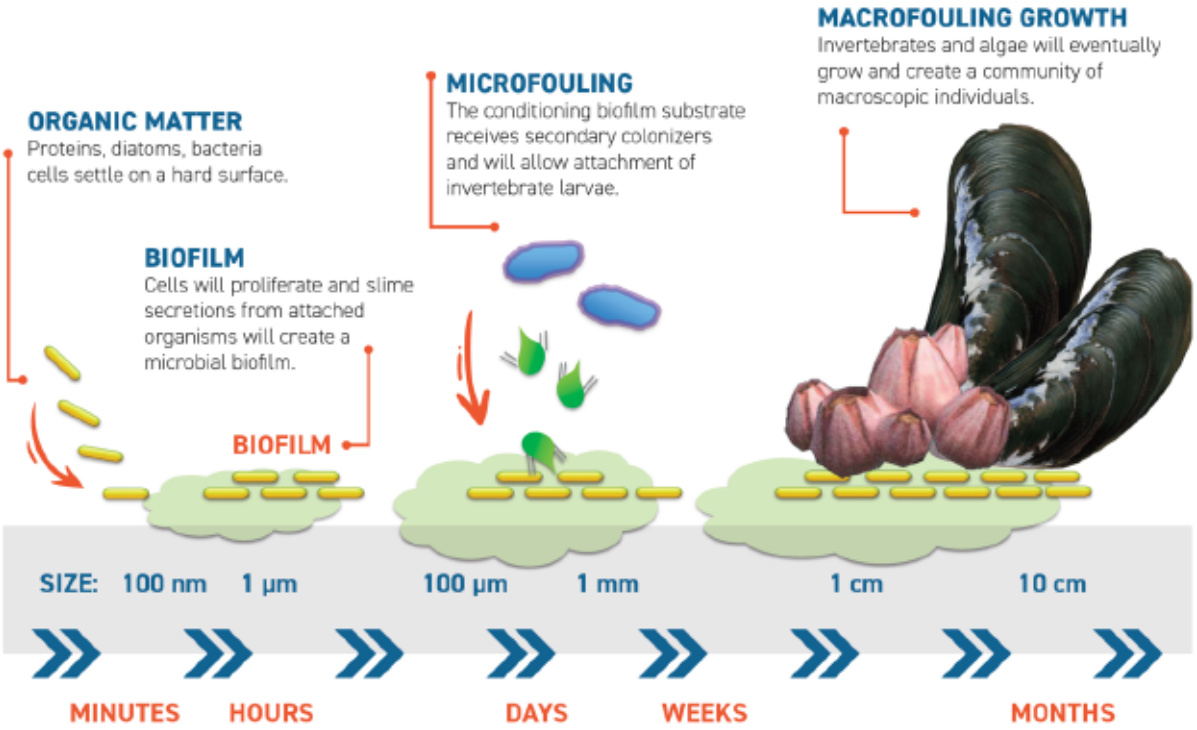


**Figure 1.1**: Schematic showing the typical successive process of biological fouling in the marine environment (taken from GEF-UNDP-IMO GloFouling Partnerships Project and GIA for Marine Biosafety, 2022).

The factors affecting biofouling are manifold including several physical, biological and chemical interactions (Mi and Elimelech, 2008).

Physical factors include temperature, surface topography, hydrodynamics (current velocity, wave exposure), light availability (Kalia, 2018; Vinagre et al., 2020), and color of the substratum (Dahlem et al., 1984). Increased temperature in water systems, such as in the tropics, has shown increased biofilm thickness due to enhanced metabolism resulting in higher growth rates and continuous reproduction throughout the year without interruptions by seasonal changes (Lee and Trott, 1973; Garrett et al., 2008). For instance, Molino et al. (2009) compared the accumulation of bacterial microfouling layers on antifouling coatings between a temperate and tropical environment in Australia and found more rapid rates of fouling in the tropics and during summer months. Also, depth (bathymetry) influences the structure of biofouling communities, especially in shallow waters which are generally more turbulent and have greater variation in physical-chemical parameters such as temperature and turbidity that influence the biofouling composition and abundance (biomass, density and coverage), compared to deeper waters (Vinagre et al., 2020). The color of a substratum relates to the amount of energy reflected and absorbed by the substratum, as well as to the temperature of the substratum, which can be determinants of biofouling settlement (Dahlem et al., 1984).

The topography of a surface dictates its roughness and wettability, the ability of a liquid to contact a solid surface. These features are reported to affect bioadhesion either by inhibiting or promoting it (Blossey, 2003; Bers et al., 2010; Bazaka et al., 2011; Lee and Kang, 2016). Carman et al. (2006) presented, for the first time, a surface that mimics the skin of sharks was effective against marine fouling organisms by altering the fluid drag, caused by anisotropic flow (Bixler and Bhushan, 2015). Another interesting topography is that of the lotus leaf, which exhibits phenomenal superhydrophobic and self-cleaning characteristics (Pechook and Pokroy, 2012; Bixler and Bhushan, 2015). The surface consists of dense microbumps that are hydrophobic in nature and therefore minimize the energy of the surface, resulting in lower adhesion.

Hydrodynamics, and static & dynamic stresses, were found to significantly affect the fouling community composition on tested antifouling coated panels (Hunsucker et al., 2016). Despite different fouling community compositions, the drag forces measured on the panels were very similar. This suggests that the frictional drag of low form and soft fouling communities was similar and that there may be a stepwise increase in frictional drag associated with the presence of mature calcareous organisms (Hunsucker et al., 2016).

The availability of light plays a crucial role in shaping the composition and growth of biofouling organisms. Specifically, macrofoulers, including photosynthetic organisms like macroalgae, tend to be more abundant in areas located within the euphotic zone, which spans from 0-40 m depth (Bartsch et al., 2008). This zone is characterized by higher light levels, elevated temperatures, and a rich abundance of plankton, which serves the primary food source for many non-photosynthetic organisms. As a consequence of a decreased light intensity with depth, within this zone, the biofouling growth and biomass generally decrease with depth (Almeida and Coolen, 2020). Biofouling is reduced by ultraviolet (UV) irradiation, which can efficiently disinfect water. Primary fouling organisms such as bacteria, algae, viruses and protozoans can be inactivated and destroyed by UV irradiation, which promotes harmful hydroxyl radicals which fragment bacterial DNA. However, many persistent molecules that promote biofouling are resistant to UV and in many cases, the oxidation performance of UV-lights alone is insufficient and needs to be combined with photocatalytic applications in order to remove persistent waste products (Penru et al., 2013; Piola et al., 2016; Braga et al., 2020; Dai et al., 2021). In addition, UV irradiation and photosynthetically active radiation (PAR) control the development of micro- and macrofouling communities by inhibiting the recruitment and growth of sensitive species and promoting the growth of resistant species. As a result, these forms of solar radiation influence the settlement cues available to competent larvae by altering the development of the microbial community (Dobretsov et al., 2010).

Biological factors affecting biofouling are microcolonies, chemotaxis, horizontal gene transfer and quorum sensing (QS). The first step in the "social" organization of biofilms is the formation

of microcolonies, groups of <50 cells that seem to spontaneously aggregate and thereby nucleate the growth of the biofilm (Wolfaardt et al., 1994). Despite decades of work, it is not well understood precisely how individual surface-attached bacteria self-organize into microcolonies (Davey and O'Toole, 2000; Zhao et al., 2013; Lawrence et al., 2016). Oliveira et al. (2016) found that individual bacterial cells actively moved towards nutrients (chemotaxis) within a developing biofilm. This ability not only allows cells to seek out favored positions on a surface in response to a chemical stimulus, but also regulates their movement with remarkable submicron precision (Pratt and Kolter, 1999; Hölscher et al., 2015). Genetically motile bacteria not only grow in length, but also in height, by detaching and reattaching, which further modifies the degree of biofouling (Picioreanu et al., 2007; Kalia, 2018).

Horizontal transfer of genetic material alters the microbial community (Hausner and Wuertz, 1999). The genetic diversity increases when the surrounding environment changes. Mobile genetic elements such as transposons, conjugative plasmids and bacteriophages are responsible for the horizontal gene transfer (Madsen et al., 2012). Bacterial communication is mediated by small molecules termed autoinducers (AIs), which are secreted by bacteria and are used to measure population densities (Waters and Bassler, 2005; Kirschner and Brennan, 2012; Salta et al., 2013; Wesseling, 2015; Kalia, 2018). As the biofilm forms and cell density rises, the concentration of AIs reaches a threshold, at which they alter gene expression (Nir and Reches, 2016). This process, termed "quorum sensing", differs between different strains of bacteria. Gram-negative bacteria use *N*-acetylated homoserine lactones (AHL) to communicate, Gram-positive bacteria respond to processed oligopeptides (Bharati and Chatterji, 2013). This behavior leads to coordinated self-organization and is provided with superior and unique survival properties (Almeida and Vasconcelos, 2015).

Comparative studies on early-stage biofilm composition dynamics face challenges due to variations in environmental conditions across different immersion sites. In addition to physical and biological factors, chemical factors such as water chemistry influence both planktonic and biofilm ecophysiology (Hall-Stoodley et al., 2004). It is crucial to recognize that biofilm community composition is directly influenced by the ecosystem, including biogeochemical and physical interactions, as well as seasonal and geographical variations. Nutrients have been shown to impact microbial biofilm communities in the intertidal zone on rocky shorelines in Hong Kong (Chiu et al., 2008), and pH and dissolved oxygen influenced the settlement of periphytic algae in a tropical estuary in Singapore (Nayar et al., 2005). Chemicals, such as NaCl, $Ca^{2+}$ and $Mg^{2+}$, can also affect biofouling (Kalia, 2018; Wang et al., 2019). Calcium ions at a certain concentration have shown to strengthen the cross-links components of EPS (Körstgens et al., 2001) and increase cell aggregation and thickening of biofilm layers (Rose and Turner, 1998). Optimal biofilm growth has been reported at a pH value between 6 to 9 in freshwater from a wastewater treatment plant (Patil et al., 2011).

## 1.2 Undesired consequences of biofouling

Biofouling is a complex, dynamic problem that globally impacts both the economy and environment (Kirschner and Brennan, 2012). Worldwide, countries spend billions of dollars in order to manage and prevent the undesired accumulation of organic molecules, microorganisms, plants, animals, and their by-products on submerged surfaces (Callow and Callow, 2011; Dobretsov et al., 2019). Biofouling impacts commercial and leisure vessels (**Figure 1.2**), naval fleets, heat exchangers in power plants, etc., by increased hull roughness and hydro- dynamic drag (Schultz, 2007), which leads to decreases in speed and maneuverability, an increase in fossil fuel consumption, and as a result increased emission of greenhouse gases (Poloczanska and Butler, 2010). Carbon dioxide emissions from shipping have been calculated to amount to more than 2.5% of global $CO_2$ release (Lewis, 2018). It has been estimated that a relatively light biofouling with diatoms resulted in efficiency penalties of 10–16%, whereas heavy calcareous fouling at full cruising speed resulted in efficiency penalties of up to 86% (Schultz et al., 2011).

Hull fouling and ballast water transfer are also the primary causes for the introduction and spread of non-indigenous marine species into ecosystems across the world (Otani et al., 2007; Piola and Johnston, 2008; Yamaguchi et al., 2009). Modern trade routes and shipping practices with relatively quick voyages and long port stays provide consistent transport of adults and larvae of fouling organisms across vast distances and biogeographical barriers (Pettengill et al., 2007). One study found 22 species of barnacles attached to the hulls of two intercontinental bulk carriers at the port in Osaka Bay, Japan. Of the 22 species identified, 14 were not previously recorded in Osaka Bay, including 4 that were not previously recorded anywhere in Japan (Otani et al., 2007).

## 1.3 How to control biofouling: past and present state of the art

In order to prevent biofouling, maritime industries use biocides or other toxic compounds applied as active ingredients in antifouling (AF) paints. Most of the biocidal paints have shown to kill non-target marine organisms and cause undesirable environmental impacts. In the 1960s, the search for more effective biocides identified organotins, e.g., tributyltin (TBT) oxide, to have a broad spectrum of biocidal properties and were therefore commercialized in AF paint products. Only when TBT showed impacts on non-target organisms such as oysters, whales and dolphins, a global ban on use on all international vessels was subsequently implemented by the IMO (International Maritime Organization; Convention on the Control of Harmful Anti-Fouling Systems on Ships) for AF coatings with TBT in 2003 and the operation of ships coated with TBT paints in 2008. Main compositions of AF paints being used in the past until 2008 were the herbicides 3-(3,4 dichlorophenyl)-1,1-dimethylurea (Diuron®) and until 2016

cybutryne (Irgarol®) (Egardt et al., 2017). These herbicides are effective against algal fouling but require *booster biocides* such as zinc pyrithione (ZnPT), copper pyrithione (CuPT), or chlorothalonil, which have negative effects on a broader range of fouling taxa (however, they can affect some non-target species at concentrations as low as TBT) (Bao et al., 2011). Many studies have shown that copper compounds are toxic to non-target marine species such as larvae of a brine shrimp (Castritsi-Catharios et al., 2007), microalga (Koppel et al., 2017), bacteria, macroalga, and crustaceans (Karlsson et al., 2010), and fish (Baldwin et al., 2011).

Modern biofouling control coatings can be classified into either "biocidal" or "non-biocidal" coatings by their composition. Biocidal coatings include controlled depletion polymers (CDPs), self-polishing copolymer (SPCs), and hybrid SPC paints. Non-biocidal coatings include fouling release coatings (FRCs), which are also termed as nonstick coatings (Chambers et al., 2006; Almeida et al., 2007). The resin-based CDPs use the hydration process to release biocides into the seawater. Seawater migrates into the CDP paint film which in turn dissolves resin and exposes biocides. However, the exponential release rate is a problem. Initially, the rate of release is wastefully high, then falls rapidly towards a point at which insufficient biocide is released to prevent the settlement of the biofouling species. The leached layers can become thick and increase the hull roughness. In general, the performance of CDP paints is considered poor but, due to its low cost, they are still preferred for vessels which have short dry-dock intervals and those operating in low biofouling regions (GEF-UNDP-IMO GloFouling Partnerships Project and GIA for Marine Biosafety, 2022).

The banning of TBT led to the development of tin-free SPC paints. SPCs have good initial hydrodynamic performance due to their smooth surface and the self-polishing action as the name suggests. The dissolution rate of biocides, e.g., copper and zinc pyrithione, is controlled via interaction with seawater, resulting in better AF performances. SPCs can remain effective for up to 5 years and therefore these coatings are preferred for vessels which have longer dry-dock intervals. The biocide release mechanism of hybrid SPCs may be regarded as a hybrid of self-polishing and hydration, combining SPC acrylic polymers with a certain amount of resin. The performance and price of hybrid SPCs, therefore, are midway between the CDPs (resin-based) and SPCs (acrylic-based). The main alternatives to biocidal AF coatings are widely known as FRCs. FRCs have attracted a great deal of attention in recent years, as they are capable of being fabricated with such low surface energy materials as silicone, which is environmental-friendly, efficient, and cheap. However, due to the mode of action of these coatings, they are most suitable for use on vessels which reach higher speeds and have higher levels of activity (GEF-UNDP-IMO GloFouling Partnerships Project and GIA for Marine Biosafety, 2022).
One of the most widely applied AF coatings, Sea-Nine 211™ (Röhm & Haas; Philadelphia, PA, USA (Jacobson and Willingham, 2000)), includes an active biocidal ingredient, known as dichlorooctylisothiazolinone (DCOIT, Kathon 930, C-9 or DCOI). DCOIT can diffuse across the cell walls and membranes, binding to proteins and enzymes, blocking activity in biofilms,

target and non-target organisms (Silva et al., 2020). The half-life of DCOIT is much shorter than traditional biocides and depends on environmental conditions, ranging from less than one day to 10 days or more, and can be influenced by several biotic and abiotic factors, such as microorganisms, photolysis, hydrolysis, pH and salinity (da Silva et al., 2021). Toxic effects have been observed across a diversity of organisms including bacteria, fungi, algae, bivalves, echinoderms, ascidians, fish, copepods, decapods, and soft corals (Cima et al., 2013; Wendt et al., 2016; Chen et al., 2017; Martins et al., 2018; Moon et al., 2019; Su et al., 2019; Fonseca et al., 2020; Ferreira et al., 2021). Although the toxicity mechanism of DCOIT is not fully understood, embryotoxicity, immunosuppression, oxidative stress, reproductive and endocrine disruption in marine organisms have been reported (Campos et al., 2022).

However, some studies have shown effective AF properties of DCOIT encapsulated in silica nanocapsules which can decrease the toxicity towards non-target organisms (Maia et al., 2015; Dos Santos et al., 2020). The rationale behind the encapsulation/immobilization technology is the prevention of direct biocidal interaction with coating components, the control of leaching rate, and thus, the decrease of the absolute quantity of biocides needed to prepare a formulation with identical AF efficacy, increasing the coating lifetime and reducing potential environmental threats (Maia et al., 2012, 2015; Martins et al., 2017; Gutner-Hoch et al., 2018).

**Figure 1.2**: Polyvinyl chloride (PVC) tile overgrown with soft and hard fouling organisms; incl. coral spat after 3 months in a seawater aquarium at ZMT (photo left). Leisure boat's hull overgrown with algae and barnacles after one season in the German Baltic Sea near Kappeln (photo center). Mooring buoy overgrown with barnacles and blue mussels after one season in the German North Sea near Husum (photo right).

Current AF research focuses on the design of environmentally benign and bioinspired solutions including engineered microtopographies, as mentioned in **section 1.1** (Lee and Kang, 2016; Tian et al., 2020; Kumar et al., 2021), enzyme-mimicry or photocatalytic coatings (Al-Belushi et al., 2020; Dobretsov et al., 2020; Wang et al., 2021), as described for nanoparticles below in this section, and natural product antifoulants found in different marine organisms, such as sponges, macroalgae, and corals (Niemann et al., 2015; Soliman et al., 2017; Sánchez-Lozano et al., 2019).

A recent approach aims to prevent fouling by targeting the early stages of biofilm formation without the use of biocidal agents. Nanoparticles (NPs) function by interfering with bacterial cell-to-cell communication (i.e., quorum sensing). Based on reports and first scientific publications (Hartog et al., 2012; Herget et al., 2017, 2018; Korschelt et al., 2018a), indicating that NPs can exhibit enzyme-like activities and show in vitro biocompatibility, research on NP enzyme mimics that might have the potential to be functional even inside cells or living organisms has seen an upsurge in recent years. NPs can be surface functionalized for specific targeting, and they can tolerate changes in reaction conditions more easily when compared to enzymes. Moreover, they can be manufactured cost-efficiently up to industrial scales. One key feature of NPs is their large surface to volume ratio leading to high chemical activity (Herget et al., 2018).

In solution, NPs are stabilized typically with surfactants and/or polymers. Their reactivity may be higher than that of enzymes because any surface site can be catalytically active, whereas enzymes only have a single binding site, although with exceptional specificity and selectivity. Vanadium-dependent haloperoxidase catalyzes the oxidation of halides in presence of hydrogen peroxide ($H_2O_2$) to hypohalous acids (HOX) according to: $Br^- + H_2O_2 \rightarrow HOBr + H_2O$. HOX can react to form halogenated organic compounds, such as hypohalous acids which combat biofilm formation through their biocidal activity or the formation of signaling molecules involved in intracellular communication. When cell-to-cell communication is blocked by halogenated (and therefore inactive) compounds, bacteria cannot form organized community structures such as biofilms. NPs that incorporate mixed valent $Ce^{3+}/Ce^{4+}$ surface sites directly affect the catalytic activity. $Ce^{3+}$ ions are known to catalyze the halogenation of malonic acid. Thus, the antibacterial activity of NPs is presumably not a result of superoxide dismutase (SOD) activity, but of its halogenating properties. NPs showed a strong brominating activity, as demonstrated with phenol red in the presence of $Br^-$ and $H_2O_2$. Bromination reactions in the presence of NPs and the marine alga *Corallina officinalis* showed similar results (Herget et al., 2017), illustrating the oxidative halogenation properties of NPs.

Laboratory and field tests with paint formulations containing 2 wt% of $CeO_{2-x}$ NPs showed a reduction in biofouling comparable to $Cu_2O$, one of the most typical biocidal ingredients in AF paints. Bacterial cultures containing $CeO_{2-x}$ NPs, bromide and $H_2O_2$ showed virtually no colonization compared to negative controls. The metal oxide showed strongly reduced algal growth in field tests (Herget et al., 2017; Korschelt et al., 2018b). NPs have the potential to be non-toxic and sustainable substitutes for conventional inorganic/organic biocides. $CeO_{2-x}$ NPs have been reported to have peroxidase, SOD, catalase, phosphatase and esterase properties (Korschelt et al., 2018b). $CeO_{2-x}$ nanorods may have a broad future application in paints, textiles, polymer membranes for water desalination of filters, for the reclamation of waste water, aquaculture systems, on bridge piers, naval vessels, or in offshore wind parks (Herget et al., 2017; Wang et al., 2021). An ideal $CeO_{2-x}$ NP AF formulation contains a durable biomimetic

catalyst incorporated into an insoluble and stable, but porous matrix. The porosity provides sufficient surface area and allows mass transfer of $H_2O_2$, halogenide and the substrate molecules. The products are released after the reaction and leave the catalyst in the matrix behind, where it can recover its activity. Haloperoxidase mimics allow designing stable antibacterial materials with high chemical stability and low environmental toxicity due to the insolubility of NP in water, low costs, constant availability of the substrates ($H_2O_2$ and halide) which are required for a dynamic antibacterial activity (HOX formation), and intrinsic activity at substrate concentrations comparable to those encountered in aqueous environments.

## 1.4 Tropical corals under stress in a rapidly changing environment

Tropical coral reefs, the 'rainforests of the sea', are among the most biodiverse and productive ecosystems on earth (Knowlton and Jackson, 2008). They occupy less than 0.1% of the ocean surface (Spalding and Grenfell, 1997), yet, they are home to more than 25% of marine species (Plaisance et al., 2011). Coral reefs provide humans within critical ecosystem services in terms of food, livelihoods and coastal protection (Moberg and Folke, 1999; Burke and Reytar, 2011; Cinner et al., 2012; Kennedy et al., 2013b; Pendleton et al., 2016).

Coral reefs have undergone a significant decline of around 50% in their distribution and abundance in the past 30 years (Gardner et al., 2005; Bruno and Selig, 2007; De'ath et al., 2012) due to various factors, including pollution, storms, overfishing, and unsustainable coastal development (Burke and Reytar, 2011; Halpern et al., 2015; Cheal et al., 2017). However, the most significant threat to coral reefs in recent years has been climate change, particularly the impact of heat stress caused by rising temperatures (Hoegh-Guldberg, 1999; Baker et al., 2008; Spalding and Brown, 2015; Hughes et al., 2017b). Even a slight temperature increase of 1°C above the long-term summer maximum for an area (reference period 1985–1993) sustained for 4-6 weeks can lead to mass coral bleaching and mortality, as stated with very high confidence by the working group (WG) II Fifth Assessment Report (AR5) of the Intergovernmental Panel on Climate Change (IPCC; Hoegh-Guldberg et al., 2018). Furthermore, ocean warming and acidification can reduce the growth and calcification rates of corals, making them less competitive against other benthic organisms such as macroalgae or seaweeds (Dove et al., 2013; Reyes-Nivia et al., 2013, 2014)

Average warming of the global mean surface temperature (GMST) of 0.87°C in recent years (2006-2015) has led to a substantial proportion of coral reefs experiencing large-scale mortalities that have led to reduced coral populations (Hoegh-Guldberg, 2014a, 2014b). According to Hughes et al. (2017), prominent coral reef ecosystems as Australia's Great Barrier Reef have lost as much as 50% of their shallow water corals.

Predicted bleaching events (Hoegh-Guldberg, 1999) have come to pass during the summers of 2016-2017 (Hughes et al., 2017b). Additionally, there is a high degree of certainty in projections of declining coral populations. Advances in modeling techniques have allowed for predictions of extensive coral reef loss by mid-century, even under low-emissions scenarios (Hoegh-Guldberg, 1999; Donner et al., 2005; Donner, 2009; van Hooidonk and Huber, 2012; Frieler et al., 2013; Van Hooidonk et al., 2016).

It has been predicted that achieving emission reduction targets in line with the Paris Agreement's ambitious goal of limiting global warming to 1.5°C will still result in the loss of 70-90% of reef-building corals compared to today (Hoegh-Guldberg et al., 2018). Moreover, a temperature rise of 2°C or more above pre-industrial levels would lead to the loss of 99% of corals (Frieler et al., 2013; Hoegh-Guldberg, 2014b; Schleussner et al., 2016; Hughes et al., 2017a). The models used in these assessments often incorporate assumptions that are considered to be highly conservative, and in some cases, include 'optimistic' assumptions such as rapid thermal adaptation of 0.2°C-1°C per decade (Donner et al., 2005) or 0.4°C per decade (Schleussner et al., 2016). However, there is little evidence supporting the notion that corals can adapt to climate change at such high rates, and recovery from mass mortality events typically takes much longer, often exceeding 15 years (Baker et al., 2008).

According to probability analysis, the likelihood of coral bleaching and mortality is 25% lower under 1.5°C instead of 2°C sea temperature increase scenarios (King et al., 2017). Variations in the rates of heating across different areas suggest that there may be temporary climate refugia, which could aid in the regeneration of coral reefs if protected from risks unrelated to climate change (Caldeira, 2013; Van Hooidonk et al., 2013; Cacciapaglia and van Woesik, 2015; Keppel and Kavousi, 2015).

Kersting et al. (2017), suggested locations in higher latitudes are reporting the arrival of reef-building corals, which could be valuable in terms of the role of limited refugia and reef structures. Deep-water (30-150m) or mesophotic coral reefs may play an important role due to their ability to evade the extreme conditions of shallow waters, such as heat and storms (Bongaerts et al., 2010; Holstein et al., 2016). However, according to Bongaerts et al. (2017), these ecosystems may have limited capacity to assist in the recovery of damaged shallow water areas.

The susceptibility of corals to heat stress makes it clear that even relatively brief periods of overshoot (i.e., decades) would result in severe harm to coral reefs. If 70-90% of today's coral reefs disappeared, the depletion of resources would raise poverty levels for the millions of people who rely on these valuable ecosystems along tropical coastlines (Spalding et al., 2014; Halpern et al., 2015).

The disappearance of habitat-building corals has a domino effect on other reef-dependent species such as fish, and this has far-reaching implications for various industries, including tourism and fisheries. This issue is particularly concerning for coastal communities in the tropics, many of which depend on functional reefs for food, livelihoods, and coastal protection (Wilson et al., 2006; Graham, 2014; Graham et al., 2015; Cinner et al., 2016; Pendleton et al., 2016). Furthermore, the impacts of increasingly intense storms exacerbate the problem by physically destroying coral communities and reefs (Cheal et al., 2017). The issue is further compounded by ocean acidification, which weakens coral skeletons, contributes to disease, and slows the recovery of coral communities after mortality events (Gardner et al., 2005; Dove et al., 2013; Kennedy et al., 2013a; Webster et al., 2013; Hoegh-Guldberg, 2014b; Anthony, 2016). Also, decalcifying organisms such as excavating sponges have been found to exhibit increased activity in response to ocean acidification (Kline et al., 2012; Dove et al., 2013; Fang et al., 2013, 2014; Reyes-Nivia et al., 2013, 2014).

With the challenges facing coastal communities' food security and livelihoods, it is increasingly crucial to plan for adaptation options like the diversification of livelihoods and the establishment of new sustainable industries. Coastal living faces various threats and challenges, including rising sea levels, which will exacerbate the issues arising from the degradation of coral reefs, particularly for small island developing states (SIDS) and low-lying tropical nations. Considering the magnitude and expense of these interventions, it would be advantageous to implement them sooner rather than later.

## 1.5 Successful recruitment of corals endangered by fouling

It is not only maritime industries that are affected by biofouling, the ecological function of coral reefs can also be negatively impacted by excessive fouling, which often creates uninhabitable substrate for corals' survival. High mortality after larval settlement in corals can be caused by competition with other benthic organisms (Vermeij and Sandin, 2008; Vermeij et al., 2009; Arnold et al., 2010; Arnold and Steneck, 2011). Competition with benthic algae, often triggered by excess nutrients associated with runoff is recognized as a key threat to coral settlement and the survival and growth of coral recruits and the success of adult corals (Carpenter and Edmunds, 2006; Box and Mumby, 2007; Birrell et al., 2008; Linares et al., 2012; Karcher et al., 2020). Fouling can impact coral spat (newly settled corals) through competition for space and direct overgrowth by microorganisms or motile propagules of other macroorganisms (**Figure 1.3**; McCook et al., 2001). Furthermore, the microtopography provided by fouling may provide a refuge for microbial pathogens (Nugues et al., 2004) or corallivorous invertebrates. Allelopathy (Fong et al., 2019), shading (McCook et al., 2001), alteration of fine-scale water movement, and other microenvironmental changes induced by fouling algae may also impede coral survival or fitness of coral spat (Hauri et al., 2010).

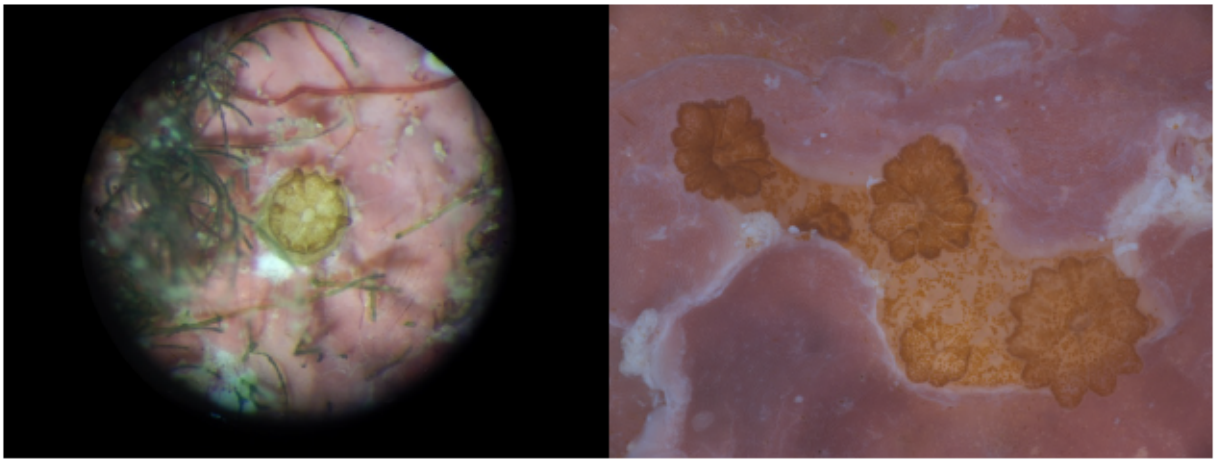

**Figure 1.3**: Coral settler (*Colpophyllia natans*) surrounded by crustose coralline algae (CCA) and turf algae (photo left). *Acropora millepora* coral settlers overgrown by CCA (photo right).

The functioning and recovery of coral reefs following disturbance events depends on the successful recruitment of corals (Ricardo et al., 2017). The most severe demographic bottleneck for corals occurs in their earliest life stages as larvae (Chamberland et al., 2017). Coral larvae select a site on the reef substrate for permanent attachment using external chemical cues that induce metamorphosis (Morse et al., 1996; Heyward and Negri, 1999; Webster et al., 2004). Some biofilms and crustose coralline algae (CCA) are strong inducers of settlement of coral larvae (Heyward and Negri, 1999; Negri et al., 2001; Tebben et al., 2011, 2015; Sneed et al., 2014). Previous studies have shown that the induction of attachment in larvae has been triggered by CCA (Pollock et al., 2017; Jorissen et al., 2021; Abdul Wahab et al., 2023) including by their associated bacteria (Negri et al., 2001; Tebben et al., 2011; Tran and Hadfield, 2011). Tebben et al. (2015) found two classes of CCA cell wall-associated compounds, glycoglycerolipids and polysaccharides, which induced settlement and metamorphosis at equivalent concentrations as present in live CCA. Other studies reported the induction of metamorphosis in coral larvae by specific bacterial isolates of the genus *Pseudoalteromonas* in laboratory assays with tetrabromopyrrole (TBP) being the causative bacterial metabolite responsible (Tebben et al., 2011; Sneed et al., 2014).

However, the bacterial genus *Pseudoalteromonas* has been shown to possess unusual and intriguing features concerning ecologically-relevant questions. A number of studies were able to show the antibacterial and AF properties of *Pseudoalteromonas* spp. resulting in the settlement inhibition or cytotoxicity of various algal species and invertebrate larvae (Holmström et al., 1996, 2002; Bowman, 2007). A neuropeptide, GLW-amide, has shown to induce metamorphosis, but often without attachment in *Acropora tenuis* and *Acropora palmata* (Iwao et al., 2002; Erwin and Szmant, 2010; Grasso et al., 2011; Moeller et al., 2019). Moeller et al. (2019) demonstrated coral larvae settlement was induced by the cnidarian typic neurotransmitters dopamine, glutamic acid and epinephrine in the species *Leptastrea purpurea*. Dopamine showed a moderate settlement and metamorphosis response of 54% in larvae.

However, the results obtained from this experiment revealed that none of the tested compounds induced larval settlement as effective as the positive control (CCA pieces) with 98%.

While CCA have been shown to be one of the most preferred natural substrates that induce coral settlement and recruitment, other studies have demonstrated that CCA can also outcompete and overgrow coral spat and lead to spat mortality under certain conditions (Harrington et al., 2004; Jorissen et al., 2020). In literature, so called "promoter" and "inhibitor" CCA species emphasize the importance to identify CCA species and match beneficial CCA-coral pairs for optimal growth of both benthic organisms (Buenau et al., 2012; Abdul Wahab et al., 2023). Therefore, control of CCA, amongst other algae, is an important consideration for improving coral spat survival (Tebben et al., 2014; ***Chapter 5***) in parallel to decreasing anthropogenically driven nutrient discharges that foster algal growth (Littler et al., 2006).

## 1.6 Knowledge gaps and objectives

As more tropical reefs worldwide undergo climate- and eutrophication-driven phase-shifts from coral- to fleshy algal-dominated cover, interactions between fouling organisms and corals become more pronounced and frequent (Anton et al., 2020; Karcher et al., 2020; Adam et al., 2021). In this context, innovative antifouling (AF) coatings could have broad application in coral restoration activities. The application of low toxicity or non-biocidal AF coatings on settlement surfaces for coral larvae may enhance the viability and profitability of sexually propagated corals by improving the survival and growth of coral spat that make it through critical early life stages. Several studies tested the effects of past tributyltin (TBT), Diuron® and Cu-based AFs on coral spat performance (Negri and Heyward, 2001; Negri et al., 2002, 2005, 2011; Smith et al., 2003; Cantin et al., 2007; Negri and Marshall, 2009). However, the effects of modern AF coatings on marine species, especially corals, have been rarely evaluated since their introduction after 2008, when TBT was globally prohibited (Dafforn et al., 2011). By contrast, DCOIT, as a biocidal ingredient in a range of AF coatings, has been investigated and evaluated to a greater extent, but with no testing of hard corals or coral larvae to date. Additional research and methodological development are needed to investigate the ability of newly developed AF coatings to reduce competition from biofouling and increase coral survival to size-escape levels (Doropoulos et al., 2012). Ultimately, this could benefit restoration programs by complementing current methodologies. Furthermore, sensitive techniques to assess the effects of AF coatings on the behavior of coral larvae are required to select coatings that do not inhibit larvae from settlement on adjacent surfaces. To address these knowledge gaps, innovative AFs were tested in respect to their ability to (1) reduce fouling in tropical conditions, (2) affect larval swimming behavior (using an automated tracking software EthoVision XT), (3) affect larval settlement and (4) improve the survival of spat. This study applied and tested three coatings (antiadhesive, cerium dioxide ($CeO_{2-x}$) nanoparticle, and encapsulated biocide

dichlorooctylisothiazolinone (DCOIT)) with reportedly high AF efficacy and potential low toxicity (Detty et al., 2014; Maia et al., 2015; Herget et al., 2017). The thesis chapters specifically explored:

**Chapter 2**

**(i)** the AF efficacy of the coatings to reduce biofouling on settlement surfaces (*plugs*) under tropical conditions

**(ii)** the fouling community (CCA, green/brown algae, bare substrate) composition on coated and uncoated areas of settlement plugs

**(iii)** settlement preferences of *A. tenuis* coral larvae on coated and uncoated areas of pre-conditioned settlement plugs

**Chapter 3**

**(iv)** early post-settlement survival (14, 42, 69 days post-settlement) and growth (after 14 days) of *A. millepora* coral settlers on coated and uncoated areas of non-conditioned settlement plugs

**Chapter 4**

**(v)** the swimming behavior (velocity and activity) of *A. millepora* coral larvae in response to the AF coatings

**(vi)** the feasibility of the experimental setup, including its adaptation for coral larvae, with the software EthoVision XT

The ultimate goal of the study was to tackle the question of how AF coatings can potentially contribute to coral restoration practices by learning more about: (1) their antifouling efficacy, (2) their potential deterrent or toxic effects on coral spat and (3) their potential application and efficacy to enhance coral spat survival and growth on coral deployment devices.

## 1.7 Research questions

Considering the knowledge gaps and objectives of this study, the overarching research question of this thesis is:

> What are the abilities and limits of the herein investigated antifouling coatings to potentially enhance reef restoration efforts?

To address this question, three sub-questions are asked and investigated in their corresponding chapters:

1. How effectively do the coatings inhibit fouling and shape the fouling community on "coral plugs"? (***Chapter 2, 5***)
2. To what degree do the coatings affect coral spat performance (settlement, survival, growth, swimming behavior)? (***Chapters 2, 3, 4, 5***)
3. Is coral spat performance different between coated and uncoated areas on the plugs within and between antifouling treatments? How could antifouling treated substrates be further investigated and applied in the future? (***Chapters 2, 3, 4, 5***)

## 1.8 Chapter and publication outline

The work presented in this thesis was conducted at the Leibniz Centre for Tropical Marine Research (ZMT) in Bremen, Germany, and the Australian Institute of Marine Science (AIMS) in Townsville, Australia. At AIMS, experiments were performed in natural filtered seawater in large outdoor flow-through aquaria, as well as indoors in different temperature-controlled rooms of the National Sea Simulator (SeaSim).

Following the general introduction, this thesis includes three manuscripts, two of which have already been published (***Chapters 2***, ***4***), while ***Chapter 3*** is in preparation for submission. Together, these studies provide a first overview of the opportunities and limits to enhance reef restoration efforts with antifouling coatings. In a final discussion (***Chapter 5***), the key results and findings of the three chapters are integrated and evaluated in the context of the current state of knowledge. Furthermore, the applied methodologies along with the significance of the results are assessed in a broader, holistic context in order to identify future research and application recommendations.

The thesis is structured as follows, with personal contributions of the PhD candidate outlined in **Table 1.1**: Contribution (in %) of the PhD candidate Lisa Röpke to the conceptualization, data acquisition and analysis, interpretation of results, and preparation of the manuscripts, including visualization of results (in figures and tables) for each of the three chapters presented in this thesis.

### Chapter 2

In ***Chapter 2***, the AF coatings were investigated for their ability to inhibit algal fouling on "coral plugs" with coated and uncoated areas, as there was a potential risk that the chemicals of the coated areas could affect coral settlement on uncoated areas through spill-over effects. Fouling succession was tracked for 37 days and, in addition, settlement of *Acropora tenuis* larvae was measured to determine whether AF coatings were a settlement deterrent. The study provides insights into the efficacy to reduce biofouling and the extent to which crustose coralline algae (CCA), green/brown algae, and bare substrate were shaped by the coatings. Furthermore, settlement preferences of coral larvae on and next to the coatings reveal opportunities for potential application of the coatings in coral aquaculture.

This chapter has been published as:

*Roepke LK, Brefeld D, Soltmann U, Randall CJ, Negri AP, Kunzmann A (2022) Antifouling coatings can reduce algal growth while preserving coral settlement. Sci Rep 12, 15935. https://doi.org/10.1038/s41598-022-19997-6*

### Chapter 3

In ***Chapter 3***, the fully- and partially-coated AF "coral plugs" were tested on the survival and growth of *Acropora millepora* spat. The spat were monitored on the plugs at regular intervals (0, 14, 42, 69 days post-settlement). The results of this study contribute to the understanding of possible deterrent effects of the coatings on early coral spat and provide insights into which of the coatings could be used to promote survival and growth of seeded corals. In addition, the findings highlight options for future AF-coated seeding device design, which could complement other coral restoration activities.

This chapter is in preparation for submission as:

*Roepke LK, Brefeld D, Soltmann U, Randall CJ, Negri AP and Kunzmann A (in prep.) Effects of antifoulings on survival and growth of coral spat for reef restoration.*

### Chapter 4

In ***Chapter 4***, the effect of the AF coatings was tested on the swimming velocity and activity of *Acropora millepora* coral larvae, as behavioral responses are considered sensitive and effective indicators of organism stress. The behavior of 32 coral larvae per AF treatment were recorded, each for 25 min, in a custom designed dark box with two camera recording sets in parallel. Tracking of coral larval swimming behavior with the software Noldus EthoVision XT was identified as a reliable and feasible method for assessing potential non-lethal stress responses to AF coatings. As changes in behavior could have significant consequences for larval survival and settlement, they are important endpoints to consider. For methodological standardization and implementation of coral toxicity tests, this study features a detailed guide for video-processing and track analysis of *A. millepora* coral larvae in EthoVision.

This chapter has been published as:

*Roepke LK, Brefeld D, Soltmann U, Randall CJ, Negri AP and Kunzmann A (2022) Applying behavioral studies to the ecotoxicology of corals: A case study on Acropora millepora. Front Mar Sci 9:1002924. doi: 10.3389/fmars.2022.1002924*

The contribution of the PhD candidate to each chapter of the present thesis is given in **Table 1.1**. Additionally, each chapter contains an authorship contribution statement as requested by the respective journals.

**Table 1.1**: Contribution (in %) of the PhD candidate Lisa Röpke to the conceptualization, data acquisition and analysis, interpretation of results, and preparation of the manuscripts, including visualization of results (in figures and tables) for each of the three chapters presented in this thesis.

| *Task* | *Chapter 2* | *Chapter 3* | *Chapter 4* |
|---|---|---|---|
| *Concept, coordination and design* | 95 | 95 | 95 |
| *Acquisition of data* | 90 | 90 | 60 |
| *Data analysis and interpretation* | 80 | 80 | 60 |
| *Preparation of Figures and Tables* | 90 | 90 | 90 |
| *Drafting of manuscript* | 100 | 100 | 100 |

## 1.9 References


Abarzua, S., and Jakubowski, S. (1995). Biotechnological investigation for the prevention of biofouling. I. Biological and biochemical principles for the prevention of biofouling. *Mar. Ecol. Prog. Ser.* 123, 301–312.

Abdul Wahab, M. A., Ferguson, S., Snekkevik, V. K., McCutchan, G., Jeong, S., Severati, A., et al. (2023). Hierarchical settlement behaviours of coral larvae to common coralline algae. *Sci. Rep.* 13, 5795. doi:10.1038/s41598-023-32676-4.

Adam, T. C., Burkepile, D. E., Holbrook, S. J., Carpenter, R. C., Claudet, J., Loiseau, C., et al. (2021). Landscape-scale patterns of nutrient enrichment in a coral reef ecosystem: implications for coral to algae phase shifts. *Ecol. Appl.* 31. doi:10.1002/eap.2227.

Al-Belushi, M. A., Myint, M. T. Z., Kyaw, H. H., Al-Naamani, L., Al-Mamari, R., Al-Abri, M., et al. (2020). ZnO nanorod-chitosan composite coatings with enhanced antifouling properties. *Int. J. Biol. Macromol.* 162, 1743–1751. doi:10.1016/j.ijbiomac.2020.08.096.

Almeida, E., Diamantino, T. C., and de Sousa, O. (2007). Marine paints: The particular case of antifouling paints. *Prog. Org. Coatings* 59, 2–20. doi:10.1016/j.porgcoat.2007.01.017.

Almeida, J. R., and Vasconcelos, V. (2015). Natural antifouling compounds: Effectiveness in preventing invertebrate settlement and adhesion. *Biotechnol. Adv.* 33, 343–357. doi:10.1016/j.biotechadv.2015.01.013.

Almeida, L. P., and Coolen, J. W. P. (2020). Modelling thickness variations of macrofouling communities on offshore platforms in the Dutch North Sea. *J. Sea Res.* 156, 101836. doi:10.1016/j.seares.2019.101836.

Anthony, K. R. N. (2016). Coral Reefs under Climate Change and Ocean Acidification: Challenges and Opportunities for Management and Policy. *Annu. Rev. Environ. Resour.* 41, 59–81. doi:10.1146/annurev-environ-110615-085610.

Anton, A., Randle, J. L., Garcia, F. C., Rossbach, S., Ellis, J. I., Weinzierl, M., et al. (2020). Differential thermal tolerance between algae and corals may trigger the proliferation of algae in coral reefs. *Glob. Chang. Biol.* 26, 4316–4327. doi:10.1111/gcb.15141.

Arnold, S. N., and Steneck, R. S. (2011). Settling into an increasingly hostile world: The rapidly closing "recruitment window" for corals. *PLoS One* 6. doi:10.1371/journal.pone.0028681.

Arnold, S. N., Steneck, R. S., and Mumby, P. J. (2010). Running the gauntlet: Inhibitory effects of algal turfs on the processes of coral recruitment. *Mar. Ecol. Prog. Ser.* 414, 91–105. doi:10.3354/meps08724.

Baker, A. C., Glynn, P. W., and Riegl, B. (2008). Climate change and coral reef bleaching : An ecological assessment of long-term impacts, recovery trends and future outlook. *Estuar. Coast. Shelf Sci.* 80, 435–471. doi:10.1016/j.ecss.2008.09.003.

Baldwin, D. H., Tatara, C. P., and Scholz, N. L. (2011). Copper-induced olfactory toxicity in salmon and steelhead: Extrapolation across species and rearing environments. *Aquat. Toxicol.* 101, 295–297. doi:10.1016/j.aquatox.2010.08.011.

Bao, V. W. W., Leung, K. M. Y., Qiu, J. W., and Lam, M. H. W. (2011). Acute toxicities of five commonly used antifouling booster biocides to selected subtropical and cosmopolitan marine species. *Mar. Pollut. Bull.* 62, 1147–1151. doi:10.1016/j.marpolbul.2011.02.041.

Bartsch, I., Wiencke, C., Bischof, K., Buchholz, C. M., Buck, B. H., Eggert, A., et al. (2008). The genus *Laminaria sensu lato*: Recent insights and developments. *Eur. J. Phycol.* 43, 1–86. doi:10.1080/09670260701711376.

Bazaka, K., Crawford, R. J., Nazarenko, E. L., and Ivanova, E. P. (2011). Bacterial extracellular polysaccharides. *Adv. Exp. Med. Biol.* 715, 213–226. doi:10.1007/978-94-007-0940-9_13.

Bers, A. V., Diaz, E. R., da Gama, B. A. P., Vieira-Silva, F., Dobretsov, S., Valdivia, N., et al. (2010). Relevance of mytilid shell microtopographies for fouling defence - a global comparison. *Biofouling* 26, 367–377. doi:10.1080/08927011003605888.

Bharati, B. K., and Chatterji, D. (2013). Quorum sensing and pathogenesis: Role of small signalling molecules in bacterial persistence. *Curr. Sci.* 105, 643–656.

Birrell, C. L., McCook, L. J., Willis, B. L., and Diaz-Pulido, G. A. (2008). "Effects of benthic algae on the replenishment of corals and the implications for the resilience of coral reefs," in *Oceanography and Marine Biology: An Annual Review* (CRC Press), 25–63.

Bixler, G. D., and Bhushan, B. (2015). Rice and butterfly wing effect inspired low drag and antifouling surfaces: A review. *Crit. Rev. Solid State Mater. Sci.* 40, 1–37. doi:10.1080/10408436.2014.917368.

Blossey, R. (2003). Self-cleaning surfaces — virtual realities. *Nat. Publ. Gr.* 2, 301–306.

Bongaerts, P., Ridgway, T., Sampayo, E. M., and Hoegh-Guldberg, O. (2010). Assessing the "deep reef refugia" hypothesis: Focus on Caribbean reefs. *Coral Reefs* 29, 309–327. doi:10.1007/s00338-009-0581-x.

Bongaerts, P., Riginos, C., Brunner, R., Englebert, N., Smith, S. R., and Hoegh-Guldberg, O. (2017). Deep reefs are not universal refuges: Reseeding potential varies among coral species. *Sci. Adv.* 3. doi:10.1126/sciadv.1602373.

Bowman, J. P. (2007). Bioactive compound synthetic capacity and ecological significance of marine bacterial genus *Pseudoalteromonas*. *Mar. Drugs* 5, 220–241. doi:10.3390/md504220.

Box, S. J., and Mumby, P. J. (2007). Effect of macroalgal competition on growth and survival of juvenile Caribbean corals. *Mar. Ecol. Prog. Ser.* 342, 139–149.

Braga, C., Hunsucker, K., Gardner, H., and Swain, G. (2020). A novel design to investigate the impacts of UV exposure on marine biofouling. *Appl. Ocean Res.* 101. doi:10.1016/j.apor.2020.102226.

Branda, S. S., Vik, Å., Friedman, L., and Kolter, R. (2005). Biofilms: The matrix revisited. *Trends Microbiol.* 13, 20–26. doi:10.1016/j.tim.2004.11.006.

Bruno, J. F., and Selig, E. R. (2007). Regional decline of coral cover in the Indo-Pacific: Timing, extent, and subregional comparisons. *PLoS One* 2, e711. doi:10.1371/journal.pone.0000711.

Buenau, K. E., Price, N. N., and Nisbet, R. M. (2012). Size dependence, facilitation, and microhabitats mediate space competition between coral and crustose coralline algae in a spatially explicit model. *Ecol. Modell.* 237–238, 23–33. doi:10.1016/j.ecolmodel.2012.04.013.

Burke, L., and Reytar, K. (2011). Reefs at Risk Revisited : Technical Notes on Modeling Threats to the World ' s Coral Reefs Reefs at Risk Project Purpose. 1–19.

Cacciapaglia, C., and van Woesik, R. (2015). Reef-coral refugia in a rapidly changing ocean. *Glob. Chang. Biol.* 21, 2272–2282. doi:10.1111/gcb.12851.

Caldeira, K. (2013). Coral Bleaching: Coral "refugia" amid heating seas. *Nat. Clim. Chang.* 3, 444–445. doi:10.1038/nclimate1888.

Callow, J. A., and Callow, M. E. (2011). Trends in the development of environmentally friendly fouling-resistant marine coatings. *Nat. Commun.* 2. doi:10.1038/ncomms1251.

Campos, B. G. de, Fontes, M. K., Gusso-Choueri, P. K., Marinsek, G. P., Nobre, C. R., Moreno, B. B., et al. (2022). A preliminary study on multi-level biomarkers response of the tropical oy ster *Crassostrea brasiliana* to exposure to the antifouling biocide DCOIT. *Mar. Pollut. Bull.* 174, 113241. doi:10.1016/j.marpolbul.2021.113241.

Cantin, N. E., Negri, A. P., and Willis, B. L. (2007). Photoinhibition from chronic herbicide exposure reduces reproductive output of reef-building corals. *Mar. Ecol. Prog. Ser.* 344, 81–93. doi:10.3354/meps07059.

Carman, M. L., Estes, T. G., Feinberg, A. W., Schumacher, J. F., Wilkerson, W., Wilson, L. H., et al. (2006). Engineered antifouling microtopographies - Correlating wettability with cell attachment. *Biofouling* 22, 11–21. doi:10.1080/08927010500484854.

Carpenter, R. C., and Edmunds, P. J. (2006). Local and regional scale recovery of *Diadema* promotes recruitment of scleractinian corals. *Ecol. Lett.* 9, 268–277. doi:10.1111/j.1461-0248.2005.00866.x.

Castritsi-Catharios, J., Bourdaniotis, N., and Persoone, G. (2007). A new simple method with high precision for determining the toxicity of antifouling paints on brine shrimp larvae (*Artemia*): First results. *Chemosphere* 67, 1127–1132. doi:10.1016/j.chemosphere.2006.11.033.

Chamberland, V. F., Snowden, S., Marhaver, K. L., Petersen, D., and Vermeij, M. J. A. (2017). The reproductive biology and early life ecology of a common Caribbean brain coral, *Diploria labyrinthiformis* (Scleractinia: Faviinae). *Coral Reefs* 36, 83–94. doi:10.1007/s00338-016-1504-2.

Chambers, L. D., Stokes, K. R., Walsh, F. C., and Wood, R. J. K. (2006). Modern approaches to marine antifouling coatings. *Surf. Coatings Technol.* 201, 3642–3652. doi:10.1016/j.surfcoat.2006.08.129.

Chaudhury, M. K., Finlay, J. A., Jun, Y. C., Callow, M. E., and Callow, J. A. (2005). The influence of elastic modulus and thickness on the release of the soft-fouling green alga Ulva linza (syn. *Enteromorpha linza*) from poly(dimethylsiloxane) (PDMS) model networks. *Biofouling* 21, 41–48. doi:10.1080/08927010500044377.

Cheal, A. J., MacNeil, M. A., Emslie, M. J., and Sweatman, H. (2017). The threat to coral reefs from more intense cyclones under climate change. *Glob. Chang. Biol.* 23, 1511–1524. doi:10.1111/gcb.13593.

Chen, L., Au, D. W. T., Hu, C., Peterson, D. R., Zhou, B., and Qian, P. Y. (2017). Identification of Molecular Targets for 4,5-Dichloro-2-n-octyl-4-isothiazolin-3-one (DCOIT) in Teleosts: New Insight into Mechanism of Toxicity. *Environ. Sci. Technol.* 51, 1840–1847. doi:10.1021/acs.est.6b05523.

Chiu, J. M. Y., Zhang, R., Wang, H., Thiyagarajan, V., and Qian, P. Y. (2008). Nutrient effects on intertidal community: From bacteria to invertebrates. *Mar. Ecol. Prog. Ser.* 358, 41–50. doi:10.3354/meps07310.

Cima, F., Ferrari, G., Ferreira, N. G. C., Rocha, R. J. M., Serôdio, J., Loureiro, S., et al. (2013). Preliminary evaluation of the toxic effects of the antifouling biocide Sea-Nine 211™ in the soft coral *Sarcophyton cf. glaucum* (Octocorallia, Alcyonacea) based on PAM fluorometry and biomarkers. *Mar. Environ. Res.* 83, 16–22. doi:10.1016/j.marenvres.2012.10.004.

Cinner, J. E., Mcclanahan, T. R., Graham, N. A. J., Daw, T. M., Maina, J., Stead, S. M., et al. (2012). Vulnerability of coastal communities to key impacts of climate change on coral reef fisheries. *Glob. Environ. Chang.* 22, 12–20. doi:10.1016/j.gloenvcha.2011.09.018.

Cinner, J. E., Pratchett, M. S., Graham, N. A. J., Messmer, V., Fuentes, M. M. P. B., Ainsworth, T., et al. (2016). A framework for understanding climate change impacts on coral reef social–ecological systems. *Reg. Environ. Chang.* 16, 1133–1146. doi:10.1007/s10113-015-0832-z.

da Silva, A. R., Guerreiro, A. da S., Martins, S. E., and Sandrini, J. Z. (2021). DCOIT unbalances the antioxidant defense system in juvenile and adults of the marine bivalve *Amarilladesma mactroides* (Mollusca: Bivalvia). *Comp. Biochem. Physiol. Part - C Toxicol. Pharmacol.* 250, 109169. doi:10.1016/j.cbpc.2021.109169.

Dafforn, K. A., Lewis, J. A., and Johnston, E. L. (2011). Antifouling strategies: History and regulation, ecological impacts and mitigation. *Mar. Pollut. Bull.* 62, 453–465. doi:10.1016/j.marpolbul.2011.01.012.

Dahlem, C., Moran, P. J., and Grant, T. R. (1984). Larval settlement of marine sessile invertebrates on surfaces of different colour and position. *Ocean Sci. Eng.* 9, 225–236.

Dai, H., Sun, T., Han, T., Li, X., Guo, Z., Wang, X., et al. (2021). Interactions between cerium

dioxide nanoparticles and humic acid: Influence of light intensities and molecular weight fractions. *Environ. Res.* 195, 110861. doi:10.1016/j.envres.2021.110861.

Davey, M. E., and O'Toole, G. A. (2000). Microbial biofilms: from ecology to molecular genetics. *Microbiol. Mol. Biol. Rev.* 64, 847–67. Available at: http://www.ncbi.nlm.nih.gov/pubmed/11104821%0Ahttp://www.pubmedcentral.nih.gov/articlerender.fcgi?artid=PMC99016.

De'ath, G., Fabricius, K. E., Sweatman, H., and Puotinen, M. (2012). The 27 – year decline of coral cover on the Great Barrier Reef and its causes. *Proc. Natl. Acad. Sci. U. S. A.* 109, 17995–17999. doi:10.1073/pnas.1208909109.

Detty, M. R., Ciriminna, R., Bright, F. V., and Pagliaro, M. (2014). Environmentally Benign Sol-Gel Antifouling and Foul-Releasing Coatings. *Acc. Chem. Res.* 47, 678–687. doi:10.1021/ar400240n.

Dobretsov, S., Abed, R. M. M., Muthukrishnan, T., Sathe, P., Al-Naamani, L., Queste, B. Y., et al. (2019). Living on the edge: biofilms developing in oscillating environmental conditions. *Biofouling* 34, 1064–1077. doi:10.1080/08927014.2018.1539707.

Dobretsov, S., Sathe, P., Bora, T., Barry, M., Myint, M. T. Z., and Abri, M. Al (2020). Toxicity of Different Zinc Oxide Nanomaterials at 3 Trophic Levels: Implications for Development of Low-Toxicity Antifouling Agents. *Environ. Toxicol. Chem.* 39, 1343–1354. doi:10.1002/etc.4720.

Dobretsov, S. V., Gosselin, L., and Qian, P. Y. (2010). Effects of solar PAR and UV radiation on tropical biofouling communities. *Mar. Ecol. Prog. Ser.* 402, 31–43. doi:10.3354/meps08455.

Donner, S. D. (2009). Coping with commitment: Projected thermal stress on coral reefs under different future scenarios. *PLoS One* 4. doi:10.1371/journal.pone.0005712.

Donner, S. D., Skirving, W. J., Little, C. M., Oppenheimer, M., and Hoegh-Gulberg, O. (2005). Global assessment of coral bleaching and required rates of adaptation under climate change. *Glob. Chang. Biol.* 11, 2251–2265. doi:10.1111/j.1365-2486.2005.01073.x.

Doropoulos, C., Ward, S., Marshell, A., Diaz-Pulido, G., and Mumby, P. J. (2012). Interactions among chronic and acute impacts on coral recruits: The importance of size-escape thresholds. *Ecology* 93, 2131–2138. doi:10.1890/12-0495.1.

Dos Santos, J. V. N., Martins, R., Fontes, M. K., Galv, B., Bruni, M., and Maia, F. (2020). Can Encapsulation of the Biocide DCOIT Affect the Anti-Fouling Efficacy and Toxicity on Tropical Bivalves? *Appl. Sci.* 10, 1–12. doi:8579; doi:10.3390/app10238579.

Dove, S. G., Kline, D. I., Pantos, O., Angly, F. E., and Tyson, G. W. (2013). Future reef decalcification under a business-as-usual CO2 emission scenario. *Proc. Natl. Acad. Sci. U. S. A.* 110, 1–6. doi:10.1073/pnas.1302701110.

Egardt, J., Nilsson, P., and Dahllöf, I. (2017). Sediments indicate the continued use of banned antifouling compounds. *Mar. Pollut. Bull.* 125, 282–288. doi:10.1016/j.marpolbul.2017.08.035.

Erwin, P. M., and Szmant, A. M. (2010). Settlement induction of *Acropora palmata* planulae by a GLW-amide neuropeptide. *Coral Reefs* 29, 929–939. doi:10.1007/s00338-010-0634-1.

Fang, J. K. H., Mello-Athayde, M. A., Schönberg, C. H. L., Kline, D. I., Hoegh-Guldberg, O., and Dove, S. (2013). Sponge biomass and bioerosion rates increase under ocean warming and acidification. *Glob. Chang. Biol.* 19, 3581–3591. doi:10.1111/gcb.12334.

Fang, J. K. H., Schönberg, C. H. L., Mello-Athayde, M. A., Hoegh-Guldberg, O., and Dove, S. (2014). Effects of ocean warming and acidification on the energy budget of an excavating sponge. *Glob. Chang. Biol.* 20, 1043–1054. doi:10.1111/gcb.12369.

Ferreira, V., Pavlaki, M. D., Martins, R., Monteiro, M. S., Maia, F., Tedim, J., et al. (2021). Effects of nanostructure antifouling biocides towards a coral species in the context of

global changes. *Sci. Total Environ.* 799, 149324. doi:10.1016/j.scitotenv.2021.149324.
Fitridge, I., Dempster, T., Guenther, J., and de Nys, R. (2012). The impact and control of biofouling in marine aquaculture: A review. *Biofouling* 28, 649–669. doi:10.1080/08927014.2012.700478.
Fong, J., Lim, Z. W., Bauman, A. G., Valiyaveettil, S., Liao, L. M., Yip, Z. T., et al. (2019). Allelopathic effects of macroalgae on *Pocillopora acuta* coral larvae. *Mar. Environ. Res.* 151. doi:10.1016/j.marenvres.2019.06.007.
Fonseca, V. B., Guerreiro, A. da S., Vargas, M. A., and Sandrini, J. Z. (2020). Effects of DCOIT (4,5-dichloro-2-octyl-4-isothiazolin-3-one) to the haemocytes of mussels *Perna perna*. *Comp. Biochem. Physiol. Part - C Toxicol. Pharmacol.* 232, 108737. doi:10.1016/j.cbpc.2020.108737.
Frieler, K., Meinshausen, M., Golly, A., Mengel, M., Lebek, K., Donner, S. D., et al. (2013). Limiting global warming to 2C is unlikely to save most coral reefs. *Nat. Clim. Chang.* 3, 165–170. doi:10.1038/nclimate1674.
Gardner, T. A., Côté, I. M., Gill, J. A., Grant, A., and Watkinson, A. R. (2005). Hurricanes and Caribbean Coral Reefs: Impacts, recovery patterns, and role in long-term decline. *Ecology* 86, 174–184.
Garrett, T. R., Bhakoo, M., and Zhang, Z. (2008). Bacterial adhesion and biofilms on surfaces. *Prog. Nat. Sci.* 18, 1049–1056. doi:10.1016/j.pnsc.2008.04.001.
GEF-UNDP-IMO GloFouling Partnerships Project and GIA for Marine Biosafety (2022). Analysing the Impact of Marine Biofouling on the Energy Efficiency of Ships and the GHG Abatement Potential of Biofouling Management Measure.
Graham, N. A. J. (2014). Habitat complexity: Coral structural loss leads to fisheries declines. *Curr. Biol.* 24, R359–R361. doi:10.1016/j.cub.2014.03.069.
Graham, N. A. J., Jennings, S., MacNeil, M. A., Mouillot, D., and Wilson, S. K. (2015). Predicting climate-driven regime shifts versus rebound potential in coral reefs. *Nature* 518, 94–97. doi:10.1038/nature14140.
Grasso, L. C., Negri, A. P., Fôret, S., Saint, R., Hayward, D. C., Miller, D. J., et al. (2011). The biology of coral metamorphosis: Molecular responses of larvae to inducers of settlement and metamorphosis. *Dev. Biol.* 353, 411–419. doi:10.1016/j.ydbio.2011.02.010.
Gutner-Hoch, E., Martins, R., Oliveira, T., Maia, F., Soares, A., Loureiro, S., et al. (2018). Antimacrofouling Efficacy of Innovative Inorganic Nanomaterials Loaded with Booster Biocides. *J. Mar. Sci. Eng.* 6, 6. doi:10.3390/jmse6010006.
Hall-Stoodley, L., Costerton, J. W., and Stoodley, P. (2004). Bacterial biofilms: From the natural environment to infectious diseases. *Nat. Rev. Microbiol.* 2, 95–108. doi:10.1038/nrmicro821.
Hall-Stoodley, L., and Stoodley, P. (2009). Evolving concepts in biofilm infections. *Cell. Microbiol.* 11, 1034–1043. doi:10.1111/j.1462-5822.2009.01323.x.
Halpern, B. S., Frazier, M., Potapenko, J., Casey, K. S., Koenig, K., Longo, C., et al. (2015). Spatial and temporal changes in cumulative human impacts on the world's ocean. *Nat. Commun.*, 1–7. doi:10.1038/ncomms8615.
Harrington, L., Fabricius, K., De'ath, G., and Negri, A. (2004). Recognition and Selection of Settlement Substrata Determine Post-Settlement Survival in Corals. *Ecology* 85, 3428–3437. Available at: https://pdfs.semanticscholar.org/b6b9/8971ac0350e1f014c5fb251f5c111529c662.pdf.
Hartog, A. F., Stoll, B., Jochum, K. P., Wever, R., Natalio, F., Andre, R., et al. (2012). Vanadium pentoxide nanoparticles mimic vanadium haloperoxidases and thwart biofilm formation. *Nat. Nanotechnol.*, 1–6. doi:10.1038/nnano.2012.91.
Hauri, C., Fabricius, K. E., Schaffelke, B., and Humphrey, C. (2010). Chemical and physical environmental conditions underneath mat- and canopy-forming macroalgae, and their

effects on understorey corals. *PLoS One* 5, 1–9. doi:10.1371/journal.pone.0012685.
Hausner, M., and Wuertz, S. (1999). High rates of conjugation in bacterial biofilms as determined by quantitative in situ analysis. *Appl. Environ. Microbiol.* 65, 3710–3713. doi:10.1128/aem.65.8.3710-3713.1999.
Hentzer, M., Teitzel, G. M., Balzer, G. J., Heydorn, A., Molin, S., Givskov, M., et al. (2001). Alginate overproduction affects *Pseudomonas aeruginosa* biofilm structure and function. *J. Bacteriol.* 183, 5395–5401. doi:10.1128/JB.183.18.5395-5401.2001.
Herget, K., Frerichs, H., Pfitzner, F., Tahir, M. N., and Tremel, W. (2018). Functional Enzyme Mimics for Oxidative Halogenation Reactions that Combat Biofilm Formation. *Adv. Mater.* 30, 1–28. doi:10.1002/adma.201707073.
Herget, K., Hubach, P., Pusch, S., Deglmann, P., Götz, H., Gorelik, T. E., et al. (2017). Haloperoxidase Mimicry by CeO2-x Nanorods Combats Biofouling. *Adv. Mater.* 29, 1–8. doi:10.1002/adma.201603823.
Heyward, A. J., and Negri, A. P. (1999). Natural inducers for coral larval metamorphosis. *Coral Reefs* 18, 273–279. doi:10.1007/s003380050193.
Hoegh-Guldberg, O. (1999). Climate change, coral bleaching and the future of the world's coral reefs. *Mar. Freshw. Res.* 50, 839. doi:10.1071/MF99078.
Hoegh-Guldberg, O. (2014a). Coral reef sustainability through adaptation: Glimmer of hope or persistent mirage? *Curr. Opin. Environ. Sustain.* 7, 127–133. doi:10.1016/j.cosust.2014.01.005.
Hoegh-Guldberg, O. (2014b). Coral reefs in the anthropocene: Persistence or the end of the line? *Geol. Soc. Spec. Publ.* 395, 167–183. doi:10.1144/SP395.17.
Hoegh-Guldberg, O., Jacob, D., Taylor, M., Bindi, M., Brown, S., Camilloni, I., et al. (2018). "Impacts of 1.5°C of Global Warming on Natural and Human Systems," in *Global Warming of 1.5°C. An IPCC Special Report on the impacts of global warming of 1.5°C above pre-industrial levels and related global greenhouse gas emission pathways, in the context of strengthening the global response to the threat of climate change,* eds. V. Masson-Delmotte, P. Zhai, H.-O. Pörtner, D. Roberts, J. Skea, P. R. Shukla, et al. (Cambridge, UK and New York, NY, USA: Cambridge University Press), 175–312. doi:10.1017/9781009157940.005.
Holmström, C., Egan, S., Franks, A., McCloy, S., and Kjelleberg, S. (2002). Antifouling activities expressed by marine surface associated *Pseudoalteromonas* species. *FEMS Microbiol. Ecol.* 41, 47–58. doi:10.1016/S0168-6496(02)00239-8.
Holmström, C., James, S., Egan, S., and Kjelleberg, S. (1996). Inhibition of common fouling organisms by marine bacterial isolates with special reference to the role of pigmented bacteria. *Biofouling* 10, 251–259. doi:10.1080/08927019609386284.
Hölscher, T., Bartels, B., Lin, Y. C., Gallegos-Monterrosa, R., Price-Whelan, A., Kolter, R., et al. (2015). Motility, Chemotaxis and Aerotaxis Contribute to Competitiveness during Bacterial Pellicle Biofilm Development. *J. Mol. Biol.* 427, 3695–3708. doi:10.1016/j.jmb.2015.06.014.
Holstein, D. M., Paris, C. B., Vaz, A. C., and Smith, T. B. (2016). Modeling vertical coral connectivity and mesophotic refugia. *Coral Reefs* 35, 23–37. doi:10.1007/s00338-015-1339-2.
Hori, K., and Matsumoto, S. (2010). Bacterial adhesion: From mechanism to control. *Biochem. Eng. J.* 48, 424–434. doi:10.1016/j.bej.2009.11.014.
Hughes, T. P., Barnes, M. L., Bellwood, D. R., Cinner, J. E., Cumming, G. S., Jackson, J. B. C., et al. (2017a). Coral reefs in the Anthropocene. *Nature* 546. doi:10.1038/nature22901.
Hughes, T. P., Kerry, J. T., Álvarez-Noriega, M., Álvarez-Romero, J. G., Anderson, K. D., Baird, A. H., et al. (2017b). Global warming and recurrent mass bleaching of corals. *Nature* 543, 373–377. doi:10.1038/nature21707.

Hunsucker, J. T., Hunsucker, K. Z., Gardner, H., and Swain, G. (2016). Influence of hydrodynamic stress on the frictional drag of biofouling communities. *Biofouling* 32, 1209–1221. doi:10.1080/08927014.2016.1242724.

Iwao, K., Fujisawa, T., and Hatta, M. (2002). A cnidarian neuropeptide of the GLWamide family induces metamorphosis of reef-building corals in the genus *Acropora*. *Coral Reefs* 21, 127–129. doi:10.1007/s00338-002-0219-8.

Jacobson, A. H., and Willingham, G. L. (2000). Sea-nine antifoulant: An environmentally acceptable alternative to organotin antifoulants. *Sci. Total Environ.* 258, 103–110. doi:10.1016/S0048-9697(00)00511-8.

Jorissen, H., Baumgartner, C., Steneck, R. S., and Nugues, M. M. (2020). Contrasting effects of crustose coralline algae from exposed and subcryptic habitats on coral recruits. *Coral Reefs* 39, 1767–1778. doi:10.1007/s00338-020-02002-9.

Jorissen, H., Galand, P. E., Bonnard, I., Meiling, S., Raviglione, D., Meistertzheim, A. L., et al. (2021). Coral larval settlement preferences linked to crustose coralline algae with distinct chemical and microbial signatures. *Sci. Rep.* 11, 1–11. doi:10.1038/s41598-021-94096-6.

Kalia, V. C. (2018). *Biotechnological applications of quorum sensing inhibitors*. doi:10.1007/978-981-10-9026-4.

Karcher, D. B., Roth, F., Carvalho, S., El-Khaled, Y. C., Tilstra, A., Kürten, B., et al. (2020). Nitrogen eutrophication particularly promotes turf algae in coral reefs of the central Red Sea. *PeerJ* 2020, 1–25. doi:10.7717/peerj.8737.

Karlsson, J., Ytreberg, E., and Eklund, B. (2010). Toxicity of anti-fouling paints for use on ships and leisure boats to non-target organisms representing three trophic levels. *Environ. Pollut.* 158, 681–687. doi:10.1016/j.envpol.2009.10.024.

Kennedy, E. V., Perry, C. T., Halloran, P. R., Iglesias-Prieto, R., Schönberg, C. H. L., Wisshak, M., et al. (2013a). Avoiding coral reef functional collapse requires local and global action. *Curr. Biol.* 23, 912–918. doi:10.1016/j.cub.2013.04.020.

Kennedy, E. V, Perry, C. T., Halloran, P. R., Iglesias-prieto, R., Scho, C. H. L., Wisshak, M., et al. (2013b). Report Avoiding Coral Reef Functional Collapse Requires Local and Global Action. 912–918. doi:10.1016/j.cub.2013.04.020.

Keppel, G., and Kavousi, J. (2015). Effective climate change refugia for coral reefs. *Glob. Chang. Biol.* 21, 2829–2830. doi:10.1111/gcb.12936.

Kersting, D. K., Cebrian, E., Verdura, J., and Ballesteros, E. (2017). A new *Cladocora caespitosa* population with unique ecological traits. *Mediterr. Mar. Sci.* 18, 38–42. doi:10.12681/mms.1955.

King, A. D., Karoly, D. J., and Henley, B. J. (2017). Australian climate extremes at 1.5 °C and 2 °C of global warming. *Nat. Clim. Chang.* 7, 412–416. doi:10.1038/nclimate3296.

Kirschner, C. M., and Brennan, A. B. (2012). Bio-inspired antifouling strategies. *Annu. Rev. Mater. Res.* 42, 211–229. doi:10.1146/annurev-matsci-070511-155012.

Kline, D. I., Teneva, L., Schneider, K., Miard, T., Chai, A., Marker, M., et al. (2012). A short-term in situ CO2 enrichment experiment on Heron Island (GBR). *Sci. Rep.* 2, 1–9. doi:10.1038/srep00413.

Knowlton, N., and Jackson, J. B. C. (2008). Shifting baselines, local impacts, and global change on coral reefs. *PLoS Biol.* 6, 0215–0220. doi:10.1371/journal.pbio.0060054.

Koppel, D. J., Gissi, F., Adams, M. S., King, C. K., and Jolley, D. F. (2017). Chronic toxicity of five metals to the polar marine microalga *Cryothecomonas armigera* – Application of a new bioassay. *Environ. Pollut.* 228, 211–221. doi:10.1016/j.envpol.2017.05.034.

Korschelt, K., Schwidetzky, R., Pfitzner, F., Strugatchi, J., Schilling, C., Von Der Au, M., et al. (2018a). CeO2-: X nanorods with intrinsic urease-like activity. *Nanoscale* 10, 13074–13082. doi:10.1039/c8nr03556c.

Korschelt, K., Tahir, M. N., and Tremel, W. (2018b). A Step into the Future: Applications of

Nanoparticle Enzyme Mimics. *Chem. - A Eur. J.* 24, 9703–9713. doi:10.1002/chem.201800384.

Körstgens, V., Flemming, H. C., Wingender, J., and Borchard, W. (2001). Influence of calcium ions on the mechanical properties of a model biofilm of mucoid *Pseudomonas aeruginosa*. *Water Sci. Technol.* 43, 49–57. doi:10.2166/wst.2001.0338.

Kumar, A., Al-Jumaili, A., Bazaka, O., Ivanova, E. P., Levchenko, I., Bazaka, K., et al. (2021). Functional nanomaterials, synergisms, and biomimicry for environmentally benign marine antifouling technology. *Mater. Horizons* 8, 3201–3238. doi:10.1039/d1mh01103k.

Lawrence, J. R., Swerhone, G. D. W., Kuhlicke, U., and Neu, T. R. (2016). In situ evidence for metabolic and chemical microdomains in the structured polymer matrix of bacterial microcolonies . *FEMS Microbiol. Ecol.* 92, fiw183. doi:10.1093/femsec/fiw183.

Lee, S., and Kang, S. (2016). Influences of zeta potential, water absorption and surface roughness of porous ceramics on marine bio-fouling. *Int. J. Bio-Science Bio-Technology* 8, 35–44. doi:10.14257/ijbsbt.2016.8.2.04.

Lee, S. W., and Trott, L. B. (1973). Marine succession of fouling organisms in Hong Kong, with a comparison of woody substrates and common, locally-available, antifouling paints. *Mar. Biol.* 20, 101–108. doi:10.1007/BF00351449.

Lewis, J. A. (2018). Battling biofouling with, and without, biocides. *Chem. Aust.*, 26–29. Available at: https://search.informit.org/doi/10.3316/informit.659357711949386.

Linares, C., Cebrian, E., and Coma, R. (2012). Effects of turf algae on recruitment and juvenile survival of gorgonian corals. *Mar. Ecol. Prog. Ser.* 452, 81–88. doi:10.3354/meps09586.

Littler, M. M., Littler, D. S., and Brooks, B. L. (2006). Harmful algae on tropical coral reefs: Bottom-up eutrophication and top-down herbivory. *Harmful Algae* 5, 565–585. doi:10.1016/j.hal.2005.11.003.

Madsen, J. S., Burmølle, M., Hansen, L. H., and Sørensen, S. J. (2012). The interconnection between biofilm formation and horizontal gene transfer. *FEMS Immunol. Med. Microbiol.* 65, 183–195. doi:10.1111/j.1574-695X.2012.00960.x.

Maia, F., Silva, A. P., Fernandes, S., Cunha, A., Almeida, A., Tedim, J., et al. (2015). Incorporation of biocides in nanocapsules for protective coatings used in maritime applications. *Chem. Eng. J.* 270, 150–157. doi:10.1016/j.cej.2015.01.076.

Maia, F., Tedim, J., Lisenkov, A. D., Salak, A. N., Zheludkevich, M. L., and Ferreira, M. G. S. (2012). Silica nanocontainers for active corrosion protection. *Nanoscale* 4, 1287–1298. doi:10.1039/c2nr11536k.

Martins, R., Oliveira, T., Santos, C., Kuznetsova, A., Ferreira, V., Avelelas, F., et al. (2017). Effects of a novel anticorrosion engineered nanomaterial on the bivalve: *Ruditapes philippinarum*. *Environ. Sci. Nano* 4, 1064–1076. doi:10.1039/c6en00630b.

Martins, S. E., Fillmann, G., Lillicrap, A., and Thomas, K. V (2018). Review: Ecotoxicity of organic and organo-metallic antifouling co-biocides and implications for environmental hazard and risk assessments in aquatic ecosystems. *Biofouling* 34, 34–52. doi:10.1080/08927014.2017.1404036.

McCook, L. J., Jompa, J., and Diaz-Pulido, G. (2001). Competition between corals and algae on coral reefs: A review of evidence and mechanisms. *Coral Reefs* 19, 400–417. doi:10.1007/s003380000129.

Mi, B., and Elimelech, M. (2008). Chemical and physical aspects of organic fouling of forward osmosis membranes. *J. Memb. Sci.* 320, 292–302. doi:10.1016/j.memsci.2008.04.036.

Moberg, F., and Folke, C. (1999). Ecological goods and services of coral reef ecosystems. *Ecol. Econ.* 29, 215–233. doi:10.1016/S0921-8009(99)00009-9.

Moeller, M., Nietzer, S., and Schupp, P. J. (2019). Neuroactive compounds induce larval settlement in the scleractinian coral *Leptastrea purpurea*. *Sci. Rep.* 9, 1–9. doi:10.1038/s41598-019-38794-2.

Molino, P. J., Childs, S., Eason Hubbard, M. R., Carey, J. M., Burgman, M. A., and Wetherbee, R. (2009). Development of the primary bacterial microfouling layer on antifouling and fouling release coatings in temperate and tropical environments in Eastern Australia. *Biofouling* 25, 149–162. doi:10.1080/08927010802592917.

Moon, Y. S., Kim, M., Hong, C. P., Kang, J. H., and Jung, J. H. (2019). Overlapping and unique toxic effects of three alternative antifouling biocides (Diuron, Irgarol 1051 ® , Sea-Nine 211 ® ) on non-target marine fish. *Ecotoxicol. Environ. Saf.* 180, 23–32. doi:10.1016/j.ecoenv.2019.04.070.

Morse, A. N. C., Iwao, K., Baba, M., Shimoike, K., Hayashibara, T., and Omori, M. (1996). An ancient chemosensory mechanism brings new life to coral reefs. *Biol. Bull.* 191, 149–154. doi:10.2307/1542917.

Müller, W. E. G., Wang, X., Proksch, P., Perry, C. C., Osinga, R., Gardères, J., et al. (2013). Principles of Biofouling Protection in Marine Sponges: A Model for the Design of Novel Biomimetic and Bio-inspired Coatings in the Marine Environment? *Mar. Biotechnol.* 15, 375–398. doi:10.1007/s10126-013-9497-0.

Nayar, S., Goh, B. P. L., and Chou, L. M. (2005). Settlement of marine periphytic algae in a tropical estuary. *Estuar. Coast. Shelf Sci.* 64, 241–248. doi:10.1016/j.ecss.2005.01.016.

Negri, A., and Marshall, P. (2009). TBT contamination of remote marine environments: Ship groundings and ice-breakers as sources of organotins in the Great Barrier Reef and Antarctica. *J. Environ. Manage.* 90. doi:10.1016/j.jenvman.2008.06.009.

Negri, A. P., Flores, F., Röthig, T., and Uthicke, S. (2011). Herbicides increase the vulnerability of corals to rising sea surface temperature. *Limnol. Oceanogr.* 56, 471–485. doi:10.4319/lo.2011.56.2.0471.

Negri, A. P., and Heyward, A. J. (2001). Inhibition of coral fertilisation and larval metamorphosis by tributyltin and copper. *Mar. Environ. Res.* 51, 17–27. doi:10.1016/S0141-1136(00)00029-5.

Negri, A. P., Smith, L. D., Webster, N. S., and Heyward, A. J. (2002). Understanding ship-grounding impacts on a coral reef: Potential effects of anti-foulant paint contamination on coral recruitment. *Mar. Pollut. Bull.* 44, 111–117. doi:10.1016/S0025-326X(01)00128-X.

Negri, A. P., Webster, N. S., Hill, R. T., and Heyward, A. J. (2001). Metamorphosis of broadcast spawning corals in response to bacteria isolated from crustose algae. *Mar. Ecol. Prog. Ser.* 223, 121–131.

Negri, A., Vollhardt, C., Humphrey, C., Heyward, A., Jones, R., Eaglesham, G., et al. (2005). Effects of the herbicide diuron on the early life history stages of coral. *Mar. Pollut. Bull.* 51, 370–383. doi:10.1016/j.marpolbul.2004.10.053.

Niemann, H., Hagenow, J., Chung, M.-Y., Hellio, C., Weber, H., and Proksch, P. (2015). SAR of Sponge-Inspired Hemibastadin Congeners Inhibiting Blue Mussel PhenolOxidase. *Mar. Drugs* 13, 3061–3071. doi:10.3390/md13053061.

Nir, S., and Reches, M. (2016). Bio-inspired antifouling approaches: The quest towards non-toxic and non-biocidal materials. *Curr. Opin. Biotechnol.* 39, 48–55. doi:10.1016/j.copbio.2015.12.012.

Nugues, M. M., Smith, G. W., Van Hooidonk, R. J., Seabra, M. I., and Bak, R. P. M. (2004). Algal contact as a trigger for coral disease. *Ecol. Lett.* 7, 919–923. doi:10.1111/j.1461-0248.2004.00651.x.

O'Toole, G. A., and Kolter, R. (1998). Flagellar and twitching motility are necessary for *Pseudomonas aeruginosa* biofilm development. *Mol. Microbiol.* 30, 295–304. doi:10.1046/j.1365-2958.1998.01062.x.

Oliveira, H., Boas, D. V., Mesnage, S., Kluskens, L. D., Lavigne, R., Sillankorva, S., et al. (2016). Structural and enzymatic characterization of ABgp46, a novel phage endolysin with broad anti-gram-negative bacterial activity. *Front. Microbiol.* 7, 1–9.

doi:10.3389/fmicb.2016.00208.
Otani, M., Oumi, T., Uwai, S., Hanyuda, T., Prabowo, R. E., Yamaguchi, T., et al. (2007). Occurrence and diversity of barnacles on international ships visiting Osaka Bay, Japan, and the risk of their introduction. *Biofouling* 23, 277–286. doi:10.1080/08927010701315089.
Patil, S. A., Harnisch, F., Koch, C., Hübschmann, T., Fetzer, I., Carmona-Martínez, A. A., et al. (2011). Electroactive mixed culture derived biofilms in microbial bioelectrochemical systems: The role of pH on biofilm formation, performance and composition. *Bioresour. Technol.* 102, 9683–9690. doi:10.1016/j.biortech.2011.07.087.
Pechook, S., and Pokroy, B. (2012). Self-assembling, bioinspired wax crystalline surfaces with time-dependent wettability. *Adv. Funct. Mater.* 22, 745–750. doi:10.1002/adfm.201101721.
Pendleton, L., Comte, A., Langdon, C., Ekstrom, J. A., Cooley, R., Suatoni, L., et al. (2016). Coral Reefs and People in a High-CO 2 World : Where Can Science Make a Difference to People ? 1–21. doi:10.1371/journal.pone.0164699.
Penru, Y., Guastalli, A. R., Esplugas, S., and Baig, S. (2013). Disinfection of Seawater: Application of UV and Ozone. *Ozone Sci. Eng.* 35, 63–70. doi:10.1080/01919512.2012.722050.
Pettengill, J. B., Wendt, D. E., Schug, M. D., and Hadfield, M. G. (2007). Biofouling likely serves as a major mode of dispersal for the polychaete tubeworm *Hydroides elegans* as inferred from microsatellite loci. *Biofouling* 23, 161–169. doi:10.1080/08927010701218952.
Picioreanu, C., Head, I. M., Katuri, K. P., van Loosdrecht, M. C. M., and Scott, K. (2007). A computational model for biofilm-based microbial fuel cells. *Water Res.* 41, 2921–2940. doi:10.1016/j.watres.2007.04.009.
Piola, R. F., and Johnston, E. L. (2008). The potential for translocation of marine species via small-scale disruptions to antifouling surfaces. *Biofouling* 24, 145–155. doi:10.1080/08927010801930480.
Piola, R., Salters, B., Grandison, C., Ciacic, M., and Hietbrink, R. (2016). Assessing the use of Low Voltage UV-light Emitting Miniature LEDs for Marine Biofouling Control.
Plaisance, L., Caley, M. J., Brainard, R. E., and Knowlton, N. (2011). The diversity of coral reefs: What are we missing? *PLoS One* 6. doi:10.1371/journal.pone.0025026.
Pollock, F. J., Katz, S. M., van de Water, J. A. J. M., Davies, S. W., Hein, M., Torda, G., et al. (2017). Coral larvae for restoration and research: a large-scale method for rearing *Acropora millepora* larvae, inducing settlement, and establishing symbiosis. *PeerJ* 5, e3732. doi:10.7717/peerj.3732.
Poloczanska, E. S., and Butler, A. J. (2010). "Biofouling and Climate Change," in *Biofouling*, 333–347. doi:10.1002/9781444315462.ch23.
Pratt, L. A., and Kolter, R. (1999). Genetic analyses of bacterial biofilm formation. *Curr. Opin. Microbiol.* 2, 598–603. doi:10.1016/S1369-5274(99)00028-4.
Reyes-Nivia, C., Diaz-Pulido, G., and Dove, S. (2014). Relative roles of endolithic algae and carbonate chemistry variability in the skeletal dissolution of crustose coralline algae. *Biogeosciences* 11, 4615–4626. doi:10.5194/bg-11-4615-2014.
Reyes-Nivia, C., Diaz-Pulido, G., Kline, D., Hoegh-Guldberg, O., and Dove, S. (2013). Ocean acidification and warming scenarios increase microbioerosion of coral skeletons. *Glob. Chang. Biol.* 19, 1919–1929. doi:10.1111/gcb.12158.
Ricardo, G. F., Jones, R. J., Nordborg, M., and Negri, A. P. (2017). Settlement patterns of the coral *Acropora millepora* on sediment-laden surfaces. *Sci. Total Environ.* 609, 277–288. doi:10.1016/j.scitotenv.2017.07.153.
Rittschof, D. (2000). Natural product antifoulants: One perspective on the challenges related to

coatings development. *Biofouling* 15, 119–127. doi:10.1080/08927010009386303.
Rose, R. K., and Turner, S. J. (1998). Fluoride-Induced Enhancement of Diffusion in Streptococcal Model Plaque Biofilms. *Caries Res.* 32, 227–232. doi:10.1159/000016457.
Salta, M., Wharton, J. A., Blache, Y., Stokes, K. R., and Briand, J. F. (2013). Marine biofilms on artificial surfaces: Structure and dynamics. *Environ. Microbiol.* 15, 2879–2893. doi:10.1111/1462-2920.12186.
Sánchez-Lozano, I., Hernández-Guerrero, C. J., Muñoz-Ochoa, M., and Hellio, C. (2019). Biomimetic approaches for the development of new antifouling solutions: Study of incorporation of macroalgae and sponge extracts for the development of new environmentally-friendly coatings. *Int. J. Mol. Sci.* 20, 1–18. doi:10.3390/ijms20194863.
Schleussner, C. F., Lissner, T. K., Fischer, E. M., Wohland, J., Perrette, M., Golly, A., et al. (2016). Differential climate impacts for policy-relevant limits to global warming: The case of 1.5 °C and 2 °C. *Earth Syst. Dyn.* 7, 327–351. doi:10.5194/esd-7-327-2016.
Schultz, M. P. (2007). Effects of coating roughness and biofouling on ship resistance and powering. *Biofouling* 23, 331–341. doi:10.1080/08927010701461974.
Schultz, M. P., Bendick, J. A., Holm, E. R., and Hertel, W. M. (2011). Economic impact of biofouling on a naval surface ship. *Biofouling* 27, 87–98. doi:10.1080/08927014.2010.542809.
Silva, V., Silva, C., Soares, P., Garrido, E. M., Borges, F., and Garrido, J. (2020). Isothiazolinone Biocides: Chemistry, Biological, and Toxicity Profiles. *Molecules* 25, 10.3390/molecules25040991. doi:10.3390/molecules25040991.
Sivadon, P., Barnier, C., Urios, L., and Grimaud, R. (2019). Biofilm formation as a microbial strategy to assimilate particulate substrates. *Environ. Microbiol. Rep.* 11, 749–764. doi:10.1111/1758-2229.12785.
Smith, L. D., Negri, A. P., Philipp, E., Webster, N. S., and Heyward, A. J. (2003). The effects of antifoulant-paint-contaminated sediments on coral recruits and branchlets. *Mar. Biol.* 143, 651–657. doi:10.1007/s00227-003-1107-7.
Sneed, J. M., Sharp, K. H., Ritchie, K. B., and Paul, V. J. (2014). The chemical cue tetrabromopyrrole from a biofilm bacterium induces settlement of multiple Caribbean corals. *Proc. R. Soc. B Biol. Sci.* 281, 1–9. doi:10.1098/rspb.2013.3086.
Soliman, Y. A. A., Brahim, A. M., Moustafa, A. H., and Hamed, M. A. F. (2017). Antifouling evaluation of extracts from Red Sea soft corals against primary biofilm and biofouling. *Asian Pac. J. Trop. Biomed.* 7, 991–997. doi:10.1016/j.apjtb.2017.09.016.
Spalding, M. D., and Brown, B. E. (2015). Warm-water coral refs and climate change. *Science* 350, 769–771. doi:10.1126/science.aad0349.
Spalding, M. D., and Grenfell, A. M. (1997). New estimates of global and regional coral reef areas. *Coral Reefs* 16, 225–230. doi:10.1007/s003380050078.
Spalding, M. D., Ruffo, S., Lacambra, C., Meliane, I., Hale, L. Z., Shepard, C. C., et al. (2014). The role of ecosystems in coastal protection: Adapting to climate change and coastal hazards. *Ocean Coast. Manag.* 90, 50–57. doi:10.1016/j.ocecoaman.2013.09.007.
Su, Y., Li, H., Xie, J., Xu, C., Dong, Y., Han, F., et al. (2019). Toxicity of 4,5-dichloro-2-n-octyl-4-isothiazolin-3-one (DCOIT) in the marine decapod *Litopenaeus vannamei*. *Environ. Pollut.* 251, 708–716. doi:10.1016/j.envpol.2019.05.030.
Tebben, J., Guest, J. R., Sin, T. M., Steinberg, P. D., and Harder, T. (2014). Corals like it waxed: Paraffin-based antifouling technology enhances coral spat survival. *PLoS One* 9, 1–8. doi:10.1371/journal.pone.0087545.
Tebben, J., Motti, C. A., Siboni, N., Tapiolas, D. M., Negri, A. P., Schupp, P. J., et al. (2015). Chemical mediation of coral larval settlement by crustose coralline algae. *Sci. Rep.* 5, 1–11. doi:10.1038/srep10803.
Tebben, J., Tapiolas, D. M., Motti, C. A., Abrego, D., Negri, A. P., Blackall, L. L., et al. (2011).

Induction of larval metamorphosis of the coral *Acropora millepora* by tetrabromopyrrole isolated from a *Pseudoalteromonas* bacterium. *PLoS One* 6, 1–8. doi:10.1371/journal.pone.0019082.

Tian, L., Yin, Y., Jin, H., Bing, W., Jin, E., Zhao, J., et al. (2020). Novel marine antifouling coatings inspired by corals. *Mater. Today Chem.* 17, 100294. doi:10.1016/j.mtchem.2020.100294.

Tran, C., and Hadfield, M. G. (2011). Larvae of *Pocillopora damicornis* (Anthozoa) settle and metamorphose in response to surface-biofilm bacteria. *Mar. Ecol. Prog. Ser.* 433, 85–96. doi:10.3354/meps09192.

Van Hooidonk, R., and Huber, M. (2012). Effects of modeled tropical sea surface temperature variability on coral reef bleaching predictions. *Coral Reefs* 31, 121–131. doi:10.1007/s00338-011-0825-4.

Van Hooidonk, R., Maynard, J. A., and Planes, S. (2013). Temporary refugia for coral reefs in a warming world. *Nat. Clim. Chang.* 3, 508–511. doi:10.1038/nclimate1829.

Van Hooidonk, R., Maynard, J., Tamelander, J., Gove, J., Ahmadia, G., Raymundo, L., et al. (2016). Local-scale projections of coral reef futures and implications of the Paris Agreement. *Sci. Rep.* 6, 1–8. doi:10.1038/srep39666.

Vermeij, M. J. A., and Sandin, S. A. (2008). Density-dependent settlement and mortality structure the earliest life phases of a coral population. *Ecology* 89, 1994–2004. doi:10.1890/07-1296.1.

Vermeij, M. J. A., Smith, J. E., Smith, C. M., Vega Thurber, R., and Sandin, S. A. (2009). Survival and settlement success of coral planulae: Independent and synergistic effects of macroalgae and microbes. *Oecologia* 159, 325–336. doi:10.1007/s00442-008-1223-7.

Vinagre, P. A., Simas, T., Cruz, E., Pinori, E., and Svenson, J. (2020). Marine biofouling: A European database for the marine renewable energy sector. *J. Mar. Sci. Eng.* 8. doi:10.3390/JMSE8070495.

Wahl, M. (1989). Marine epibiosis. I. Fouling and antifouling: some basic aspects. *Mar. Ecol. Prog. Ser.* 58, 175–189. doi:10.3354/meps058175.

Wang, N., Li, W., Ren, Y., Duan, J., Zhai, X., Guan, F., et al. (2021). Investigating the properties of nano core-shell CeO2@C as haloperoxidase mimicry catalyst for antifouling applications. *Colloids Surfaces A Physicochem. Eng. Asp.* 608, 125592. doi:10.1016/j.colsurfa.2020.125592.

Wang, T., Flint, S., and Palmer, J. (2019). Magnesium and calcium ions: roles in bacterial cell attachment and biofilm structure maturation. *Biofouling* 35, 959–974. doi:10.1080/08927014.2019.1674811.

Waters, C. M., and Bassler, B. L. (2005). Quorum Sensing: Cell-to-Cell Communication in Bacteria. *Annu. Rev. Cell Dev. Biol.* 21, 319–346. doi:10.1146/annurev.cellbio.21.012704.131001.

Webster, N. S., Smith, L. D., Heyward, A. J., Watts, J. E. M., Webb, R. I., Blackall, L. L., et al. (2004). Metamorphosis of a scleractinian coral in response to microbial biofilms. *Appl. Environ. Microbiol.* 70, 1213–1221. doi:10.1128/AEM.70.2.1213.

Webster, N. S., Uthicke, S., Botté, E. S., Flores, F., and Negri, A. P. (2013). Ocean acidification reduces induction of coral settlement by crustose coralline algae. *Glob. Chang. Biol.* 19, 303–315. doi:10.1111/gcb.12008.

Weitere, M., Erken, M., Majdi, N., Arndt, H., Norf, H., Reinshagen, M., et al. (2018). The food web perspective on aquatic biofilms. *Ecol. Monogr.* 88, 543–559. doi:10.1002/ecm.1315.

Wendt, I., Backhaus, T., Blanck, H., and Arrhenius, Å. (2016). The toxicity of the three antifouling biocides DCOIT, TPBP and medetomidine to the marine pelagic copepod *Acartia tonsa*. *Ecotoxicology* 25, 871–879. doi:10.1007/s10646-016-1644-8.

Wesseling, W. (2015). Beneficial biofilms in marine aquaculture? Linking points of biofilm

formation mechanisms in *Pseudomonas aeruginosa* and *Pseudoalteromonas* species. *AIMS Bioeng*. 2, 104–125. doi:10.3934/bioeng.2015.3.104.

Wilson, S. K., Graham, N. A. J., Pratchett, M. S., Jones, G. P., and Polunin, N. V. C. (2006). Multiple disturbances and the global degradation of coral reefs: Are reef fishes at risk or resilient? *Glob. Chang. Biol.* 12, 2220–2234. doi:10.1111/j.1365-2486.2006.01252.x.

Wolfaardt, G. M., Lawrence, J. R., Robarts, R. D., Caldwell, S. J., and Caldwell, D. E. (1994). Multicellular organization in a degradative biofilm community. *Appl. Environ. Microbiol.* 60, 434–446. doi:10.1128/aem.60.2.434-446.1994.

Yamaguchi, T., Prabowo, R. E., Ohshiro, Y., Shimono, T., Jones, D., Kawai, H., et al. (2009). The introduction to Japan of the Titan barnacle, *Megabalanus coccopoma* (Darwin, 1854) (Cirripedia: Balanomorpha) and the role of shipping in its translocation. *Biofouling* 25, 325–333. doi:10.1080/08927010902738048.

Zhao, J., Wang, Z., Dai, Y., and Xing, B. (2013). Mitigation of CuO nanoparticle-induced bacterial membrane damage by dissolved organic matter. *Water Res.* 47, 4169–4178. doi:10.1016/j.watres.2012.11.058.

# Chapter 2: Antifouling coatings can reduce algal growth while preserving coral settlement

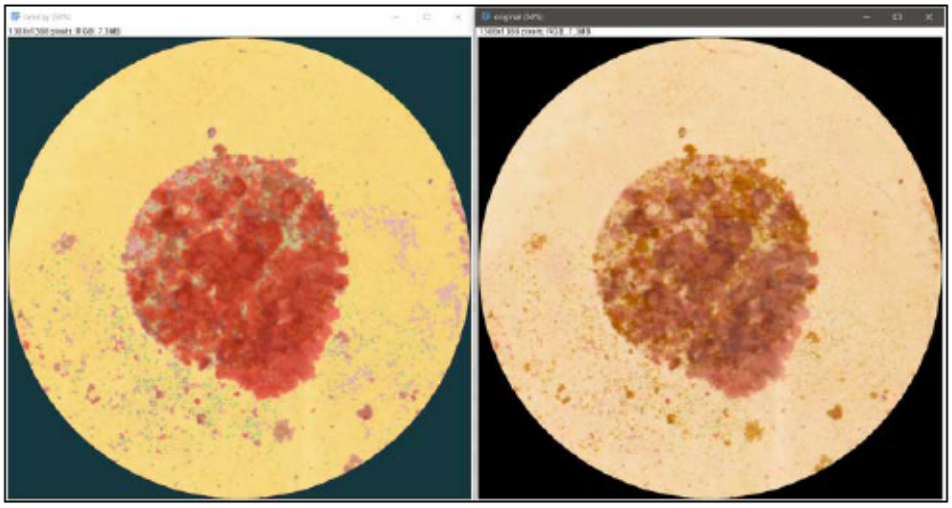

*Published as:*
*Roepke LK, Brefeld D, Soltmann U, Randall CJ, Negri AP, Kunzmann A (2022) Antifouling coatings can reduce algal growth while preserving coral settlement. Sci Rep 12, 15935. https://doi.org/10.1038/s41598-022-19997-6*

## Abstract

In the early stages after larval settlement, coral spat can be rapidly overgrown and outcompeted by algae, reducing overall survival for coral reef replenishment and supply for restoration programs. Here we investigated three antifouling (AF) coatings for their ability to inhibit algal fouling on coral settlement plugs, a commonly-used restoration substrate. Plugs were either fully or partially coated with the AF coatings and incubated in mesocosm systems with partial recirculation for 37 days to track fouling succession. In addition, settlement of *Acropora tenuis* larvae was measured to determine whether AF coatings were a settlement deterrent. Uncoated control plugs became heavily fouled, yielding only 4-8% bare substrate on upper surfaces after 37 days. During this period, an encapsulated dichlorooctylisothiazolinone (DCOIT)-coating was most effective in reducing fouling, yielding 61-63% bare substrate. Antiadhesive and cerium dioxide ($CeO_{2-x}$) nanoparticle (NP) coatings were less effective, yielding 11-17% and 2% bare substrate, respectively. Average settlement of *A. tenuis* larvae on the three types of AF-coated plugs did not statistically differ from settlement on uncoated controls. However, settlement on the NP-coating was generally the highest and was significantly higher than settlement found on the antiadhesive- and DCOIT-coating. Furthermore, on plugs only partially-covered with AF coatings, larval settlement on coated NP- areas was significantly higher than settlement on coated antiadhesive- and DCOIT-areas. These results demonstrate that AF coatings can reduce fouling intensity on biologically-relevant timescales while preserving robust levels of coral settlement. This represents an important step towards reducing fine-scale competition with benthic fouling organisms in coral breeding and propagation.


**Key words: biofouling, coral larvae, Trainable Weka Segmentation, coral restoration, algal community, benthic competition**

## 1. Introduction

Tropical coral reefs are under increasing pressure [1–3] from multiple anthropogenic threats including ocean warming and acidification on a global scale and eutrophication, pollution and increased human activities in coastal areas [4–6]. An estimated 20% of reefs worldwide have been lost as a consequence of natural and anthropogenic disturbances, and a further 15% are in a critical state and likely to be lost within the next few decades [4,7]. Successful reproduction and recruitment of corals is critical for the recovery of scleractinian coral species and for increasing reef resilience [8]. High mortality after larval settlement in corals can be caused by accidental removal by grazing fish [9,10], competition with other benthic organisms [11,12], sedimentation [13,14], and direct corallivory [10]. Competition with benthic algae, often triggered by excess nutrients

associated with runoff is also recognized as a key threat to coral settlement and the survival of newly settled corals (spat) [15,16].

Algal growth occurs following the primary colonization of hard benthic surfaces by microbial (bacteria, fungi, protozoa, etc.) biofilms [17], and the settlement of corals can be either induced or inhibited by these early fouling communities, depending on the colonizing taxa [18]. Some biofilms and crustose coralline algae (CCA) are strong inducers of settlement of coral larvae [19–23]. However, the interaction between corals and other fouling organisms, such as filamentous algae, can be detrimental to larval settlement and to the survival of coral spat, juveniles and the success of adult corals [24–26]. Fouling can impact coral spat through competition for space and direct overgrowth by microorganisms or motile propagules of other macroorganisms [27]. Furthermore, the microtopography provided by fouling may provide a refuge for microbial pathogens [28] or corallivorous invertebrates. Allelopathy [29], shading [27], alteration of fine-scale water movement, and other microenvironmental changes induced by fouling algae may also impede coral survival or fitness of coral spat [30].

Declining coral cover and health, and increasing environmental pressures on tropical coral reefs, have motivated the development of novel restoration techniques and the establishment of restoration programs around the globe [31–33]. A key strategy for large-scale reef restoration is to deliver captured or cultivated coral larvae onto the reef, either directly [34–36] or on deployment devices [37–39]. The benefits of using sexually produced coral propagules for this purpose include improvements in genetic diversity, scalability and cost [38,40,41], as well as retention of species diversity and community composition [41]. Deploying spat onto reefs using devices also, at least temporarily, overcomes challenges associated with the settlement process, including a lack of available substrate or settlement cues [42–44], the presence of settlement inhibitors [45–47], and direct competition with surrounding benthos. The application of antifouling (AF) technologies onto deployment devices to increase the survival of sexually propagated corals is a potential strategy to support coral spat and recruit survival over the first vulnerable months [48].

AF paints containing biocides that inhibit the establishment of algal and invertebrate communities have been applied on ship hulls to increase efficacy since the mid 19th century [49]. High concentrations of tributyltin (TBT) and copper-based AF paints that can contaminate coral reefs following groundings have previously been considered a threat to coral larval settlement [50] and spat survival [51]. However, the banning of TBT and further regulation of copper in AF paints has led to the development of alternative formulations that either contain no biocides or less toxic biocides that rapidly degrade, reviewed in Almeida *et al*. (2007) [49]. One of the most widely applied AF coatings, Sea-Nine 211™ (Röhm & Haas; Philadelphia, PA, USA [52]), includes an active biocidal ingredient, known as dichlorooctylisothiazolinone (DCOIT, Kathon 930, C-9 or DCOI). DCOIT can diffuse across the cell walls and membranes, binding to proteins and enzymes, blocking activity in biofilms, target and non-target organisms [53]. The half-life of

DCOIT depends on environmental conditions, ranging from less than one day to 10 days or more, and can be influenced by several biotic and abiotic factors, such as microorganisms, photolysis, hydrolysis, pH and salinity [54]. Toxic effects have been observed across a diversity of organisms including bacteria, fungi, algae, bivalves, echinoderms, ascidians, fish, copepods, decapods, and soft corals [55–62]. Although the toxicity mechanism of DCOIT is not fully understood, embryotoxicity, immunosuppression, oxidative stress, reproductive and endocrine disruption in marine organisms have been reported [63]. However, some studies have shown effective AF properties of DCOIT encapsulated in silica nanocapsules which can decrease the toxicity towards non-target organisms [64,65]. Yet, no study to date has investigated the effects of DCOIT on hard corals, or encapsulated in a sol-gel.

Non-biocidal antifoulants include silicon-based sol-gel coatings, which are produced by a wet-chemical technique used for the fabrication of metal oxides. The sol (or solution) gradually forms a gel-like network containing both a liquid and a solid phase. The antiadhesive surface properties of these coatings can prevent the attachment of fouling organisms and facilitate their release at higher water velocities. The antiadhesive effect is achieved through low surface energies (with weak molecular attraction), amphiphilic properties (both hydrophilic and hydrophobic properties) and a precisely tuned surface roughness tuned to inhibit primary fouling [66]. Other recently developed non-biocidal AFs are based on nanoparticles, which disrupt bacterial cell-to-cell communication (i.e., quorum sensing) to inhibit the formation of biofilms and mitigate or delay later colonization by algae [67]. One example includes cerium ($Ce^{3+}/Ce^{4+}$)-modified sites across the high surface area of NPs, which enhance the catalytic oxidation of halides, resulting in the formation of biocidal compounds which combat biofilm formation or the formation of signaling molecules involved in intracellular communication [68–70]. Laboratory and field tests with paint formulations containing 2 wt% $CeO_{2-x}$ NPs showed a higher reduction in biofouling than $Cu_2O$, the most common biocidal ingredient in AF paints [68,70].

Only a single study has attempted to reduce fouling on surfaces to improve coral spat survival [48]. That study demonstrated how the application of two different paraffin waxes in close proximity to early coral spat significantly reduced fouling and improved survival, and no differences in coral settlement between wax treatments and uncoated controls were found. Further research is needed on the potential for recently-developed AF coatings to mitigate competition from biofouling and increase the likelihood of coral survival to size-escape thresholds (*sensu* Doropoulos *et al.*, 2012)[71]. This would ultimately improve the feasibility of sexual propagation techniques for reef-restoration programs.

In this study, we manufactured and tested the efficacy of three distinct AF coatings: an antiadhesive, a cerium dioxide nanoparticle (NP) coating, and an encapsulated DCOIT-coating. In addition, we investigated the settlement of *A. tenuis* coral larvae on fully-coated (FC) and partially-coated (PC) settlement surfaces ("coral plugs" or "plugs"). Our objectives were to (1)

explore the AF efficacy to reduce biofouling, (2) explore the fouling community (CCA, green/brown algae, bare substrate) composition and (3) assess coral-settlement preferences on coated and uncoated areas of pre-conditioned plugs. Our ultimate goal was to test whether the coatings reduced algal growth without inhibiting larval settlement adjacent to the coatings.

## 2. Materials & Methods

### 2.1. Coral plug preparation and coating design

Coral plugs (top disc diameter: 3 cm) made from white Portland cement were purchased (AquaPerfekt, Germany; Dyckerhoff WEISS CEM 1) and the layer of sand (Raunheimer quartz sand) on top of the surfaces was removed with a diamond saw blade on a circular saw. A smooth finish was achieved by sanding and polishing the plug's surfaces on very fine wet sandpaper (STARCKE® (SiC) waterproof Matador 220, 800, 2500). The uniformly smooth top surfaces were then coated with three different AF coatings following the methods described below. For each AF coating, half of the plug replicates were fully-coated (FC) and the other half were partially-coated (PC) (**Figure 2.1**), leaving a circular control area in the center of each plug uncoated (**Figure 2.1**). A circular sticker (12 mm Ø) was applied to the plug and prevented the coating in an area of approximately 10 mm Ø, since the sol spread out slightly underneath the sticker (approximately 88% coated and 12% uncoated). Control plugs were not coated. The purpose of including FC plugs, was to explore the antifouling efficacy, fouling community composition and coral larval settlement preferences among the AF treatments. PC plugs were used to further explore fine-scale antifouling efficacy, fouling community composition and coral larval settlement preferences, when offered the choice to settle on an uncoated or coated area.

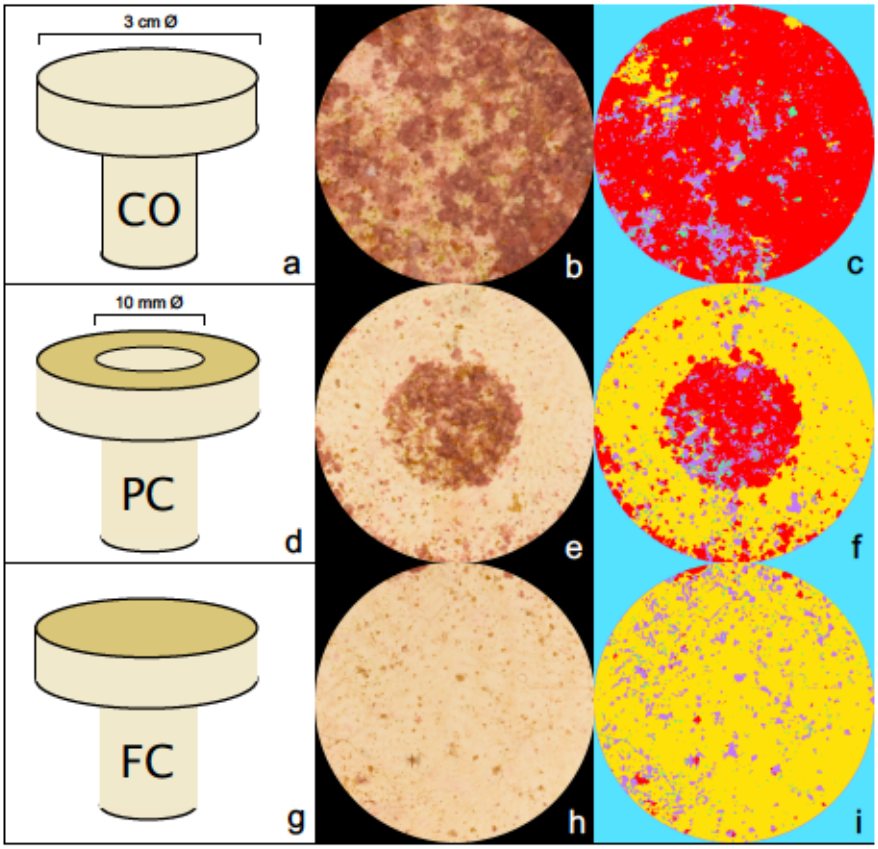


**Figure 2.1**: Uncoated Control (CO; a), partially-coated (PC; d), and fully-coated (FC; g) plugs, cropped images of CO (b), PC (e), and FC (h) DCOIT plugs (after 37 days in the aquaria), and the segmentation of fouling classes on the same CO (c), PC (f), and FC (i) DCOIT plugs, using machine learning-based image classification with the Trainable Weka Segmentation (TWS) in ImageJ. Each fouling class was segmented using a specific color (c, f, i): red (CCA), violet (brown algae), green (green algae), yellow (bare substrate), blue (background).

## 2.2. AF coating manufacturing

### 2.2.1. $CeO_{2-x}$ nanoparticle coating

Cerium oxide nanoparticles (NPs) were manufactured according to Ji *et al*. (2012)[72] and the Supporting Information in Herget *et al*. (2017)[73] with minor adjustments as described below. The process involved: (i) the production of nanoparticles, (ii) the catalytic activity testing, (iii) the production of coating solution A which included tetraethoxysilane (TEOS) and (iiii) the production of coating solution B which included TEOS and 3-glycidyloxypropyltriethoxysilane (GLYEO) (all technical details can be found in the Supporting Information). The plugs were coated 3 times, with a base coat and two overcoats. First, plugs were dip-coated with coating solution A, followed by a second and third coating applied by a soaked felt (textile) with solution B. The combination of an initial dip coating using a $SiO_2$-sol with $CeO_{2-x}$ and the subsequent overcoats using an epoxy-modified sol with $CeO_{2-x}$ gave good results in terms of adhesion and uniformity of the coatings. On the unmodified basecoat, the epoxy-modified sols showed good coating adhesion, with fewer tendencies to crack. For the overcoats, a more

homogeneous distribution of the $CeO_{2-x}$ particles was achieved by using a felt for the coating application. Test coatings on Poly (methyl methacrylate) (PMMA) tiles (16 $cm^2$) revealed a coating weight of 14.4 mg/16 $cm^2$ (0.9 mg/$cm^2$). The final concentration of ceria NPs in the coating solution was 35.7 wt%. Thus, the final surface density of ceria NPs was approximately 0.32 mg/$cm^2$.

### 2.2.2. Antiadhesive coating

Following and adapting the methods by Sokolova *et al.* (2012)[74] and Detty *et al.* (2014)[66] a silica-based sol-gel was produced from *n*-octadecyl-trimethoxysilane (C18, 0.675 g, CAS 3069-42-9, abcr GmbH, Karlsruhe), tridecafluoro-1,1,2,2-tetrahydrooctyltriethoxysilane (TDF, 3.675 g, CAS 51851-37-7, abcr GmbH, Karlsruhe), *n*-octyltriethoxysilane (C8, 22.4 g, CAS 2943-75-1, abcr GmbH, Karlsruhe), and tetraethylorthosilicate (TEOS, 18.75 g, CAS 78-10-4 abcr GmbH, Karlsruhe) in a molar ratio of 1:4:45:50. The modified silica alkoxides were mixed with 59.5 mL of ethanol and 11.4 mL of HCl (0.1 M) and stirred for 24 h at room temperature for sol formation. Prior to coating the surface, the plugs were cleaned with ethanol and their surfaces were activated by microwave plasma (working pressure 10 Pa in air, activation time 2.5 min., Creaetch 250 Plasma MV, Creavac GmbH) to ensure good coating adhesion. Coatings were applied by the dip-coating technique and cured at 100 °C for one hour.

### 2.2.3. DCOIT coating

Dichlorooctylisothiazolinone (DCOIT; $C_{11}H_{17}Cl_2NOS$; TCI America; CAS RN 64359-81-5; Product number D4157) was dissolved in ethanol and attached to hydrophobic pyrogenic silicic acid, each batch containing 0.5 g DCOIT in 2 mL ethanol and 0.1 g hydrophobisated silicic acid powder. After gentle stirring, the mixture was incubated overnight at room temperature, loosely covered, to allow ethanol to evaporate. Subsequently, the DCOIT loaded silicic acid powder was incorporated in two different sol-gels: 1. an aqueous $SiO_2$-sol made from TEOS and 3-glycidyloxypropyl-triethoxysilane (9 mL TEOS, 1 mL 3-glycidyloxypropyl-triethoxysilane, 60 mL $H_2O$ and 30 mL 0.01M HCl were stirred for 20 h) and 2. a hydrophobic $SiO_2$-sol (same antiadhesive coating as in section 2.2.2). Each $SiO_2$-sol with 20 mL volume contained 0.1 g of DCOIT loaded silicic acid powder. After mixture, the dispersions were sonicated (UP100H, Hielscher Ultrasonics GmbH, Teltow, Germany) for 3 min, followed by a 5 min cooling period to prevent heating of the dispersions, followed by another 3 min sonication. Prior to coating the surface, the plugs were cleaned with ethanol and their surfaces were activated in microwave plasma (working pressure 10 Pa in air, activation time 2.5 min., Creaetch 250 Plasma MV, Creavac GmbH). Plug surfaces were dip-coated in the hydrophilic sol first, then dried and tempered at 100 °C for one hour. Afterwards, the second hydrophobic sol was applied by dip-coating, then dried and tempered at 100 °C for an hour. To estimate the embedded DCOIT concentration per area, DCOIT was extracted from the coatings with ethanol. The concentration was measured photometrically at 280 nm. A DCOIT concentration of 3.2 mg/$cm^2$ was determined.

## 2.3. Fouling experiment

### 2.3.1. Experimental setup

Plugs were kept in three replicate outdoor holding mesocosm aquaria (280 L) located in the quarantine area of the National Sea Simulator (SeaSim) of the Australian Institute of Marine Science (AIMS) in Townsville, Australia. Each tank contained 15 replicate plugs per treatment (15 plugs x 7 treatments including the control treatment). In total, 315 plugs were tested (3 tanks x 105 plugs). Each aquarium was independent of the others, with a separate recirculation system and an independent, temperature-controlled sump. Fresh filtered seawater was circulated into each experimental tank at a rate of three full water exchanges (turnovers) per day. Temperature was maintained at 26 °C and measured every 60 min. (HOBO Pendant® Temperature/Light 64K Data Logger, Onset Computer Corporation, Bourne, MA) and salinity was kept in the range of 34.5 to 35.5 PSU. Water circulation in the tanks was maintained by Maxspect Gyre 200 series pumps (constant speed mode, 20% force). Tanks received natural sunlight attenuated by ~70% with shade cloth: maximum Photosynthetically Active Radiation (PAR) light intensity was 250 µmol photons $m^{-2}$ $s^{-1}$. PVC plug trays (custom-fabricated: 40 x 20 x 5 cm (length x width x height), holes (1.2 cm Ø) for coral plugs arranged in rows A-E with 10 holes per row) were used to maintain the coral plugs horizontally within the tanks. Tray positions were swapped circularly on a weekly basis to minimize within-tank effects (i.e., unequal shading or local water flow) on fouling across the plugs. To 'seed' the plugs with a biofilm, approximately 3 kg of live rock (comprising reef rubble with typical fouling communities incl. CCA) was added to each tank 3 weeks before plugs were introduced.

### 2.3.2. Fouling quantification in ImageJ

To monitor and quantify the fouling intensity on the plugs, plug surfaces were photographed at regular intervals (after 9, 23 and 37 days) using a Nikon D810 with a Nikon AF-S 60 mm f/2.8 G Micro ED Lens outfitted with four Ikelite DS160 strobes mounted on a trolley with standardized distance and angle to each plug surface. The monitoring intervals were chosen based on other studies with similar coatings [66,68]. Six plugs were photographed at once. All image analyses were performed in ImageJ version 1.53c [75,76]. To obtain images of single plugs, each plug was cropped out of the original image using a standardized circular region of interest (ROI; **Figure 2.1**). The ROI was slightly smaller (2.5 cm Ø) than the plug surface's diameter, to easily accommodate all plugs. Subsequently, the Trainable Weka Segmentation (TWS) plugin in the Fiji distribution of the image processing program ImageJ [77] was used to segment images into different classes by the use of machine-learning based image classification models. The analysis was adapted from the "Trainable Weka Segmentation User Manual" published as Supplementary data in Arganda-Carreras *et al.* (2017)[78], but other studies have previously applied similar approaches to quantify biofouling with the TWS [79–82]. More recently, Macadam *et al.* (2021)[83] successfully used a similar machine-learning tool to measure coral spat survival, size, and color. In this study, each plug image was segmented into 5 different classes: crustose

coralline algae (CCA), green algae, brown algae, bare substrate and background. Green and brown algae were subsequently combined into a single category "green/brown alga" for statistical analysis, as the TWS classification of green and brown algae did not consistently achieve the same accuracy as for the category CCA and bare substrate. The initial model training stack was created using nine randomly selected images, one from each tank and monitoring period (3 tanks x 3 monitoring periods = 9 plug images). After loading the image stack into the TWS plugin, a minimum of three ROIs were selected for each fouling class on every image and the base model was trained using the default image features. By selecting just one image feature at a time and re-training the model, the most promising image features were chosen based on their minimization of the "out of bag error" (OOBE). The OOBE is a recommended option in TWS to measure the prediction error of the machine learning models by utilizing bootstrap aggregating methods. A lower OOBE indicates a better model performance. Features with no substantial reduction of the OOBE were excluded from the model. The minimization of the OOBE by each of the chosen image features was confirmed by excluding one feature at a time and re-training the model. By removing features, which did not minimize the OOBE in this step-wise backward-selection, a set of five features (variance, minimum, maximum, structure & neighbors) were chosen for further analyses. If the initial model segmented the image satisfactorily into the chosen fouling classes, the classifier was applied to all images and its accuracy was validated visually. The initial model was optimized using four more training stacks of formerly mis-segmented images (mis-segmentations of CCA, green/brown algae and bare substrate after visual validation). In total, 40 images of plugs were used for model training. Classes were balanced and the default classifier with 200 boosted regression trees, each considering 2 random features, was used. The OOBE for the final model was 0.591%. Pixels of areas with overlapping fouling classes (e.g., brown algae overgrowing CCA) were classified as the "more dominant" class, resulting in each pixel being assigned only to a single class. Corresponding areas were included during model training. After classification, the fraction of each class from the total plug surface was measured by using the particle analyzer in ImageJ. The segmented 8-bit images include a look-up table (LUT) in which each class is specified with a specific color (**Figure 2.1**). Using the thresholding tool, segments of one class were extracted and masks were produced. Using the particle analyzer, the percentage of each area belonging to one class was calculated and the results were exported to Microsoft Excel 2019. The classification of the PC plugs was performed for the whole surface area (coated and uncoated). Afterwards, each image was segmented into coated and uncoated regions and the remaining analyses were conducted as for the FC plugs. The cropped images, as well as the ROIs, segmented images, and the final model and training data can be accessed from a on-line repository here: https://doi.org/10.25845/ws1n-ah16.

## 2.4. Coral settlement experiment

### 2.4.1. Coral collection and larval husbandry

Fragments of gravid colonies (25–40 cm diameter) of the scleractinian coral *Acropora tenuis* (Dana, 1846) were collected from Davies Reef (18° 49'35.70"S 147° 37'36.46"E; 4 m depth) on December 12, 2019 under permit G12/35236.1 issued by the Great Barrier Reef Marine Park Authority. Colonies were transported to the SeaSim and maintained in 1700 L semi-recirculating holding tanks until spawning. Temperatures were held at 26–27 °C, to match the seawater temperature at the collection site. Spawning occurred on 17th December 2019 and the coral gametes from seven parental colonies were collected and fertilized. Symbiont-free larval cultures were maintained at densities <500 larvae per L, indoors, in 70 L flow-through rearing tanks (1.5 turnovers per day) supplied with 1 µm filtered seawater at 27 °C [84,85]. Larvae remained in those conditions until the experiment commenced.

### 2.4.2. Experimental setup

*A. tenuis* larvae (each 800–1000 $\mu$m in length) were competent to undergo attachment and metamorphosis after 5 days, as determined by routine settlement assays in the laboratory [19]. Settlement was defined here as the change in life stage from "free-swimming" or "loosely-attached, elongated" larvae to a squat, firmly attached and disc-shaped form, with pronounced flattening of the oral–aboral axis and with septal mesenteries radiating from the central mouth region [19]. The same plugs that were photographed to quantify fouling intensity (described above), were subsequently used to test larval settlement success in this experiment. Due to handling time restrictions (pipetting larvae and counting coral spat), the number of experimental plugs for settlement was reduced to 30 plugs per treatment (chosen haphazardly, 7 treatments: control, FC NPs, FC antiadhesive, FC DCOIT, PC NPs, PC antiadhesive, PC DCOIT), for a total of 210 plugs. After snapping off the stem of each plug, the plugs were isolated from each other by placing them in individual 200 mL glass jars, haphazardly interspersed, and filled with 150 mL of 1 µm filtered seawater. Prior to the start of the experiment, clear glass jars (7 cm Ø, 11 cm height) were cleaned with 20 mL acetone each, left to dry under a drying cabinet, and then rinsed in filtered seawater. To prevent larvae from attaching and undergoing metamorphosis on the side or underside of the plug, plugs were gently set into a thin layer (about 2 cm depth) of fine glass beads (1 mm Ø) placed at the bottom of each jar. Prior to filling the glass jars, the newly purchased beads were rinsed in freshwater twice and then spread as a thin layer (0.5 cm depth) on aluminium foil to dry in an oven at 50 °C for 5 hours. The glass jars and glass beads were generic (no brand). 15 randomly selected 11-day-old larvae were pipetted gently into each jar. No settlement inducers were added, because each fouled plug surface contained a biofilm that included crustose coralline algae (CCA). Larvae were incubated under artificial lighting (Hydra FiftyTwo HD LED, Aquaria Illumination, Allentown, USA) at an intensity of approximately 40 $\mu$mol photons $m^{-2}$ $s^{-1}$ (12:12 h light:dark cycle) and at a

constant water temperature of 26.7 °C. Settlement was assessed after 24 h under a stereo microscope and was considered normal if a larva had undergone attachment to the plug surface and metamorphosis into a polyp, as described above. All other larvae (swimming, loosely attached, dead and partially disintegrated) were counted as not settled.

## 2.5. Statistical analysis

All statistical analyses were performed in R version 4.2.0 [86] and the data were manipulated and visualized using packages of the 'tidyverse' [87].

Fouling intensity on the FC and PC plugs was measured as percent coverage by fouling class (CCA, green/brown algae, bare substrate). To investigate differences in fouling intensity after 37 days (end of experiment) between AF treatments, linear mixed models (LMM) were fitted using the package 'nlme' [88]. The last timepoint of the analysis shows the overall efficacy of the AF coatings and was therefore considered to be the most informative timepoint from a biological and ecological standpoint as less algae-coral competition is hypothesized with less algae fouling. On the FC plugs, fouling coverage was modeled as a function of fouling class and AF treatment. The fouling coverage on the PC plugs was modeled as a function of the area (coated vs. uncoated), fouling class and AF treatment. Both models used a square-root transformation of the response to stabilize heteroscedasticity of the residuals, and included 'tank' as a random effect. Furthermore, the fouling classes were corrected for unequal variances using the 'varIdent' function in the weights argument. Model fit was visually assessed using standard diagnostic plots of the normalized residuals. ANOVA tables (type II tests) were computed for both models using the 'car' package [89] in order to identify statistically significant fixed effects and their interactions. When significant, post-hoc tests for pairwise comparisons between treatments were performed using the 'emmeans' package [90]. On the FC plugs, differences in fouling coverage between treatments were assessed within each fouling class. On the PC plugs, differences in fouling coverage were investigated between the coated and uncoated area, for each treatment within fouling classes. The p-value was adjusted for multiple comparisons with the Tukey method. The presented estimated marginal means were back-transformed from the square-root to the response scale for interpretation (**Supplementary Figure S2.1** and **Figure S2.2**). The estimated contrasts are provided in the Supplementary Information.

Settlement was expressed as settler (spat) density (settlers/cm$^2$). On the FC plugs, the settler density was calculated by dividing the total number of settlers on each plug by the total surface area (7.069 cm$^2$). On the PC plugs, the settler density was calculated by dividing the number of settlers on the uncoated and coated area of each plug by the respective surface area (uncoated: 6.283 cm$^2$; coated: 0.785 cm$^2$). To investigate differences in settler density among treatments,

LMMs were fitted. On the FC plugs, the settler density was estimated as a function of treatment using the package 'glmmTMB' [91]. To account for the correlation of observations from the same tank, "tank" was added as a random factor. On the PC plugs, settler density was modeled as a function of treatment and area (uncoated/coated) using the package 'nlme' [88]. "Tank" again was used as a random factor and all treatment-area-fouling class combinations were corrected for unequal variances using the 'varIdent' function in the weights argument. The response variables (settler density) of both models were square-root transformed to stabilize heterogeneity in the residuals and improve model fit. Satisfaction of model assumptions was checked by using standard R model diagnostic plots. Plots were based on 'response' residuals on the FC plugs and on 'normalized' residuals on the PC plugs. ANOVA tables (type II tests) for both models were computed again using the 'car' package [89]. If significant, pairwise post-hoc tests were performed using the 'emmeans' package [90] for all group combinations. P-values were adjusted for multiple comparisons using the Tukey method. Tests were performed on the square-root and back-transformed for visualization (**Figure 2.4**, **Figure 2.5**). Coefficients remained on the square-root.

## 3. Results

### 3.1. Biofouling

#### 3.1.1. Biofouling: fully-coated plugs

Settlement plugs became progressively colonized with green/brown algae and crustose coralline algae (CCA) over the course of the experiment, and rapid fouling was evident after 9 days on all surfaces. Between 9 and 23 days, all plugs shifted towards higher fouling cover, except for DCOIT-coated plugs (**Figure 2.2**; **Supplementary Table S2.1**). Antifouling treatments had a statistically significant effect on the fouling community composition after 37 days (LMM: $\chi^2(6) = 504.29, p < 0.001$). This analysis focused on comparing treatments withing fouling classes, while the "full" pairwise results including treatment-fouling class interactions are shared in the Supplementary Information (**Table S2.4**). After 37 days, bare substrate was significantly different ($p < 0.001$) among all treatments, except between the NP treatment and control. Bare substrate on the DCOIT-coated plugs averaged 62.8 ± 3.3% (mean ± SE; **Supplementary Table S2.1**) and was significantly higher ($p < 0.001$) than average bare substrate on the antiadhesive-coated plugs (17.4 ± 2.2%; **Figure 2.2** and **Supplementary Figure S2.1**; **Supplementary Table S2.1** and **Table S2.3**) and all other plugs. Bare substrate on the antiadhesive-coated plugs was significantly higher ($p < 0.001$) than average bare substrate on the NP-coated (2.3 ± 0.4%) and control plugs (4.5 ± 0.6%; **Figure 2.2** and **Supplementary Figure S2.1**; **Supplementary Table S2.1** and **Table S2.3**). Green/brown algae were the most dominant fouling class in all treatments throughout the experiment (average of 52.1% across all treatments by day 37). However, after 37 days, average green/brown algae

coverage on the DCOIT treatment (36.2% ± 3.4%) and antiadhesive treatment (42.3% ± 4.5%) was significantly lower than on the nanoparticle treatment (65% ± 5.3%) and the control (64.8% ± 5.1%; **Figure 2.2** and **Supplementary Figure S2.1**; **Supplementary Table S2.1** and **Table S2.3**). On control plugs, CCA cover increased from 0.5% to 30.7% between days 9 and 37 (**Figure 2.2**; **Supplementary Table S2.1**). CCA coverages on the nanoparticle-coated and control plugs were very similar after 9, 23 and 37 days (**Figure 2.2**). After 37 days, only 1.1 ± 0.3% CCA cover was measured on the DCOIT treatment, significantly less CCA ($p < 0.001$) as compared to all other treatments and the control. There were no differences in CCA coverage among the NP, antiadhesive and control treatments (**Figure 2.2** and **Supplementary Figure S2.1**; **Supplementary Table S2.1** and **Table S2.3**).

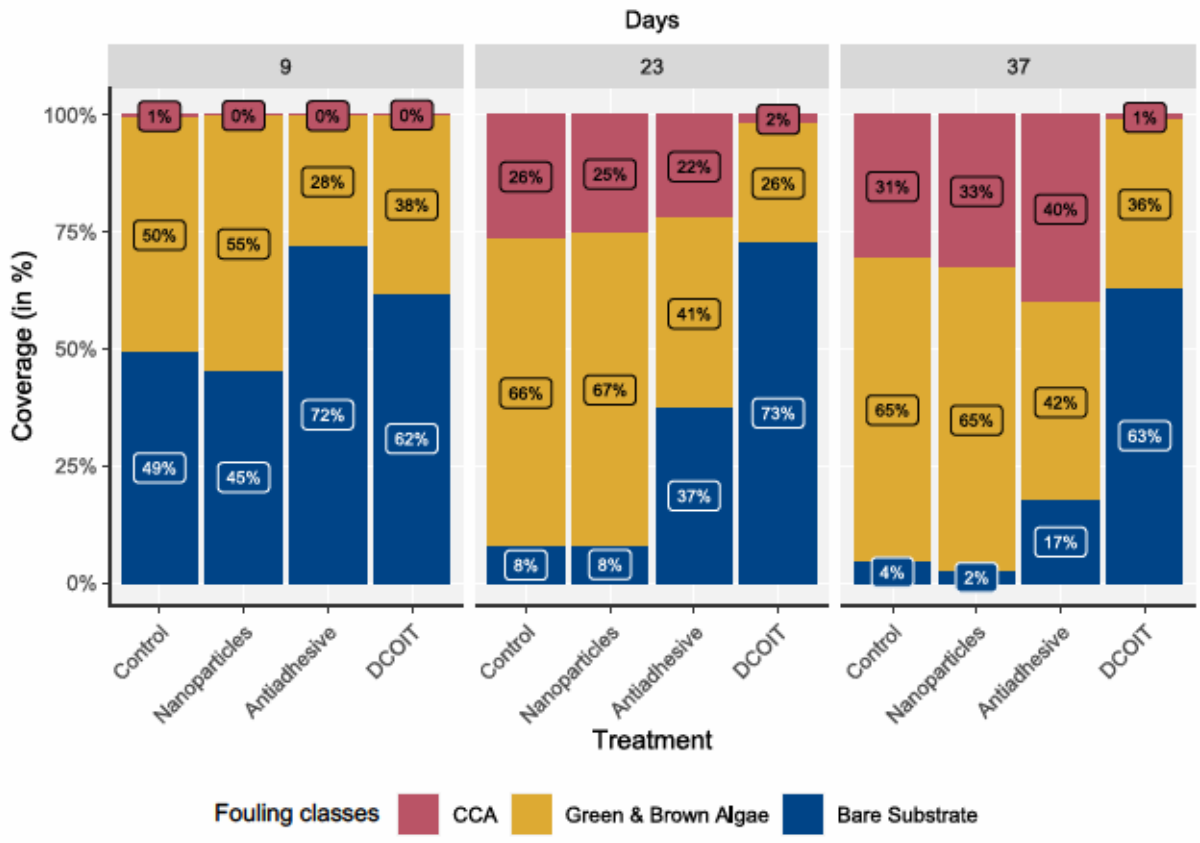


**Figure 2.2**: Fully-coated (FC) plugs (Nanoparticles, Antiadhesive, DCOIT) and uncoated Control plugs (n=45 plugs per treatment) were incubated in semi-recirculating seawater systems prior to coral settlement trials to examine the mean coverage (%) of fouling classes (CCA, Green/brown algae, Bare substrate) over time (after 9, 23,37 days). Note that bare substrate coverage at experimental start (day 0) was 100% (**Supplementary Table S2.1**).

### 3.1.2. Biofouling: partially-coated plugs

Fouling class coverages on the coated and uncoated control areas of the PC plugs were generally similar to fouling on the FC and uncoated control plugs, respectively (**Figure 2.2**) throughout the experiment. There was a significant three-way interaction among AF treatment, area (coated

vs. uncoated) and fouling classes after 37 days (LMM: $\chi^2$ (4) = 167.204, $p < 0.001$), suggesting that the differences between coated and uncoated areas were not consistent for all treatments and fouling classes. The "full" pairwise results including area-treatment-fouling class interactions are shared in the Supplementary Information (**Table S2.8**). After 23 and 37 days, the uncoated areas of the antiadhesive-coated and DCOIT-coated treatments were similar to the control plugs, whereas the coated areas of these treatments had more bare substrate (**Figure 2.3**; **Supplementary Table S2.5**). There were significant differences in bare substrate coverage between coated and uncoated areas across all AF treatments, but only DCOIT significantly reduced CCA and green/brown algae coverage (**Figure 2.3**; **Supplementary Figure S2.2** and **Supplementary Table S2.7**). Bare substrate averaged 60.9 ± 3.3% (mean ± SE) on the coated areas and was significantly higher ($p < 0.001$) than bare substrate on the uncoated areas (8.1 ± 1.2%) of the PC DCOIT plugs (**Figure 2.3**; **Supplementary Figure S2.2** and **Supplementary Table S2.5** and **Table S2.7**). CCA were significantly more abundant (22.5 ± 4%; $p = 0.005$) on the uncoated areas than on the coated areas (5.2 ± 1.3%) of the PC DCOIT plugs. Green/brown algae were dominant ($p < 0.001$) on the uncoated areas in contrast to the coated areas (33.9 ± 3.3%) of the PC DCOIT plugs. Bare substrate on the PC antiadhesive plugs differed significantly between coated and uncoated areas ($p = 0.008$), with more bare substrate on the coated areas. In contrast, significantly more bare substrate was found on the uncoated areas of the nanoparticle treatment ($p = 0.049$) (**Figure 2.3**; **Supplementary Figure S2.2** and **Supplementary Table S2.5** and **Table S2.7**).

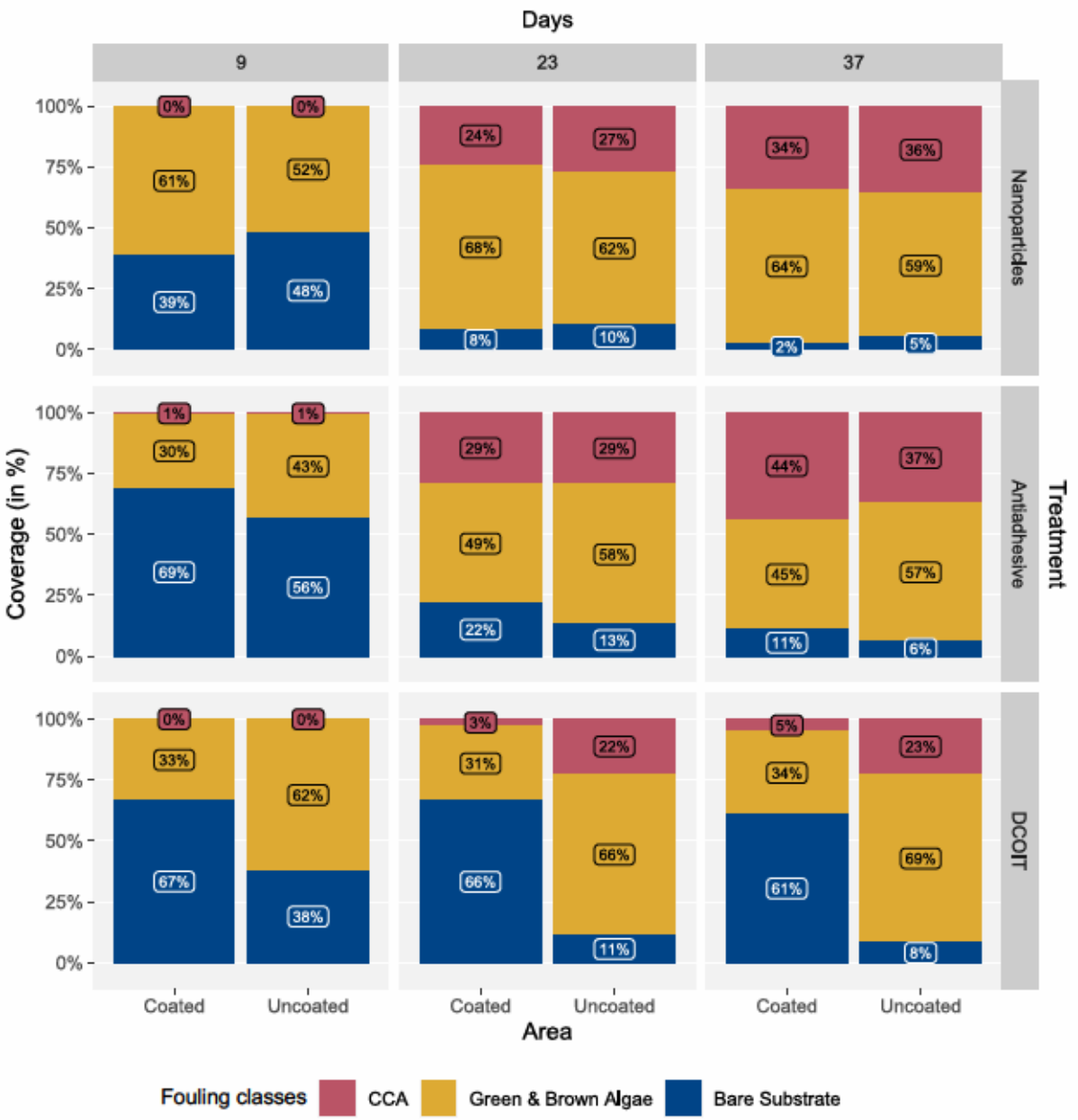


**Figure 2.3**: Partially-coated (PC) plugs (Nanoparticles, Antiadhesive, DCOIT) with coated and uncoated areas (n=45 plugs per treatment) were incubated in semi-recirculating seawater systems prior to coral settlement trials to examine the mean coverage (%) of fouling classes (CCA, Green/brown algae, Bare substrate) over time (after 9, 23,37 days). Note that bare substrate coverage at experimental start (day 0) was 100% (**Supplementary Table S2.5**).

## 3.2. Settlement

### 3.2.1. Settlement: fully-coated plugs

The average settlement success on control plugs was 0.8 ± 0.1 settlers/cm2 (mean ± SE), typical of settlement on fouled plugs 82. On the fully-coated (FC) plugs, there was a statistically significant effect of treatment on larval settlement (LMM: $\chi 2(3) = 15.559$, $p < 0.01$). A. tenuis

settlement was highest on the NP-coated plugs with an average of 0.8 ± 0.1 settlers/cm2 and similarly high with the control plugs, while the lowest settlement was found on the antiadhesive-coated plugs (0.5 ± 0.1 settlers/cm2) (**Figure 2.4**; **Supplementary Table S2.9** and **Table S2.11**). Coral larval settlement on the DCOIT-coated plugs (0.6 ± 0.1 settlers/cm2) was higher than on the antiadhesive-coated plugs, and did statistically differ from settlement on the nanoparticle-coated plugs ($p = 0.014$; **Figure 2.4**; **Supplementary Table S2.9**, **Table S2.10** and **Table S2.11**).

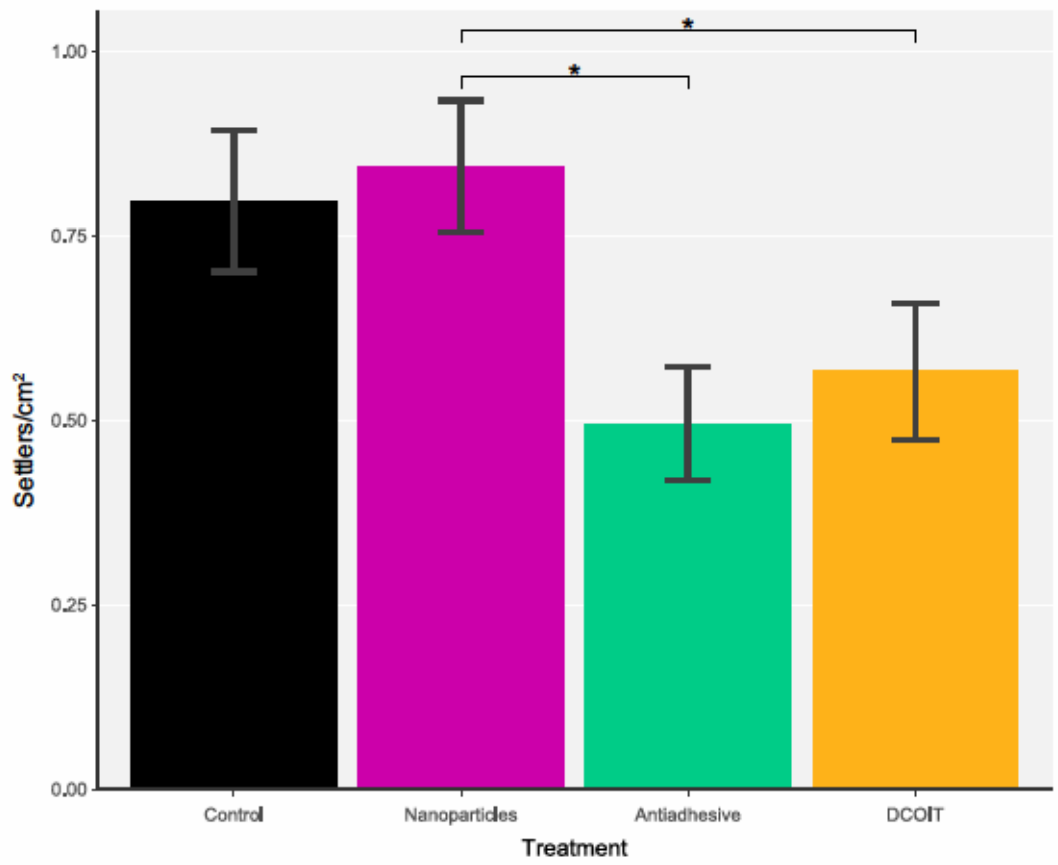


**Figure 2.4**: Pre-conditioned fully-coated (FC) plugs (Nanoparticles, Antiadhesive, DCOIT) and uncoated Control plugs (n=30 plugs per treatment) were tested for mean coral larval settlement (settlers per cm2) in individual glass jars (one plug with 15 larvae per jar). Error bars represent SEM. Asterisks indicate statistically significant differences based on pairwise post-hoc tests with least-squares means (**Supplementary Table S2.9** and **Table S2.11**; *$p < 0.05$).

### 3.2.2. Settlement: partially-coated plugs

Mean settlement densities (settlers/cm²) differed significantly among treatments and between areas (coated/uncoated) (LMM: $\chi2(2) = 6.6274$, $p < 0.05$), and settlement patterns on the PC plugs were similar to the FC plugs. Settlement on the coated NP areas, with 0.9 ± 0.1 settlers/cm² (mean ± SE), was significantly higher than settlement on the coated antiadhesive areas ($p < 0.001$) and coated DCOIT areas ($p = 0.004$) (**Figure 2.5**; **Supplementary Table S2.11** and **Table S2.14**). *A. tenuis* settlement on the uncoated areas of the antiadhesive coating

(0.9 ± 0.3 m settlers/cm²) and DCOIT coating (1.2 ± 0.3 settlers/cm²) was much higher than on the coated areas in close vicinity on the same plugs, however, not significantly (**Figure 2.5**; **Supplementary Table S2.12**, **Table S2.13** and **Table S2.14**).

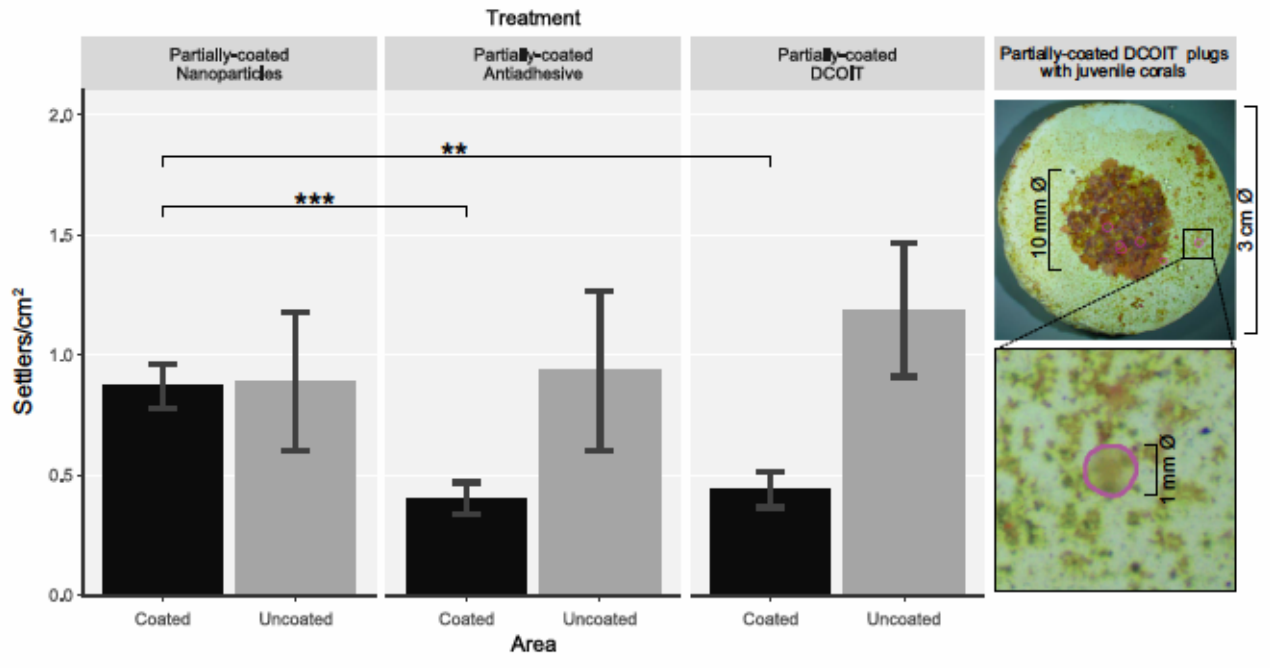


**Figure 2.5**: Pre-conditioned partially-coated (PC) plugs (Nanoparticles, Antiadhesive, DCOIT) with coated and uncoated areas (n=30 plugs per treatment) were tested for mean coral larval settlement (settlers per cm2) in individual glass jars (one plug with 15 larvae per jar). Error bars represent SEM. Asterisks indicate statistically significant differences based on pairwise post-hoc tests with estimated marginal means (**Supplementary Table S2.12** and **Table S2.14**; *p < 0.05, **p < 0.01, ***p < 0.001). Images (right) show coral settlers (circled in magenta) on a PC DCOIT plug.

## 4. Discussion

The effects of non-biocidal and recently-developed antifouling (AF) coatings on marine species have been rarely evaluated since their introduction after 2008, when tributyltin (TBT) was globally prohibited [92]. By contrast, DCOIT, as a biocidal ingredient in a range of AF coatings, has been investigated and evaluated to a greater extent, but with no testing of hard corals or coral larvae to date. Here, three coatings with reportedly high AF efficacy and potential low toxicity [64,66,68] were tested, to explore whether any of these coatings caused reduced algae growth without reducing coral larval settlement (indicating low deterrent or toxic effects). Two of the three AF coatings, the encapsulated DCOIT and antiadhesive coating, showed effective and localized antifouling action, while the $CeO_{2-x}$ coating formulation was ineffective. Coral settlement on the fully-coated (FC) plugs of all treatments did not differ from settlement on the control; however, coral larvae tended to settle on an uncoated area if given the choice (in partially-coated (PC) antiadhesive and DCOIT treatments), leading to higher settler densities in

that area. These results indicate that larval settlement on and around the AF coatings is possible, and that the AF coatings can reduce fouling and competition with newly settled corals.

### 4.1. Antifouling efficacy and *A. tenuis* settlement: $CeO_{2-x}$ nanoparticle coating

The $CeO_{2-x}$ nanoparticle (NP) coating did not actively inhibit fouling or change fouling community composition compared with the uncoated control. This contrasted with Herget *et al*. (2017)[68] and Wu *et al*. (2021)[93] who demonstrated beneficial antifouling of stainless-steel plates coated with $CeO_{2-x}$ NP in freshwater and seawater environments. The enzymatic activity of the $CeO_{2-x}$ nanoparticles (NPs) catalyzes the oxidation of halides in presence of hydrogen peroxide ($H_2O_2$) to hypohalous acids (HOX) according to: $Br^- + H_2O_2 \rightarrow HOBr + H_2O$. HOX can react in follow-up reactions to halogenated organic compounds. Hypohalous acids combat biofilm formation through their biocidal activity or the formation of signaling molecules involved in intracellular communication. When cell-to-cell communication is blocked by halogenated compounds, bacteria cannot form organized community structures such as biofilms. As the catalytic activity of the NPs was tested in their unconsolidated form, we assumed their activity in the coating would still be present. Future studies could test this activity in the coating just prior to any field tests. Furthermore, the concentration of NPs in our coating could have been too low for the expected antifouling activity and future approaches could test for different NP concentrations in the coatings. Although several studies report substantial reductions in bacterial adhesion [68,93–95], literature on suppressed macrofouling species in natural seawater is very scarce [96]. Interestingly, Xu *et al*. (2019)[97] reported increased biofilm formation and growth of bacterial strains from wastewater treatment plants at $CeO_{2-x}$ NP concentrations < 4 mg/L, whereas the opposite effect was observed at $CeO_{2-x}$ NP concentrations higher than 10 mg/L. Concentrations of 0.5 and 2 mg/L were reported to enhance the surface hydrophobicity, aggregating ability, and the α-, and β-D-glucopyranose polysaccharide production of the bacterial strains. In addition, Xu *et al*. (2018, 2019)[97,98] reported similar findings of ROS-induced acceleration of quorum sensing molecules and activation of inherent resistance capacity by bacteria. Thus, ROS generated by non-lethal $CeO_{2-x}$ NP concentrations may accelerate bacterial biofouling and subsequent macrofouling. Clearly more studies to optimise the composition of NP antifoulants are needed to assess their potential to reduce fouling in seawater under tropical conditions.

In our study, *A. tenuis* larval settlement on the $CeO_{2-x}$ NP coated surfaces was higher than on the uncoated control, and was significantly higher on the FC plugs and coated PC plugs than on the antiadhesive- or DCOIT-coating. Also, when given the choice on PC plugs, larvae chose to settle on both coated and uncoated areas equally. However, ROS-mediated manipulation by the $CeO_{2-x}$ NPs could have created subtle effects, or effects that cancelled each other out in terms of settlement outcomes. For example, there may have been positive or negative effects of

generated ROS on both the fouling community beyond the resolution of this study and there could have been effects directly on the larvae as they contacted the surface in their search for a site to settle.

### 4.2. Antifouling efficacy and *A. tenuis* settlement: Antiadhesive coating

The antiadhesive coating showed the second highest AF efficacy, although it was much lower than that of the DCOIT coating. Our findings are in agreement with previous reports on the same or similar sol-gel coating types. For example, Tang *et al.* (2005)[99] found inhibition of zoospore settlement of the marine fouling alga *Ulva linza* after exposure to turbulent flow on sol-gel-derived xerogel films with *n*-octyltriethoxysilane (C8), tetraethylorthosilane (TEOS) and tetramethylorthosilane (TMOS), similar to the constituents of the coatings used in the present study. Also, their xerogel was found to act as a fouling-release surface for juveniles of the tropical barnacle *Balanus amphitrite*. Similarly, Gunari *et al.* (2011)[100] showed good AF results with *n*-octadecyl-trimethoxysilane (C18), C8 and TEOS on the settlement of barnacle cyprids, removal of juvenile barnacles (*B. amphitrite*) and settlement of zoospores of the alga *U. linza*. Sokolova *et al.* (2012)[74] tested an identical sol-gel xerogel coating (1:4:45:50; C18/TDF/C8/TEOS) containing the same constituents in the same molar ratios as tested here. That study found higher releases of juvenile barnacles and *Ulva* sp. sporelings, as compared with the C18/C8/TEOS formulation [100]. The C18/TDF/C8/TEOS xerogel contributes to the increased fraction of barnacles removed via shear [66].

However, Sokolova *et al.* (2012)[74] pointed out that sometimes opposing patterns in the settlement and release of different fouling organisms make it difficult to design a single surface to minimize settlement of all fouling organisms [99]. The goal of our study was to identify an AF coating that potentially inhibited harmful (i.e. competitive) fouling, while not deterring coral larval settlement (i.e. not inhibiting the sensitive settlement process). The antiadhesive sol-gel performed very well to inhibit CCA and green/brown algae but was also one of the two coatings that significantly reduced coral settlement, as compared to the highest settlement found on the nanoparticle treatment. In the choice experiment, *A. tenuis* settlement was approximately 50% lower on the coated areas of the PC antiadhesive plugs than on the uncoated areas (although not statistically significant). This could indicate disadvantageous surface properties of the coating for coral larval settlement. Unlike the DCOIT coating, sol-gel does not contain a known biocide, so the inhibition of settlement is likely to be physical, and any unlikely potential for deterrent or toxic effects should be investigated by assessing the survival of spat on, and adjacent to, the sol-gel coating. Interestingly, the abundance of CCA on the antiadhesive sol-gel coating was no different from the control, suggesting that the sol-gel coating might create a favorable environment for CCA growth and could be further investigated as a method to encourage the

colonization of surfaces with CCA that are advantageous for larval settlement in coral propagation and supply for restoration programs.

### 4.3. Antifouling efficacy and *A. tenuis* settlement: encapsulated DCOIT-coating

To date, very few studies have assessed the effects of encapsulated DCOIT in tropical marine species [65]. Even less is known about the effects of encapsulated DCOIT integrated in a coating, as compared to its free form, on marine species [64]. The rationale behind the encapsulation/immobilization technology is the prevention of direct biocidal interaction with coating components, the control of leaching rate, and thus, the decrease of the absolute quantity of biocides needed to prepare a formulation with identical AF efficacy, increasing the coating lifetime and reducing potential environmental threats [64,101–103]. Only one study by Ferreira *et al.* (2021)[62] compared the effects of free (non-integrated in a coating) and encapsulated DCOIT on the soft coral *Sarcophyton glaucum*. The authors found reduced toxicity of encapsulated DCOIT on the coral fragments compared with free DCOIT, as measured by coral polyp retraction, photosynthetic efficacy, and oxidative-stress markers. Our study demonstrated the high AF efficacy of encapsulated DCOIT with a very localized area of effect. The biofouling analysis showed clear differences in fouling between coated and uncoated areas on the same plugs, indicating that antifouling activity was isolated to the coating's surface with negligible leaching of antifoulants onto adjacent uncoated areas (1-3 mm away).

In this study, the settlement of *A. tenuis* directly on the FC DCOIT-coated areas was not significantly lower than settlement on the control plugs. These results suggest that either the coating has generally low deterrent or toxic effects, or that the potential toxicity declined sufficiently during the 37 days of pre-conditioning so as not to impede settlement. Inhibition of larval settlement is very sensitive to contaminants, including the AF biocides copper and TBT [50,104], and the lack of response to DCOIT in this no-choice experiment is strong evidence that the coating was not harmful at the time of the assay. Nevertheless, when larvae were able to choose between DCOIT-coated and uncoated surfaces (on PC plugs), almost 3 times more larvae chose to settle on the uncoated surface of PC plugs (per $cm^2$). It is possible that this was due to a subtle influence of the DCOIT itself (e.g., toxicity or textural), but these results could be further investigated by focusing on freshly applied DCOIT, as well as leaching rates and spatial and temporal effects on the physiological, and molecular responses of the larvae. Alternatively, the uncoated area of PC plugs may have developed a stronger inductive microbial biofilm for larval settlement [18] independently of, or influenced by, the adjacent DCOIT coating. Future research could investigate fouling organisms quantitatively, including bacterial species abundances and specific taxonomic occurrences on and next to the coatings. Moreover, long-term survival of coral spat and the associated benthic community on and next to the coating could be investigated.

The DCOIT coating worked particularly well to suppress CCA growth. With 1% coverage on the FC plugs and 5% on the coated areas of the PC plugs, CCA growth was strongly inhibited as compared to the control plugs with 31% CCA, and the uncoated areas with 23% CCA (PC plugs) after 37 days. This finding could indicate high toxicity towards CCA and could be particularly relevant for industrial maritime sectors. Although many studies have shown the importance of CCA as a cue for coral settlement [19,23,105], studies have demonstrated that CCA can also outcompete coral spat and lead to spat mortality under certain conditions [106,107]. Therefore, control of CCA overgrowth is an important consideration for improving survival in coral propagation for restoration purposes [38]. Our results support those of Figueiredo *et al.* (2019) [108] who demonstrated good AF performance of encapsulated DCOIT with reduced toxicity towards non-target species, including microalgae, rotifers, bivalves, crustaceans and echinoderms.

## 5. Conclusion & Future considerations

Two of the three types of AF coatings successfully inhibited macroalgal competitors of coral spat in mesocosm aquaria over 37 days. Our results also suggest no detrimental effects of the 37-day old coatings on coral larvae during settlement. However, these findings could be further evaluated by testing freshly applied coatings and determining possible toxic leaching effects in time-series experiments lasting for several weeks to months. Now that promising AF candidates have been identified, further studies could be conducted to assess their potential benefits on the survival and growth of coral spat over the first months post-settlement. Tebben *et al.* (2014)[48] demonstrated that a non-toxic paraffin wax-based AF was able to improve the survival of early coral spat that were in close proximity (within mm) of the wax coating. A similar approach of settling larvae directly onto a deployment substrate immediately adjacent to, or surrounded by, DCOIT or antiadhesive AF coatings, may offer strong protection against overgrowth by algae. While biocide-containing AFs ($Cu_2O$) have been effective in reducing fouling in coral fragments in nurseries for reef restoration [109], the biocide-free antiadhesive is likely to be more suitable for application on coral settlement surfaces for deployment into the field where biocides such as $Cu_2O$ or DCOIT are prohibited.

## Data availability

The raw data of the fouling quantification with the Trainable Weka Segmentation in ImageJ can be accessed publicly on-line here: https://doi.org/10.25845/ws1n-ah16.

## References


1. Gardner, T. A., Côté, I. M., Gill, J. A., Grant, A. & Watkinson, A. R. Long-term region-wide declines in Caribbean corals. *Science* **301**, 958–960 (2003).
2. Bruno, J. F. & Selig, E. R. Regional decline of coral cover in the Indo-Pacific: Timing, extent, and subregional comparisons. *PLoS One* **2**, e711 (2007).
3. De'Ath, G., Fabricius, K. E., Sweatman, H. & Puotinen, M. The 27-year decline of coral cover on the Great Barrier Reef and its causes. *Proc. Natl. Acad. Sci. U. S. A.* **109**, 17995–17999 (2012).
4. Hughes, T. P., Graham, N. A. J., Jackson, J. B. C., Mumby, P. J. & Steneck, R. S. Rising to the challenge of sustaining coral reef resilience. *Trends Ecol. Evol.* **25**, 633–642 (2010).
5. Pandolfi, J. M., Connolly, S. R., Marshall, D. J. & Cohen, A. L. Projecting coral reef futures under global warming and ocean acidification. *Science* **333**, 418–422 (2011).
6. Hughes, T. P. *et al.* Global warming and recurrent mass bleaching of corals. *Nature* **543**, 373–377 (2017).
7. Bindoff, N. L. *et al. Chapter 5: Changing Ocean, Marine Ecosystems, and Dependent Communities. IPCC Special Report on the Ocean and Cryosphere in a Changing Climate* (2019).
8. Richmond, R. H. Reproduction and recruitment in corals: critical links in the persistence of reefs. in *Life and Death of Coral Reefs* (ed. Birkeland, C. E.) 175–197 (Springer US, 1997). doi:10.1007/978-1-4615-5995-5_8.
9. Trapon, M. L., Pratchett, M. S., Hoey, A. S. & Baird, A. H. Influence of fish grazing and sedimentation on the early post-settlement survival of the tabular coral *Acropora cytherea*. *Coral Reefs* **32**, 1051–1059 (2013).
10. Gallagher, C. & Doropoulos, C. Spatial refugia mediate juvenile coral survival during coral–predator interactions. *Coral Reefs* **36**, 51–61 (2017).
11. Vermeij, M. J. A. & Sandin, S. A. Density-dependent settlement and mortality structure the earliest life phases of a coral population. *Ecology* **89**, 1994–2004 (2008).
12. Vermeij, M. J. A., Smith, J. E., Smith, C. M., Vega Thurber, R. & Sandin, S. A. Survival and settlement success of coral planulae: Independent and synergistic effects of macroalgae and microbes. *Oecologia* **159**, 325–336 (2009).
13. Ricardo, G. F., Jones, R. J., Nordborg, M. & Negri, A. P. Settlement patterns of the coral *Acropora millepora* on sediment-laden surfaces. *Sci. Total Environ.* **609**, 277–288 (2017).
14. Brunner, C. A., Uthicke, S., Ricardo, G. F., Hoogenboom, M. O. & Negri, A. P. Climate change doubles sedimentation-induced coral recruit mortality. *Sci. Total Environ.* **768**, (2021).
15. Birrell, C. L., McCook, L. J., Willis, B. L. & Diaz-Pulido, G. A. Effects of benthic algae on the replenishment of corals and the implications for the resilience of coral reefs. in *Oceanography and Marine Biology: An Annual Review* 25–63 (CRC Press, 2008).
16. Karcher, D. B. *et al.* Nitrogen eutrophication particularly promotes turf algae in coral reefs of the central Red Sea. *PeerJ* **2020**, 1–25 (2020).

17. Kirschner, C. M. & Brennan, A. B. Bio-inspired antifouling strategies. *Annu. Rev. Mater. Res.* **42**, 211–229 (2012).
18. Webster, N. S. *et al.* Metamorphosis of a scleractinian coral in response to microbial biofilms. *Appl. Environ. Microbiol.* **70**, 1213–21 (2004).
19. Heyward, A. J. & Negri, A. P. Natural inducers for coral larval metamorphosis. *Coral Reefs* **18**, 273–279 (1999).
20. Negri, A. P., Webster, N. S., Hill, R. T. & Heyward, A. J. Metamorphosis of broadcast spawning corals in response to bacteria isolated from crustose algae. *Mar. Ecol. Prog. Ser.* **223**, 121–131 (2001).
21. Tebben, J. *et al.* Induction of larval metamorphosis of the coral *Acropora millepora* by tetrabromopyrrole isolated from a Pseudoalteromonas bacterium. *PLoS One* **6**, 1–8 (2011).
22. Sneed, J. M., Sharp, K. H., Ritchie, K. B. & Paul, V. J. The chemical cue tetrabromopyrrole from a biofilm bacterium induces settlement of multiple Caribbean corals. *Proc. R. Soc. B Biol. Sci.* **281**, 1–9 (2014).
23. Tebben, J. *et al.* Chemical mediation of coral larval settlement by crustose coralline algae. *Sci. Rep.* **5**, 1–11 (2015).
24. Carpenter, R. C. & Edmunds, P. J. Local and regional scale recovery of *Diadema* promotes recruitment of scleractinian corals. *Ecol. Lett.* **9**, 268–277 (2006).
25. Box, Steve, J. & Mumby, Peter, J. Effect of macroalgal competition on growth and survival of juvenile Caribbean corals. *Mar. Ecol. Prog. Ser.* **342**, 139–149 (2007).
26. Linares, C., Cebrian, E. & Coma, R. Effects of turf algae on recruitment and juvenile survival of gorgonian corals. *Mar. Ecol. Prog. Ser.* **452**, 81–88 (2012).
27. McCook, L. J., Jompa, J. & Diaz-Pulido, G. Competition between corals and algae on coral reefs: A review of evidence and mechanisms. *Coral Reefs* **19**, 400–417 (2001).
28. Nugues, M. M., Smith, G. W., Van Hooidonk, R. J., Seabra, M. I. & Bak, R. P. M. Algal contact as a trigger for coral disease. *Ecol. Lett.* **7**, 919–923 (2004).
29. Fong, J. *et al.* Allelopathic effects of macroalgae on *Pocillopora acuta* coral larvae. *Mar. Environ. Res.* **151**, 104745; 10.1016/j.marenvres.2019.06.007 (2019).
30. Hauri, C., Fabricius, K. E., Schaffelke, B. & Humphrey, C. Chemical and physical environmental conditions underneath mat- and canopy-forming macroalgae, and their effects on understorey corals. *PLoS One* **5**, 1–9 (2010).
31. Bay, L. K. *et al. Reef Restoration and Adaptation Program : Intervention Technical Summary. A report provided to the Australian Government by the Reef Restoration and Adaptation Program*. (2019).
32. Anthony, K. R. N. *et al.* Interventions to help coral reefs under global change—A complex decision challenge. *PLoS One* **15**, 1–14 (2020).
33. Vardi, T. *et al.* Six priorities to advance the science and practice of coral reef restoration worldwide. *Restor. Ecol.* **29**, 1–7 (2021).
34. Heyward, A. J., Rees, M. & Smith, L. D. Coral spawning slicks harnessed for large-scale coral culture. *Progr. Abstr. Int. Conf. Sci. Asp. Coral Reef Assessment, Monit. Restor.* **104**, 188–189 (1999).
35. Harrison, P., Villanueva, R. & Dela Cruz, D. *Coral Reef Restoration using Mass Coral Larval Reseeding*. (2016).

36. dela Cruz, D. W. & Harrison, P. L. Enhancing coral recruitment through assisted mass settlement of cultured coral larvae. *PLoS One* **15**, e0242847; 10.1371/journal.pone.0242847 (2020).
37. Chamberland, V. F., Snowden, S., Marhaver, K. L., Petersen, D. & Vermeij, M. J. A. The reproductive biology and early life ecology of a common Caribbean brain coral, *Diploria labyrinthiformis* (Scleractinia: Faviinae). *Coral Reefs* **36**, 83–94 (2017).
38. Randall, C. J. *et al*. Sexual production of corals for reef restoration in the Anthropocene. *Mar. Ecol. Prog. Ser.* **635**, 203–232 (2020).
39. Miller, M. W. *et al*. Settlement yields in large-scale in situ culture of Caribbean coral larvae for restoration. *Restor. Ecol.* (2021) doi:10.1111/rec.13512.
40. Baria-Rodriguez, M. V., dela Cruz, D. W., Dizon, R. M., Yap, H. T. & Villanueva, R. D. Performance and cost-effectiveness of sexually produced *Acropora granulosa* juveniles compared with asexually generated coral fragments in restoring degraded reef areas. *Aquat. Conserv. Mar. Freshw. Ecosyst.* **29**, 891–900 (2019).
41. Doropoulos, C., Elzinga, J., ter Hofstede, R., van Koningsveld, M. & Babcock, R. C. Optimizing industrial-scale coral reef restoration: comparing harvesting wild coral spawn slicks and transplanting gravid adult colonies. *Restor. Ecol.* **27**, 758–767 (2019).
42. Kuffner, I. B., Andersson, A. J., Jokiel, P. L., Rodgers, K. S. & MacKenzie, F. T. Decreased abundance of crustose coralline algae due to ocean acidification. *Nat. Geosci.* **1**, 114–117 (2008).
43. Webster, N. S., Uthicke, S., Botté, E. S., Flores, F. & Negri, A. P. Ocean acidification reduces induction of coral settlement by crustose coralline algae. *Glob. Chang. Biol.* **19**, 303–315 (2013).
44. Randall, C. J., Giuliano, C., Heyward, A. J. & Negri, A. P. Enhancing Coral Survival on Deployment Devices With Microrefugia. *Front. Mar. Sci.* **8**, 662263; 10.3389/fmars.2021.662263 (2021).
45. Kuffner, I. B. *et al*. Inhibition of coral recruitment by macroalgae and cyanobacteria. *Mar. Ecol. Prog. Ser.* **323**, 107–117 (2006).
46. Arnold, S. N., Steneck, R. S. & Mumby, P. J. Running the gauntlet: Inhibitory effects of algal turfs on the processes of coral recruitment. *Mar. Ecol. Prog. Ser.* **414**, 91–105 (2010).
47. Speare, K. E., Duran, A., Miller, M. W. & Burkepile, D. E. Sediment associated with algal turfs inhibits the settlement of two endangered coral species. *Mar. Pollut. Bull.* **144**, 189–195 (2019).
48. Tebben, J., Guest, J. R., Sin, T. M., Steinberg, P. D. & Harder, T. Corals like it waxed: Paraffin-based antifouling technology enhances coral spat survival. *PLoS One* **9**, 1–8 (2014).
49. Almeida, E., Diamantino, T. C. & de Sousa, O. Marine paints: The particular case of antifouling paints. *Prog. Org. Coatings* **59**, 2–20 (2007).
50. Negri, A. P., Smith, L. D., Webster, N. S. & Heyward, A. J. Understanding ship-grounding impacts on a coral reef: Potential effects of anti-foulant paint contamination on coral recruitment. *Mar. Pollut. Bull.* **44**, 111–117 (2002).
51. Smith, L. D., Negri, A. P., Philipp, E., Webster, N. S. & Heyward, A. J. The effects of antifoulant-paint-contaminated sediments on coral recruits and branchlets. *Mar. Biol.*

**143**, 651–657 (2003).
52. Jacobson, A. H. & Willingham, G. L. Sea-nine antifoulant: An environmentally acceptable alternative to organotin antifoulants. *Sci. Total Environ.* **258**, 103–110 (2000).
53. Silva, V. *et al.* Isothiazolinone Biocides: Chemistry, Biological, and Toxicity Profiles. *Molecules* **25**, 10.3390/molecules25040991 (2020).
54. da Silva, A. R., Guerreiro, A. da S., Martins, S. E. & Sandrini, J. Z. DCOIT unbalances the antioxidant defense system in juvenile and adults of the marine bivalve Amarilladesma mactroides (Mollusca: Bivalvia). *Comp. Biochem. Physiol. Part - C Toxicol. Pharmacol.* **250**, 109169 (2021).
55. Cima, F. *et al.* Preliminary evaluation of the toxic effects of the antifouling biocide Sea-Nine 211™ in the soft coral *Sarcophyton cf. glaucum* (Octocorallia, Alcyonacea) based on PAM fluorometry and biomarkers. *Mar. Environ. Res.* **83**, 16–22 (2013).
56. Wendt, I., Backhaus, T., Blanck, H. & Arrhenius, Å. The toxicity of the three antifouling biocides DCOIT, TPBP and medetomidine to the marine pelagic copepod *Acartia tonsa*. *Ecotoxicology* **25**, 871–879 (2016).
57. Chen, L. *et al.* Identification of Molecular Targets for 4,5-Dichloro-2-n-octyl-4-isothiazolin-3-one (DCOIT) in Teleosts: New Insight into Mechanism of Toxicity. *Environ. Sci. Technol.* **51**, 1840–1847 (2017).
58. Martins, S. E., Fillmann, G., Lillicrap, A. & Thomas, K. V. Review: Ecotoxicity of organic and organo-metallic antifouling co-biocides and implications for environmental hazard and risk assessments in aquatic ecosystems. *Biofouling* **34**, 34–52 (2018).
59. Moon, Y. S., Kim, M., Hong, C. P., Kang, J. H. & Jung, J. H. Overlapping and unique toxic effects of three alternative antifouling biocides (Diuron, Irgarol 1051 ® , Sea-Nine 211 ® ) on non-target marine fish. *Ecotoxicol. Environ. Saf.* **180**, 23–32 (2019).
60. Su, Y. *et al.* Toxicity of 4,5-dichloro-2-n-octyl-4-isothiazolin-3-one (DCOIT) in the marine decapod *Litopenaeus vannamei*. *Environ. Pollut.* **251**, 708–716 (2019).
61. Fonseca, V. B., Guerreiro, A. da S., Vargas, M. A. & Sandrini, J. Z. Effects of DCOIT (4,5-dichloro-2-octyl-4-isothiazolin-3-one) to the haemocytes of mussels *Perna perna*. *Comp. Biochem. Physiol. Part C Toxicol. Pharmacol.* **232**, 108737; 10.1016/j.cbpc.2020.108737 (2020).
62. Ferreira, V. *et al.* Effects of nanostructure antifouling biocides towards a coral species in the context of global changes. *Sci. Total Environ.* **799**, 149324 (2021).
63. Campos, B. G. de *et al.* A preliminary study on multi-level biomarkers response of the tropical oyster Crassostrea brasiliana to exposure to the antifouling biocide DCOIT. *Mar. Pollut. Bull.* **174**, 113241 (2022).
64. Maia, F. *et al.* Incorporation of biocides in nanocapsules for protective coatings used in maritime applications. *Chem. Eng. J.* **270**, 150–157 (2015).
65. Dos Santos, J. V. N. *et al.* Can Encapsulation of the Biocide DCOIT Affect the Anti-Fouling Efficacy and Toxicity on Tropical Bivalves? *Appl. Sci.* **10**, 1–12 (2020).
66. Detty, M. R., Ciriminna, R., Bright, F. V. & Pagliaro, M. Environmentally Benign Sol-Gel Antifouling and Foul-Releasing Coatings. *Acc. Chem. Res.* **47**, 678–687 (2014).
67. Korschelt, K., Tahir, M. N. & Tremel, W. A Step into the Future: Applications of Nanoparticle Enzyme Mimics. *Chem. - A Eur. J.* **24**, 9703–9713 (2018).
68. Herget, K. *et al.* Haloperoxidase Mimicry by CeO2-x Nanorods Combats Biofouling.

*Adv. Mater.* **29**, 1–8 (2017).
69. Korschelt, K. *et al.* CeO2-: X nanorods with intrinsic urease-like activity. *Nanoscale* **10**, 13074–13082 (2018).
70. Herget, K., Frerichs, H., Pfitzner, F., Tahir, M. N. & Tremel, W. Functional Enzyme Mimics for Oxidative Halogenation Reactions that Combat Biofilm Formation. *Adv. Mater.* **30**, 1–28 (2018).
71. Doropoulos, C., Ward, S., Marshell, A., Diaz-Pulido, G. & Mumby, P. J. Interactions among chronic and acute impacts on coral recruits: The importance of size-escape thresholds. *Ecology* **93**, 2131–2138 (2012).
72. Ji, Z. *et al.* Designed synthesis of CeO2 nanorods and nanowires for studying toxicological effects of high aspect ratio nanomaterials. *ACS Nano* **6**, 5366–5380 (2012).
73. Herget, K. *et al.* Supporting Information: Haloperoxidase Mimicry by CeO2-x Nanorods Combats Biofouling. *Adv. Mater.* **29**, 1603823 (2017).
74. Sokolova, A. *et al.* Spontaneous multiscale phase separation within fluorinated xerogel coatings for fouling-release surfaces. *Biofouling* **28**, 143–157 (2012).
75. Schneider, C. A., Rasband, W. S. & Eliceiri, K. W. NIH Image to ImageJ: 25 years of image analysis. *Nat. Methods* **9**, 671–675 (2012).
76. ImageJ Release Notes. https://imagej.nih.gov/ij/notes.html.
77. Arganda-Carreras, I. *et al.* Trainable Weka Segmentation: A machine learning tool for microscopy pixel classification. *Bioinformatics* **33**, 2424–2426 (2017).
78. Arganda-Carreras, I. *et al.* Supplementary data: Trainable Weka Segmentation: A machine learning tool for microscopy pixel classification: Trainable Weka Segmentation User Manual. (2017) doi:10.1093/bioinformatics/btx180.
79. Vyas, N., Sammons, R. L., Addison, O., Dehghani, H. & Walmsley, A. D. A quantitative method to measure biofilm removal efficiency from complex biomaterial surfaces using SEM and image analysis. *Sci. Rep.* **6**, 2–11 (2016).
80. Carbone, D. A., Gargano, I., Pinto, G., De Natale, A. & Pollio, A. Evaluating microalgae attachment to surfaces: A first approach towards a laboratory integrated assessment. *Chem. Eng. Trans.* **57**, 73–78 (2017).
81. Moreno Osorio, J. H. *et al.* Early colonization stages of fabric carriers by two Chlorella strains. *J. Appl. Phycol.* **32**, 3631–3644 (2020).
82. Ricardo, G. F. *et al.* Impacts of water quality on *Acropora* coral settlement: The relative importance of substrate quality and light. *Sci. Total Environ.* **777**, 10.1016/j.scitotenv.2021.146079 (2021).
83. Macadam, A., Nowell, C. J. & Quigley, K. Machine learning for the fast and accurate assessment of fitness in coral early life history. *Remote Sens.* **13**, 1–17 (2021).
84. Negri, A. P. & Heyward, A. J. Inhibition of Fertilization and Larval Metamorphosis of the Coral *Acropora millepora* (Ehrenberg, 1834) by Petroleum Products. *Mar. Pollut. Bull.* **41**, 420–427 (2000).
85. Nordborg, F. M., Flores, F., Brinkman, D. L., Agustí, S. & Negri, A. P. Phototoxic effects of two common marine fuels on the settlement success of the coral *Acropora tenuis*. *Sci. Rep.* **8**, 1–12 (2018).
86. R Core Team. R: A Language and Environment for Statistical Computing. (2021).
87. Wickham, H. *et al.* Welcome to the Tidyverse. *J. Open Source Softw.* **4**, 1686;

10.21105/joss.01686 (2019).
88. Pinheiro, J., Bates, D., Debroy, S., Sarkar, D. & R Core Team. Linear and Nonlinear Mixed Effects Models Contact. *Linear nonlinear Mix. Eff. Model.* **3**, 103–135 (2021).
89. Fox, J. & Weisberg, S. *An R Companion to Applied Regression*. (Sage Publications, 2019).
90. Lenth, R. V. Emmeans: estimated marginal means. https://cran.r-project.org/package=emmeans (2021).
91. Brooks, M. E. *et al*. glmmTMB balances speed and flexibility among packages for zero-inflated generalized linear mixed modeling. *R J.* **9**, 378–400 (2017).
92. Dafforn, K. A., Lewis, J. A. & Johnston, E. L. Antifouling strategies: History and regulation, ecological impacts and mitigation. *Mar. Pollut. Bull.* **62**, 453–465 (2011).
93. Wu, R. *et al*. Room temperature synthesis of defective cerium oxide for efficient marine anti-biofouling. *Adv. Compos. Hybrid Mater.* doi.org/110.1007/s42114-021-00256-7 (2021).
94. Hu, M. *et al*. Nanozymes in Nanofibrous Mats with Haloperoxidase-like Activity to Combat Biofouling. *ACS Appl. Mater. Interfaces* **10**, 44722–44730 (2018).
95. He, X. *et al*. Haloperoxidase Mimicry by CeO2-x Nanorods of Different Aspect Ratios for Antibacterial Performance. *ACS Sustain. Chem. Eng.* **8**, 6744–6752 (2020).
96. Saxena, P. & Harish. Nanoecotoxicological Reports of Engineered Metal Oxide Nanoparticles on Algae. *Curr. Pollut. Reports* **4**, 128–142 (2018).
97. Xu, Y. *et al*. Effects of cerium oxide nanoparticles on bacterial growth and behaviors: induction of biofilm formation and stress response. *Environ. Sci. Pollut. Res.* **26**, 9293–9304 (2019).
98. Xu, Y. *et al*. Mechanistic understanding of cerium oxide nanoparticle-mediated biofilm formation in Pseudomonas aeruginosa. *Environ. Sci. Pollut. Res.* **25**, 34765–34776 (2018).
99. Tang, Y. *et al*. Hybrid xerogel films as novel coatings for antifouling and fouling release. *Biofouling* **21**, 59–71 (2005).
100. Gunari, N. *et al*. The control of marine biofouling on xerogel surfaces with nanometer-scale topography. *Biofouling* **27**, 137–149 (2011).
101. Maia, F. *et al*. Silica nanocontainers for active corrosion protection. *Nanoscale* **4**, 1287–1298 (2012).
102. Martins, R. *et al*. Effects of a novel anticorrosion engineered nanomaterial on the bivalve: *Ruditapes philippinarum*. *Environ. Sci. Nano* **4**, 1064–1076 (2017).
103. Gutner-Hoch, E. *et al*. Antimacrofouling Efficacy of Innovative Inorganic Nanomaterials Loaded with Booster Biocides. *J. Mar. Sci. Eng.* **6**, 6 (2018).
104. Negri, A. P. & Heyward, A. J. Inhibition of coral fertilisation and larval metamorphosis by tributyltin and copper. *Mar. Environ. Res.* **51**, 17–27 (2001).
105. Morse, D. E., Hooker, N., Morse, A. N. C. & Jensen, R. A. Control of larval metamorphosis and recruitment in sympatric agariciid corals. *J. Exp. Mar. Bio. Ecol.* **116**, 193–217 (1988).
106. Harrington, L., Fabricius, K., De'ath, G. & Negri, A. Recognition and Selection of Settlement Substrata Determine Post-Settlement Survival in Corals. *Ecology* **85**, 3428–3437 (2004).

107. Jorissen, H., Baumgartner, C., Steneck, R. S. & Nugues, M. M. Contrasting effects of crustose coralline algae from exposed and subcryptic habitats on coral recruits. *Coral Reefs* **39**, 1767–1778 (2020).
108. Figueiredo, J. *et al*. Toxicity of innovative anti-fouling nano-based solutions to marine species. *Environ. Sci. Nano* **6**, 1418–1429 (2019).
109. Shafir, S., Abady, S. & Rinkevich, B. Improved sustainable maintenance for mid-water coral nursery by the application of an anti-fouling agent. *J. Exp. Mar. Bio. Ecol.* **368**, 124–128 (2009).

## Acknowledgements

The authors would like to thank Constanze von Waldthausen, Sebastian Flotow and Christian Brandt for their technical support at ZMT and Florita Flores for her guidance and lab support at AIMS. The authors also thank the staff at the National Sea Simulator at AIMS for assistance with experimental setup and field collections. We acknowledge the Bindal People as the Traditional Owners where this work took place. We pay our respects to their Elders past, present and emerging and we acknowledge their continuing spiritual connection to their land and sea country. This work was partially funded by the Australian Institute of Marine Science, the University of Bremen and graduate school GLOMAR, the BMWK (Federal Ministry for Economic Affairs and Climate Action—ZIM program) and the DSM (German Foundation Marine Conservation) and was supported by the Reef Restoration and Adaptation Program which is funded by the partnership between the Australian Governments Reef Trust and the Great Barrier Reef Foundation.

## Author contributions

L.K.R. conceptualized and coordinated the study, with guidance provided by D.B., U.S., C.J.R., A.P.N. and A.K.; L.K.R. and D.B. performed the experiments, analyzed the data and prepared figures/tables; L.K.R. wrote the manuscript with input from U.S. and D.B.; C.J.R. and A.P.N. substantively revised the manuscript; all authors read and approved the manuscript.

## Supplementary Information (SI)

### SI Materials and Methods

#### $CeO_{2-x}$ nanoparticle coating

(i) The production of nanoparticles

An aqueous solution of NaOH (100 mL, 9.0 M, 37.8 g) was directly poured into a rapidly stirred solution of cerium(III) nitrate hexahydrate (20 mL, 5.2 g, 0.05 M) in MilliQ-water. After being vigorously stirred for 30 min, the lilac suspension was transferred into a stainless steel autoclave with Teflon insert (total volume: 300 mL) and heated to 100 °C for 24 hours. The lilac product was separated from the turbid suspension by centrifugation (3000 rpm, 10 min) and washed two times with MilliQ-water (15 mL each). After drying at 60 °C overnight, the resulting yellow product was ground in a vibrating ball mill for two minutes at 30 rpm. The milling yielded agglomerates of the size < 20 $\mu$m.

(ii) The catalytic activity testing

For catalytic activity testing, 25 $\mu$g of NPs in 1 mL MilliQ-water were mixed with a vortex oscillator for 3 sec and exposed to ultrasound (Bandelin electronic GmbH & Co. KG, SONOPULS HD 2070.2 Homogenisator with MS 72) twice (15 sec each). The catalytic haloperoxidase-like activity of the NPs was successfully demonstrated using the phenol red (PR; Sigma Aldrich; CAS 143-74-8) bromination assay following the methods and optimized parameters in Table S3 in Herget *et al*. (2017) [1,2]. Spectrophotometrically measured samples containing $CeO_{2-x}$ NPs[a], PR[b], $NH_4Br$ (Sigma Aldrich; CAS 12124-97-9)[c] and $H_2O_2$ (Sigma Aldrich; CAS 7722-84-1)[d] were added up to a volume of 300 $\mu$l (7 $\mu$l[a], 47 $\mu$l[b], 186 $\mu$l[c], 60 $\mu$l [d]).

(iii) The production of coating solution A

Prior to coating, the plugs were cleaned with ethanol and activated using microwave plasma (as above). Two different coating solutions were produced. Coating solution A was made from 100 mL of tetraethoxysilane (TEOS) and mixed with 420 mL of ethanol (96%) and 20 mL of 0.01 M HCl and stirred overnight at room temperature for hydrolysis. An acidic silica nano-sol with a solids content of about 6 wt% was formed.

(iiii) The production of coating solution B

Coating solution B was made from 75 g tetraethoxysilane (TEOS), 25 g 3-glycidyloxypropyltriethoxysilane (GLYEO), 420 mL ethanol (96%) and 20 mL 0.01 M HCl and stirred overnight at room temperature for hydrolysis. The solids content of coating solution B was also about 6 wt%. 30 mL (= 1.8 g $SiO_2$) of each coating solution was mixed with 1 g of ceria (cerium dioxide) powder. Before adding the ceria NPs to the sols, the ceria powder was dispersed in MilliQ-water and the pH was adjusted to 7.5 with 1N HCl. A pH of about 5 was reached at which the ready-to-coat sols had a sufficient pot life of 1-2 days.

SI Figures

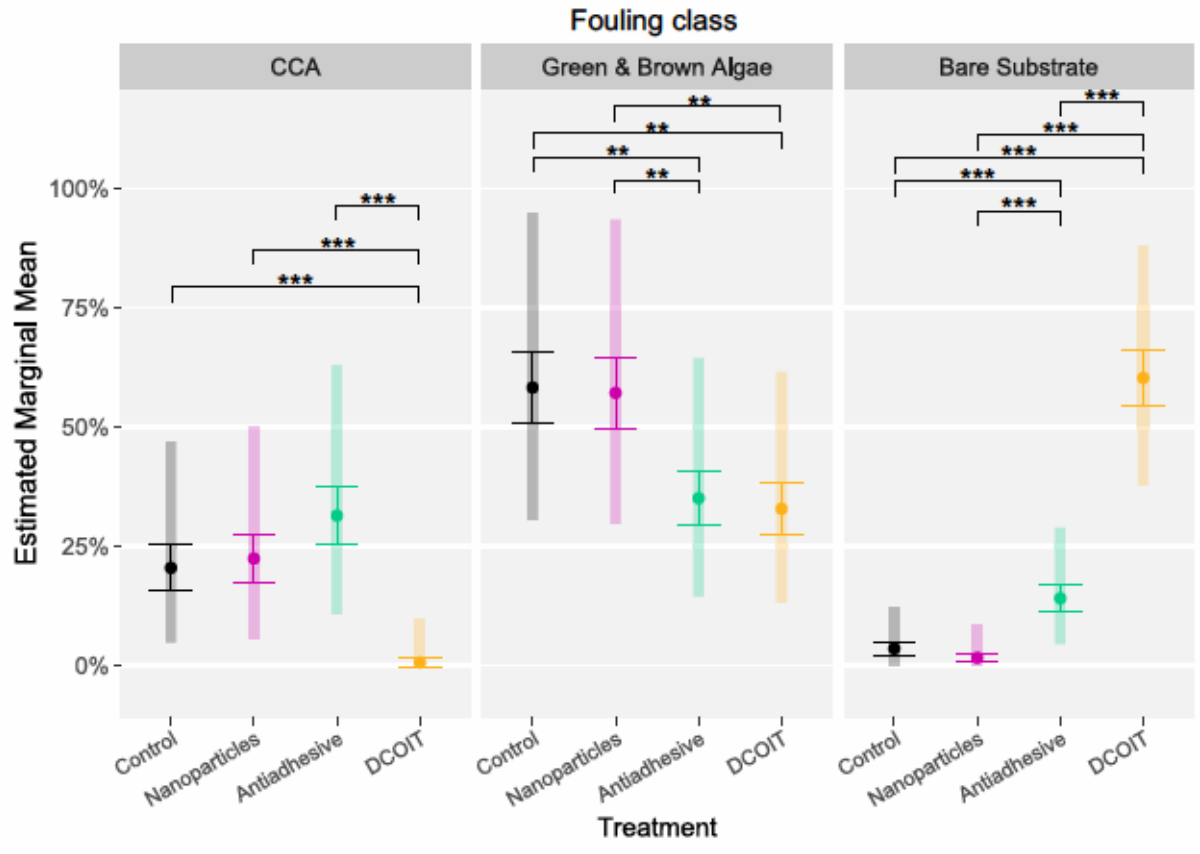


**Figure S2.1**: Estimated marginal means, SE and upper and lower confidence levels (CL) of the fouling classes on the fully-coated (FC) plugs after 37 days. Estimates were back-transformed from the square-root scale. Asterisks indicate statistically significant differences of pairwise post-hoc tests based on estimated marginal means (**Supplementary Table S2.2** and **Table S2.3**; *p < 0.05, **p < 0.01, ***p < 0.001).

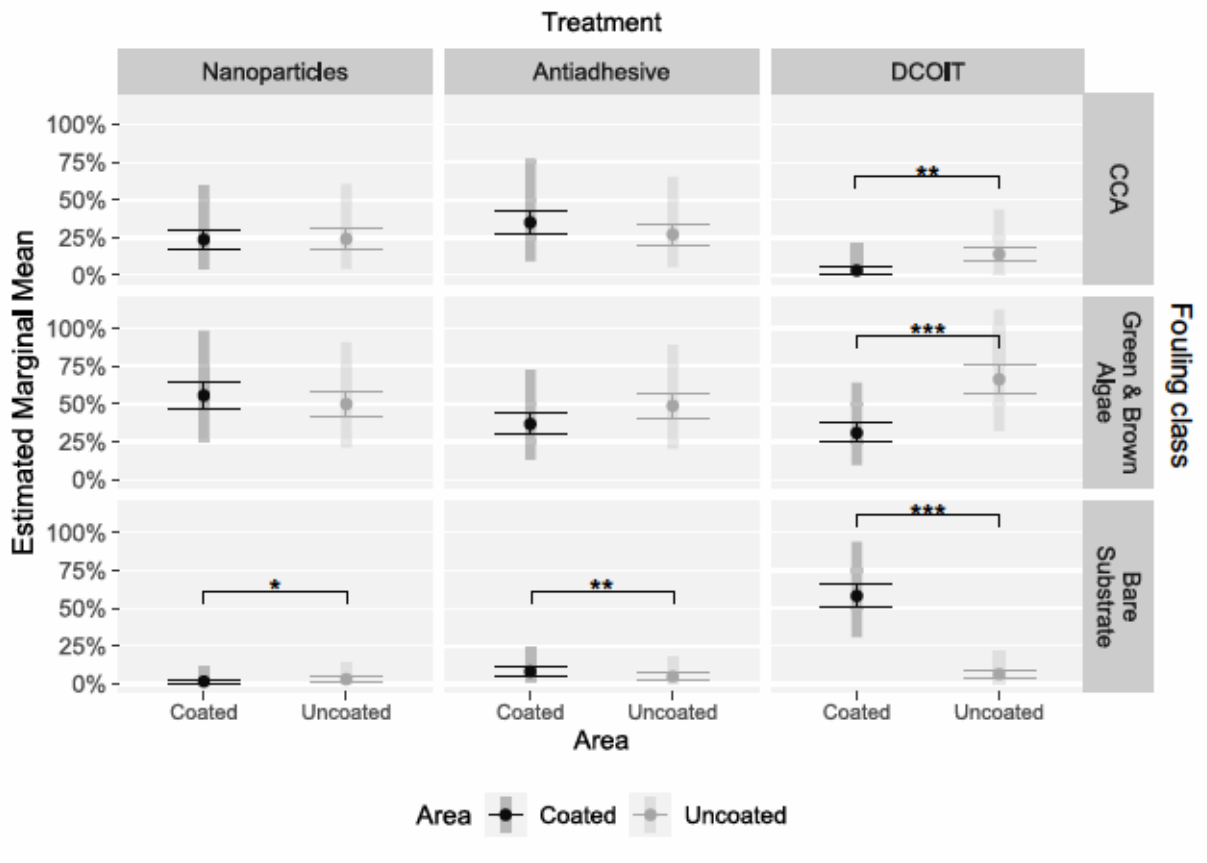


**Figure S2.2**: Estimated marginal means, SE and confidence levels of the fouling classes per area (coated/uncoated) on the partially-coated (PC) plugs after 37 days. Estimated were back-transformed from the square-root scale. Asterisks indicate statistically significant differences of pairwise post-hoc tests based on estimated marginal means (**Supplementary Table S2.5** and **Table S2.7**; *p < 0.05, **p < 0.01, ***p < 0.001).

## SI Tables

**Table S2.1**: Summary statistics of fouling coverage data for each fouling class (CCA, green/brown algae, bare substrate) and treatment (Control, Nanoparticles, Antiadhesive, DCOIT) combination at each monitoring period (9, 23, 37 days) on the fully-coated (FC) plugs. Values represent mean percent fouling coverage (%). N (= 45) corresponds to the number of plugs in each treatment measured repeatedly for each monitoring period.

| Fouling class | Days | Treatment | Mean fouling coverage | Standard error |
|---|---|---|---|---|
| CCA | 9 | Control | 0.5 | 0.1 |
| CCA | 23 | Control | 26.5 | 4.2 |
| CCA | 37 | Control | 30.7 | 5.2 |
| Green/brown Algae | 9 | Control | 50.4 | 5.1 |
| Green/brown Algae | 23 | Control | 66 | 4.8 |
| Green/brown Algae | 37 | Control | 64.8 | 5.1 |
| Bare Substrate | 9 | Control | 49.1 | 5.1 |
| Bare Substrate | 23 | Control | 7.5 | 1.1 |
| Bare Substrate | 37 | Control | 4.5 | 0.6 |
| CCA | 9 | Nanoparticles | 0.3 | 0 |
| CCA | 23 | Nanoparticles | 25.3 | 4.3 |
| CCA | 37 | Nanoparticles | 32.8 | 5.4 |
| Green/brown Algae | 9 | Nanoparticles | 54.7 | 5.4 |
| Green/brown Algae | 23 | Nanoparticles | 67 | 5 |
| Green/brown Algae | 37 | Nanoparticles | 65 | 5.3 |
| Bare Substrate | 9 | Nanoparticles | 45.1 | 5.5 |
| Bare Substrate | 23 | Nanoparticles | 7.7 | 1.6 |
| Bare Substrate | 37 | Nanoparticles | 2.3 | 0.4 |
| CCA | 9 | Antiadhesive | 0.4 | 0.1 |
| CCA | 23 | Antiadhesive | 22.1 | 3.3 |
| CCA | 37 | Antiadhesive | 40.3 | 5.3 |
| Green/brown Algae | 9 | Antiadhesive | 27.8 | 4.9 |
| Green/brown Algae | 23 | Antiadhesive | 40.8 | 4.7 |
| Green/brown Algae | 37 | Antiadhesive | 42.3 | 4.5 |
| Bare Substrate | 9 | Antiadhesive | 71.8 | 4.9 |
| Bare Substrate | 23 | Antiadhesive | 37.1 | 4.2 |
| Bare Substrate | 37 | Antiadhesive | 17.4 | 2.2 |
| CCA | 9 | DCOIT | 0.1 | 0 |
| CCA | 23 | DCOIT | 1.8 | 0.8 |
| CCA | 37 | DCOIT | 1.1 | 0.3 |
| Green/brown Algae | 9 | DCOIT | 38.3 | 5 |
| Green/brown Algae | 23 | DCOIT | 25.6 | 4.9 |
| Green/brown Algae | 37 | DCOIT | 36.2 | 3.4 |
| Bare Substrate | 9 | DCOIT | 61.6 | 5 |
| Bare Substrate | 23 | DCOIT | 72.5 | 5.2 |
| Bare Substrate | 37 | DCOIT | 62.8 | 3.3 |

**Table S2.2:** Estimated marginal means (EMM), standard error (SE), degrees of freedom (df) and upper and lower confidence levels (CL) of each fouling class (CCA, green/brown algae, bare substrate) and treatment (Control, Nanoparticles, Antiadhesive, DCOIT) combination after 37 days on the fully-coated (FC) plugs. Intervals (EMM, SE, CL) were back-transformed from the square-root scale.

| Treatment | Fouling class | EMM | Standard error | df | Lower CL | Upper CL |
|---|---|---|---|---|---|---|
| Control | CCA | 20.4 | 4.9 | 2 | 4.8 | 47 |
| Nanoparticles | CCA | 22.4 | 5.1 | 2 | 5.8 | 49.9 |
| Antiadhesive | CCA | 31.4 | 6.1 | 2 | 10.7 | 63 |
| DCOIT | CCA | 0.6 | 0.9 | 2 | 0 | 9.7 |
| Control | Green/brown Algae | 58.2 | 7.5 | 2 | 30.5 | 94.9 |
| Nanoparticles | Green/brown Algae | 57.1 | 7.4 | 2 | 29.7 | 93.5 |
| Antiadhesive | Green/brown Algae | 35 | 5.8 | 2 | 14.5 | 64.5 |
| DCOIT | Green/brown Algae | 32.8 | 5.6 | 2 | 13.1 | 61.5 |
| Control | Bare Substrate | 3.5 | 1.4 | 2 | 0.1 | 12.3 |
| Nanoparticles | Bare Substrate | 1.6 | 1 | 2 | 0 | 8.3 |
| Antiadhesive | Bare Substrate | 14.1 | 2.8 | 2 | 4.5 | 28.9 |
| DCOIT | Bare Substrate | 60.3 | 5.9 | 2 | 37.7 | 88.1 |

**Table S2.3**: Results of pairwise post-hoc tests of fouling coverage data after 37 days on the fully-coated (FC) plugs based on estimated marginal means. Fouling coverage was compared between treatments (Control, Nanoparticles, Antiadhesive, DCOIT), within fouling classes (CCA, green/brown algae, bare substrate). Note that the estimated contrasts are on the square-root scale. Tests were performed on the square-root scale. The p-value was adjusted for multiple comparisons (family of 4 estimates) with the Tukey method. Significant codes indicate: * < 0.05, ** < 0.01, *** < 0.001.

| Compared treatment pair | Fouling class | Estimated contrast | Standard error | df | t ratio | p-value |
|---|---|---|---|---|---|---|
| Control - Nanoparticles | CCA | -0.2 | 0.6 | 526 | -0.347 | 0.986 |
| Control - Antiadhesive | CCA | -1.1 | 0.6 | 526 | -1.774 | 0.287 |
| Control - DCOIT | CCA | 3.7 | 0.6 | 526 | 6.127 | < 0.001 *** |
| Nanoparticles - Antiadhesive | CCA | -0.9 | 0.6 | 526 | -1.427 | 0.483 |
| Nanoparticles - DCOIT | CCA | 3.9 | 0.6 | 526 | 6.474 | < 0.001 *** |
| Antiadhesive - DCOIT | CCA | 4.8 | 0.6 | 526 | 7.901 | < 0.001 *** |
| Control - Nanoparticles | Green/brown Algae | 0.1 | 0.5 | 526 | 0.142 | 0.999 |
| Control - Antiadhesive | Green/brown Algae | 1.7 | 0.5 | 526 | 3.317 | 0.005 ** |
| Control - DCOIT | Green/brown Algae | 1.9 | 0.5 | 526 | 3.684 | 0.001 ** |
| Nanoparticles - Antiadhesive | Green/brown Algae | 1.6 | 0.5 | 526 | 3.175 | 0.009 ** |
| Nanoparticles - DCOIT | Green/brown Algae | 1.8 | 0.5 | 526 | 3.542 | 0.002 ** |
| Antiadhesive - DCOIT | Green/brown Algae | 0.2 | 0.5 | 526 | 0.367 | 0.983 |
| Control - Nanoparticles | Bare Substrate | 0.6 | 0.3 | 526 | 2.351 | 0.088 |
| Control - Antiadhesive | Bare Substrate | -1.9 | 0.3 | 526 | -7.087 | < 0.001 *** |
| Control - DCOIT | Bare Substrate | -5.9 | 0.3 | 526 | -22.318 | < 0.001 *** |
| Nanoparticles - Antiadhesive | Bare Substrate | -2.5 | 0.3 | 526 | -9.438 | < 0.001 *** |
| Nanoparticles - DCOIT | Bare Substrate | -6.5 | 0.3 | 526 | -24.669 | < 0.001 *** |
| Antiadhesive - DCOIT | Bare Substrate | -4 | 0.3 | 526 | -15.231 | < 0.001 *** |

**Table S2.4**: Results of full pairwise post-hoc tests of fouling coverage data after 37 days on the fully-coated (FC) plugs based on estimated marginal means. Fouling coverage was compared between all treatments (Control, Nanoparticles, Antiadhesive, DCOIT) and fouling class (CCA, green/brown algae, bare substrate) combinations. Note that the estimated contrasts are on the square-root scale. Tests were performed on the square-root scale. The p-value was adjusted for multiple comparisons (family of 12 estimates) with the Tukey method. Significant codes indicate: * < 0.05, ** < 0.01, *** < 0.001.

| Compared treatment-fouling class pair | Estimated contrast | Standard error | df | t ratio | p-value |
|---|---|---|---|---|---|
| Control CCA - Nanoparticles CCA | -0.2 | 0.6 | 526 | -0.347 | 1 |
| Control CCA - Antiadhesive CCA | -1.1 | 0.6 | 526 | -1.774 | 0.831 |
| Control CCA - DCOIT CCA | 3.7 | 0.6 | 526 | 6.127 | < 0.001 *** |
| Control CCA - Control Green/brown Algae | -3.1 | 0.6 | 526 | -5.504 | < 0.001 *** |
| Control CCA - Nanoparticles Green/brown Algae | -3 | 0.6 | 526 | -5.375 | < 0.001 *** |
| Control CCA - Antiadhesive Green/brown Algae | -1.4 | 0.6 | 526 | -2.474 | 0.359 |
| Control CCA - DCOIT Green/brown Algae | -1.2 | 0.6 | 526 | -2.139 | 0.595 |
| Control CCA - Control Bare Substrate | 2.6 | 0.5 | 526 | 5.617 | < 0.001 *** |
| Control CCA - Nanoparticles Bare Substrate | 3.3 | 0.5 | 526 | 6.935 | < 0.001 *** |
| Control CCA - Antiadhesive Bare Substrate | 0.8 | 0.5 | 526 | 1.643 | 0.892 |
| Control CCA - DCOIT Bare Substrate | -3.2 | 0.5 | 526 | -6.899 | < 0.001 *** |
| Nanoparticles CCA - Antiadhesive CCA | -0.9 | 0.6 | 526 | -1.427 | 0.958 |
| Nanoparticles CCA - DCOIT CCA | 3.9 | 0.6 | 526 | 6.474 | < 0.001 *** |
| Nanoparticles CCA - Control Green/brown Algae | -2.9 | 0.6 | 526 | -5.13 | < 0.001 *** |
| Nanoparticles CCA - Nanoparticles Green/brown Algae | -2.8 | 0.6 | 526 | -5 | < 0.001 *** |
| Nanoparticles CCA - Antiadhesive Green/brown Algae | -1.2 | 0.6 | 526 | -2.099 | 0.624 |
| Nanoparticles CCA - DCOIT Green/brown Algae | -1 | 0.6 | 526 | -1.764 | 0.837 |
| Nanoparticles CCA - Control Bare Substrate | 2.9 | 0.5 | 526 | 6.067 | < 0.001 *** |
| Nanoparticles CCA - Nanoparticles Bare Substrate | 3.5 | 0.5 | 526 | 7.386 | < 0.001 *** |
| Nanoparticles CCA - Antiadhesive Bare Substrate | 1 | 0.5 | 526 | 2.094 | 0.628 |
| Nanoparticles CCA - DCOIT Bare Substrate | -3 | 0.5 | 526 | -6.448 | < 0.001 *** |
| Antiadhesive CCA - DCOIT CCA | 4.8 | 0.6 | 526 | 7.901 | < 0.001 *** |
| Antiadhesive CCA - Control Green/brown Algae | -2 | 0.6 | 526 | -3.589 | 0.019 * |
| Antiadhesive CCA - Nanoparticles Green/brown Algae | -2 | 0.6 | 526 | -3.46 | 0.029 * |
| Antiadhesive CCA - Antiadhesive Green/brown Algae | -0.3 | 0.6 | 526 | -0.559 | 1 |
| Antiadhesive CCA - DCOIT Green/brown Algae | -0.1 | 0.6 | 526 | -0.223 | 1 |
| Antiadhesive CCA - Control Bare Substrate | 3.7 | 0.5 | 526 | 7.92 | < 0.001 *** |
| Antiadhesive CCA - Nanoparticles Bare Substrate | 4.3 | 0.5 | 526 | 9.239 | < 0.001 *** |
| Antiadhesive CCA - Antiadhesive Bare Substrate | 1.9 | 0.5 | 526 | 3.946 | 0.005 ** |
| Antiadhesive CCA - DCOIT Bare Substrate | -2.2 | 0.5 | 526 | -4.595 | < 0.001 *** |
| DCOIT CCA - Control Green/brown Algae | -6.8 | 0.6 | 526 | -12.118 | < 0.001 *** |
| DCOIT CCA - Nanoparticles Green/brown Algae | -6.8 | 0.6 | 526 | -11.989 | < 0.001 *** |
| DCOIT CCA - Antiadhesive Green/brown Algae | -5.1 | 0.6 | 526 | -9.088 | < 0.001 *** |
| DCOIT CCA - DCOIT Green/brown Algae | -4.9 | 0.6 | 526 | -8.752 | < 0.001 *** |
| DCOIT CCA - Control Bare Substrate | -1.1 | 0.5 | 526 | -2.337 | 0.451 |
| DCOIT CCA - Nanoparticles Bare Substrate | -0.5 | 0.5 | 526 | -1.019 | 0.997 |
| DCOIT CCA - Antiadhesive Bare Substrate | -3 | 0.5 | 526 | -6.311 | < 0.001 *** |
| DCOIT CCA - DCOIT Bare Substrate | -7 | 0.5 | 526 | -14.853 | < 0.001 *** |

| | | | | | |
|---|---|---|---|---|---|
| Control Green & Brown Algae - Nanoparticles Green/brown Algae | 0.1 | 0.5 | 526 | 0.142 | 1 |
| Control Green & Brown Algae - Antiadhesive Green/brown Algae | 1.7 | 0.5 | 526 | 3.317 | 0.045 * |
| Control Green & Brown Algae - DCOIT Green/brown Algae | 1.9 | 0.5 | 526 | 3.684 | 0.013 * |
| Control Green & Brown Algae - Control Bare Substrate | 5.7 | 0.4 | 526 | 14.028 | < 0.001 *** |
| Control Green & Brown Algae - Nanoparticles Bare Substrate | 6.4 | 0.4 | 526 | 15.54 | < 0.001 *** |
| Control Green & Brown Algae - Antiadhesive Bare Substrate | 3.9 | 0.4 | 526 | 9.472 | < 0.001 *** |
| Control Green & Brown Algae - DCOIT Bare Substrate | -0.1 | 0.4 | 526 | -0.319 | 1 |
| Nanoparticles Green/brown Algae - Antiadhesive Green/brown Algae | 1.6 | 0.5 | 526 | 3.175 | 0.069 |
| Nanoparticles Green/brown Algae - DCOIT Green/brown Algae | 1.8 | 0.5 | 526 | 3.542 | 0.022 * |
| Nanoparticles Green/brown Algae - Control Bare Substrate | 5.7 | 0.4 | 526 | 13.85 | < 0.001 *** |
| Nanoparticles Green/brown Algae - Nanoparticles Bare Substrate | 6.3 | 0.4 | 526 | 15.361 | < 0.001 *** |
| Nanoparticles Green/brown Algae - Antiadhesive Bare Substrate | 3.8 | 0.4 | 526 | 9.294 | < 0.001 *** |
| Nanoparticles Green/brown Algae - DCOIT Bare Substrate | -0.2 | 0.4 | 526 | -0.498 | 1 |
| Antiadhesive Green/brown Algae - DCOIT Green/brown Algae | 0.2 | 0.5 | 526 | 0.367 | 1 |
| Antiadhesive Green/brown Algae - Control Bare Substrate | 4 | 0.4 | 526 | 9.85 | < 0.001 *** |
| Antiadhesive Green/brown Algae - Nanoparticles Bare Substrate | 4.7 | 0.4 | 526 | 11.362 | < 0.001 *** |
| Antiadhesive Green/brown Algae - Antiadhesive Bare Substrate | 2.2 | 0.4 | 526 | 5.295 | < 0.001 *** |
| Antiadhesive Green/brown Algae - DCOIT Bare Substrate | -1.8 | 0.4 | 526 | -4.497 | < 0.001 *** |
| DCOIT Green/brown Algae - Control Bare Substrate | 3.8 | 0.4 | 526 | 9.388 | < 0.001 *** |
| DCOIT Green/brown Algae - Nanoparticles Bare Substrate | 4.5 | 0.4 | 526 | 10.899 | < 0.001 *** |
| DCOIT Green/brown Algae - Antiadhesive Bare Substrate | 2 | 0.4 | 526 | 4.832 | < 0.001 *** |
| DCOIT Green/brown Algae - DCOIT Bare Substrate | -2 | 0.4 | 526 | -4.96 | < 0.001 *** |
| Control Bare Substrate - Nanoparticles Bare Substrate | 0.6 | 0.3 | 526 | 2.351 | 0.441 |
| Control Bare Substrate - Antiadhesive Bare Substrate | -1.9 | 0.3 | 526 | -7.087 | < 0.001 *** |
| Control Bare Substrate - DCOIT Bare Substrate | -5.9 | 0.3 | 526 | -22.318 | < 0.001 *** |
| Nanoparticles Bare Substrate - Antiadhesive Bare Substrate | -2.5 | 0.3 | 526 | -9.438 | < 0.001 *** |
| Nanoparticles Bare Substrate - DCOIT Bare Substrate | -6.5 | 0.3 | 526 | -24.669 | < 0.001 *** |

| | | | | | |
|---|---|---|---|---|---|
| Antiadhesive Bare Substrate - DCOIT Bare Substrate | -4 | 0.3 | 526 | -15.231 | < 0.001 *** |

**Table S2.5**: Summary statistics of fouling coverage data for each fouling class (CCA, green/brown algae, bare substrate), treatment (Nanoparticles, Antiadhesive, DCOIT) and area (coated/uncoated) combination at each monitoring period (9, 23, 37 days) on the partially-coated (PC) plugs. Values represent mean percent fouling coverage (%) per area. N (= 45) corresponds to the number of plugs in each treatment measured repeatedly for each monitoring period.

| Fouling class | Days | Treatment | Area | Mean fouling coverage | Standard error |
|---|---|---|---|---|---|
| CCA | 9 | Nanoparticles | Coated | 0.4 | 0.1 |
| CCA | 9 | Nanoparticles | Uncoated | 0.4 | 0.1 |
| CCA | 23 | Nanoparticles | Coated | 24.1 | 4.3 |
| CCA | 23 | Nanoparticles | Uncoated | 27.2 | 4.4 |
| CCA | 37 | Nanoparticles | Coated | 34.1 | 5.6 |
| CCA | 37 | Nanoparticles | Uncoated | 36.1 | 5.7 |
| Green/brown Algae | 9 | Nanoparticles | Coated | 60.8 | 5.7 |
| Green/brown Algae | 9 | Nanoparticles | Uncoated | 51.5 | 5.4 |
| Green/brown Algae | 23 | Nanoparticles | Coated | 68 | 4.8 |
| Green/brown Algae | 23 | Nanoparticles | Uncoated | 62.5 | 5.3 |
| Green/brown Algae | 37 | Nanoparticles | Coated | 63.6 | 5.5 |
| Green/brown Algae | 37 | Nanoparticles | Uncoated | 59 | 5.5 |
| Bare Substrate | 9 | Nanoparticles | Coated | 38.9 | 5.6 |
| Bare Substrate | 9 | Nanoparticles | Uncoated | 48.1 | 5.4 |
| Bare Substrate | 23 | Nanoparticles | Coated | 7.9 | 2.4 |
| Bare Substrate | 23 | Nanoparticles | Uncoated | 10.3 | 2.5 |
| Bare Substrate | 37 | Nanoparticles | Coated | 2.3 | 0.5 |
| Bare Substrate | 37 | Nanoparticles | Uncoated | 4.9 | 1.1 |
| CCA | 9 | Antiadhesive | Coated | 0.7 | 0.1 |
| CCA | 9 | Antiadhesive | Uncoated | 0.8 | 0.2 |
| CCA | 23 | Antiadhesive | Coated | 29.3 | 4.6 |
| CCA | 23 | Antiadhesive | Uncoated | 29.5 | 4.6 |
| CCA | 37 | Antiadhesive | Coated | 43.9 | 5.5 |
| CCA | 37 | Antiadhesive | Uncoated | 37.4 | 5.4 |
| Green/brown Algae | 9 | Antiadhesive | Coated | 30.5 | 5.5 |
| Green/brown Algae | 9 | Antiadhesive | Uncoated | 42.8 | 5 |
| Green/brown Algae | 23 | Antiadhesive | Coated | 49 | 4.9 |
| Green/brown Algae | 23 | Antiadhesive | Uncoated | 57.6 | 5 |
| Green/brown Algae | 37 | Antiadhesive | Coated | 45.1 | 5 |
| Green/brown Algae | 37 | Antiadhesive | Uncoated | 56.5 | 5.2 |
| Bare Substrate | 9 | Antiadhesive | Coated | 68.8 | 5.5 |
| Bare Substrate | 9 | Antiadhesive | Uncoated | 56.5 | 5 |
| Bare Substrate | 23 | Antiadhesive | Coated | 21.7 | 2.8 |
| Bare Substrate | 23 | Antiadhesive | Uncoated | 12.9 | 1.6 |
| Bare Substrate | 37 | Antiadhesive | Coated | 11 | 1.8 |
| Bare Substrate | 37 | Antiadhesive | Uncoated | 6.1 | 0.9 |
| CCA | 9 | DCOIT | Coated | 0.1 | 0 |
| CCA | 9 | DCOIT | Uncoated | 0.2 | 0 |
| CCA | 23 | DCOIT | Coated | 2.9 | 1.6 |

| | | | | | |
|---|---|---|---|---|---|
| CCA | 23 | DCOIT | Uncoated | 22.4 | 3.4 |
| CCA | 37 | DCOIT | Coated | 5.2 | 1.3 |
| CCA | 37 | DCOIT | Uncoated | 22.5 | 4 |
| Green/brown Algae | 9 | DCOIT | Coated | 33.3 | 4.6 |
| Green/brown Algae | 9 | DCOIT | Uncoated | 62 | 5.8 |
| Green/brown Algae | 23 | DCOIT | Coated | 30.6 | 4.6 |
| Green/brown Algae | 23 | DCOIT | Uncoated | 66.5 | 3.6 |
| Green/brown Algae | 37 | DCOIT | Coated | 33.9 | 3.3 |
| Green/brown Algae | 37 | DCOIT | Uncoated | 69.4 | 3.9 |
| Bare Substrate | 9 | DCOIT | Coated | 66.5 | 4.6 |
| Bare Substrate | 9 | DCOIT | Uncoated | 37.8 | 5.8 |
| Bare Substrate | 23 | DCOIT | Coated | 66.5 | 4.9 |
| Bare Substrate | 23 | DCOIT | Uncoated | 11.1 | 1.5 |
| Bare Substrate | 37 | DCOIT | Coated | 60.9 | 3.3 |
| Bare Substrate | 37 | DCOIT | Uncoated | 8.1 | 1.2 |

**Table S2.6**: Estimated marginal means (EMM), standard error (SE), degrees of freedom (df) and upper and lower confidence levels (CL) of each area (coated/uncoated), treatment (Nanoparticles, Antiadhesive, DCOIT) and fouling class (CCA, green/brown algae, bare substrate) combination after 37 days on the areas (coated vs. uncoated) of the partially-coated (PC) plugs. Intervals (EMM, SE, CL) were back-transformed from the square-root scale.

| Area | Treatment | Fouling class | EMM | Standard error | df | Lower CL | Upper CL |
|---|---|---|---|---|---|---|---|
| Coated | Nanoparticles | CCA | 23.7 | 6.5 | 2 | 4 | 59.7 |
| Uncoated | Nanoparticles | CCA | 24.1 | 6.5 | 2 | 4.2 | 60.4 |
| Coated | Antiadhesive | CCA | 35 | 7.9 | 2 | 9.3 | 77 |
| Uncoated | Antiadhesive | CCA | 27 | 6.9 | 2 | 5.5 | 65 |
| Coated | DCOIT | CCA | 3.1 | 2.4 | 2 | 0 | 21.5 |
| Uncoated | DCOIT | CCA | 14 | 5 | 2 | 0.8 | 43.5 |
| Coated | Nanoparticles | Green/brown Algae | 55.6 | 8.5 | 2 | 25 | 98.3 |
| Uncoated | Nanoparticles | Green/brown Algae | 50 | 8.1 | 2 | 21.3 | 90.8 |
| Coated | Antiadhesive | Green/brown Algae | 36.7 | 6.9 | 2 | 13 | 72.6 |
| Uncoated | Antiadhesive | Green/brown Algae | 48.8 | 8 | 2 | 20.5 | 89.2 |
| Coated | DCOIT | Green/brown Algae | 30.8 | 6.3 | 2 | 9.6 | 64.2 |
| Uncoated | DCOIT | Green/brown Algae | 66.3 | 9.3 | 2 | 32.3 | 112.4 |
| Coated | Nanoparticles | Bare Substrate | 1.5 | 1.2 | 2 | 0 | 10.8 |
| Uncoated | Nanoparticles | Bare Substrate | 2.9 | 1.6 | 2 | 0 | 14.3 |
| Coated | Antiadhesive | Bare Substrate | 8.1 | 2.7 | 2 | 0.6 | 24.1 |
| Uncoated | Antiadhesive | Bare Substrate | 4.7 | 2.1 | 2 | 0 | 18 |
| Coated | DCOIT | Bare Substrate | 58.1 | 7.3 | 2 | 30.8 | 94 |
| Uncoated | DCOIT | Bare Substrate | 6.3 | 2.4 | 2 | 0.2 | 21 |

**Table S2.7**: Results of pairwise post-hoc tests of fouling coverage data (CCA, green/brown algae, bare substrate) after 37 days on the partially-coated (PC) plugs based on estimated marginal means. Fouling coverage was compared between areas (coated/uncoated), within treatment (Nanoparticles, Antiadhesive, DCOIT) and fouling class (CCA, green/brown algae, bare substrate). Note that the estimated contrasts are on the square-root scale. Tests were performed on the square-root scale. Significant codes indicate: * < 0.05, ** < 0.01, *** < 0.001.

| Compared treatment-area pair | Fouling class | Estimated contrast | Standard error | df | t ratio | p-value |
|---|---|---|---|---|---|---|
| Nanoparticles: Coated - Uncoated | CCA | 0 | 0.7 | 790 | -0.064 | 0.949 |
| Antiadhesive: Coated - Uncoated | CCA | 0.7 | 0.7 | 790 | 1.029 | 0.304 |
| DCOIT: Coated - Uncoated | CCA | -2 | 0.7 | 790 | -2.828 | 0.005 ** |
| Nanoparticles: Coated - Uncoated | Green/brown Algae | 0.4 | 0.5 | 790 | 0.779 | 0.436 |
| Antiadhesive: Coated - Uncoated | Green/brown Algae | -0.9 | 0.5 | 790 | -1.844 | 0.066 |
| DCOIT: Coated - Uncoated | Green/brown Algae | -2.6 | 0.5 | 790 | -5.167 | < 0.001 *** |
| Nanoparticles: Coated - Uncoated | Bare Substrate | -0.5 | 0.3 | 790 | -1.968 | 0.049 * |
| Antiadhesive: Coated - Uncoated | Bare Substrate | 0.7 | 0.3 | 790 | 2.647 | 0.008 ** |
| DCOIT: Coated - Uncoated | Bare Substrate | 5.1 | 0.3 | 790 | 20.395 | < 0.001 *** |

**Table S2.8**: Results of full pairwise post-hoc tests of fouling coverage data after 37 days on the partially-coated (PC) plugs based on estimated marginal means. Fouling coverage was compared between all area (coated/uncoated), treatment (Nanoparticles, Antiadhesive, DCOIT) and fouling class (CCA, green/brown algae, bare substrate) combinations. Note that the estimated contrasts are on the square-root scale. Tests were performed on the square-root scale. The p-value was adjusted for multiple comparisons (family of 18 estimates) with the Tukey method. Significant codes indicate: * < 0.05, ** < 0.01, *** < 0.001.

| Compared area-treatment-fouling class pair | Estimated contrast | Standard error | df | t ratio | p-value |
|---|---|---|---|---|---|
| Coated Nanoparticles CCA - Uncoated Nanoparticles CCA | 0 | 0.7 | 790 | -0.064 | 1 |
| Coated Nanoparticles CCA - Coated Antiadhesive CCA | -1.1 | 0.7 | 790 | -1.514 | 0.99 |
| Coated Nanoparticles CCA - Uncoated Antiadhesive CCA | -0.3 | 0.7 | 790 | -0.485 | 1 |
| Coated Nanoparticles CCA - Coated DCOIT CCA | 3.1 | 0.7 | 790 | 4.447 | 0.001 ** |
| Coated Nanoparticles CCA - Uncoated DCOIT CCA | 1.1 | 0.7 | 790 | 1.62 | 0.979 |
| Coated Nanoparticles CCA - Coated Nanoparticles Green/brown Algae | -2.6 | 0.6 | 790 | -4.284 | 0.003 ** |
| Coated Nanoparticles CCA - Uncoated Nanoparticles Green/brown Algae | -2.2 | 0.6 | 790 | -3.64 | 0.032 * |
| Coated Nanoparticles CCA - Coated Antiadhesive Green/brown Algae | -1.2 | 0.6 | 790 | -1.976 | 0.88 |
| Coated Nanoparticles CCA - Uncoated Antiadhesive Green/brown Algae | -2.1 | 0.6 | 790 | -3.502 | 0.05 |
| Coated Nanoparticles CCA - Coated DCOIT Green/brown Algae | -0.7 | 0.6 | 790 | -1.138 | 1 |
| Coated Nanoparticles CCA - Uncoated DCOIT Green/brown Algae | -3.3 | 0.6 | 790 | -5.413 | < 0.001 *** |

| | | | | | |
|---|---|---|---|---|---|
| Coated Nanoparticles CCA - Coated Nanoparticles Bare Substrate | 3.6 | 0.5 | 790 | 6.98 | < 0.001 *** |
| Coated Nanoparticles CCA - Uncoated Nanoparticles Bare Substrate | 3.2 | 0.5 | 790 | 6.036 | < 0.001 *** |
| Coated Nanoparticles CCA - Coated Antiadhesive Bare Substrate | 2 | 0.5 | 790 | 3.878 | 0.014 * |
| Coated Nanoparticles CCA - Uncoated Antiadhesive Bare Substrate | 2.7 | 0.5 | 790 | 5.148 | < 0.001 *** |
| Coated Nanoparticles CCA - Coated DCOIT Bare Substrate | -2.8 | 0.5 | 790 | -5.285 | < 0.001 *** |
| Coated Nanoparticles CCA - Uncoated DCOIT Bare Substrate | 2.3 | 0.5 | 790 | 4.498 | 0.001 ** |
| Uncoated Nanoparticles CCA - Coated Antiadhesive CCA | -1 | 0.7 | 790 | -1.449 | 0.994 |
| Uncoated Nanoparticles CCA - Uncoated Antiadhesive CCA | -0.3 | 0.7 | 790 | -0.421 | 1 |
| Uncoated Nanoparticles CCA - Coated DCOIT CCA | 3.1 | 0.7 | 790 | 4.512 | 0.001 ** |
| Uncoated Nanoparticles CCA - Uncoated DCOIT CCA | 1.2 | 0.7 | 790 | 1.684 | 0.969 |
| Uncoated Nanoparticles CCA - Coated Nanoparticles Green/brown Algae | -2.6 | 0.6 | 790 | -4.21 | 0.004 ** |
| Uncoated Nanoparticles CCA - Uncoated Nanoparticles Green/brown Algae | -2.2 | 0.6 | 790 | -3.566 | 0.04 * |
| Uncoated Nanoparticles CCA - Coated Antiadhesive Green/brown Algae | -1.2 | 0.6 | 790 | -1.902 | 0.911 |
| Uncoated Nanoparticles CCA - Uncoated Antiadhesive Green/brown Algae | -2.1 | 0.6 | 790 | -3.428 | 0.063 |
| Uncoated Nanoparticles CCA - Coated DCOIT Green/brown Algae | -0.6 | 0.6 | 790 | -1.064 | 1 |
| Uncoated Nanoparticles CCA - Uncoated DCOIT Green/brown Algae | -3.2 | 0.6 | 790 | -5.339 | < 0.001 *** |
| Uncoated Nanoparticles CCA - Coated Nanoparticles Bare Substrate | 3.7 | 0.5 | 790 | 7.066 | < 0.001 *** |
| Uncoated Nanoparticles CCA - Uncoated Nanoparticles Bare Substrate | 3.2 | 0.5 | 790 | 6.122 | < 0.001 *** |
| Uncoated Nanoparticles CCA - Coated Antiadhesive Bare Substrate | 2.1 | 0.5 | 790 | 3.964 | 0.01 |
| Uncoated Nanoparticles CCA - Uncoated Antiadhesive Bare Substrate | 2.7 | 0.5 | 790 | 5.234 | < 0.001 *** |
| Uncoated Nanoparticles CCA - Coated DCOIT Bare Substrate | -2.7 | 0.5 | 790 | -5.199 | < 0.001 *** |
| Uncoated Nanoparticles CCA - Uncoated DCOIT Bare Substrate | 2.4 | 0.5 | 790 | 4.584 | < 0.001 *** |
| Coated Antiadhesive CCA - Uncoated Antiadhesive CCA | 0.7 | 0.7 | 790 | 1.029 | 1 |
| Coated Antiadhesive CCA - Coated DCOIT CCA | 4.1 | 0.7 | 790 | 5.961 | < 0.001 *** |
| Coated Antiadhesive CCA - Uncoated DCOIT CCA | 2.2 | 0.7 | 790 | 3.133 | 0.145 |
| Coated Antiadhesive CCA - Coated Nanoparticles Green/brown Algae | -1.5 | 0.6 | 790 | -2.548 | 0.494 |

| | | | | | |
|---|---|---|---|---|---|
| Coated Antiadhesive CCA - Uncoated Nanoparticles Green/brown Algae | -1.2 | 0.6 | 790 | -1.904 | 0.91 |
| Coated Antiadhesive CCA - Coated Antiadhesive Green/brown Algae | -0.1 | 0.6 | 790 | -0.24 | 1 |
| Coated Antiadhesive CCA - Uncoated Antiadhesive Green/brown Algae | -1.1 | 0.6 | 790 | -1.766 | 0.952 |
| Coated Antiadhesive CCA - Coated DCOIT Green/brown Algae | 0.4 | 0.6 | 790 | 0.598 | 1 |
| Coated Antiadhesive CCA - Uncoated DCOIT Green/brown Algae | -2.2 | 0.6 | 790 | -3.677 | 0.028 * |
| Coated Antiadhesive CCA - Coated Nanoparticles Bare Substrate | 4.7 | 0.5 | 790 | 8.994 | < 0.001 *** |
| Coated Antiadhesive CCA - Uncoated Nanoparticles Bare Substrate | 4.2 | 0.5 | 790 | 8.05 | < 0.001 *** |
| Coated Antiadhesive CCA - Coated Antiadhesive Bare Substrate | 3.1 | 0.5 | 790 | 5.892 | < 0.001 *** |
| Coated Antiadhesive CCA - Uncoated Antiadhesive Bare Substrate | 3.7 | 0.5 | 790 | 7.162 | < 0.001 *** |
| Coated Antiadhesive CCA - Coated DCOIT Bare Substrate | -1.7 | 0.5 | 790 | -3.271 | 0.1 |
| Coated Antiadhesive CCA - Uncoated DCOIT Bare Substrate | 3.4 | 0.5 | 790 | 6.512 | < 0.001 *** |
| Uncoated Antiadhesive CCA - Coated DCOIT CCA | 3.4 | 0.7 | 790 | 4.932 | < 0.001 *** |
| Uncoated Antiadhesive CCA - Uncoated DCOIT CCA | 1.5 | 0.7 | 790 | 2.105 | 0.813 |
| Uncoated Antiadhesive CCA - Coated Nanoparticles Green/brown Algae | -2.3 | 0.6 | 790 | -3.728 | 0.023 * |
| Uncoated Antiadhesive CCA - Uncoated Nanoparticles Green/brown Algae | -1.9 | 0.6 | 790 | -3.084 | 0.165 |
| Uncoated Antiadhesive CCA - Coated Antiadhesive Green/brown Algae | -0.9 | 0.6 | 790 | -1.419 | 0.995 |
| Uncoated Antiadhesive CCA - Uncoated Antiadhesive Green/brown Algae | -1.8 | 0.6 | 790 | -2.946 | 0.23 |
| Uncoated Antiadhesive CCA - Coated DCOIT Green/brown Algae | -0.4 | 0.6 | 790 | -0.581 | 1 |
| Uncoated Antiadhesive CCA - Uncoated DCOIT Green/brown Algae | -2.9 | 0.6 | 790 | -4.857 | < 0.001 *** |
| Uncoated Antiadhesive CCA - Coated Nanoparticles Bare Substrate | 4 | 0.5 | 790 | 7.625 | < 0.001 *** |
| Uncoated Antiadhesive CCA - Uncoated Nanoparticles Bare Substrate | 3.5 | 0.5 | 790 | 6.682 | < 0.001 *** |
| Uncoated Antiadhesive CCA - Coated Antiadhesive Bare Substrate | 2.4 | 0.5 | 790 | 4.524 | < 0.001 *** |
| Uncoated Antiadhesive CCA - Uncoated Antiadhesive Bare Substrate | 3 | 0.5 | 790 | 5.793 | < 0.001 *** |
| Uncoated Antiadhesive CCA - Coated DCOIT Bare Substrate | -2.4 | 0.5 | 790 | -4.64 | < 0.001 *** |
| Uncoated Antiadhesive CCA - Uncoated DCOIT Bare Substrate | 2.7 | 0.5 | 790 | 5.143 | < 0.001 *** |
| Coated DCOIT CCA - Uncoated DCOIT CCA | -2 | 0.7 | 790 | -2.828 | 0.298 |
| Coated DCOIT CCA - Coated Nanoparticles Green/brown Algae | -5.7 | 0.6 | 790 | -9.384 | < 0.001 *** |

| | | | | | |
|---|---|---|---|---|---|
| Coated DCOIT CCA - Uncoated Nanoparticles Green/brown Algae | -5.3 | 0.6 | 790 | -8.74 | < 0.001 *** |
| Coated DCOIT CCA - Coated Antiadhesive Green/brown Algae | -4.3 | 0.6 | 790 | -7.076 | < 0.001 *** |
| Coated DCOIT CCA - Uncoated Antiadhesive Green/brown Algae | -5.2 | 0.6 | 790 | -8.602 | < 0.001 *** |
| Coated DCOIT CCA - Coated DCOIT Green/brown Algae | -3.8 | 0.6 | 790 | -6.238 | < 0.001 *** |
| Coated DCOIT CCA - Uncoated DCOIT Green/brown Algae | -6.4 | 0.6 | 790 | -10.514 | < 0.001 *** |
| Coated DCOIT CCA - Coated Nanoparticles Bare Substrate | 0.6 | 0.5 | 790 | 1.064 | 1 |
| Coated DCOIT CCA - Uncoated Nanoparticles Bare Substrate | 0.1 | 0.5 | 790 | 0.12 | 1 |
| Coated DCOIT CCA - Coated Antiadhesive Bare Substrate | -1.1 | 0.5 | 790 | -2.038 | 0.85 |
| Coated DCOIT CCA - Uncoated Antiadhesive Bare Substrate | -0.4 | 0.5 | 790 | -0.768 | 1 |
| Coated DCOIT CCA - Coated DCOIT Bare Substrate | -5.9 | 0.5 | 790 | -11.201 | < 0.001 *** |
| Coated DCOIT CCA - Uncoated DCOIT Bare Substrate | -0.7 | 0.5 | 790 | -1.419 | 0.995 |
| Uncoated DCOIT CCA - Coated Nanoparticles Green/brown Algae | -3.7 | 0.6 | 790 | -6.142 | < 0.001 *** |
| Uncoated DCOIT CCA - Uncoated Nanoparticles Green/brown Algae | -3.3 | 0.6 | 790 | -5.497 | < 0.001 *** |
| Uncoated DCOIT CCA - Coated Antiadhesive Green/brown Algae | -2.3 | 0.6 | 790 | -3.833 | 0.016 * |
| Uncoated DCOIT CCA - Uncoated Antiadhesive Green/brown Algae | -3.2 | 0.6 | 790 | -5.359 | < 0.001 *** |
| Uncoated DCOIT CCA - Coated DCOIT Green/brown Algae | -1.8 | 0.6 | 790 | -2.995 | 0.205 |
| Uncoated DCOIT CCA - Uncoated DCOIT Green/brown Algae | -4.4 | 0.6 | 790 | -7.271 | < 0.001 *** |
| Uncoated DCOIT CCA - Coated Nanoparticles Bare Substrate | 2.5 | 0.5 | 790 | 4.825 | < 0.001 *** |
| Uncoated DCOIT CCA - Uncoated Nanoparticles Bare Substrate | 2 | 0.5 | 790 | 3.882 | 0.013 * |
| Uncoated DCOIT CCA - Coated Antiadhesive Bare Substrate | 0.9 | 0.5 | 790 | 1.724 | 0.962 |
| Uncoated DCOIT CCA - Uncoated Antiadhesive Bare Substrate | 1.6 | 0.5 | 790 | 2.994 | 0.206 |
| Uncoated DCOIT CCA - Coated DCOIT Bare Substrate | -3.9 | 0.5 | 790 | -7.439 | < 0.001 *** |
| Uncoated DCOIT CCA - Uncoated DCOIT Bare Substrate | 1.2 | 0.5 | 790 | 2.343 | 0.651 |
| Coated Nanoparticles Green/brown Algae - Uncoated Nanoparticles Green/brown Algae | 0.4 | 0.5 | 790 | 0.779 | 1 |
| Coated Nanoparticles Green/brown Algae - Coated Antiadhesive Green/brown Algae | 1.4 | 0.5 | 790 | 2.79 | 0.321 |
| Coated Nanoparticles Green/brown Algae - Uncoated Antiadhesive Green/brown Algae | 0.5 | 0.5 | 790 | 0.946 | 1 |

| | | | | | |
|---|---|---|---|---|---|
| Coated Nanoparticles Green/brown Algae - Coated DCOIT Green/brown Algae | 1.9 | 0.5 | 790 | 3.803 | 0.018 * |
| Coated Nanoparticles Green/brown Algae - Uncoated DCOIT Green/brown Algae | -0.7 | 0.5 | 790 | -1.364 | 0.997 |
| Coated Nanoparticles Green/brown Algae - Coated Nanoparticles Bare Substrate | 6.2 | 0.4 | 790 | 15.749 | < 0.001 *** |
| Coated Nanoparticles Green/brown Algae - Uncoated Nanoparticles Bare Substrate | 5.7 | 0.4 | 790 | 14.505 | < 0.001 *** |
| Coated Nanoparticles Green/brown Algae - Coated Antiadhesive Bare Substrate | 4.6 | 0.4 | 790 | 11.662 | < 0.001 *** |
| Coated Nanoparticles Green/brown Algae - Uncoated Antiadhesive Bare Substrate | 5.3 | 0.4 | 790 | 13.335 | < 0.001 *** |
| Coated Nanoparticles Green/brown Algae - Coated DCOIT Bare Substrate | -0.2 | 0.4 | 790 | -0.415 | 1 |
| Coated Nanoparticles Green/brown Algae - Uncoated DCOIT Bare Substrate | 4.9 | 0.4 | 790 | 12.478 | < 0.001 *** |
| Uncoated Nanoparticles Green/brown Algae - Coated Antiadhesive Green/brown Algae | 1 | 0.5 | 790 | 2.011 | 0.863 |
| Uncoated Nanoparticles Green/brown Algae - Uncoated Antiadhesive Green/brown Algae | 0.1 | 0.5 | 790 | 0.167 | 1 |
| Uncoated Nanoparticles Green/brown Algae - Coated DCOIT Green/brown Algae | 1.5 | 0.5 | 790 | 3.024 | 0.191 |
| Uncoated Nanoparticles Green/brown Algae - Uncoated DCOIT Green/brown Algae | -1.1 | 0.5 | 790 | -2.143 | 0.79 |
| Uncoated Nanoparticles Green/brown Algae - Coated Nanoparticles Bare Substrate | 5.9 | 0.4 | 790 | 14.764 | < 0.001 *** |
| Uncoated Nanoparticles Green/brown Algae - Uncoated Nanoparticles Bare Substrate | 5.4 | 0.4 | 790 | 13.521 | < 0.001 *** |
| Uncoated Nanoparticles Green/brown Algae - Coated Antiadhesive Bare Substrate | 4.2 | 0.4 | 790 | 10.677 | < 0.001 *** |
| Uncoated Nanoparticles Green/brown Algae - Uncoated Antiadhesive Bare Substrate | 4.9 | 0.4 | 790 | 12.35 | < 0.001 *** |
| Uncoated Nanoparticles Green/brown Algae - Coated DCOIT Bare Substrate | -0.6 | 0.4 | 790 | -1.4 | 0.996 |
| Uncoated Nanoparticles Green/brown Algae - Uncoated DCOIT Bare Substrate | 4.6 | 0.4 | 790 | 11.493 | < 0.001 *** |
| Coated Antiadhesive Green/brown Algae - Uncoated Antiadhesive Green/brown Algae | -0.9 | 0.5 | 790 | -1.844 | 0.931 |
| Coated Antiadhesive Green/brown Algae - Coated DCOIT Green/brown Algae | 0.5 | 0.5 | 790 | 1.013 | 1 |
| Coated Antiadhesive Green/brown Algae - Uncoated DCOIT Green/brown Algae | -2.1 | 0.5 | 790 | -4.154 | 0.005 ** |
| Coated Antiadhesive Green/brown Algae - Coated Nanoparticles Bare Substrate | 4.8 | 0.4 | 790 | 12.22 | < 0.001 *** |
| Coated Antiadhesive Green/brown Algae - Uncoated Nanoparticles Bare Substrate | 4.3 | 0.4 | 790 | 10.976 | < 0.001 *** |
| Coated Antiadhesive Green/brown Algae - Coated Antiadhesive Bare Substrate | 3.2 | 0.4 | 790 | 8.132 | < 0.001 *** |
| Coated Antiadhesive Green/brown Algae - Uncoated Antiadhesive Bare Substrate | 3.9 | 0.4 | 790 | 9.806 | < 0.001 *** |
| Coated Antiadhesive Green/brown Algae - Coated DCOIT Bare Substrate | -1.6 | 0.4 | 790 | -3.945 | 0.011 * |

| | | | | | |
|---|---|---|---|---|---|
| Coated Antiadhesive Green/brown Algae - Uncoated DCOIT Bare Substrate | 3.5 | 0.4 | 790 | 8.949 | < 0.001 *** |
| Uncoated Antiadhesive Green/brown Algae - Coated DCOIT Green/brown Algae | 1.4 | 0.5 | 790 | 2.857 | 0.28 |
| Uncoated Antiadhesive Green/brown Algae - Uncoated DCOIT Green/brown Algae | -1.2 | 0.5 | 790 | -2.31 | 0.676 |
| Uncoated Antiadhesive Green/brown Algae - Coated Nanoparticles Bare Substrate | 5.8 | 0.4 | 790 | 14.553 | < 0.001 *** |
| Uncoated Antiadhesive Green/brown Algae - Uncoated Nanoparticles Bare Substrate | 5.3 | 0.4 | 790 | 13.309 | < 0.001 *** |
| Uncoated Antiadhesive Green/brown Algae - Coated Antiadhesive Bare Substrate | 4.1 | 0.4 | 790 | 10.465 | < 0.001 *** |
| Uncoated Antiadhesive Green/brown Algae - Uncoated Antiadhesive Bare Substrate | 4.8 | 0.4 | 790 | 12.139 | < 0.001 *** |
| Uncoated Antiadhesive Green/brown Algae - Coated DCOIT Bare Substrate | -0.6 | 0.4 | 790 | -1.611 | 0.98 |
| Uncoated Antiadhesive Green/brown Algae - Uncoated DCOIT Bare Substrate | 4.5 | 0.4 | 790 | 11.282 | < 0.001 *** |
| Coated DCOIT Green/brown Algae - Uncoated DCOIT Green/brown Algae | -2.6 | 0.5 | 790 | -5.167 | < 0.001 *** |
| Coated DCOIT Green/brown Algae - Coated Nanoparticles Bare Substrate | 4.3 | 0.4 | 790 | 10.939 | < 0.001 *** |
| Coated DCOIT Green/brown Algae - Uncoated Nanoparticles Bare Substrate | 3.8 | 0.4 | 790 | 9.695 | < 0.001 *** |
| Coated DCOIT Green/brown Algae - Coated Antiadhesive Bare Substrate | 2.7 | 0.4 | 790 | 6.851 | < 0.001 *** |
| Coated DCOIT Green/brown Algae - Uncoated Antiadhesive Bare Substrate | 3.4 | 0.4 | 790 | 8.524 | < 0.001 *** |
| Coated DCOIT Green/brown Algae - Coated DCOIT Bare Substrate | -2.1 | 0.4 | 790 | -5.226 | < 0.001 *** |
| Coated DCOIT Green/brown Algae - Uncoated DCOIT Bare Substrate | 3 | 0.4 | 790 | 7.667 | < 0.001 *** |
| Uncoated DCOIT Green/brown Algae - Coated Nanoparticles Bare Substrate | 6.9 | 0.4 | 790 | 17.475 | < 0.001 *** |
| Uncoated DCOIT Green/brown Algae - Uncoated Nanoparticles Bare Substrate | 6.4 | 0.4 | 790 | 16.232 | < 0.001 *** |
| Uncoated DCOIT Green/brown Algae - Coated Antiadhesive Bare Substrate | 5.3 | 0.4 | 790 | 13.388 | < 0.001 *** |
| Uncoated DCOIT Green/brown Algae - Uncoated Antiadhesive Bare Substrate | 6 | 0.4 | 790 | 15.061 | < 0.001 *** |
| Uncoated DCOIT Green/brown Algae - Coated DCOIT Bare Substrate | 0.5 | 0.4 | 790 | 1.311 | 0.998 |
| Uncoated DCOIT Green/brown Algae - Uncoated DCOIT Bare Substrate | 5.6 | 0.4 | 790 | 14.204 | < 0.001 *** |
| Coated Nanoparticles Bare Substrate - Uncoated Nanoparticles Bare Substrate | -0.5 | 0.3 | 790 | -1.968 | 0.884 |
| Coated Nanoparticles Bare Substrate - Coated Antiadhesive Bare Substrate | -1.6 | 0.3 | 790 | -6.466 | < 0.001 *** |
| Coated Nanoparticles Bare Substrate - Uncoated Antiadhesive Bare Substrate | -1 | 0.3 | 790 | -3.819 | 0.017 * |
| Coated Nanoparticles Bare Substrate - Coated DCOIT Bare Substrate | -6.4 | 0.3 | 790 | -25.57 | < 0.001 *** |

| | | | | | |
|---|---|---|---|---|---|
| Coated Nanoparticles Bare Substrate - Uncoated DCOIT Bare Substrate | -1.3 | 0.3 | 790 | -5.175 | < 0.001 *** |
| Uncoated Nanoparticles Bare Substrate - Coated Antiadhesive Bare Substrate | -1.1 | 0.3 | 790 | -4.499 | 0.001 ** |
| Uncoated Nanoparticles Bare Substrate - Uncoated Antiadhesive Bare Substrate | -0.5 | 0.3 | 790 | -1.851 | 0.928 |
| Uncoated Nanoparticles Bare Substrate - Coated DCOIT Bare Substrate | -5.9 | 0.3 | 790 | -23.603 | < 0.001 *** |
| Uncoated Nanoparticles Bare Substrate - Uncoated DCOIT Bare Substrate | -0.8 | 0.3 | 790 | -3.207 | 0.119 |
| Coated Antiadhesive Bare Substrate - Uncoated Antiadhesive Bare Substrate | 0.7 | 0.3 | 790 | 2.647 | 0.42 |
| Coated Antiadhesive Bare Substrate - Coated DCOIT Bare Substrate | -4.8 | 0.3 | 790 | -19.104 | < 0.001 *** |
| Coated Antiadhesive Bare Substrate - Uncoated DCOIT Bare Substrate | 0.3 | 0.3 | 790 | 1.291 | 0.998 |
| Uncoated Antiadhesive Bare Substrate - Coated DCOIT Bare Substrate | -5.4 | 0.3 | 790 | -21.751 | < 0.001 *** |
| Uncoated Antiadhesive Bare Substrate - Uncoated DCOIT Bare Substrate | -0.3 | 0.3 | 790 | -1.356 | 0.997 |
| Coated DCOIT Bare Substrate - Uncoated DCOIT Bare Substrate | 5.1 | 0.3 | 790 | 20.395 | < 0.001 *** |

**Table S2.9**: Summary statistics of settlement data per treatment (Control, Nanoparticles, Antiadhesive, DCOIT) on the fully-coated (FC) plugs. Values represent total settlement and mean settlers per $cm^2$. N corresponds to the number of plugs in individual jars containing 15 coral larvae per jar.

| Treatment | n | Total settlers | Mean settlers/$cm^2$ | Standard deviation | Standard error |
|---|---|---|---|---|---|
| Control | 30 | 169 | 0.8 | 0.5 | 0.1 |
| Nanoparticles | 30 | 179 | 0.8 | 0.5 | 0.1 |
| Antiadhesive | 30 | 105 | 0.5 | 0.4 | 0.1 |
| DCOIT | 30 | 120 | 0.6 | 0.5 | 0.1 |

**Table S2.10**: Estimated marginal means (EMM), standard error (SE), degrees of freedom (df) and upper and lower confidence levels (95% and 5%, respectively) of settlers per $cm^2$ in each treatment (Control, Nanoparticles, Antiadhesive, DCOIT) on the fully-coated (FC) plugs. Intervals (EMM, SE, CL) were back-transformed from the square-root scale.

| Treatment | EMM | Standard error | df | Lower CL | Upper CL |
|---|---|---|---|---|---|
| Control | 0.7 | 0.2 | 114 | 0.4 | 1.1 |
| Nanoparticles | 0.8 | 0.2 | 114 | 0.4 | 1.2 |
| Antiadhesive | 0.4 | 0.1 | 114 | 0.2 | 0.7 |
| DCOIT | 0.4 | 0.1 | 114 | 0.2 | 0.7 |

**Table S2.11**: Results of pairwise post-hoc tests of settlement data on the fully-coated (FC) plugs based on estimated marginal means. Settler density was compared between all treatment (Control, Nanoparticles, Antiadhesive, DCOIT) combinations. The p-value was adjusted for multiple comparisons (family of 4 estimates) with the Tukey method. Note that the estimated contrasts are on the square-root scale. Tests were performed on the square-root scale. Significant codes indicate: * < 0.05, ** < 0.01, *** < 0.001.

| Compared treatment pair | Estimated contrast | Standard error | df | t ratio | p-value |
|---|---|---|---|---|---|
| Control - Nanoparticles | -0.1 | 0.1 | 114 | -0.604 | 0.93 |
| Control - Antiadhesive | 0.2 | 0.1 | 114 | 2.446 | 0.074 |
| Control - DCOIT | 0.2 | 0.1 | 114 | 2.463 | 0.071 |
| Nanoparticles - Antiadhesive | 0.3 | 0.1 | 114 | 3.05 | 0.015 * |
| Nanoparticles - DCOIT | 0.3 | 0.1 | 114 | 3.067 | 0.014 * |
| Antiadhesive - DCOIT | 0 | 0.1 | 114 | 0.017 | 1 |

**Table S2.12**: Summary statistics of settlement data for each treatment (Nanoparticles, Antiadhesive, DCOIT) and area (coated/uncoated) combination on the partially-coated (PC) plugs. Values represent total settlement and mean settler density/cm² per area (coated vs. uncoated). N (= 30) corresponds to the number of plugs in individual jars containing 15 coral larvae per jar.

| Treatment | Area | Total settlers | Mean settlers/cm² | Standard error |
|---|---|---|---|---|
| Partially-coated Nanoparticles | Coated | 164 | 0.9 | 0.1 |
| Partially-coated Nanoparticles | Uncoated | 168 | 0.9 | 0.3 |
| Partially-coated Antiadhesive | Coated | 76 | 0.4 | 0.1 |
| Partially-coated Antiadhesive | Uncoated | 176 | 0.9 | 0.3 |
| Partially-coated DCOIT | Coated | 83 | 0.4 | 0.1 |
| Partially-coated DCOIT | Uncoated | 224 | 1.2 | 0.3 |

**Table S2.13**: Estimated marginal means (EMM), standard error (SE), degrees of freedom (df) and confidence levels (CL) of the settlers/cm² for each area (coated/uncoated), within each partially-coated (PC) treatment (Nanoparticles (PN), Antiadhesive (PA), DCOIT (PD)). Intervals were back-transformed from the square-root scale.

| Treatment-Area | EMM | Standard error | df | Lower CL | Upper CL |
|---|---|---|---|---|---|
| PN-Coated | 0.7 | 0.2 | 2 | 0.1 | 2.1 |
| PN-Uncoated | 0.3 | 0.2 | 2 | 0 | 1.8 |
| PA-Coated | 0.3 | 0.1 | 2 | 0 | 1.2 |
| PA-Uncoated | 0.3 | 0.2 | 2 | 0 | 1.9 |
| PD-Coated | 0.3 | 0.1 | 2 | 0 | 1.3 |
| PD-Uncoated | 0.6 | 0.3 | 2 | 0 | 2.4 |

**Table S2.14**: Results of pairwise post-hoc tests of settlement data on the partially-coated (PC) plugs based on estimated marginal means. Settler density was compared between all area (coated/uncoated) and treatment (Nanoparticles (PN), Antiadhesive (PA), DCOIT (PD)) combinations. Note that the estimated contrasts are on the square-root scale. Tests were performed on the square-root scale. The p-value was adjusted for multiple comparisons (family of 7 estimates) with the Tukey method. Significant codes indicate: * < 0.05, ** < 0.01, *** < 0.001.

| Compared treatment-area pair | Estimated contrast | Standard error | df | t ratio | p-value |
|---|---|---|---|---|---|
| PN Coated - PA Coated | 0.4 | 0.1 | 172 | 4.113 | < 0.001 *** |
| PN Coated - PD Coated | 0.3 | 0.1 | 172 | 3.69 | 0.004 ** |
| PN Coated - PN Uncoated | 0.3 | 0.2 | 172 | 2.087 | 0.299 |
| PN Coated - PA Uncoated | 0.3 | 0.2 | 172 | 1.952 | 0.374 |
| PN Coated - PD Uncoated | 0.1 | 0.2 | 172 | 0.618 | 0.99 |
| PA Coated - PD Coated | 0 | 0.1 | 172 | -0.385 | 0.999 |
| PA Coated - PN Uncoated | 0 | 0.2 | 172 | -0.123 | 1 |
| PA Coated - PA Uncoated | 0 | 0.2 | 172 | -0.285 | 1 |
| PA Coated - PD Uncoated | -0.3 | 0.2 | 172 | -1.71 | 0.527 |
| PD Coated - PN Uncoated | 0 | 0.2 | 172 | 0.085 | 1 |
| PD Coated - PA Uncoated | 0 | 0.2 | 172 | -0.074 | 1 |
| PD Coated - PD Uncoated | -0.2 | 0.2 | 172 | -1.486 | 0.674 |
| PN Uncoated - PA Uncoated | 0 | 0.2 | 172 | -0.122 | 1 |
| PN Uncoated - PD Uncoated | -0.2 | 0.2 | 172 | -1.181 | 0.845 |
| PA Uncoated - PD Uncoated | -0.2 | 0.2 | 172 | -1.064 | 0.895 |

## SI References


1. Herget, K. *et al*. Haloperoxidase Mimicry by CeO2-x Nanorods Combats Biofouling. *Adv. Mater.* **29**, 1–8 (2017).
2. Herget, K. *et al*. Supporting Information: Haloperoxidase Mimicry by CeO2-x Nanorods Combats Biofouling. *Adv. Mater.* **29**, (2017).

# Chapter 3: Effects of antifoulings on survival and growth of coral spat for reef restoration

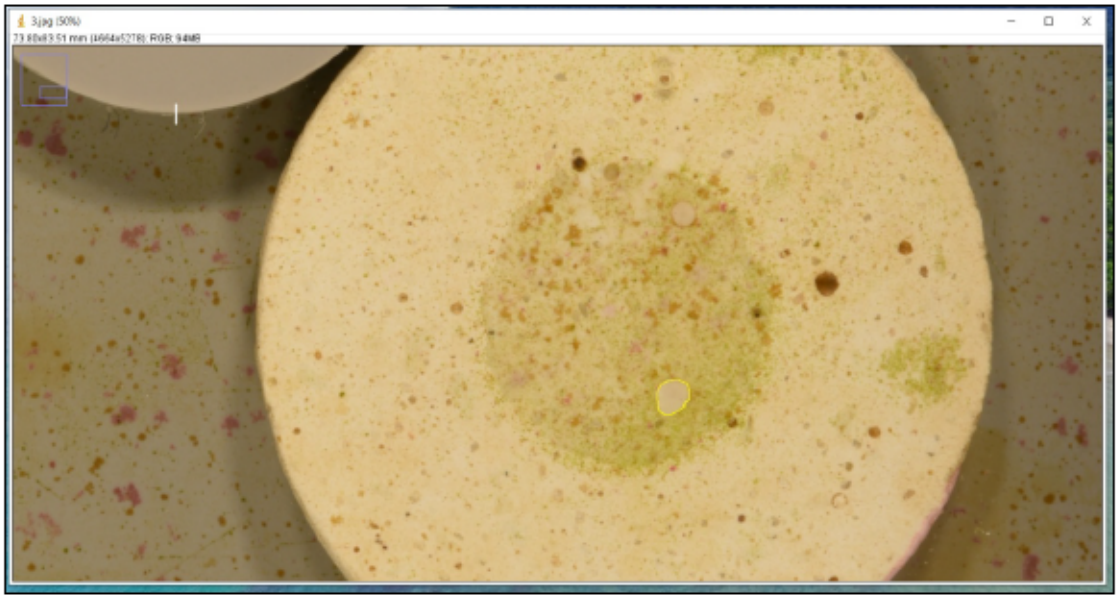

*In preparation for submission as:*
*Roepke LK, Brefeld D, Soltmann U, Randall CJ, Negri AP and Kunzmann A (in prep.) Effects of antifoulings on survival and growth of coral spat for reef restoration.*

## Abstract

Survival of coral spat after larval settlement can be a bottleneck to reef recovery, and diverse strategies are required to overcome this issue in reef restoration programs. One such approach includes the application of innovative antifouling (AF) coatings on seeding devices, which have been shown to successfully decrease competitive algal growth while preserving coral settlement. Building on this success, we tested the effects of AF coatings on the next stages of coral ontogeny: survival and growth of *Acropora millepora* settlers. Settlement plugs were either fully or partially coated, seeded with coral larvae, and then the settled corals were monitored at regular intervals for survival and growth (0, 14, 42, 69 days post-settlement). Survival across treatments after 69 days averaged between 12.0 - 28.6%. Larvae refused to settle on an encapsulated dichlorooctylisothiazolinone (DCOIT) coating. However, the survival of settlers directly next to the coating on partially-coated plugs was the highest (28.6%) and significantly higher than on the control plugs (16.4%). The coral growth rate per 14 days was particularly high on the coated antiadhesive and uncoated DCOIT areas, however not significantly different from the uncoated control plugs. Based on these results and previously published findings, we suggest that the antiadhesive and DCOIT coatings are most effective at promoting survival and growth of seeded corals. The findings of this and previous studies provide insights for AF coated seeding device design, which could be used to complement other coral restoration activities.

**Key words: biofouling, coral larvae, restoration, benthic competition, propagation technique**

# 1. Introduction

Tropical coral reef ecosystems are threatened by a combination of global and local factors (Harborne et al., 2017; Hoegh-Guldberg et al., 2017), with the potential for devasting ecosystem collapses and keystone species extinctions by 2050 (Bindoff et al., 2019) unless action is taken to protect these species and address existing stressors. Thermal stress events have led to over 70% of the world's reefs experiencing consecutive or prolonged bleaching events, causing widespread damage to living corals (Eakin et al., 2019). The growing intensity and frequency of coral bleaching events is also impeding the natural recovery of reefs between disturbances (Fabricius et al., 2017; Ortiz et al., 2018; Hughes et al., 2019). Some damaged reefs have shown natural resilience and recovery (Graham et al., 2011; Australian Institute of Marine Science, 2022), but others have failed to recover due to a lack of coral recruitment, unstable substrate, or phase shifts to macroalgal-dominated ecosystems (Fox et al., 2003; Hughes et al., 2007; Graham et al., 2015; Kenyon et al., 2020). Successful reproduction and recruitment are crucial for coral recovery (Richmond, 1997), yet, newly settled coral spat can face high mortality due to competition from other benthic organisms (Vermeij and Sandin, 2008; Vermeij et al., 2009).

Reef management in the 21st century must adopt a combination of conservation approaches, including preventative measures to reduce local and global stressors, combined with habitat restoration to enhance adaptive potential and rebuild damaged reefs (Bay et al., 2019; Richards et al., 2019; Vardi et al., 2021). A key strategy for large-scale reef restoration is to deploy captured or cultivated coral larvae and juveniles onto the reef either directly or through deployment devices (Heyward et al., 1999; Harrison et al., 2016; Chamberland et al., 2017; dela Cruz and Harrison, 2020; Randall et al., 2020; Miller et al., 2021). Using sexually produced coral propagules offers benefits such as increased genetic diversity, scalability, cost efficiency, and retention of species diversity and community composition (Baria-Rodriguez et al., 2019; Doropoulos et al., 2019; Randall et al., 2020). Deployment devices can also overcome challenges such as a lack of substrate or settlement cues, the presence of settlement inhibitors, and competition with surrounding benthos (Kuffner et al., 2006, 2008; Arnold et al., 2010; Webster et al., 2013; Speare et al., 2019; Randall et al., 2021).

Primary colonization of hard benthic surfaces by biofilms, such as bacteria, fungi, and protozoa, precedes algal growth (Kirschner and Brennan, 2012). These early fouling communities can either induce or inhibit coral settlement depending on the colonizing taxa (Webster et al., 2004). Some biofilms and crustose coralline algae (CCA) promote coral larval settlement (Heyward and Negri, 1999; Negri et al., 2001; Tebben et al., 2011, 2015; Sneed et al., 2014). However, interactions with other fouling organisms, such as filamentous algae, can impede larval settlement (Carpenter and Edmunds, 2006) and reduce the survival and growth of coral juveniles (Box and Mumby, 2007; Linares et al., 2012). Fouling can negatively impact coral spat through competition for space and overgrowth by other microorganisms (McCook et al.,

2001). Furthermore, the microtopography provided by fouling can provide a refuge for microbial pathogens or corallivorous invertebrates (Nugues et al., 2004). Allelopathy, shading, altered water movement, and other changes to the microenvironment induced by fouling algae all have the potential to impede coral fitness and survival (McCook et al., 2001; Hauri et al., 2010; Fong et al., 2019).

Antifouling (AF) paints with biocides, such as tributyltin (TBT) and copper, that prevent the growth of algae and invertebrates have been utilized on ship hulls to boost efficiency since the mid 19th century (Almeida et al., 2007). However, due to its negative environmental impact and toxicity, TBT was banned under the 'International Convention for the Control and Management of Ships' Ballast Water and Sediments' in 2003. As a result of the ban on TBT, and the regulation of copper in AF paints, new and less toxic formulations have emerged, as reviewed in Almeida et al. (2007). The use of innovative AF technologies on coral deployment devices could potentially improve the survival of sexually propagated corals during the first critical months (Tebben et al., 2014; Roepke et al., 2022a).

One of the most commonly used AF coatings, Sea-Nine 211™ (Röhm & Haas; Philadelphia, PA, USA; Jacobson and Willingham (2000)), contains the biocidal component dichlorooctylisothiazolinone (DCOIT, Kathon 930, C-9 or DCOI). DCOIT has been shown to penetrate cell membranes and bind to proteins and enzymes, disrupting the function of both target and non-target organisms (Silva et al., 2020). The mechanism of DCOITs' toxicity is not well understood, but previous studies have linked it to embryotoxicity, immunosuppression, oxidative stress, and reproductive and endocrine disruption (Campos et al., 2022b). Efforts to mitigate its toxicity include encapsulation in silica nanocapsules, which have been shown to reduce its harmful effects on non-target organisms (Maia et al., 2015; Dos Santos et al., 2020). However, the effects of DCOIT on hard corals, with DCOIT tested in its free form, consolidated in a coating, encapsulated, or a combination thereof, remains underrepresented in current research (Ferreira et al., 2021; Roepke et al., 2022a, 2022b).

Non-biocidal AF alternatives include silicone-based sol-gel coatings, which are made using a wet-chemical process to create metal oxides. The sol solution transforms into a gel-like structure with both liquid and solid elements. The surface properties of these coatings prevent fouling organisms from adhering to the surface and facilitate their release at higher water velocities. The antiadhesive effect is the result of low surface energy levels (with limited molecular attraction), having both hydrophilic and hydrophobic traits, and a carefully crafted roughness to inhibit primary fouling (Detty et al., 2014). Another advancement in non-biocidal AFs utilizes nanoparticles (NPs), which interfere with bacterial communication (i.e., quorum sensing) to prevent biofilm formation and curb or postpone the colonization of algae (Korschelt et al., 2018b). Some such technologies include cerium ($Ce^{3+}/Ce^{4+}$)- modification on the large surface area of NPs, which boosts the catalytic oxidation of halides and generates biocidal

compounds that counteract biofilm growth and the formation of signaling molecules involved in intracellular communication (Herget et al., 2017, 2018; Korschelt et al., 2018a). Laboratory and field trials using paint with 2 wt% $CeO_{2-x}$ NPs showed a greater reduction in biofouling compared to $Cu_2O$, one of the most frequently used biocidal components in AF paints (Herget et al., 2017, 2018).

Despite the potential of antifoulants to reduce competitive algal growth, limited research has focused on decreasing fouling on surfaces to enhance coral settlement (Roepke et al., 2022a) and survival of coral spat (Tebben et al., 2014). The latter study demonstrated that coatings of two different types of paraffin waxes immediate adjacent to coral spat significantly decreased fouling and increased early post-settlement survival after 39 days. There was no difference in coral settlement between the wax treatments and untreated controls. Additional research is needed to investigate the ability of newly developed AF coatings to reduce competition from biofouling and increase coral survival to size-escape levels (*sensu* Doropoulos et al., 2012). Ultimately, this could benefit restoration programs by complementing current methodologies. To that end, our objective was to test the effects of three innovative and distinct AF coatings (antiadhesive, cerium dioxide nanoparticles (NPs), encapsulated DCOIT), on the early post-settlement survival (14, 42, 69 days post-settlement) and growth rate (per 14 days) of *A. millepora* coral settlers on fully coated (FC) and partially coated (PC) 'coral plugs' (plugs).

## 2. Materials & Methods

### 2.1. Coral plug preparation and coating design

Coral plugs (top disc diameter: 3 cm) made from white Portland cement were purchased (AquaPerfekt, Germany; Dyckerhoff WEISS CEM 1) and the layer of sand (Raunheimer quartz sand) on top of the surfaces was removed with a diamond saw blade on a circular saw. A smooth finish was achieved by sanding and polishing the plug's surfaces on very fine wet sandpaper (STARCKE® (SiC) waterproof Matador 220, 800, 2500). The uniformly smooth top surfaces were then coated with three different AF coatings following the methods described in Roepke et al. (2022). For each AF coating, half of the plug replicates were fully-coated (FC) (**Figure 3.1c**) while the other half were partially-coated (PC) (**Figure 3.1b**) with a circular area in the center of each plug uncoated. A circular sticker (12 mm Ø) was applied to the plug and prevented the coating in an area of approximately 10 mm Ø, since the sol spread out slightly underneath the sticker (approximately 88% coated and 12% uncoated). Control plugs (**Figure 3.1a**) were not coated. The purpose of including FC plugs was to explore the coral settler's survival and growth among the AF treatments. PC plugs were used to further explore hypothesized fine-scale effects of the AF coatings on survival and growth of *A. millepora* spat. Although, very locally active antifouling with robust settlement was shown for the herein

investigated coatings (Roepke et al., 2022a), there is a potential risk and assumption that the chemicals of the coated areas could affect coral spat on uncoated areas through leaching or spill-over effects. Therefore, and since the coatings could potentially be used in various ways to create algal-free areas with or without coral spat directly on top, it is important to compare survival and growth not only on coated vs. uncoated areas (PC plugs) within treatments, but also between treatments.

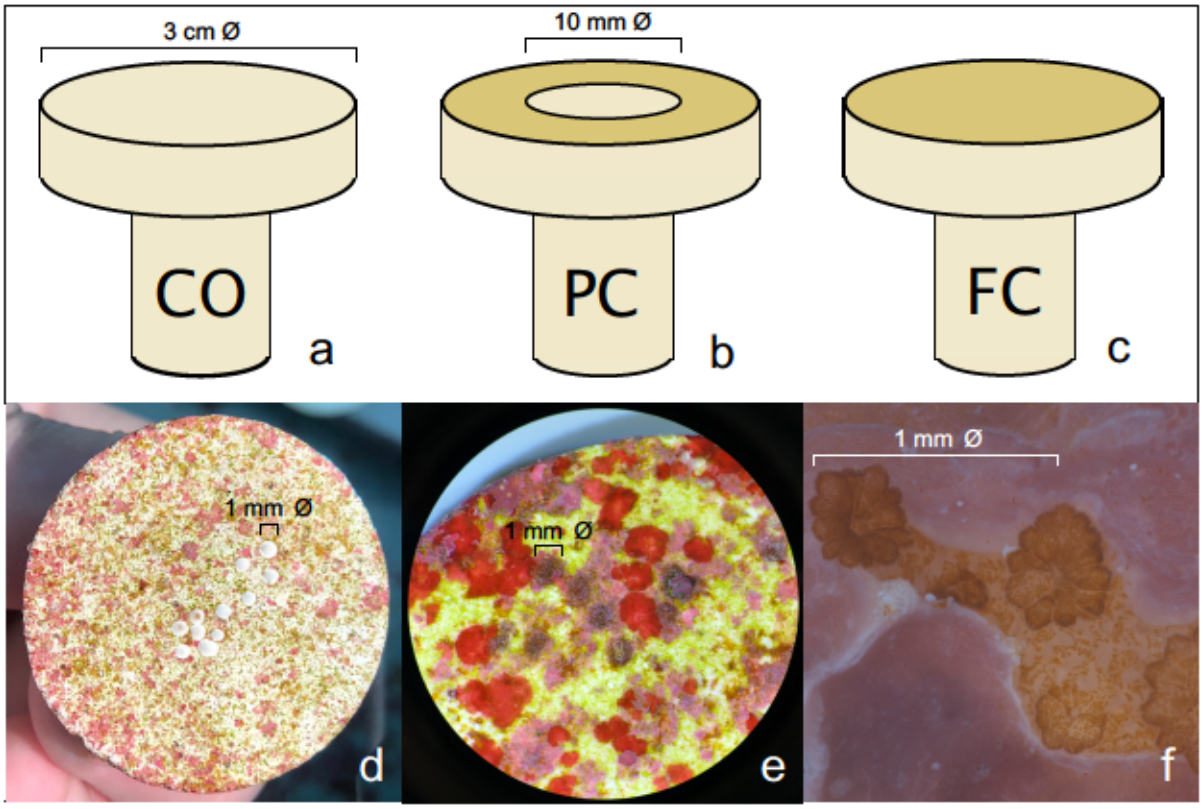


**Figure 3.1**: Top row: Schematic of uncoated Control (CO; a), partially-coated (PC; b), and fully-coated (FC; c) plugs. Bottom row: Control plug surface with fouling organisms and coral spat after 14 days (d), 42 days (e), and 69 days (f) in the tank.

## 2.2. Indoor settlement tank setup

Plugs were maintained in seven settlement tanks (60 L) located in an aquarium room of the National Sea Simulator (SeaSim) of the Australian Institute of Marine Science (AIMS) in Townsville, Australia. Each tank contained 45 replicate plugs of the same treatment (45 plugs x 7 treatments including the control treatment = total of 315 plugs). Each aquarium was independent, with a separate open-circulation system and room-controlled temperature setting ensuring constant 26 °C water temperature. The plugs were left in the tanks for three days to allow for the elution of any excess AF chemicals in the coatings. Afterwards, small crushed particles (approx. 1-4 mm²) of the crustose coralline alga *Porolithon onkodes* were placed on top of the FC and PC plugs to induce larval settlement on the unconditioned (no biofilm) plugs.

The CCA particles were distributed as evenly as possible across the whole plug surface, regardless of treatment, to avoid any settlement preference in one area.

## 2.3. Coral collection and larval husbandry

Fragments of gravid colonies (25–40 cm diameter) of the scleractinian coral *Acropora millepora* (Ehrenberg, 1834) were collected from Falcon Island (18° 45.796'S 146° 31.926'E; 2 m depth) in November 2019 ahead of the full moon, under permit G12/35236.1 issued by the Great Barrier Reef Marine Park Authority. Colonies were transported to the National Sea Simulator (SeaSim) and maintained in 1700 L semi-recirculating holding tanks until spawning. Temperatures were held at 26–27 °C, to match the seawater temperature at the collection site. Spawning occurred on 15th November 2019 and the coral gametes from eight parental colonies were collected and fertilized. Symbiont-free larval cultures were maintained at densities <500 larvae per L, indoors, in round, 500 L fibreglass flow-through rearing tanks (1.5 turnovers per day) supplied with 1 µm filtered seawater (FSW) at 27 °C (Negri and Heyward, 2000; Nordborg et al., 2018). Larvae used in this experiment originated from one culture tank only and remained in this tank until the experiment commenced.

## 2.4. Coral settlement

*A. millepora* larvae were competent to undergo attachment and metamorphosis after 5 days, as determined by routine settlement assays in the laboratory (Heyward and Negri, 1999). Settlement was defined here as the change in life stage from 'free-swimming' or 'loosely-attached, elongated' larvae to a squat, firmly attached and disc-shaped form, with pronounced flattening of the oral–aboral axis and with septal mesenteries radiating from a central mouth (Heyward and Negri, 1999). All other larvae (swimming, loosely attached, dead and partially disintegrated) were counted as not settled. Test settlement trials revealed no settlement of *A. millepora* larvae on FC DCOIT plugs. Therefore, this treatment was excluded from the experiment (7 treatments reduced to 6). Also, only 3 larvae settled onto the coated areas of the PC DCOIT plugs in the main settlement experiment, and therefore this treatment was also excluded from further analysis. Between the 25th of November until the 3rd of December 2019, during a period of 8 days, each settlement tank received a total of ≅ 2500 larvae. Points of time in settlement differed between treatments, as larvae did not settle equally onto each coating. For instance, sufficient larval settlement on the Antiadhesive coating was achieved later than in the other treatments.

Settlement was assessed each day under a stereo microscope, and as soon as a plug housed a minimum of 2 settlers, CCA particles were removed and plugs were translocated to 60 L tanks

as described in 2.2. for grow-out. Plugs with sufficient settlement remained in these tanks until all plugs showed sufficient settlement. On day 9 (after 8 days of settlement), plugs were then allocated to their positions on PVC plug trays (custom-fabricated: 40 x 20 x 5 cm (length x width x height), holes (1.2 cm Ø) for coral plugs arranged in rows A-E with 10 holes per row) and transferred to three replicate outdoor aquaria (280 L) located in the quarantine area of the SeaSim.

## 2.5. Outdoor aquaria

Each of three replicate aquaria contained 15 replicate plugs per treatment (15 plugs × 6 treatments including the control treatment = 90 plugs), for a total of 270 plugs. Each aquarium was independent, with a separate recirculation system and a temperature-controlled sump. Fresh FSW was circulated into each experimental tank at a rate of three full water exchanges (turnovers) per day. Temperature was maintained at 26 °C and measured every 60 min. (HOBO Pendant® Temperature/Light 64K Data Logger, Onset Computer Corporation, Bourne, MA) and salinity was kept in the range of 34.5 to 35.5 PSU. Water circulation in the tanks was maintained by Maxspect Gyre 200 series pumps (constant speed mode, 20% force). Tanks received natural sunlight attenuated by ~70% with shade cloth: maximum Photosynthetically Active Radiation (PAR) light intensity was 250 µmol photons $m^{-2}$ $s^{-1}$. The PVC plug trays were kept horizontally within the tanks. Tray positions were swapped circularly on a weekly basis to minimize within-tank effects (i.e., unequal shading or local water flow) on fouling, survival and growth across the plugs. To 'seed' the plugs with a biofilm, approximately 3 kg of live rock (comprising reef rubble with typical fouling communities incl. CCA) was added to each tank 3 weeks before plugs were introduced.

## 2.6. Survival and growth: monitoring and measurement

To monitor and quantify the survival and growth of coral spat, plug surfaces were photographed at regular intervals (after 0, 14, 42 and 69 days) using a Nikon D810 with a Nikon AF-S 60 mm f/2.8 G Micro ED Lens outfitted with four Ikelite DS160 strobes mounted on a trolley with a standardized distance and angle to each plug surface. Four plugs were photographed at once. A small PVC disc-shaped reference (10 mm Ø) was added before images were taken to serve as a scale bar during image analyses. The first monitoring images were taken on the same day the plugs were transferred to the outdoor holding tanks (day 9), and were repeated on days 42, and 69. All image analyses were performed in ImageJ version 1.53c (ImageJ Release Notes; Schneider et al., 2012). The standardized reference in each image allowed for the investigation of spat survival and growth over time. Spat survival was determined from the images by eyesight, and in combination with the last monitoring using a stereo microscope. Spat was either

described as dead or alive. The size of the settlers was analyzed by drawing an according perimeter (freehand function) around the live tissue borders of the settlers and extracting the 2-D surface area. As the average settler sizes in each treatment differed at the first monitoring (due to different settlement time points of larvae in each treatment; **Supplementary Table S3.3** and **Table S3.11**), growth was calculated as a rate (% increase or decrease) by dividing the settlers' sizes on day 14 (size end) by their size on day 0 (size start) according to the formula $(\frac{\text{size end } (mm^2)}{\text{size start}(mm^2)}\text{-}1 \times 100)$. Hereby, growth was normalized to the initial size of the settlers. Growth was only analyzed after the 14 days' time point, as most settlers were heavily overgrown by CCA at subsequent points.

## 2.7. Statistical analysis

All statistical analyses were performed in R version 4.2.0 (R Core Team, 2021) and the data were manipulated and visualized using packages of the 'tidyverse'(Wickham et al., 2019). Survival was rated for each coral settler on a dead/alive (0/1) scale at each monitoring time point. Differences in survival probability of coral spat amongst treatments (antiadhesive, cerium dioxide nanoparticles (NPs), encapsulated DCOIT, Control) and between areas (coated and uncoated) after 69 days were investigated by fitting binomial generalized linear mixed models (GLMMs) with a complementary log-log (cloglog) link function (analogous to proportional Hazards model). To account for tank effects and clustering of multiple settlers on the same plug, 'plug ID', nested in 'tank' was used as a random effect (varying intercepts). The number of fusions and the initial number of settlers on each plug were used as random factors only in the PC model, as they improved model fit. Model fits were visually assessed using residual diagnostic plots from the DHARMA package (Hartig, 2022). ANOVA tables (type II tests) were computed for both models using the 'car' package (Fox and Weisberg, 2019) to identify statistically significant fixed effects and their interactions. If significant, post-hoc tests for full pairwise comparisons between treatments and areas were performed using the 'emmeans' package (Lenth, 2021). P-values were adjusted for multiple comparisons with the Tukey method. As only very few larvae settled on the coated area of the PC DCOIT plugs and no larvae settled on the FC DCOIT plugs, these treatments were excluded from the analysis.

Differences in growth rates of settlers (%) per 14 days were investigated among treatments on the FC plugs and among treatments and areas (coated/uncoated) on the PC plugs using linear mixed models (LMMs). To account for tank effects and clustering of multiple settlers on the same plug, the plug ID, nested in the 'tank' was used as a random effect (varying intercepts). As the number of individuals within clusters of spat might influence growth measurements, 'number of fusions' was included as another random effect. Model fit was visually assessed using standard diagnostic residual plots. ANOVA tables (type II tests) were computed for both models using the 'lmerTest' package (Kuznetsova et al., 2017) with the Kenward-Roger

degrees of freedom (df) approximation in order to identify statistically significant fixed effects. If significant, post-hoc tests for full pairwise comparisons between treatments and areas were performed using the 'emmeans' package (Lenth, 2021). P-values were adjusted for multiple comparisons with the Tukey method. Because growth was assessed after 14 days while survival was assessed after 69 days, the number of settlers used in each analysis differed.

## 3. Results

### 3.1. Survival of spat

#### 3.1.1. Survival on fully-coated plugs

Spat survival did not statistically differ among treatments on FC plugs after 69 days (GLMM: $\chi^2(2) = 5.05$, $p = 0.08$; **Supplementary Table S3.3**). The highest survival was observed on the antiadhesive-coated plugs, averaging 24.8% compared with 16.4% on control plugs, and 18.9% on nanoparticle-coated plugs (**Table 3.1**).

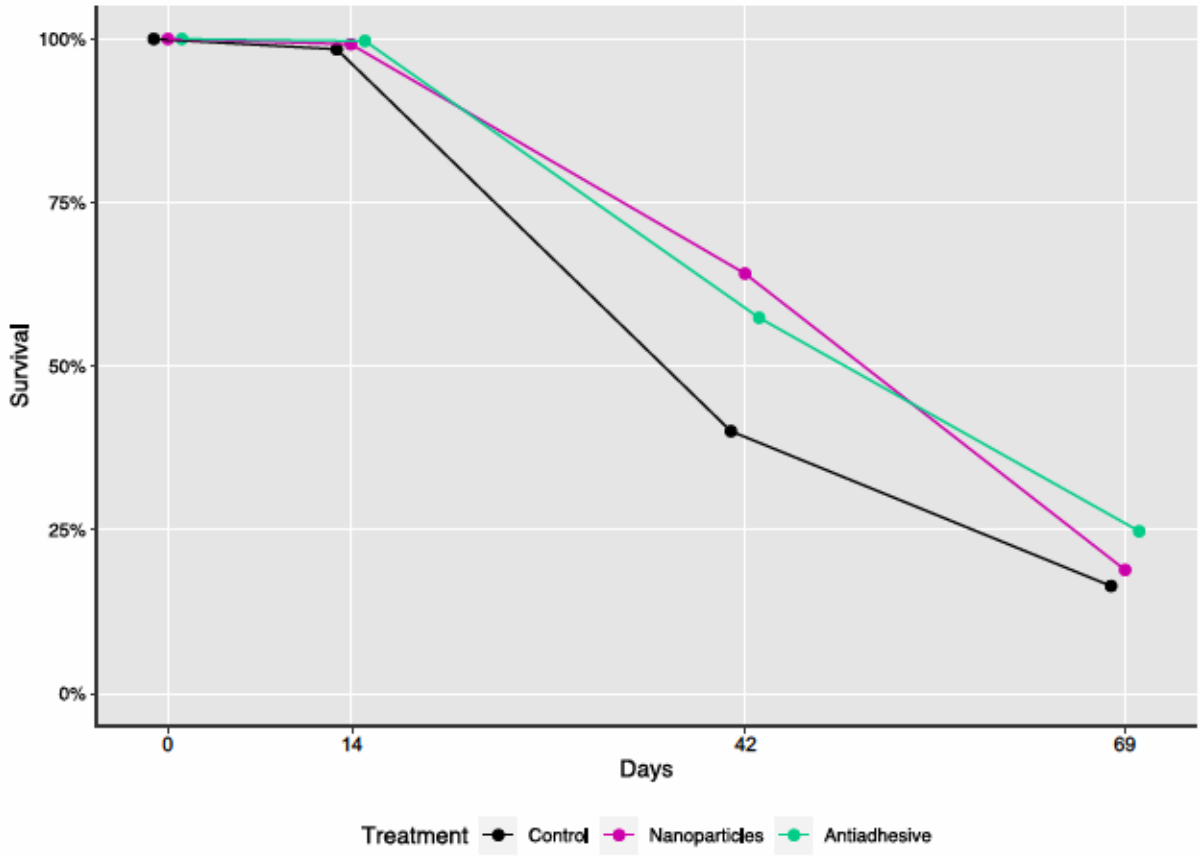


**Figure 3.2**: Total average survival (%) of *A. millepora* spat after 0, 14, 42, and 69 days on fully-coated (FC) plugs (Nanoparticles, Antiadhesive) and uncoated Control plugs (**Table 3.1**; see Supplementary **Table S3.1** for absolute spat numbers; S2 and S3).

**Table 3.1**: Total average *A. millepora* survival (%) data on fully-coated (FC) and partially-coated (PC) plugs at monitoring time points (0, 14, 42, 69 days).

| Treatment/Area | 0 days | 14 days | 42 days | 69 days |
|---|---|---|---|---|
| Control - Uncoated | 100 | 98.4 | 40.1 | 16.4 |
| FC Nanoparticles | 100 | 99.2 | 64.2 | 18.9 |
| FC Antiadhesive | 100 | 99.7 | 57.4 | 24.8 |
| PC Antiadhesive - Uncoated | 100 | 98.9 | 59.6 | 16.9 |
| PC Antiadhesive - Coated | 100 | 99.6 | 63.8 | 20.1 |
| PC DCOIT - Uncoated | 100 | 99.6 | 72.6 | 28.6 |
| PC Nanoparticles - Uncoated | 100 | 99.1 | 46.2 | 12.0 |
| PC Nanoparticles - Coated | 100 | 99.0 | 50.0 | 18.0 |

### 3.1.2. Survival: partially-coated plugs

Survival on the coated and uncoated areas of the PC plugs significantly differed between AF treatments (GLMM: $\chi^2(5) = 18.94$, $p = 0.002$; Supplementary Table S5). Survival on the coated (18.0%) and uncoated areas (12.0%) of the Nanoparticles treatment were significantly lower as to survival on the uncoated areas of the DCOIT treatment (28.6%) after 69 days (**Figure 3.3**; **Table 3.1**; **Supplementary Table S3.5**). In fact, survival on the uncoated DCOIT areas was the highest among all FC and PC treatments and significantly higher as survival on the Control plugs (**Figure 3.3**; **Table 3.1**; **Supplementary Table S3.5**). No differences in survival were found between the coated and uncoated areas within treatments (Antiadhesive, Nanoparticles; **Figure 3.3**; **Supplementary Table S3.5**).

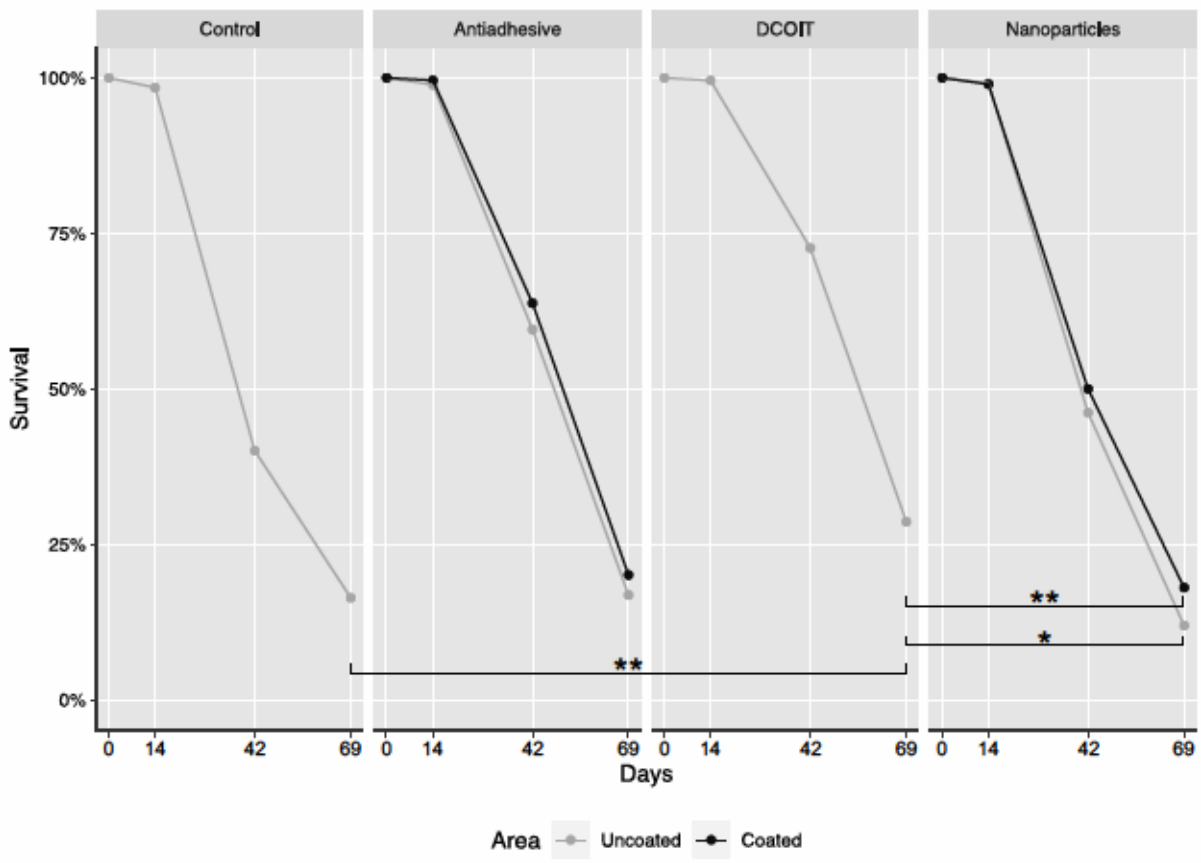


**Figure 3.3:** Total average survival (%) of *A. millepora* spat after 0, 14, 42, and 69 days on coated and uncoated areas of partially-coated (PC) plugs (Antiadhesive, DCOIT, Nanoparticles) and uncoated Control plugs. (**Table 3.1**; see **Supplementary Table S3.1** for absolute spat numbers). Asterisks indicate statistically significant differences based on pairwise post-hoc tests with estimated marginal means after 69 days (**Supplementary Table S3.4** and **Table S3.5**; *$p < 0.05$, **$p < 0.01$). Note that the treatment 'DCOIT coated' was removed from the analysis as no larvae settled on this coating.

## 3.2. Growth of spat

### 3.2.1. Growth on fully-coated plugs

On the fully-coated (FC) plugs, there was a statistically significant effect of AF treatment on the spat growth rate (LMM: $F(123.34) = 5.88$, $p = 0.004$).

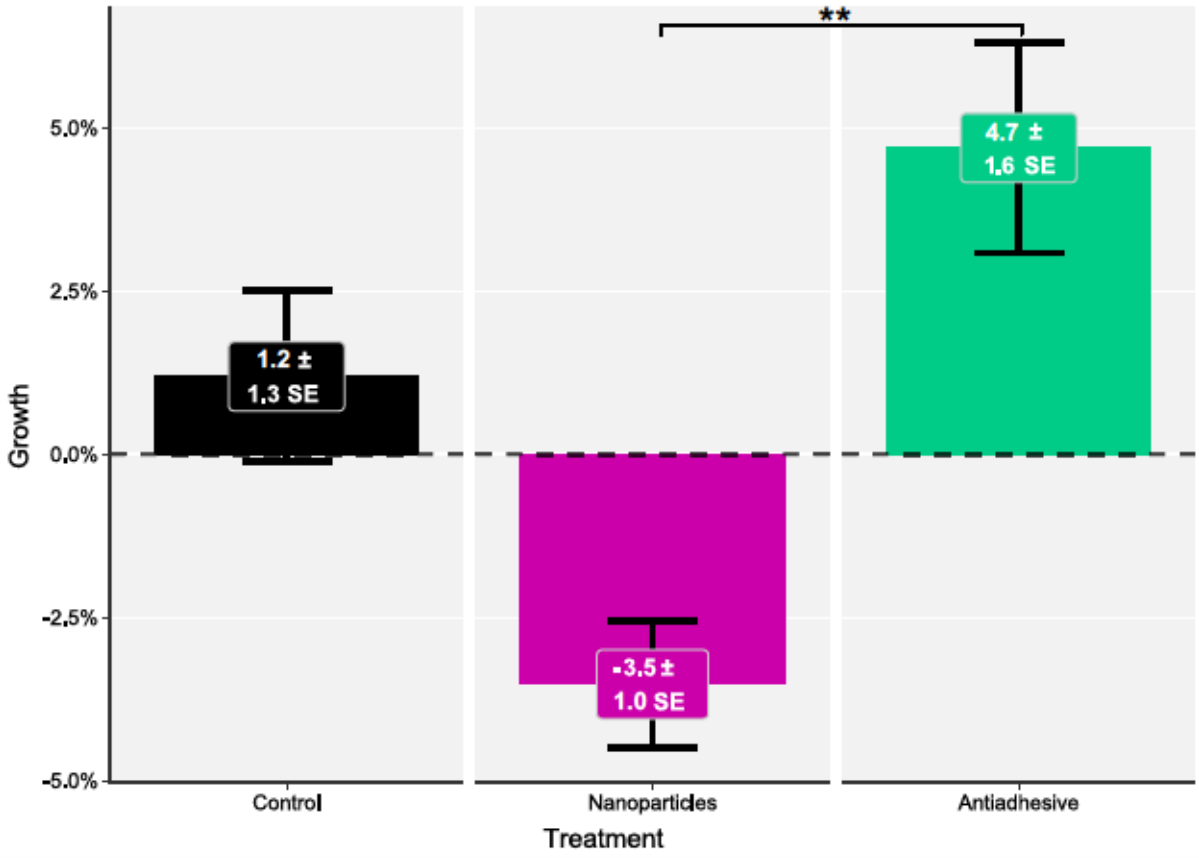


**Figure 3.4:** Growth rate (%) of *Acropora millepora* spat (n) per 14 days on fully-coated (FC) plugs (Nanoparticles (n = 286), Antiadhesive (n = 224)) and uncoated control plugs (n = 223). Error bars represent SEM. Asterisks indicate statistically significant differences based on pairwise post-hoc tests with estimated marginal means (**Supplementary Table S3.6**, **Table S3.8** and **Table S3.9**; **$p < 0.01$).

The spat growth rate on the Control plugs averaged 1.2 ± 1.3 % (mean ± SE; **Figure 3.4**. The highest average growth of 4.7 ± 1.6 % was found in the recruits growing on the Antiadhesive coated plugs, and differed significantly ($p = 0.002$) from the negative growth rate of spat on the Nanoparticle coated plugs (-3.5 ± 1.0 %; **Figure 3.4**; **Supplementary Table S3.6** and **Table S3.9**).

### 3.2.2. Growth on partially-coated plugs

The mean spat growth rate did not differ significantly among AF treatments and between areas (coated/uncoated) (LMM: $F(298.44) = 1.86$, $p = 0.101$).

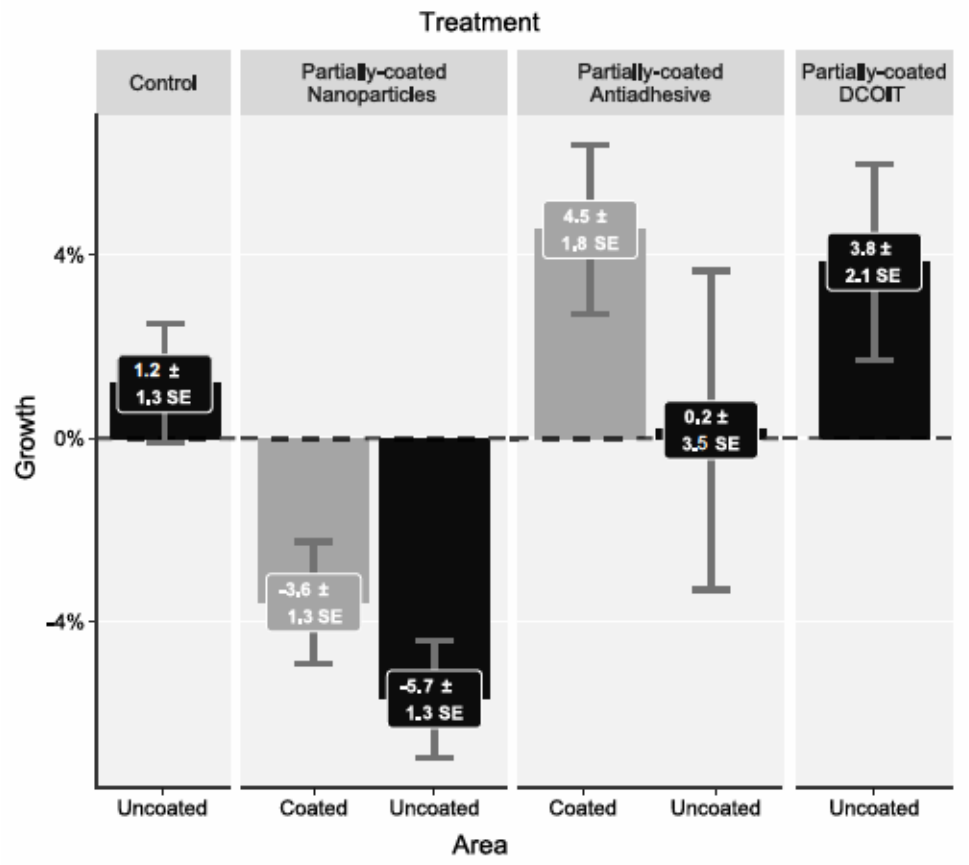


**Figure 3.5:** Growth rate (%) of *Acropora millepora* spat (n) per 14 days on partially-coated (PC) plugs: Nanoparticles Coated/Uncoated (n = 157/94), Antiadhesive Coated/Uncoated (n = 150/53), DCOIT Uncoated (n = 152), and uncoated Control plugs (n = 223). Error bars represent SEM. Asterisks indicate statistically significant differences based on pairwise post-hoc tests with estimated marginal means (**Supplementary Table S3.10**, **Table S3.12** and **Table S3.13**).

Although the spat growth rate did not significantly differ between and within treatments, growth was relatively high on the coated Antiadhesive areas (4.5 ± 1.8 % (mean ± SE)), and the uncoated DCOIT areas 3.8 ± 2.1 %, as compared to growth on the Control plugs (1.2 ± 1.3 %) and uncoated Antiadhesive areas (0.2 ± 3.5 %; **Figure 3.5**). Negative growth (due to CCA overgrowth) of coral spat was found on both, the coated and uncoated areas of the Nanoparticle treatment (-3.6 ± 1.3 %, and -5.7 ± 1.3 %, respectively; **Figure 3.5**; **Supplementary Table S3.10** and **Table S3.13**).

# 4. Discussion

Low toxicity antifouling (AF) coatings have shown promising results in reducing algal growth on coral settlement surfaces for application in reef restoration (Roepke et al., 2022a, 2022b). This study is one of very few to investigate the efficacy of three innovative AF coatings to improve early post-settlement survival and growth of coral spat by reducing competition from biofouling. While direct larval settlement onto DCOIT-coated surfaces was strongly inhibited, relatively high settlement, survival and growth was found on the uncoated areas directly adjacent to the DCOIT coating (PC DCOIT plugs). The antiadhesive coating showed robust survival and growth of coral spat, while the $CeO_{2-x}$ coating formulation was ineffective. Our results indicate a trend of enhancement for spat survival and growth on the antiadhesive and next to the DCOIT coating. By reducing competitive algal species around coral settlers, survival of corals might be enhanced due to more space and light that could be utilized for growth.

## 4.1. *A. millepora* survival and growth: $CeO_{2-x}$ nanoparticle coating

*A. millepora* survival on the FC $CeO_{2-x}$ NP surfaces did not statistically differ from survival on the FC Antiadhesive or Control surfaces. On the PC surfaces; however, survival was significantly lower on the coated and uncoated areas as compared to survival on the uncoated areas of the DCOIT-coated plugs. Growth on the FC $CeO_{2-x}$ NP surfaces was significantly lower from the highest growth gain on the FC Antiadhesive plugs. Growth on both the coated and uncoated areas of the PC $CeO_{2-x}$ NP surfaces was the lowest among all treatments, however, not statistically different from any other treatment/area.

The impact of reactive oxygen species (ROS) generated by $CeO_{2-x}$ NPs on both the fouling community and corals may have been either positive or negative; however, the extent and direction of these effects remain unclear. Roepke et al. (2022a) tested the same coatings for AF efficacy during *Acropora tenuis* coral settlement and found they did not effectively reduce fouling in comparison to uncoated plugs. It is possible that under the specific conditions of the tests ROS may accelerate bacterial biofouling and subsequent macrofouling (Xu et al., 2018, 2019), resulting in greater competition with coral spat for space and light, ultimately resulting in decreased survival and growth. Additionally, the settlers may have been directly affected by the NPs, the surface structure/porosity, the amphiphilic surface property of the sol-gel coating, which served as a basis for the $CeO_{2-x}$ NP coating, or a combination thereof. As our study did not include an inert particle/surface control (for the encapsulated DCOIT particles and $CeO_2$ NPs), observed effects are difficult to link to either physical or chemical coating effects.

Furthermore, the catalytic activity of the NPs was tested in their unconsolidated form, and it was assumed that this activity would persist in the coating. However, the poor performance of

the $CeO_{2-x}$ NP coating in preventing fouling (Roepke et al., 2022a), indicates activity may have been lost. Moreover, there is limited information on the potential effects and mode of action of $CeO_2$ nanoparticles on corals. Studies have shown that other NPs used in cosmetics can have harmful effects on corals. For instance, Tang et al. (2017) observed that ZnO nanoparticles (common in sunscreens) affect lipid profiles in *Seriatopora caliendrum*, suggesting a mechanical disturbance caused by ZnO nanoparticles. According to Corinaldesi et al. (2018), the exposure to uncoated ZnO NPs resulted in severe coral bleaching, while exposure of two coated forms of $TiO_2$ NPs over a 48 h period had no adverse effect on *Acropora* spp.. Fel et al. (2019) found a negative impact of ZnO on the photosystem II of the algal symbionts, reducing their functionality by 38% in comparison to the control group. Given the limited number of studies and variations in methodologies and differences in chemical and physical properties of NPs, caution must be exercised when interpreting these results, which require further testing (Mitchelmore et al., 2021; Moeller et al., 2021; Miller et al., 2022).

### 4.2. *A. millepora* survival and growth: Antiadhesive coating

The Antiadhesive coating showed the highest average post-settlement survival of *A. millepora* settlers after 69 days, and growth rate per 14 days, although the results were not statistically different from the Control plugs and uncoated areas of the other treatments. This type of coating has a surface with both hydrophobic and hydrophilic properties, with an overall low surface energy in the range of about 20 mN/m. Many organisms exhibit only a weak bioadhesion tendency in this range. Whether hydrophobic or hydrophilic surfaces are preferred for adhesion depends on the particular organism. For instance, diatoms adhere via hydrophilic proteins, whereas barnacles attach using hydrophobic adhesive proteins (Finlay et al., 2010). The attachment process of coral larvae is not well understood, and the potential proteins involved have not been described. Hayashibara et al. (2000) and Okubo and Motokawa (2007) assumed spirocysts, adhesive organelles at the aboral end of larvae in anthozoa, to be involved in the process of substrate attachment in different *Acropora* spp. However, the proteins and genes involved in this process remain unidentified. More recent studies found proteins and cells involved in bioadhesion in the pedal disc of the sea anemone *Exaiptasia pallida*, which offers a toolkit for molecular techniques in other species, including scleractinian corals (Davey et al., 2019; Clarke et al., 2020). The latter study was able to identify that spirocysts were not involved in the bioadhesion process of *E. pallida*, but a protein-rich adhesive secrete that is structurally and compositionally complex (see Clarke et al., 2020 and Davey et al., 2021).

Future research should aim to investigate the mechanisms and proteins involved in this important process, as bioadhesion to surfaces i.e. antiadhesive coatings could prove advantageous for coral propagation and supply for restoration programs. Roepke et al. (2022a) showed that the antiadhesive coating on the same substrates as tested herein was able to

significantly reduce fouling (CCA, green/brown algae), and potentially reduce algal competition for coral spat. However, Roepke et al. (2022a) also observed a trend of reduced settlement on the same antiadhesive coating, although not statistically different from the uncoated Control plugs and areas. As sol-gel does not contain any known toxic compounds or biocides, the reduced settlement in Roepke et al. (2022a) is likely linked to the physical surface properties of the coating. In this study, fouling after 69 days on the sol-gel was equivalent to that on uncoated Control plugs. This could indicate a limited timeframe for the antiadhesive AF to work efficiently, as the study by Roepke et al. (2022a) investigated fouling only until 37 days post introduction to natural filtered SW. This finding highlights the importance of investigating AF efficacy through time and in different environmental settings. Tebben et al. (2014) demonstrated that a non-toxic paraffin wax-based AF with antiadhesive characteristics was able to improve the survival of early coral spat after 39 days that were in close proximity (within mm) of the wax coating. Taken together, these results could be used to further test and further develop an efficient, and environmentally benign coating for coral restoration. It could also be worthwhile to look into other bioinspired AF coating alternatives in future comparison studies on AF efficacy and potential toxicity towards corals (Jin et al., 2022).

### 4.3. *A. millepora* survival and growth: encapsulated DCOIT coating

In this study, no *A. millepora* larvae settled onto the FC DCOIT plugs, despite the presence of CCA fragments to induce settlement. Only four larvae in total settled on the coated areas of the PC plugs; therefore, these treatments were excluded from the analysis. Inhibition of larval settlement is sensitive to contaminants, including the AF biocides copper and TBT (Negri and Heyward, 2001; Negri et al., 2002). Our findings are in line with a recent study by Roepke et al. (2022b), reporting a significantly reduced swimming velocity and decreased activity of *A. millepora* larvae on the DCOIT coating. The extreme reduction in larval motility observed in that study is most likely driven by the DCOIT's toxicity, although the mechanism remains unclear. DCOIT's permeable nature through cell membranes and walls can result in harm to cellular structures and functions. Additionally, its ability to disrupt the antioxidant defense system can trigger oxidative stress (Eom et al., 2019). For instance, the neotropical oyster *Crassostrea brasiliana* showed evidence of oxidative stress, lipid peroxidation, lysosomal membrane damage, and histopathological pathologies, as revealed by Campos et al. (2022), in response to DCOIT at levels consistent with those found in the environment. The presence of a toxic substance also necessitates energy for neutralization and metabolism, which could divert energy from other functions. Future studies could investigate this mechanism by assessing the spatial and temporal effects of the coating on physiological parameters (e.g., respiration) coupled with biochemical and molecular markers (e.g., enzymatic oxidative stress).

Another study performed by Roepke et al. (2022a) did demonstrate a high AF efficacy of the DCOIT coating, which worked particularly well to suppress CCA growth. This finding could

potentially explain the significantly higher survival of spat on the uncoated areas of the PC DCOIT plugs in comparison to survival on the Control plugs here. The encapsulated DCOIT could have created a positive indirect effect for survival and growth by reducing algal or bacterial fouling which benefits the coral due to less or missing competition interactions. Roepke et al. (2022a) did not find any statistical difference in settlement of *Acropora tenuis* coral larvae between uncoated Control plugs/areas and coated DCOIT plugs/areas. However, the plugs were pre-conditioned in natural FSW tanks equipped with live rocks and typical fouling communities including CCA prior to settlement, which could have contributed to the different outcomes between these studies. Therefore, pre-conditioning of plugs to establish a certain degree of fouling should be emphasized whenever settlement on DCOIT treated surfaces is initiated.

Little research has been performed on the effects of encapsulated DCOIT on tropical marine species (Dos Santos et al., 2020; Campos et al., 2022a). Furthermore, the comparison of the impact of encapsulated DCOIT to its free form remains largely unexplored (Maia et al., 2015). To date, only one study has compared the effects of free and encapsulated DCOIT on a soft coral species, *Sarcophyton glaucum* (Ferreira et al., 2021). The authors found reduced toxicity of encapsulated DCOIT on the coral fragments compared with free DCOIT, as measured by coral polyp retraction, photosynthetic efficacy, and oxidative-stress markers. Relative to the negative control, encapsulated DCOIT still caused some toxicity. The encapsulation/immobilization technology is designed to reduce the amount of biocide required while maintaining its efficacy. This is achieved by preventing direct biocidal interaction with the coating components, controlling the leaching rate, and increasing the lifespan of the coating. Moreover, this technology has been reported to reduce potential environmental threats (Maia et al., 2012, 2015; Martins et al., 2017; Gutner-Hoch et al., 2018).

In this study, spat survival among the PC plugs was the highest on the uncoated DCOIT areas, significantly higher than on the Control plugs. Spat growth on the uncoated DCOIT areas and on the coated Antiadhesive areas were also similar. These results, in combination with previous findings by (Roepke et al., 2022a, 2022b) suggest that the fresh DCOIT coating without pre-conditioning is most likely deterrent or toxic to the larvae, but that the AF activity of DCOIT is restricted to the coating's surface with negligible leaching onto adjacent uncoated areas (1-3 mm away). In addition, the potential toxicity of the coating could be dependent on either the biofilm quantity (cover) or quality (diversity/composition) on top of the coating, or the DCOIT's diffusion rate, or a combination thereof. By influencing the composition of the fouling organisms on coated areas, uncoated areas in close vicinity to coated areas can potentially generate indirect positive effects for spat's survival and growth.

## 5. Conclusions and future considerations

This study indicates that there were no negative effects of the AF coatings on the survival and growth of *A. millepora*, while the uncoated DCOIT and coated Antiadhesive coatings improved survival and growth of coral spat. While the freshly applied DCOIT coating inhibited settlement, settlement occurring adjacent to the coating led to high survival and growth. The results herein, combined with Roepke et al. (2022a, 2022b) suggest that the AF coating-design (i.e. coated next to uncoated areas) and handling-design (i.e. pre-conditioning) play important roles in the settlement, survival, and growth process of coral larvae and early post-settlers. Further research is necessary to fine-tune the coatings' diffusion rates, effective concentrations, and to understand the modes of action on corals, and effects on fouling. As more and more tropical reefs worldwide undergo phase-shifts from coral- to fleshy algal-dominated cover and coastal eutrophication increases, interactions between fouling organisms and corals become more pronounced and frequent. In this context, AF could have broad implications for coral restoration activities. The incorporation of AF measures may enhance the viability and profitability of sexually propagated corals by raising the number of corals that make it through critical early life stages.

## Author Contributions

L.K.R. conceptualized and coordinated the study, with guidance provided by D.B., U.S., C.J.R., A.P.N. and A.K.; L.K.R. and D.B. performed the experiments, analyzed the data and prepared figures/tables; L.K.R. wrote the manuscript; C.J.R. and A.P.N. substantively revised the manuscript; all authors read and approved the final draft.

## Funding

This work was partially funded by the Australian Institute of Marine Science, the University of Bremen and graduate school GLOMAR, the AiF (German Federation of Industrial Research Associations) and the DSM (German Foundation Marine Conservation) and was supported by the Reef Restoration and Adaptation Program, which is funded by a partnership between the Australian Government's Reef Trust and the Great Barrier Reef Foundation.

## Acknowledgements

The authors would like to thank Constanze von Waldthausen, Sebastian Flotow and Christian Brandt for their technical support at ZMT and Florita Flores for her guidance and lab support at AIMS. The authors also thank the staff at the National Sea Simulator at AIMS for assistance

with experimental setup and field collections. We acknowledge the Bindal People as the Traditional Owners where this work took place. We pay our respects to their Elders past, present and emerging and we acknowledge their continuing spiritual connection to their land and sea country.

## References

Almeida, E., Diamantino, T. C., and de Sousa, O. (2007). Marine paints: The particular case of antifouling paints. *Prog. Org. Coatings* 59, 2–20. doi:10.1016/j.porgcoat.2007.01.017.

Arnold, S. N., Steneck, R. S., and Mumby, P. J. (2010). Running the gauntlet: Inhibitory effects of algal turfs on the processes of coral recruitment. *Mar. Ecol. Prog. Ser.* 414, 91–105. doi:10.3354/meps08724.

Australian Institute of Marine Science (2022). Great Barrier Reef Coral Status (AIMS Long-Term Monitoring Program 2021-2022 Results). Available at: https://www.aims.gov.au/monitoring-great-barrier-reef/gbr-condition-summary-2021-22.

Baria-Rodriguez, M. V., dela Cruz, D. W., Dizon, R. M., Yap, H. T., and Villanueva, R. D. (2019). Performance and cost-effectiveness of sexually produced *Acropora granulosa* juveniles compared with asexually generated coral fragments in restoring degraded reef areas. *Aquat. Conserv. Mar. Freshw. Ecosyst.* 29, 891–900. doi:10.1002/aqc.3132.

Bay, L. K., Rocker, M., Boström-Einarsson, L., Babcock, R., Buerger, P., Cleves, P., et al. (2019). Reef Restoration and Adaptation Program : Intervention Technical Summary. A report provided to the Australian Government by the Reef Restoration and Adaptation Program.

Bindoff, N. L., Cheung, W. W. L., Kairo, J. G., Arístegui, J., Guinder, V. A., Hallberg, R., et al. (2019). Chapter 5: Changing Ocean, Marine Ecosystems, and Dependent Communities.

Box, S. J., and Mumby, P. J. (2007). Effect of macroalgal competition on growth and survival of juvenile Caribbean corals. *Mar. Ecol. Prog. Ser.* 342, 139–149.

Campos, B. G. de, do Prado e Silva, M. B. M., Avelelas, F., Maia, F., Loureiro, S., Perina, F., et al. (2022a). Toxicity of innovative antifouling additives on an early life stage of the oyster *Crassostrea gigas*: short- and long-term exposure effects. *Environ. Sci. Pollut. Res.* 29, 27534–27547. doi:10.1007/s11356-021-17842-3.

Campos, B. G. de, Fontes, M. K., Gusso-Choueri, P. K., Marinsek, G. P., Nobre, C. R., Moreno, B. B., et al. (2022b). A preliminary study on multi-level biomarkers response of the tropical oy ster *Crassostrea brasiliana* to exposure to the antifouling biocide DCOIT. *Mar. Pollut. Bull.* 174, 113241. doi:10.1016/j.marpolbul.2021.113241.

Carpenter, R. C., and Edmunds, P. J. (2006). Local and regional scale recovery of *Diadema* promotes recruitment of scleractinian corals. *Ecol. Lett.* 9, 268–277. doi:10.1111/j.1461-0248.2005.00866.x.

Chamberland, V. F., Snowden, S., Marhaver, K. L., Petersen, D., and Vermeij, M. J. A. (2017). The reproductive biology and early life ecology of a common Caribbean brain coral, *Diploria labyrinthiformis* (Scleractinia: Faviinae). *Coral Reefs* 36, 83–94. doi:10.1007/s00338-016-1504-2.

Clarke, J. L., Davey, P. A., Aldred, N., and Aldred, N. (2020). Sea anemones (*Exaiptasia pallida*) use a secreted adhesive and complex pedal disc morphology for surface attachment. *BMC Zool.* 5, 1–13. doi:10.1186/s40850-020-00054-6.

Corinaldesi, C., Marcellini, F., Nepote, E., Damiani, E., and Danovaro, R. (2018). Impact of inorganic UV filters contained in sunscreen products on tropical stony corals (*Acropora*

spp.). *Sci. Total Environ.* 637–638, 1279–1285. doi:10.1016/j.scitotenv.2018.05.108.

Davey, P. A., Power, A. M., Santos, R., Bertemes, P., Ladurner, P., Palmowski, P., et al. (2021). Omics-based molecular analyses of adhesion by aquatic invertebrates. *Biol. Rev.* 96, 1051–1075. doi:10.1111/brv.12691.

Davey, P. A., Rodrigues, M., Clarke, J. L., and Aldred, N. (2019). Transcriptional characterisation of the *Exaiptasia pallida* pedal disc. *BMC Genomics* 20, 1–15. doi:10.1186/s12864-019-5917-5.

dela Cruz, D. W., and Harrison, P. L. (2020). Enhancing coral recruitment through assisted mass settlement of cultured coral larvae. *PLoS One* 15, e0242847; 10.1371/journal.pone.0242847. doi:10.1371/journal.pone.0242847.

Detty, M. R., Ciriminna, R., Bright, F. V., and Pagliaro, M. (2014). Environmentally Benign Sol-Gel Antifouling and Foul-Releasing Coatings. *Acc. Chem. Res.* 47, 678–687. doi:10.1021/ar400240n.

Doropoulos, C., Elzinga, J., ter Hofstede, R., van Koningsveld, M., and Babcock, R. C. (2019). Optimizing industrial-scale coral reef restoration: comparing harvesting wild coral spawn slicks and transplanting gravid adult colonies. *Restor. Ecol.* 27, 758–767. doi:10.1111/rec.12918.

Doropoulos, C., Ward, S., Marshell, A., Diaz-Pulido, G., and Mumby, P. J. (2012). Interactions among chronic and acute impacts on coral recruits: The importance of size-escape thresholds. *Ecology* 93, 2131–2138. doi:10.1890/12-0495.1.

Dos Santos, J. V. N., Martins, R., Fontes, M. K., Galv, B., Bruni, M., and Maia, F. (2020). Can Encapsulation of the Biocide DCOIT Affect the Anti-Fouling Efficacy and Toxicity on Tropical Bivalves? *Appl. Sci.* 10, 1–12. doi:8579; doi:10.3390/app10238579.

Eakin, C. M., Sweatman, H. P. A., and Brainard, R. E. (2019). The 2014–2017 global-scale coral bleaching event: insights and impacts. *Coral Reefs* 38, 539–545. doi:10.1007/s00338-019-01844-2.

Eom, H. J., Haque, M. N., Nam, S. E., Lee, D. H., and Rhee, J. S. (2019). Effects of sublethal concentrations of the antifouling biocide Sea-Nine on biochemical parameters of the marine polychaete *Perinereis aibuhitensis*. *Comp. Biochem. Physiol. Part - C Toxicol. Pharmacol.* 222, 125–134. doi:10.1016/j.cbpc.2019.05.001.

Fabricius, K. E., Noonan, S. H. C., Abrego, D., Harrington, L., and De'Ath, G. (2017). Low recruitment due to altered settlement substrata as primary constraint for coral communities under ocean acidification. *Proc. R. Soc. B Biol. Sci.* 284. doi:10.1098/rspb.2017.1536.

Fel, J. P., Lacherez, C., Bensetra, A., Mezzache, S., Béraud, E., Léonard, M., et al. (2019). Photochemical response of the scleractinian coral *Stylophora pistillata* to some sunscreen ingredients. *Coral Reefs* 38, 109–122. doi:10.1007/s00338-018-01759-4.

Ferreira, V., Pavlaki, M. D., Martins, R., Monteiro, M. S., Maia, F., Tedim, J., et al. (2021). Effects of nanostructure antifouling biocides towards a coral species in the context of global changes. *Sci. Total Environ.* 799, 149324. doi:10.1016/j.scitotenv.2021.149324.

Finlay, J. A., Bennett, S. M., Brewer, L. H., Sokolova, A., Clay, G., Gunari, N., et al. (2010). Barnacle settlement and the adhesion of protein and diatom microfouling to xerogel films with varying surface energy and water wettability. *Biofouling* 26, 657–666. doi:10.1080/08927014.2010.506242.

Fong, J., Lim, Z. W., Bauman, A. G., Valiyaveettil, S., Liao, L. M., Yip, Z. T., et al. (2019). Allelopathic effects of macroalgae on *Pocillopora acuta* coral larvae. *Mar. Environ. Res.* 151. doi:10.1016/j.marenvres.2019.06.007.

Fox, H. E., Pet, J. S., Dahuri, R., and Caldwell, R. L. (2003). Recovery in rubble fields: Long-term impacts of blast fishing. *Mar. Pollut. Bull.* 46, 1024–1031. doi:10.1016/S0025-326X(03)00246-7.

Fox, J., and Weisberg, S. (2019). *An R Companion to Applied Regression*. Third Edit. Sage Publications Available at: https://socialsciences.mcmaster.ca/jfox/Books/Companion/.

Graham, N. A. J., Jennings, S., MacNeil, M. A., Mouillot, D., and Wilson, S. K. (2015). Predicting climate-driven regime shifts versus rebound potential in coral reefs. *Nature* 518, 94–97. doi:10.1038/nature14140.

Graham, N. A. J., Nash, K. L., and Kool, J. T. (2011). Coral reef recovery dynamics in a changing world. *Coral Reefs* 30, 283–294. doi:10.1007/s00338-010-0717-z.

Gutner-Hoch, E., Martins, R., Oliveira, T., Maia, F., Soares, A., Loureiro, S., et al. (2018). Antimacrofouling Efficacy of Innovative Inorganic Nanomaterials Loaded with Booster Biocides. *J. Mar. Sci. Eng.* 6, 6. doi:10.3390/jmse6010006.

Harborne, A. R., Rogers, A., Bozec, Y. M., and Mumby, P. J. (2017). Multiple Stressors and the Functioning of Coral Reefs. *Ann. Rev. Mar. Sci.* 9, 445–468. doi:10.1146/annurev-marine-010816-060551.

Harrison, P., Villanueva, R., and Dela Cruz, D. (2016). Coral Reef Restoration using Mass Coral Larval Reseeding.

Hartig, F. (2022). DHARMa: Residual Diagnostics for Hierarchical (Multi-Level / Mixed) Regression Models. Available at: https://cran.r-project.org/package=DHARMa.

Hauri, C., Fabricius, K. E., Schaffelke, B., and Humphrey, C. (2010). Chemical and physical environmental conditions underneath mat- and canopy-forming macroalgae, and their effects on understorey corals. *PLoS One* 5, 1–9. doi:10.1371/journal.pone.0012685.

Hayashibara, T., Kimura, T., and Hatta, M. (2000). Changes of cnida composition during planula development of a reef-building coral *Acropora nasuta*. *Japanese Coral Reef Soc.* 42, 39–42. doi:10.3755/jcrs.2000.39.

Herget, K., Frerichs, H., Pfitzner, F., Tahir, M. N., and Tremel, W. (2018). Functional Enzyme Mimics for Oxidative Halogenation Reactions that Combat Biofilm Formation. *Adv. Mater.* 30, 1–28. doi:10.1002/adma.201707073.

Herget, K., Hubach, P., Pusch, S., Deglmann, P., Götz, H., Gorelik, T. E., et al. (2017). Haloperoxidase Mimicry by CeO2-x Nanorods Combats Biofouling. *Adv. Mater.* 29, 1–8. doi:10.1002/adma.201603823.

Heyward, A. J., and Negri, A. P. (1999). Natural inducers for coral larval metamorphosis. *Coral Reefs* 18, 273–279. doi:10.1007/s003380050193.

Heyward, A. J., Rees, M., and Smith, L. D. (1999). Coral spawning slicks harnessed for large-scale coral culture. *Progr. Abstr. Int. Conf. Sci. Asp. Coral Reef Assessment, Monit. Restor.* 104, 188–189.

Hoegh-Guldberg, O., Poloczanska, E. S., Skirving, W., and Dove, S. (2017). Coral reef ecosystems under climate change and ocean acidification. *Front. Mar. Sci.* 4. doi:10.3389/fmars.2017.00158.

Hughes, T. P., Kerry, J. T., Baird, A. H., Connolly, S. R., Chase, T. J., Dietzel, A., et al. (2019). Global warming impairs stock–recruitment dynamics of corals. *Nature* 568, 387–390. doi:10.1038/s41586-019-1081-y.

Hughes, T. P., Rodrigues, M. J., Bellwood, D. R., Ceccarelli, D., Hoegh-Guldberg, O., McCook, L., et al. (2007). Phase Shifts, Herbivory, and the Resilience of Coral Reefs to Climate Change. *Curr. Biol.* 17, 360–365. doi:10.1016/j.cub.2006.12.049.

ImageJ Release Notes Available at: https://imagej.nih.gov/ij/notes.html.

Jacobson, A. H., and Willingham, G. L. (2000). Sea-nine antifoulant: An environmentally acceptable alternative to organotin antifoulants. *Sci. Total Environ.* 258, 103–110. doi:10.1016/S0048-9697(00)00511-8.

Jin, H., Tian, L., Bing, W., Zhao, J., and Ren, L. (2022). Bioinspired marine antifouling coatings: Status, prospects, and future. *Prog. Mater. Sci.* 124, 100889. doi:10.1016/j.pmatsci.2021.100889.

Kenyon, T. M., Doropoulos, C., Dove, S., Webb, G. E., Newman, S. P., Sim, C. W. H., et al. (2020). The effects of rubble mobilisation on coral fragment survival, partial mortality and growth. *J. Exp. Mar. Bio. Ecol.* 533, 151467. doi:10.1016/j.jembe.2020.151467.

Kirschner, C. M., and Brennan, A. B. (2012). Bio-inspired antifouling strategies. *Annu. Rev. Mater. Res.* 42, 211–229. doi:10.1146/annurev-matsci-070511-155012.

Korschelt, K., Schwidetzky, R., Pfitzner, F., Strugatchi, J., Schilling, C., Von Der Au, M., et al. (2018a). CeO2-: X nanorods with intrinsic urease-like activity. *Nanoscale* 10, 13074–13082. doi:10.1039/c8nr03556c.

Korschelt, K., Tahir, M. N., and Tremel, W. (2018b). A Step into the Future: Applications of Nanoparticle Enzyme Mimics. *Chem. - A Eur. J.* 24, 9703–9713. doi:10.1002/chem.201800384.

Kuffner, I. B., Andersson, A. J., Jokiel, P. L., Rodgers, K. S., and MacKenzie, F. T. (2008). Decreased abundance of crustose coralline algae due to ocean acidification. *Nat. Geosci.* 1, 114–117. doi:10.1038/ngeo100.

Kuffner, I. B., Walters, L. J., Becerro, M. A., Paul, V. J., Ritson-Williams, R., and Beach, K. S. (2006). Inhibition of coral recruitment by macroalgae and cyanobacteria. *Mar. Ecol. Prog. Ser.* 323, 107–117. doi:10.3354/meps323107.

Kuznetsova, A., Brockhoff, P. B., and Christensen, R. H. B. (2017). lmerTest Package: Tests in Linear Mixed Effects Models. *J. Stat. Softw.* 82, 1–26. doi:10.18637/JSS.V082.I13.

Lenth, R. V. (2021). Emmeans: estimated marginal means. Available at: https://cran.r-project.org/package=emmeans.

Linares, C., Cebrian, E., and Coma, R. (2012). Effects of turf algae on recruitment and juvenile survival of gorgonian corals. *Mar. Ecol. Prog. Ser.* 452, 81–88. doi:10.3354/meps09586.

Maia, F., Silva, A. P., Fernandes, S., Cunha, A., Almeida, A., Tedim, J., et al. (2015). Incorporation of biocides in nanocapsules for protective coatings used in maritime applications. *Chem. Eng. J.* 270, 150–157. doi:10.1016/j.cej.2015.01.076.

Maia, F., Tedim, J., Lisenkov, A. D., Salak, A. N., Zheludkevich, M. L., and Ferreira, M. G. S. (2012). Silica nanocontainers for active corrosion protection. *Nanoscale* 4, 1287–1298. doi:10.1039/c2nr11536k.

Martins, R., Oliveira, T., Santos, C., Kuznetsova, A., Ferreira, V., Avelelas, F., et al. (2017). Effects of a novel anticorrosion engineered nanomaterial on the bivalve: *Ruditapes philippinarum*. *Environ. Sci. Nano* 4, 1064–1076. doi:10.1039/c6en00630b.

McCook, L. J., Jompa, J., and Diaz-Pulido, G. (2001). Competition between corals and algae on coral reefs: A review of evidence and mechanisms. *Coral Reefs* 19, 400–417. doi:10.1007/s003380000129.

Miller, I. B., Moeller, M., Kellermann, M. Y., Nietzer, S., Di Mauro, V., Kamyab, E., et al. (2022). Towards the Development of Standardized Bioassays for Corals: Acute Toxicity of the UV Filter Benzophenone-3 to Scleractinian Coral Larvae. *Toxics* 10, 244. doi:10.3390/toxics10050244.

Miller, M. W., Latijnhouwers, K. R. W., Bickel, A., Mendoza-Quiroz, S., Schick, M., Burton, K., et al. (2021). Settlement yields in large-scale in situ culture of Caribbean coral larvae for restoration. *Restor. Ecol.* doi:10.1111/rec.13512.

Mitchelmore, C. L., Burns, E. E., Conway, A., Heyes, A., and Davies, I. A. (2021). A Critical Review of Organic Ultraviolet Filter Exposure, Hazard, and Risk to Corals. *Environ. Toxicol. Chem.* 40, 967–988. doi:10.1002/etc.4948.

Moeller, M., Pawlowski, S., Petersen-Thiery, M., Miller, I. B., Nietzer, S., Heisel-Sure, Y., et al. (2021). Challenges in Current Coral Reef Protection – Possible Impacts of UV Filters Used in Sunscreens, a Critical Review. *Front. Mar. Sci.* 8, 1–16. doi:10.3389/fmars.2021.665548.

Negri, A. P., and Heyward, A. J. (2000). Inhibition of Fertilization and Larval Metamorphosis of the Coral *Acropora millepora* (Ehrenberg, 1834) by Petroleum Products. *Mar. Pollut. Bull.* 41, 420–427.

Negri, A. P., and Heyward, A. J. (2001). Inhibition of coral fertilisation and larval metamorphosis by tributyltin and copper. *Mar. Environ. Res.* 51, 17–27.

Negri, A. P., Smith, L. D., Webster, N. S., and Heyward, A. J. (2002). Understanding ship-grounding impacts on a coral reef: Potential effects of anti-foulant paint contamination on coral recruitment. *Mar. Pollut. Bull.* 44, 111–117. doi:10.1016/S0025-326X(01)00128-X.

Negri, A. P., Webster, N. S., Hill, R. T., and Heyward, A. J. (2001). Metamorphosis of broadcast spawning corals in response to bacteria isolated from crustose algae. *Mar. Ecol. Prog. Ser.* 223, 121–131.

Nordborg, F. M., Flores, F., Brinkman, D. L., Agustí, S., and Negri, A. P. (2018). Phototoxic effects of two common marine fuels on the settlement success of the coral *Acropora tenuis*. *Sci. Rep.* 8, 1–12. doi:10.1038/s41598-018-26972-7.

Nugues, M. M., Smith, G. W., Van Hooidonk, R. J., Seabra, M. I., and Bak, R. P. M. (2004). Algal contact as a trigger for coral disease. *Ecol. Lett.* 7, 919–923. doi:10.1111/j.1461-0248.2004.00651.x.

Okubo, N., and Motokawa, T. (2007). Embryogenesis in the reef-building coral *Acropora* spp. *Zoolog. Sci.* 24, 1169–1177. doi:10.2108/zsj.24.1169.

Ortiz, J. C., Wolff, N. H., Anthony, K. R. N., Devlin, M., Lewis, S., and Mumby, P. J. (2018). Impaired recovery of the great barrier reef under cumulative stress. *Sci. Adv.* 4, 1–9. doi:10.1126/sciadv.aar6127.

R Core Team (2021). R: A Language and Environment for Statistical Computing. Available at: https://www.r-project.org/.

Randall, C. J., Giuliano, C., Heyward, A. J., and Negri, A. P. (2021). Enhancing Coral Survival on Deployment Devices With Microrefugia. *Front. Mar. Sci.* 8, 662263; 10.3389/fmars.2021.662263. doi:10.3389/fmars.2021.662263.

Randall, C. J., Negri, A. P., Quigley, K. M., Foster, T., Ricardo, G. F., Webster, N. S., et al. (2020). Sexual production of corals for reef restoration in the Anthropocene. *Mar. Ecol. Prog. Ser.* 635, 203–232. doi:10.3354/MEPS13206.

Richards, C., Briciu-Burghina, C., Jacobs, M. R., Barrett, A., and Regan, F. (2019). Assessment of antifouling potential of novel transparent sol gel coatings for application in the marine environment. *Molecules* 24. doi:10.3390/molecules24162983.

Richmond, R. H. (1997). "Reproduction and recruitment in corals: critical links in the persistence of reefs," in *Life and Death of Coral Reefs*, ed. C. E. Birkeland (Springer US), 175–197. doi:10.1007/978-1-4615-5995-5_8.

Roepke, L. K., Brefeld, D., Soltmann, U., Randall, C. J., Negri, A. P., and Kunzmann, A. (2022a). Antifouling coatings can reduce algal growth while preserving coral settlement. *Sci. Rep.* 12, 15935. doi:10.1038/s41598-022-19997-6.

Roepke, L. K., Brefeld, D., Soltmann, U., Randall, C. J., Negri, A. P., and Kunzmann, A. (2022b). Applying behavioral studies to the ecotoxicology of corals: A case study on *Acropora millepora*. *Front. Mar. Sci.* 9, 1–14. doi:10.3389/fmars.2022.1002924.

Schneider, C. A., Rasband, W. S., and Eliceiri, K. W. (2012). NIH Image to ImageJ: 25 years of image analysis. *Nat. Methods* 9, 671–675. doi:10.1038/nmeth.2089.

Silva, V., Silva, C., Soares, P., Garrido, E. M., Borges, F., and Garrido, J. (2020). Isothiazolinone Biocides: Chemistry, Biological, and Toxicity Profiles. *Molecules* 25, 10.3390/molecules25040991. doi:10.3390/molecules25040991.

Sneed, J. M., Sharp, K. H., Ritchie, K. B., and Paul, V. J. (2014). The chemical cue tetrabromopyrrole from a biofilm bacterium induces settlement of multiple Caribbean corals. *Proc. R. Soc. B Biol. Sci.* 281, 1–9. doi:10.1098/rspb.2013.3086.

Speare, K. E., Duran, A., Miller, M. W., and Burkepile, D. E. (2019). Sediment associated with algal turfs inhibits the settlement of two endangered coral species. *Mar. Pollut. Bull.* 144, 189–195. doi:10.1016/j.marpolbul.2019.04.066.

Tang, C. H., Lin, C. Y., Lee, S. H., and Wang, W. H. (2017). Membrane lipid profiles of coral responded to zinc oxide nanoparticle-induced perturbations on the cellular membrane. *Aquat. Toxicol.* 187, 72–81. doi:10.1016/j.aquatox.2017.03.021.

Tebben, J., Guest, J. R., Sin, T. M., Steinberg, P. D., and Harder, T. (2014). Corals like it waxed: Paraffin-based antifouling technology enhances coral spat survival. *PLoS One* 9, 1–8. doi:10.1371/journal.pone.0087545.

Tebben, J., Motti, C. A., Siboni, N., Tapiolas, D. M., Negri, A. P., Schupp, P. J., et al. (2015). Chemical mediation of coral larval settlement by crustose coralline algae. *Sci. Rep.* 5, 1–11. doi:10.1038/srep10803.

Tebben, J., Tapiolas, D. M., Motti, C. A., Abrego, D., Negri, A. P., Blackall, L. L., et al. (2011). Induction of larval metamorphosis of the coral *Acropora millepora* by tetrabromopyrrole isolated from a Pseudoalteromonas bacterium. *PLoS One* 6, 1–8. doi:10.1371/journal.pone.0019082.

Vardi, T., Hoot, W. C., Levy, J., Shaver, E., Winters, R. S., Banaszak, A. T., et al. (2021). Six priorities to advance the science and practice of coral reef restoration worldwide. *Restor. Ecol.* 29, 1–7. doi:10.1111/rec.13498.

Vermeij, M. J. A., and Sandin, S. A. (2008). Density-dependent settlement and mortality structure the earliest life phases of a coral population. *Ecology* 89, 1994–2004. doi:10.1890/07-1296.1.

Vermeij, M. J. A., Smith, J. E., Smith, C. M., Vega Thurber, R., and Sandin, S. A. (2009). Survival and settlement success of coral planulae: Independent and synergistic effects of macroalgae and microbes. *Oecologia* 159, 325–336. doi:10.1007/s00442-008-1223-7.

Webster, N. S., Smith, L. D., Heyward, A. J., Watts, J. E. M., Webb, R. I., Blackall, L. L., et al. (2004). Metamorphosis of a scleractinian coral in response to microbial biofilms. *Appl. Environ. Microbiol.* 70, 1213–21. doi:10.1128/AEM.70.2.1213.

Webster, N. S., Uthicke, S., Botté, E. S., Flores, F., and Negri, A. P. (2013). Ocean acidification reduces induction of coral settlement by crustose coralline algae. *Glob. Chang. Biol.* 19, 303–315. doi:10.1111/gcb.12008.

Wickham, H., Averick, M., Bryan, J., Chang, W., McGowan, L., François, R., et al. (2019). Welcome to the Tidyverse. *J. Open Source Softw.* 4, 1686; 10.21105/joss.01686. doi:10.21105/joss.01686.

Xu, Y., Wang, C., Hou, J., Wang, P., You, G., and Miao, L. (2018). Mechanistic understanding of cerium oxide nanoparticle-mediated biofilm formation in *Pseudomonas aeruginosa*. *Environ. Sci. Pollut. Res.* 25, 34765–34776. doi:10.1007/s11356-018-3418-8.

Xu, Y., Wang, C., Hou, J., Wang, P., You, G., and Miao, L. (2019). Effects of cerium oxide nanoparticles on bacterial growth and behaviors: induction of biofilm formation and stress response. *Environ. Sci. Pollut. Res.* 26, 9293–9304. doi:10.1007/s11356-019-04340-w.

# Supplementary Information: Effects of antifoulings on survival and growth of coral spat for reef restoration

## SI Tables

**Table S3.1:** Total absolute *A. millepora* spat survivors on fully-coated (FC) and partially-coated (PC) plugs at monitoring time points (0, 14, 42, 69 days). N (= 45) corresponds to the number of plugs in each treatment/area measured repeatedly for each monitoring period.

| Treatment | 0 days | 14 days | 42 days | 69 days |
|---|---|---|---|---|
| Control | 317 | 312 | 127 | 52 |
| FC Nanoparticles | 371 | 368 | 238 | 70 |
| FC Antiadhesive | 331 | 330 | 190 | 82 |
| PC Antiadhesive - Uncoated | 89 | 88 | 53 | 15 |
| PC Antiadhesive - Coated | 254 | 253 | 162 | 51 |
| PC DCOIT - Uncoated | 234 | 233 | 170 | 67 |
| PC Nanoparticles - Uncoated | 117 | 116 | 54 | 14 |
| PC Nanoparticles - Coated | 194 | 192 | 97 | 35 |

**Table S3.2:** Estimated marginal means (EMM), standard error (SE), degrees of freedom (df) and upper and lower confidence levels (CL; 95% and 5%, respectively) of ***Acropora millepora*** **survival** in each treatment (Control, Nanoparticles, Antiadhesive) after 69 days on the fully-coated (FC) plugs. Intervals (EMM, SE, CL) were back-transformed from the cloglog scale.

| Treatment | EMM | Standard error | df | Lower CL | Upper CL |
|---|---|---|---|---|---|
| Control | 0.9 | 0.1 | Inf | 0.8 | 1 |
| Nanoparticles | 0.9 | 0.1 | Inf | 0.6 | 1 |
| Antiadhesive | 0.9 | 0.1 | Inf | 0.7 | 1 |

**Table S3.3:** Pairwise statistical results of ***Acropora millepora*** **survival** data after 69 days on the fully-coated (FC) plugs based on estimated marginal means. Note that the estimated contrasts were back-transformed from the cloglog scale. The p-value was adjusted for multiple comparisons (family of 3 estimates) with the Tukey method. Significant codes indicate: * < 0.05, ** < 0.01, *** < 0.001. All statistical analyses were performed in R version 4.2.0 (R Core Team, 2021).

| Compared treatment pair | Estimated contrast | Standard error | df | z ratio | p-value |
|---|---|---|---|---|---|
| Control - Nanoparticles | 0.1 | 0.1 | Inf | 2.069 | 0.096 |
| Control - Antiadhesive | 0.1 | 0.1 | Inf | 1.796 | 0.171 |
| Nanoparticles - Antiadhesive | 0 | 0.1 | Inf | -0.259 | 0.964 |

**Table S3.4**: Estimated marginal means (EMM), standard error (SE), degrees of freedom (df) and upper and lower confidence levels (CL; 95% and 5%, respectively) of ***Acropora millepora*** **survival** in each treatment (Control, Nanoparticles, Antiadhesive, DCOIT) after 69 days on the partially-coated (PC) plugs. Intervals (EMM, SE, CL) were back-transformed from the cloglog scale.

| Treatment | EMM | Standard error | df | Lower CL | Upper CL |
|---|---|---|---|---|---|
| Nanoparticles Uncoated | 1 | 0 | Inf | 0.8 | 1 |
| Nanoparticles Coated | 1 | 0 | Inf | 0.8 | 1 |
| Antiadhesive Uncoated | 0.9 | 0.1 | Inf | 0.6 | 1 |
| Antiadhesive Coated | 0.9 | 0.1 | Inf | 0.7 | 1 |

| | | | | | |
|---|---|---|---|---|---|
| DCOIT Uncoated | 0.8 | 0.1 | Inf | 0.5 | 1 |
| Control Uncoated | 1 | 0 | Inf | 0.8 | 1 |

**Table S3.5:** Pairwise statistical results of ***Acropora millepora*** **survival** data after 69 days on the partially-coated (PC) plugs based on estimated marginal means. Note that the estimated contrasts were back-transformed from the cloglog scale. The p-value was adjusted for multiple comparisons (family of 6 estimates) with the Tukey method. Significant codes indicate: * < 0.05, ** < 0.01, *** < 0.001. All statistical analyses were performed in R version 4.2.0 (R Core Team, 2021).

| Compared treatment pair | Estimated contrast | Standard error | df | z ratio | p-value |
|---|---|---|---|---|---|
| Nanoparticles Uncoated - Nanoparticles Coated | 0 | 0 | Inf | -0.426 | 0.998 |
| Nanoparticles Uncoated - Antiadhesive Uncoated | 0.1 | 0.1 | Inf | 1.496 | 0.667 |
| Nanoparticles Uncoated - Antiadhesive Coated | 0 | 0 | Inf | 1.251 | 0.812 |
| Nanoparticles Uncoated - DCOIT Uncoated | 0.2 | 0.1 | Inf | 3.141 | 0.021 * |
| Nanoparticles Uncoated - Control Uncoated | 0 | 0 | Inf | -0.146 | 1 |
| Nanoparticles Coated - Antiadhesive Uncoated | 0.1 | 0.1 | Inf | 1.852 | 0.432 |
| Nanoparticles Coated - Antiadhesive Coated | 0 | 0.1 | Inf | 1.666 | 0.554 |
| Nanoparticles Coated - DCOIT Uncoated | 0.2 | 0.1 | Inf | 3.635 | 0.004 ** |
| Nanoparticles Coated - Control Uncoated | 0 | 0 | Inf | 0.19 | 1 |
| Antiadhesive Uncoated - Antiadhesive Coated | 0 | 0 | Inf | -0.568 | 0.993 |
| Antiadhesive Uncoated - DCOIT Uncoated | 0.1 | 0.1 | Inf | 1.429 | 0.709 |
| Antiadhesive Uncoated - Control Uncoated | -0.1 | 0.1 | Inf | -1.761 | 0.492 |
| Antiadhesive Coated - DCOIT Uncoated | 0.1 | 0.1 | Inf | 2.141 | 0.266 |
| Antiadhesive Coated - Control Uncoated | 0 | 0 | Inf | -1.557 | 0.627 |
| DCOIT Uncoated - Control Uncoated | -0.2 | 0.1 | Inf | -3.7 | 0.003 ** |

**Table S3.6:** Descriptive ***Acropora millepora*** **growth rate** data per treatment (Control, Nanoparticles, Antiadhesive) after 14 days on the fully-coated (FC) plugs. Values represent mean growth (%). N corresponds to the number of spat in each treatment measured repeatedly for each monitoring time point.

| Treatment | n | Mean growth | Standard error |
|---|---|---|---|
| Control | 223 | 1.2 | 1.3 |
| Nanoparticles | 286 | -3.5 | 1 |
| Antiadhesive | 224 | 4.7 | 1.6 |

**Table S3.7:** Descriptive ***Acropora millepora*** **size** data per treatment (Control, Nanoparticles, Antiadhesive) after 0 (beginning monitoring) & 14 days on the fully-coated (FC) plugs. Values represent mean size ($mm^2$). N corresponds to the number of spat in each treatment measured repeatedly for each monitoring time point.

| Treatment | Time point | n | Mean size | Standard error |
|---|---|---|---|---|
| Control | 0 | 223 | 1.114 | 0.019 |
| Control | 14 | 223 | 1.101 | 0.017 |
| Nanoparticles | 0 | 286 | 1.101 | 0.017 |
| Nanoparticles | 14 | 286 | 1.048 | 0.016 |
| Antiadhesive | 0 | 224 | 0.986 | 0.019 |
| Antiadhesive | 14 | 224 | 1.004 | 0.019 |

**Table S3.8:** Estimated marginal means (EMM), standard error (SE), degrees of freedom (df) and upper and lower confidence levels (CL; 95% and 5%, respectively) of ***Acropora millepora*** **growth rate** in each treatment (Control, Nanoparticles, Antiadhesive) after 14 days on the fully-coated (FC) plugs.

| Treatment | EMM | Standard error | df | Lower CL | Upper CL |
|---|---|---|---|---|---|
| Control | 2.5 | 4.1 | 5.62 | -7.8 | 12.7 |
| Nanoparticles | -2.4 | 4 | 5.328 | -12.6 | 7.8 |
| Antiadhesive | 6.4 | 4.1 | 5.634 | -3.9 | 16.6 |

**Table S3.9:** Pairwise statistical results of ***Acropora millepora*** **growth rate** data after 14 days on the fully-coated (FC) plugs based on estimated marginal means. Note that the estimated contrasts are on the cloglog scale. The p-value was adjusted for multiple comparisons (family of 3 estimates) with the Tukey method. Significant codes indicate: * < 0.05, ** < 0.01, *** < 0.001. All statistical analyses were performed in R version 4.2.0 (R Core Team, 2021).

| Compared treatment pair | Estimated contrast | Standard error | df | t ratio | p-value |
|---|---|---|---|---|---|
| Control - Nanoparticles | 4.9 | 2.6 | 120.781 | 1.916 | 0.139 |
| Control - Antiadhesive | -3.9 | 2.6 | 128.829 | -1.482 | 0.303 |
| Nanoparticles - Antiadhesive | -8.8 | 2.6 | 120.938 | -3.416 | 0.002 ** |

**Table S3.10** Descriptive ***Acropora millepora*** **growth rate** data per treatment (Control, Nanoparticles, Antiadhesive, DCOIT) after 14 days on the partially-coated (PC) plugs. Values represent mean growth (%). N corresponds to the number of spat in each treatment measured repeatedly for each monitoring time point.

| Treatment | n | Mean growth | Standard error |
|---|---|---|---|
| Control | 223 | 1.2 | 1.3 |
| Nanoparticles - Coated | 157 | -3.6 | 1.3 |
| Nanoparticles - Uncoated | 94 | -5.7 | 1.3 |
| Antiadhesive - Coated | 150 | 4.5 | 1.8 |
| Antiadhesive - Uncoated | 53 | 0.2 | 3.5 |
| DCOIT | 152 | 3.8 | 2.1 |

**Table S3.11:** Descriptive ***Acropora millepora*** **size** data per treatment (Control, Nanoparticles, Antiadhesive, DCOIT) after 0 (beginning monitoring) & 14 days on the partially-coated (PC) plugs. Values represent mean size ($mm^2$). N corresponds to the number of spat in each treatment measured repeatedly for each monitoring time point.

| Treatment | Time point | n | Mean size | Standard error |
|---|---|---|---|---|
| Control | 0 | 223 | 1.114 | 0.019 |
| Control | 14 | 223 | 1.101 | 0.017 |
| Nanoparticles Coated | 0 | 157 | 1.163 | 0.022 |
| Nanoparticles Coated | 14 | 157 | 1.108 | 0.021 |
| Nanoparticles Uncoated | 0 | 94 | 1.104 | 0.032 |
| Nanoparticles Uncoated | 14 | 94 | 1.037 | 0.032 |
| Antiadhesive Coated | 0 | 150 | 0.965 | 0.025 |
| Antiadhesive Coated | 14 | 150 | 0.985 | 0.026 |
| Antiadhesive Uncoated | 0 | 53 | 0.996 | 0.035 |
| Antiadhesive Uncoated | 14 | 53 | 0.971 | 0.037 |
| DCOIT Uncoated | 0 | 152 | 0.72 | 0.02 |
| DCOIT Uncoated | 14 | 152 | 0.739 | 0.023 |

**Table S3.12:** Estimated marginal means (EMM), standard error (SE), degrees of freedom (df) and upper and lower confidence levels (CL; 95% and 5%, respectively) of ***Acropora millepora*** **growth rate** in each treatment (Control, Nanoparticles, Antiadhesive, DCOIT) after 14 days on the partially-coated (PC) plugs.

| Treatment | EMM | Standard error | df | Lower CL | Upper CL |
|---|---|---|---|---|---|
| Control Uncoated | 1.1 | 3.4 | 5.89 | -7.2 | 9.4 |
| Nanoparticles Coated | -1.7 | 3.5 | 6.943 | -10 | 6.5 |
| Nanoparticles Uncoated | -4.5 | 3.7 | 9.23 | -12.8 | 3.8 |
| Antiadhesive Coated | 4.5 | 3.5 | 7.082 | -3.7 | 12.8 |
| Antiadhesive Uncoated | 1.7 | 4.2 | 14.569 | -7.2 | 10.6 |
| DCOIT Uncoated | 4.1 | 3.5 | 6.943 | -4.1 | 12.4 |

**Table S3.13:** Pairwise statistical results of ***Acropora millepora*** **growth rate** data after 14 days on the partially-coated (PC) plugs based on estimated marginal means. Note that the estimated contrasts are on the cloglog scale. The p-value was adjusted for multiple comparisons (family of 5 estimates) with the Tukey method. Significant codes indicate: * < 0.05, ** < 0.01, *** < 0.001. All statistical analyses were performed in R version 4.2.0 (R Core Team, 2021).

| Compared treatment pair | Estimated contrast | Standard error | df | t ratio | p-value |
|---|---|---|---|---|---|
| Control Uncoated - Nanoparticles Coated | 2.9 | 3 | 183.474 | 0.966 | 0.928 |
| Control Uncoated - Nanoparticles Uncoated | 5.7 | 3.2 | 240.05 | 1.747 | 0.502 |
| Control Uncoated - Antiadhesive Coated | -3.4 | 3 | 183.461 | -1.136 | 0.866 |
| Control Uncoated - Antiadhesive Uncoated | -0.6 | 3.7 | 338.806 | -0.157 | 1 |
| Control Uncoated - DCOIT Uncoated | -3 | 3 | 177.141 | -0.988 | 0.921 |
| Nanoparticles Coated - Nanoparticles Uncoated | 2.8 | 2.7 | 820.734 | 1.041 | 0.904 |
| Nanoparticles Coated - Antiadhesive Coated | -6.2 | 3.1 | 209.122 | -2.011 | 0.339 |
| Nanoparticles Coated - Antiadhesive Uncoated | -3.4 | 3.8 | 365.063 | -0.897 | 0.947 |
| Nanoparticles Coated - DCOIT Uncoated | -5.8 | 3.2 | 205.397 | -1.847 | 0.438 |
| Nanoparticles Uncoated - Antiadhesive Coated | -9 | 3.4 | 267.679 | -2.674 | 0.084 |
| Nanoparticles Uncoated - Antiadhesive Uncoated | -6.3 | 4.1 | 408.75 | -1.54 | 0.639 |
| Nanoparticles Uncoated - DCOIT Uncoated | -8.6 | 3.4 | 257.525 | -2.532 | 0.119 |
| Antiadhesive Coated - Antiadhesive Uncoated | 2.8 | 3.3 | 811.323 | 0.842 | 0.96 |
| Antiadhesive Coated - DCOIT Uncoated | 0.4 | 3.2 | 205.419 | 0.127 | 1 |
| Antiadhesive Uncoated - DCOIT Uncoated | -2.4 | 3.9 | 349.391 | -0.617 | 0.99 |

## SI References

R Core Team (2021). R: A Language and Environment for Statistical Computing. Available at: https://www.r-project.org/.

# Chapter 4: Applying behavioral studies to the ecotoxicology of corals: a case study on *Acropora millepora*

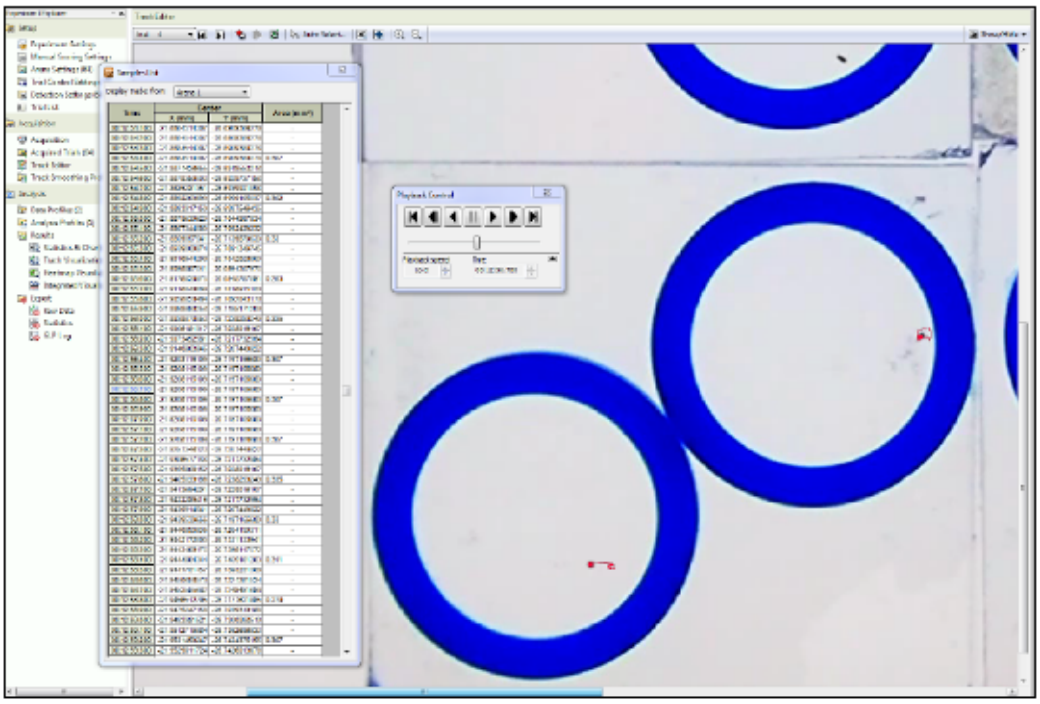

***Published as:***
***Roepke LK, Brefeld D, Soltmann U, Randall CJ, Negri AP and Kunzmann A (2022) Applying behavioral studies to the ecotoxicology of corals: A case study on Acropora millepora. Front Mar Sci 9:1002924. doi: 10.3389/fmars.2022.1002924***

## Abstract

Behavioral responses are considered sensitive and effective indicators of organism stress. As the demand for standardized coral toxicity tests grows, innovative tools that allow for automatic and quantitative measurements of these behaviors may complement ecotoxicological studies. The rapid growth of competitive marine algae in aquaculture systems is a major issue for generating coral spat for reef restoration, and the application of non-toxic antifouling (AF) coatings might effectively mitigate this issue. While these coatings do not appear to be toxic to sensitive coral larvae, their potential to affect larval mobility has not been tested. In this context, we tested the effect of three recently-developed and potentially non-toxic AF coatings: (i) antiadhesive, (ii) cerium dioxide ($CeO_{2-x}$) nanoparticle, and (iii) encapsulated biocide dichlorooctylisothiazolinone (DCOIT) on the swimming velocity and activity of *Acropora millepora* coral larvae for potential use in reef-restoration activities. The behavior of 32 coral larvae per AF treatment were recorded, each for 25 min, in a self-constructed dark box with two camera recording sets in parallel. The tracking analysis was performed with the software Noldus EthoVision XT. The mean larval swimming velocity on control tiles of 93.1 ± 5.6 mm $min^{-1}$ (and activity of 62.8 ± 5.2 %) was nearly 2-fold faster (higher) than on the antiadhesive, ($CeO_{2-x}$) nanoparticle and DCOIT coatings, respectively. Larvae exposed to the DCOIT-coated tiles remained almost stationary. Although the underlying cause and consequence of these results require further investigation, tracking of coral larval swimming behavior was identified as a reliable and feasible method for assessing potential non-lethal responses to AF coatings. As changes in behavior could have significant consequences for larval survival and settlement, they are important endpoints to consider, and the quantification of behavioral responses may be a meaningful and sensitive tool. Therefore, we recommend the use of behavioral studies for coral larval assessments in ecotoxicology as a valuable endpoint. For methodological standardization and implementation, our study also features a detailed guide for video-processing and track analysis of *A. millepora* coral larvae in EthoVision.


**Key words: locomotion, motility, biomarker, ecotoxicology, video-tracking systems, aquatic toxicology, coral toxicity**

## 1. Introduction

Tropical coral reefs are under increasing pressure (Gardner et al., 2003; Bruno and Selig, 2007; De'Ath et al., 2012) from climate change as well as increased human activities in coastal areas (Hughes et al., 2010, 2017; Pandolfi et al., 2011). While heat stress events can cause a rapid decline in coral cover (Cornwall et al., 2021), local impacts to coral reefs can exacerbate coral mortality through multi-stressor events. For instance, antifoulant releases following ship groundings have resulted in some of the most contaminated coral reefs, with TBT (tributyltin)

and Cu (copper) being highly potent inhibitors of coral larval settlement and survival, both of which are key processes in reef recovery (Negri et al., 2002). Therefore, the development of safe, non-toxic AF coatings could reduce persistent harm following such accidents. Coral health and survival can also be affected by competition with other benthic organisms (Hughes et al., 2007; Vermeij and Sandin, 2008; Vermeij et al., 2009), including macroalgae, which can be favoured by excess nutrients (Karcher et al., 2020; Adam et al., 2021). The interaction between corals and fouling organisms, particularly filamentous algae can be detrimental to larval settlement and to the survival and growth of coral recruits and the success of adult corals (Carpenter and Edmunds, 2006; Box, Steve and Mumby, Peter, 2007; Linares et al., 2012). Competition between rapidly growing algae and newly settled corals in aquaculture represents a problem for coral restoration projects, where maximising the survival of corals is critical to the feasibility of upscaling restoration towards ecologically meaningful outcomes (Randall et al., 2020). Non-toxic AF applications may prove beneficial for improving survival in coral aquaculture and restoration, an approach being developed to boost reef recovery. The application of a wax AF coating on coral settlement devices to control the benthic community composition around newly settled corals (i.e. 'spat') was found to reduce mortality (Tebben et al., 2014), which could increase the likelihood of coral survival to size-escape thresholds and consequently improve the success of sexual coral-propagation techniques (Randall et al., 2020). A recent study also demonstrated the effectiveness of two non-toxic AF coatings (same coatings as in this study) to reduce algal growth on coral settlement surfaces, a first step towards controlling fine-scale competition with benthic organisms in coral aquaculture (Roepke et al., 2022). While these AF coatings did not affect coral larval settlement, further work is required to assess their potential influence on other aspects of larval behavior such as mobility which might represent a sensitive response relevant to the application of AF coatings for shipping and in aquaculture.

Innovative non-toxic AF coatings include silicon-based sol-gel coatings which exhibit antiadhesive surface properties (herein referred to as antiadhesive coating) that prevent the attachment of fouling organisms and facilitate their release at high water velocities. The antiadhesive effect is achieved through low surface energies (with weak molecular attraction), amphiphilic properties (both hydrophilic and hydrophobic properties) and a precisely tuned surface roughness designed to inhibit primary fouling (Detty et al., 2014). Some studies have shown effective AF properties of the biocide dichlorooctylisothiazolinone (DCOIT, Kathon 930, C-9 or DCOI) encapsulated in silica nanocapsules (in this study referred to as DCOIT coating), which decreases the toxicity towards organisms (Maia et al., 2015; Vitoria et al., 2020). Other recently developed non-biocidal AFs are based on nanoparticles (NPs), which disrupt bacterial cell-to-cell communication (i.e. quorum sensing) to inhibit the formation of biofilms (herein referred to as nanoparticle coating) and mitigate or delay colonization by algae (Korschelt et al., 2018b). One example includes cerium ($Ce^{3+}/Ce^{4+}$)-modified sites across the high surface area of NPs, which enhance the catalytic oxidation of halides, resulting in the

formation of biocidal compounds that combat biofilm formation or the formation of signaling molecules involved in intracellular communication (Herget et al., 2017a, 2018; Korschelt et al., 2018a).

Studies on potential coral stressors and the effects of toxicants have garnered interest in the scientific and public community in recent years as the awareness of threats to tropical coral reef health increases. Over two decades ago, copper toxicity was tested for its inhibitory effect on coral gamete fertilization and larvae settlement (Reichelt-Brushett and Harrison, 2000; Negri and Heyward, 2001). Since then, assays have been used to identify toxicity thresholds for petroleum (Nordborg et al., 2018), AF paint (Negri et al., 2002), pesticides (Ross et al., 2015), and most recently, sunscreens and UV filters (Miller et al., 2021, 2022; Moeller et al., 2021; Pawlowski et al., 2021). However, toxicity assays often differ in methodology and experimental responses or endpoints among studies. For example, some studies have used lethal concentrations (i.e. Kwok and Ang, 2013), while other studies report sublethal endpoints including gene expression biomarkers of heat stress (Louis et al., 2017; Ishibashi et al., 2018), oxidative stress (Cima et al., 2013; Olsen et al., 2013; Marangoni et al., 2019), phototoxicity (Overmans et al., 2018), symbiont density (Cunning and Baker, 2013), bleaching response (Siebeck et al., 2006), and growth (Wijgerde et al., 2020). Standardized tests would enable the validation of coral-toxicity data related to different compounds or pathogens that are known or suspected to negatively affect individual coral species or coral ecosystems. Furthermore, robust and standardized tests, as suggested by a recent study on coral larval settlement and survival responses to UV filters (Miller et al., 2022), could help to predict biochemical, physiological and behavioral tolerance thresholds in corals (Marangoni et al., 2019; Parkinson et al., 2019) and therefore substantially improve risk assessments and help guide coral restoration efforts.

Behavioral changes that exceed the normal range of functional responses including locomotion, habitat selection, feeding, predator avoidance, competition and reproduction, have the potential to reduce fitness and survival of individuals and populations (Bridges, 1997). Behavioral end-points in aquatic ecotoxicology are characterized by short response times, high sensitivity, and are usually non-invasive, allowing for repeated measurements and time-dependent data collection (Gerhardt, 2007). For example, reductions in swimming and feeding behavior can be more sensitive than biochemical or whole organism responses (Harayashiki et al., 2016, 2018). These endpoints may be the first detectable responses of an organism to environmental perturbations, suggesting that they could be highly valuable early indicators of stress (Reichelt-Brushett and Harrison, 2004; Bertram et al., 2022). Yet, behavioral ecotoxicology has received less attention due to a lack of user-friendly tools for quantitative data acquisition (Faimali et al., 2017). As a result, little is known about behavioral stress responses in cnidarians (Ianna et al., 2020), and most studies to date have been based on tedious manual analysis of observational data such as manually tracing swimming pathways and image analysis (Reichelt-Brushett and Harrison, 2004; Kwok and Ang, 2013; Antonio-Martínez et al., 2020; Ianna et al., 2020). Some

more advanced approaches have been applied to tracking coral larvae movement including the reconstruction from film using Matlab Image Processing toolbox (Martínez-Quintana et al. (2015)). However, the recent development of inexpensive and more widely available technology has recently renewed interest in quantifying behavior and investigating relationships between behavioral and physiological activities in aquatic organisms (Faimali et al., 2017). The application of more user-friendly automatic image acquisition systems should improve the speed and reliability of accurately measuring and quantifying behavioral end-points for application in ecotoxicology (Kane et al., 2005; Bertram et al., 2022).

The software EthoVision XT (Noldus Information Technology) has been used in many aquatic behavioral studies, especially with zebrafish larvae (Groneberg et al., 2015; Tudorache et al., 2015; Thia et al., 2020). In this study, EthoVision XT was used for the first time to assess the behavior of coral larvae, including the quantification of swimming activity and velocity, in response to three recently-developed and potentially non-toxic AF coatings (antiadhesive, cerium dioxide nanoparticles, and encapsulated DCOIT). Our objectives were to (1) explore the swimming behavior of the coral larvae in response to the AF coating treatments, and (2) test the feasibility of the experimental setup, including its adaptation for coral larvae, with the software EthoVision XT. This behavioral study aimed to contribute to the suite of sub-lethal ecotoxicological protocols available to identify more universal and sensitive responses to environmental challenges for coral larvae.

## 2. Materials & Methods

### 2.1. AF coating manufacturing

Three different AF coating variants were prepared on 4 x 4 cm poly (methyl methacrylate) (PMMA) tiles, a common material used in aquaculture: (i) antiadhesive coating, (ii) DCOIT coating, and (iii) $CeO_2$ nanoparticle coating. To achieve good coating application, all tiles were cleaned by rinsing with ethanol followed by a surface activation using microwave plasma (Creaetch 250 Plasma MV, working pressure 10 Pa in air, activation time 2.5 min., Creavac GmbH), prior to coating. PMMA was selected as an inert and transparent substrate to allow tracking of larvae, having the advantage over glass of better AF adhesion.

#### 2.1.1. Antiadhesive coating

At low surface energies in the range of 20-25 mN/m, organisms usually form poor attachments to the surface, so removal by incident flow is often possible (Detty et al., 2014). To generate low surface energy coatings, a $SiO_2$ coating solution ('sol') based on modified silicon

alcoholates was prepared following the work of Sokolova et al. (2012) and Detty et al. (2014). For sol preparation, 0.675 g n-octadecyl-trimethoxysilane (CAS 3069-42-9, abcr GmbH, Karlsruhe, Germany), 3.675 g tridecafluoro-1,1,2,2-tetrahydrooctyltriethoxysilane (CAS 51851-37-7, abcr GmbH, Karlsruhe, Germany), 22.4 g n-octyltriethoxysilane (CAS 2943-75-1, abcr GmbH, Karlsruhe, Germany), and 18.75 g tetraethylorthosilicate (TEOS, CAS 78-10-4 abcr GmbH, Karlsruhe) were mixed with 59.5 mL of ethanol and 11.4 mL of HCl (0.1 M) and stirred for 24 h at room temperature for hydrolysis and sol formation. Coatings were applied by dip-coating, dried under ambient conditions and then cured at 100 °C for one hour. The final coating on the PMMA tiles was as translucent as the control tiles without any coating.

### 2.1.2. DCOIT coating

Hydrophobic pyrogenic silicic acid powder (0.1 g) was mixed with a solution of 0.5 g of dichlorooctylisothiazolinone (DCOIT; C11H17Cl2NOS; TCI America; CAS RN 64359-81-5; product number D4157) in 2 mL of ethanol. The mixture was then left overnight to evaporate the ethanol. Two different sols were used in sequence to deposit the DCOIT loaded-silicic-acid powder on the PMMA tiles. First, 20 mL of a hydrophilic sol made from TEOS and 3-glycidyloxypropyl-triethoxysilane (9 mL TEOS, 1 mL 3-glycidyloxypropyl-triethoxysilane, 60 mL $H_2O$ and 30 mL 0.01M HCl) were intensively mixed by sonication (UP100H, Hielscher Ultrasonics GmbH, Teltow, Germany) with 0.1 g of the DCOIT loaded powder. The mixture was applied to the PMMA tiles by dip-coating, dried and solidified by annealing at 100 °C for one hour. To achieve slower DCOIT release from the coatings, a second layer using a hydrophobic sol (as described in 2.1.1.) was applied on top. As for the primary coating, 0.1 g DCOIT loaded powder was mixed with 20 mL of the hydrophobic sol shortly before coating. To estimate the extractable DCOIT content from the coating, ethanol was used for extraction. Photometrically, a DCOIT content of 3.2 mg $cm^{-2}$ was measured. The final coating was similarly translucent to the control and antiadhesive coated tiles.

### 2.1.3. $CeO_2$ nanoparticle coating

Cerium oxide nanoparticles (NPs) were manufactured according to Ji et al. (2012) and the 'Supporting Information' in Herget et al. (2017). In short, 100 mL of a 9.0 M NaOH solution was poured into 20 mL of a rapidly stirred 0.05 M solution of cerium(III) nitrate hexahydrate. After stirring for 30 min, the suspension was transferred into a stainless steel autoclave with a Teflon insert and heated to 100 °C for 24 hours. The lilac product was separated from the turbid suspension by centrifugation (3000 rpm, 10 min) and washed two times with MilliQ-water. After drying at 60 °C overnight, the resulting yellow product was ground in a vibrating ball mill for two minutes at 30 rpm. The milling yielded agglomerates of the size $< 20\,\mu m$. Before adding the cerium oxide powder to the coating solutions, the powder was dispersed in water and a pH of about 7.5 was adjusted. Coatings were prepared using two different sols. Coating solution 1:

100 mL TEOS, 420 mL ethanol (96%) and 20 mL 0.01 M HCl were mixed and stirred overnight at room temperature for hydrolysis. An acidic silica nanosol with a solids content of about 6 wt% was formed. Coating solution 2: 75g TEOS, 25 g 3-glycidyloxypropyl-triethoxysilane, 420 mL ethanol (96%) and 20 mL 0.01 M HCl were mixed and stirred overnight at room temperature for hydrolysis. The solids content of the sol was also about 6 wt.%. The PMMA tiles were coated 3 times. 1st coat: dip coating of the tiles by using a mixture of 1 g cerium oxide powder dispersed within 30 mL of coating solution 1. 2nd and 3rd coat: coating application by felt using 1 g cerium oxide dispersed within 30 mL of coating solution 2. The combination of an initial dip coating using a $SiO_2$-sol with cerium oxide and the subsequent overcoats using an epoxy-modified sol with cerium oxide gave good adhesion and uniformity of the coatings. Test coatings showed a coating weight of 0.9 mg $cm^{-2}$. The amount of ceria NPs in the coatings solutions was 35.7 wt%. In total, approximately 0.32 mg of ceria NPs were embedded per $cm^2$. The final coating on the tiles was slightly opaque compared with the other coatings and control.

## 2.2. Coral collection and larval husbandry

Gravid colonies (25–40 cm diameter) of the scleractinian coral *Acropora millepora* (Ehrenberg, 1834) were collected from Falcon Island (18° 45.796'S 146° 31.926'E; 2 m depth) in November 2019 under permit G12/35236.1, issued by the Great Barrier Reef Marine Park Authority to the Australian Institute of Marine Science (AIMS). Colonies were transported to the National Sea Simulator (SeaSim) at AIMS and maintained at ambient temperature in outdoor 1700 L flow-through holding tanks until spawning. On 15th November 2019, spawning occurred and the coral gametes from eight *A. millepora* parental colonies were collected and fertilized *en masse*. Symbiont-free larval cultures were maintained at densities <500 larvae per L, indoors, in flow-through rearing tanks supplied with 0.4 µm filtered natural seawater at 27.0 ± 0.5 °C (as described in Negri and Heyward, 2000; Nordborg et al., 2018). Flow-through seawater (1.5 turnovers per day) and an air stone ring at the base of each tank provided saturating aeration and created a gentle curtain of bubbles to keep larvae away from a submerged cylindrical mesh filter (100 $\mu$m) at the outflow. The average water quality parameters during larval culture were (range): pH 8.06 (8.01-8.13), salinity 35.9 (35.4-36.4), $NH_4$ 0.19 (0.13-0.27) $\mu$mol/L, $PO_4$ 0.08 (0.06-0.11) $\mu$mol/L, $NO_3$ 1.80 (1.25-2.93) $\mu$mol/L, $SiO_2$ 2.91 (2.44-4.31) $\mu$mol/L, alkalinity 2291 (2267-2321) $\mu$mol/Kg and dissolved inorganic carbon 2010 (1984-2052) $\mu$mol/Kg. Each day, a sub-sample of larvae in the rearing tanks was tested for settlement competency on 3D-printed polylactic acid (PLA) discs. 13 days after fertilization, larvae were found competent to settle and the experiment commenced. Immediately prior to each filming session (total of 8 sessions on the same day), new larvae from the same batch and rearing tank were collected.

## 2.3. Filming setup

To investigate the effects of the AF coatings on larval behavior, coral larvae were filmed while moving freely on top of AF coated (antiadhesive, nanoparticle, DCOIT) and uncoated (control) PMMA tiles (approx. 4 x 4 cm) in a laboratory experiment. Prior to the experiment, all tiles were rinsed with fresh 1-µm filtered natural seawater to avoid any particle contamination on the surfaces. Silicone sealing rings with an inner diameter of 15 mm were then placed on top of the PMMA tiles and filled with fresh 650 µL of 1-µm filtered natural seawater, creating small "pools" that kept the larvae on the tiles above the AF coatings (**Figure 4.1**). The silicone rings self-sealed against the PMMA tiles. Room temperature was kept at 28.5 °C which maintained water temperature in the pools at a stable 27.0 °C throughout the experiment. Two silicone rings, each holding a single 13-day-old larva, were placed on each tile. Shortly prior to each filming session, larvae were gently pipetted into the previously filled pools with as little excess water from the pipette. Four tiles, one for each treatment, were arranged to be filmed at the same time by one camera (**Figure 4.1**; Olympus TG-5). Each filming session included two sets of 4 tiles (1 tile per treatment), each filmed by a single camera. This totaled two cameras and 8 tiles per session (and 2 tiles per treatment per session) (**Figure 4.2**. Tiles were coated on both sides and each side was used in a single trial (16 tiles per treatment). By conducting eight filming sessions of 28 minutes each, the tracks of 32 larvae were recorded for each treatment. After each filming session, silicone rings were rinsed with filtered seawater and applied on top of new tiles from the same treatment. New larvae from the rearing tank were introduced to fresh filtered seawater in each test. To prevent light reflections on the water surface and to increase the contrast between the larvae and the background for filming, the translucent tiles were placed inside a dark box on top of a light table. The light table was made from translucent white diffusive plastic and was lit from below by two LED light bars (ARLEC Model UC450, 4W, Cool White), providing equal lighting for all tiles (**Figure 4.2**). To provide an even surface for the tiles, a thick (2 cm) transparent PMMA block was placed on top of the light table. Both cameras were placed at an equal distance above the tiles (top-down view) and optical camera zoom was used to frame the tiles in the videos, ensuring no distortion around the edges. Recordings of both cameras were started simultaneously. The cameras were set to record at a resolution of 1920x1080 pixels (1080p/Full HD) and 25 frames per second. The recordings stopped automatically after 28 minutes when a file size of about four gigabytes was reached (limit of FAT32 formatted SD cards).

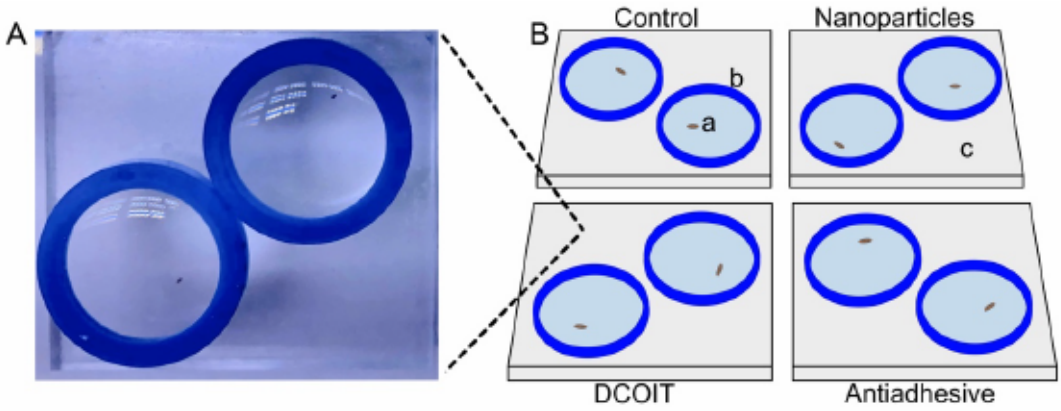


**Figure 4.1:** Tile setup beneath one camera. Actual image (A) of one tile setup (here: DCOIT tile). Schematic diagram (B) with coral larvae (a), silicone sealing ring (b), PMMA tile (c).

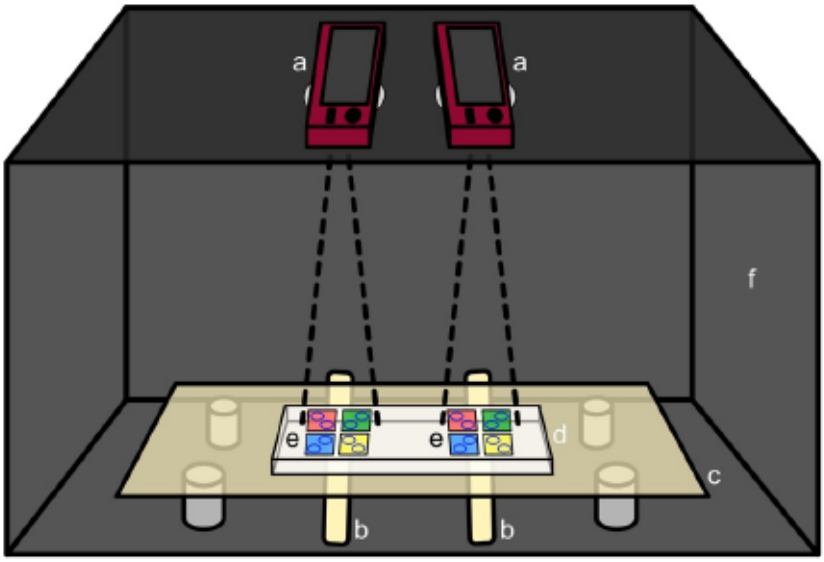


**Figure 4.2:** Filming setup including both cameras (a), light bars (b), light table (c), PMMA block (d), both tile setups (e) and the dark box (f). The 4 tile colors notionally represent tiles of each of the 4 treatment types (control, DCOIT, antiadhesive, and nanoparticle).

## 2.4. Video processing and data analysis in EthoVision XT

The video editing program XMedia Recode (version 3.4.8.3) (Dörfler, 2019) was used for post-production of the video files. The first two and the last one minute of each video were cut to acquire clips with a duration of 25 minutes. This procedure ensured a steady video quality by eliminating possible effects from camera handling and allowed the larvae a couple minutes of acclimation. Based on literature (Faimali et al., 2017), and given the lack of information for coral larval swimming video-tracking analyses, 25 minutes of behavior observations was selected, allowing substantial observation durations and multiple tests with larvae of the same age. Before track-analysis, the video files were post-processed to enhance the contrast between

the larvae and the background (see Supplementary Material for details). Subsequently, videos were converted from the original format (.mov) to .avi video-container-format for further application in the tracking software. EthoVision® XT (version 10.1.856; Noldus, Wageningen, Netherlands; Spink et al., 2001) was used to analyze larval behavior. The software generated data (every tenth of a second for each individual larva) of the distance moved (in mm) and the swimming activity (moving/not moving). "Minimal distance moved" in the EthoVision software's "Track Smoothing Profiles" tab was set to record track changes only when the larvae moved more than 0.25 mm (direct distance; see Supplementary Material). The velocity of each larva while moving was calculated by dividing the total distance a larva travelled by the duration of time spent moving during the trial (as measured by EthoVision). The threshold velocity of the larvae considered "moving" was set to 0.033 mm $s^{-1}$ (~1.98 mm $min^{-1}$), whereas the threshold for "not moving" was a velocity below 0.02 mm $s^{-1}$ (~1.21 mm $min^{-1}$). If a larva travelled more than 1.98 mm $min^{-1}$ initially, but lost speed below this threshold, "moving" was still detected. Below 1.21 mm $min^{-1}$, however, no movement was measured. These settings suppressed noise by ensuring recordings of actual larval movements and minimizing "jitter of detail" video effects, that could have biased the data.

All acquired tracks were checked, and where necessary, corrected manually to ensure high data accuracy (see Supplementary Material for a detailed guide to the track analysis in EthoVision XT). EthoVision XT created result summaries of the trial statistics (raw data for the calculation of the velocity while moving) and group statistics, which were transferred to Microsoft Excel 2019.

## 2.5. Statistical analysis

All statistical analyses were performed in R version 4.1.1 (R Core Team, 2021) and the data were manipulated and visualized using packages of the 'tidyverse' (Wickham et al., 2019) and 'car' (Fox and Weisberg, 2019). To investigate differences in larval swimming velocity and activity amongst the AF treatments, linear mixed effects models (LMM) were fitted using the package 'nlme' (Pinheiro et al., 2021).

Swimming velocity while moving ($\frac{\text{cumulative distance moved (in mm)}}{\text{time moving (in min)}}$), and swimming activity (*time moving (in percent)*) were used as response variables. The swimming activity was log-transformed (after adding a small constant), and the swimming velocity was square-root transformed to stabilize heteroscedasticity in the residuals. Treatment was always included as the sole fixed effect. Weights were adjusted to allow for unequal variances among treatments.

The filming "session" was used as a proxy for time of day and included in each model as a random effect to account for possible variation due to diurnal patterns of larval behavior. Likelihood-ratio tests between the LMMs with "session" and baseline generalized least squares

(GLS) models without random effects revealed that including the variable "session" significantly improved model performance in all cases ($p < 0.05$). Adding the "position" of the rings on the coated tiles (inner / outer corner of tile) as a random effect did not significantly improve model fit and was therefore omitted from all models.

Restricted maximum likelihood (REML) estimation was used for all models and statistical significance of the treatment effect was assessed using the 'anova' function included in 'nlme' (Pinheiro et al., 2021). The model was diagnosed and the satisfaction of model assumptions was checked using standard R model diagnostic plots with normalized residuals. Pairwise post-hoc tests based on estimated marginal means were run with the package 'emmeans' (Lenth, 2021) to find differences between each treatment pair. The p-value was adjusted for multiple testing with the Tukey method. Tests were performed on the log-/sqrt-scale and back-transformed for visualization. (**Figure 4.3, Figure 4.4**).

## 3. Results

### 3.1. Swimming velocity

Larval swimming velocity differed among AF treatments (LMM: $\chi^2(3) = 94.7$, $p < 0.001$). With a mean velocity of 93.1 ± 5.6 mm min$^{-1}$ (mean ± SE; **Table 4.1**), *A. millepora* larvae moved significantly faster on the control tiles than on all the AF tiles: larvae on the antiadhesive-coated tiles averaged 58 ± 5 mm min$^{-1}$ ($p < 0.001$), while the nanoparticle-coated tiles averaged 48.1 ± 3.8 mm min$^{-1}$ ($p < 0.001$) and the DCOIT-coated tiles averaged 37.7 ± 1.5 mm min$^{-1}$ ($p < 0.001$). Larval swimming velocity did not differ between the antiadhesive-coated and nanoparticle-coated tiles ($p = 0.278$). Velocity was lower on the DCOIT-coated tiles than on the antiadhesive- ($p < 0.001$) and nanoparticle-coated tiles ($p = 0.034$) (**Figure 4.3**; **Table 4.1**). Pairwise statistical results of swimming velocity data can be viewed in the **Supplementary Table S4.3**.

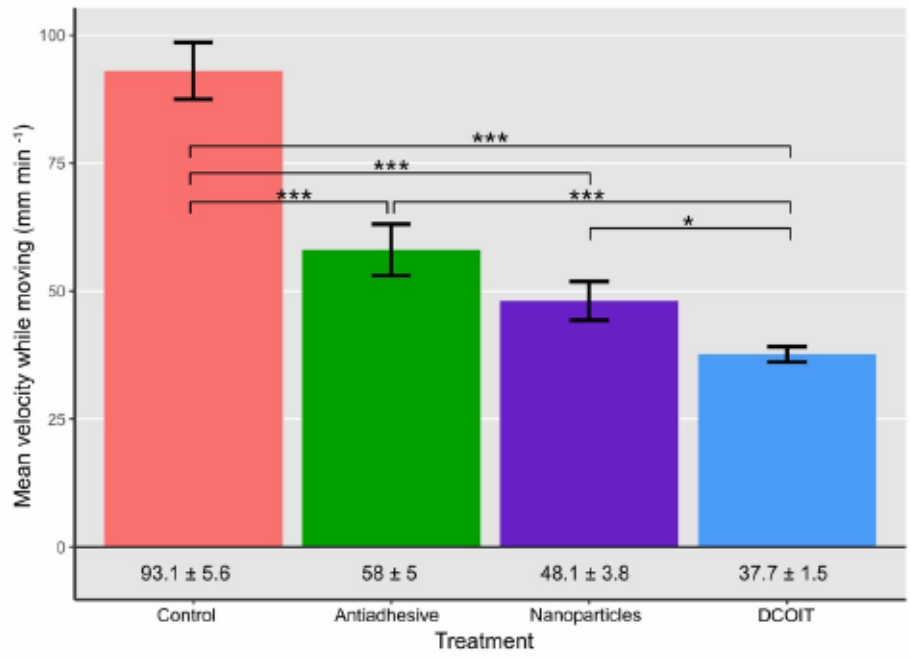


**Figure 4.3:** Average larval swimming velocity (mm $min^{-1}$) in each treatment and control (n = 32 larvae per treatment). Numbers below bars indicate mean velocity ± SE in the corresponding treatment. Error bars represent SEM. Asterisks indicate statistically significant differences based on pairwise post-hoc tests with estimated marginal means (**Supplementary Table S4.1, Table S4.3**; *p < 0.05, **p < 0.01, ***p < 0.001).

## 3.2. Swimming activity

Larval activity (time spent moving vs. not moving) also significantly differed among AF treatments (LMM: $\chi^2(3) = 285.43$, $p < 0.001$), and followed a similar pattern to swimming velocity. The larvae on the control tiles spent the majority of their time swimming (moving) (62.8 ± 5.2 % (mean ± SE); **Table 4.1**), and moved significantly more than on the antiadhesive-coated tiles (22.9 ± 5.2 %; $p < 0.001$), the nanoparticle-coated tiles (14.1 ± 3.4 %; $p < 0.001$) and the DCOIT-coated tiles ($p < 0.001$) (**Figure 4.4**; **Table 4.1**). On the DCOIT-coated tiles, larvae were predominantly still, moving an average of only 1.5 ± 0.4 % of the trial duration (**Table 4.1**). Pairwise statistical results of swimming activity data are available in the **Supplementary Table S4.4**.

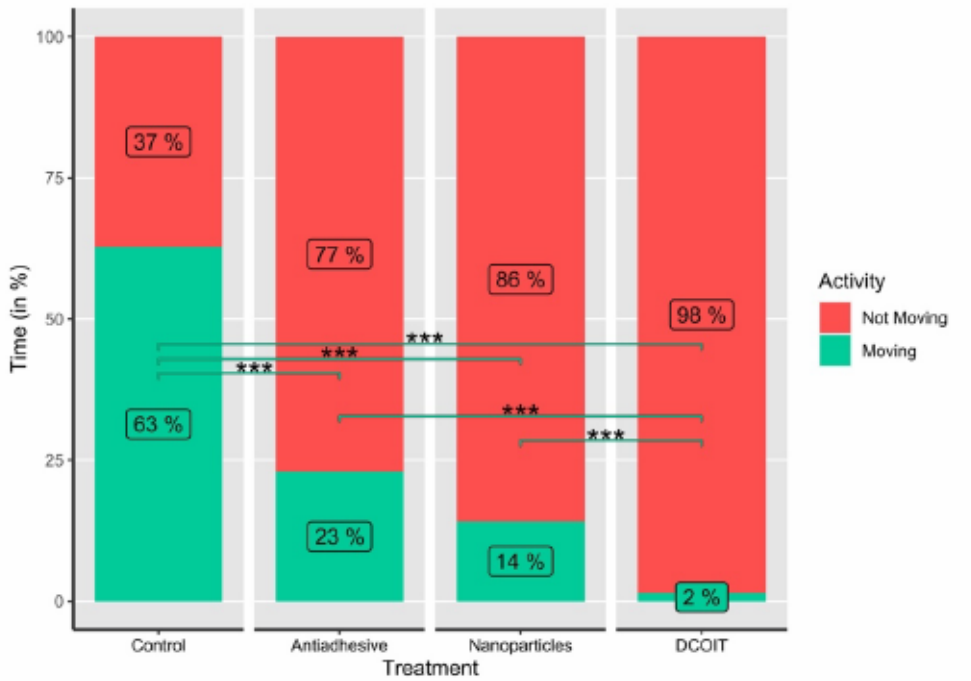


**Figure 4.4:** Average larval swimming activity (moving/not moving; in %) in each treatment and control (n=32), as indicated by the percentages (rounded) in the bars. Asterisks indicate statistically significant differences based on pairwise post-hoc tests with estimated marginal means (**Supplementary Table S4.2, Table S4.4**; *p < 0.05, **p < 0.01, ***p < 0.001).

**Table 4.1**: Mean swimming velocity (mm $min^{-1}$) and activity (%; moving) ± SE (standard error), velocity ranges (mm min-1; min. – max.) and mean distance travelled (mm) ± SE of *Acropora millepora* larvae per treatment (Control, Nanoparticles, Antiadhesive, DCOIT) on the coated PMMA tiles.

| Treatment | Mean velocity (mm $min^{-1}$) ± SE | Range in velocity (mm $min^{-1}$) | Mean distance travelled (mm) ± SE | Mean activity (%) ± SE |
|---|---|---|---|---|
| Control | 93.1 ± 5.6 | 38.1 – 152.3 | 1607.4 ± 175.3 | 62.8 ± 5.2 |
| Antiadhesive | 58 ± 5 | 37.7 – 130.2 | 512.1 ± 146.4 | 22.9 ± 5.2 |
| Nanoparticles | 48.1 ± 3.8 | 37.6 – 43.8 | 248.9 ± 105.8 | 14.1 ± 3.4 |
| DCOIT | 37.7 ± 1.5 | 0 – 66 | 14.6 ± 4.4 | 1.5 ± 0.4 |

## 4. Discussion

The effects of innovative antifouling (AF) coatings on marine species, especially corals, have been rarely evaluated since their introduction after 2008, when tributyltin (TBT) was globally prohibited (Dafforn et al., 2011). Here, three coatings with reportedly high AF efficacy and low potential toxicity (Detty et al., 2014; Maia et al., 2015; Herget et al., 2017a) were tested on the swimming activity and velocity of *Acropora millepora* coral larvae. In all three antifouling treatments, larvae moved significantly slower and in general less often than in the control

treatment. As the methodology of track-analysis with the software EthoVision XT is well-established for other aquatic organisms (i.e. zebrafish and amphipods), it was an additional goal to test the reliability and feasibility of this method with coral larvae. A comprehensive guide for video-processing and analysis is provided (see Supplementary Material). Our results document the potential of this method to identify behavioral effects in coral larvae, although the underlying cause of the changes to swimming behavior requires further investigation.

Like planulae of most coral species (Harrison and Wallace, 1990), *A. millepora* larvae are very active swimmers and exhibited typical straight, curved and spiraled swimming patterns with peridic stopping on the PMMA. The significantly higher motility of the larvae in the control treatment could be explained by the relatively smooth PMMA surface properties, which likely provided a featureless environment for the larvae who were consequently less likely to stop and explore; these smooth tiles did not offer any potentially attractive cues for settlement, nor was there any microtopography available. Therefore, larvae maintained 'normal' or 'typical' swimming and searching behavior in the absence of chemical and physical settlement cues. In this context, the high motility observed in the control could be considered 'normal' and indicative of active larval swimming, in the absence of settlement cues. It was not possible for the technique to distinguish between slow swimming and 'crawling' behavior. Crawling, which implies a slow swimming speed behavior with random swimming stops in between would have been tracked as "not moving" once the velocity of the larva was below 1.21 mm $min^{-1}$ (to eliminate jitter/noise). However, if a larvae travelled slowly or crawled for a substantial period, this would be captured in the mean velocity metric and activity data of the larvae in the treatments. Future studies could test for changes to normal swimming behavior in response to AF treatments on other biologically inert materials.

## 4.1. Effects of the coatings onto swimming behavior

By contrast, all the AF treatments tested caused a reduction in swimming speed and larval activity. In the absence of an inductive cue, reduced motility could be explained by either toxic action of the antifoulant ingredient (DCOIT, $CeO_2$), other biochemical interactions of the coatings with the larvae, or characteristics of the AF coating surface properties that confuse larval behavior, resulting in cessation of searching, or both (Negri et al., 2002), either of which could ultimately result in recruitment failure. However, further research is needed to characterize 'normal' behavior in the presence of settlement cues, which would also likely reduce swimming speed and activity, as the larvae probe the substrate, attach and metamorphose (Randall et al., 2020). Indeed, this expected reduction in swimming activity in response to settlement cues could be similar to the swimming speeds and activity seen in some AF treatments. Therefore, normal swimming behavior on different materials in the presence and absence of settlement cues requires further characterization.

The antiadhesive coating showed a much milder effect on the motility of the larvae than the DCOIT-coating. Sol-gel does not contain a biocide, so the inhibition of swimming is likely to be physical, and the reduced motility of the larvae compared with the control could be a result of different surface properties. This coating type is characterized by an amphiphilic surface with both hydrophilic and hydrophobic properties and interferes with fouling in multiple ways. For example, diatoms bind through hydrophilic proteins, while barnacles bind through hydrophobic adhesive proteins (Finlay et al., 2010); hence, amphiphilic coatings can either reduce or amplify bioadhesion and protein adsorption (Detty et al., 2014). Reduced motility of the *A. millepora* larvae may have been due to recognition of surface properties attractive for settlement (although no attachment or metamorphosis occurred in the short timeframe of the assays), or unlikely and unknown toxic effects of the sol-gel coating onto the larvae. Any disadvantageous surface properties of the coating and any unlikely potential for toxicity should be investigated further by assessing the survival of recruits on, and adjacent to, the sol-gel.

The rationale behind the encapsulation of DCOIT in the coating is the reduction of direct biocidal interactions with coating components, the control of leaching rate, and thus, a decrease in the absolute quantity of biocide needed to prepare a formulation with identical AF efficacy. Ultimately, the lifetime of the coating is increased and potential environmental threats are reduced (Maia et al., 2012, 2015; Martins et al., 2017; Gutner-Hoch et al., 2018; Figueiredo et al., 2020). However, the strong effect of this treatment on larval behavior indicates that this coating may cause stress, although the mechanism underpinning this behavioral change is unknown. Future studies could address the potential toxicity of this coating with different biocide concentrations (incl. $EC_{50}$ values) on physiological parameters (e.g. respiration) coupled with biochemical markers (e.g. enzymatic oxidative stress). When a toxicant is present, it requires energy to metabolize and counteract, which could take energy away from other functions. In order to reduce energy expenditure, a larva may reduce its swimming velocity and overall activity, and try to settle and metamorphose into a recruit as soon as possible (Kwok et al., 2016). However, DCOIT can also damage cellular structures and functions as it diffuses easily through membranes and cell walls and can also cause a blockage of the antioxidant defense system, leading to oxidative stress (Eom et al., 2019). Campos et al. (2022) found oxidative stress, lipid peroxidation, damaged lysosomal membranes and increased histopathological pathologies in the neotropical oyster *Crassostrea brasiliana* in response to DCOIT at environmentally relevant concentrations. Negative effects of DCOIT in bivalves (Fonseca et al., 2020), including decreased activity of GST (glutathione S-transferase), SOD (superoxide dismutase) and CAT (catalase) in the gills and digestive gland have also been reported (da Silva et al., 2021). To date, very few studies have assessed the effects of encapsulated DCOIT in tropical marine species (Dos Santos et al., 2020; Campos et al., 2022a). Only one study by Ferreira *et al*. (2021) compared the effects of free (non-integrated in a coating) and encapsulated DCOIT on a soft coral, *Sarcophyton glaucum*. The authors found reduced toxicity of encapsulated DCOIT on the coral fragments compared with free DCOIT, as

measured by coral polyp retraction, reduced photosynthetic efficacy and the elevated production of oxidative-stress markers. Relative to the negative control, encapsulated DCOIT still caused some toxicity. The extreme and significant reduction of *A. millepora* larval motility (velocity and activity) observed here is most likely driven by the DCOIT's toxicity, rather than the surface roughness. Ultimately, a potential consequence of substantially reduced velocity and activity could be a reduction in larval dispersal and the disruption of the coral's life cycle by limiting a larva's ability to seek a suitable habitat for settlement. This toxicity-based hypothesis could be tested with control experiments, in which larvae have no direct contact with the coating, and experiments that test the same surface coating (texture and composition) but without DCOIT incorporation.

The $CeO_2$ nanoparticle's antifouling property is created by the enzymatic activity of the nanoparticles which catalyze the oxidation of halides in presence of hydrogen peroxide ($H_2O_2$) to hypohalous acids which can subsequently react to halogenated organic compounds. Hypohalous acids combat biofilm formation through their biocidal activity or by disrupting the formation of signaling molecules involved in intracellular communication (Herget et al., 2017a, 2018). In our study, the significant reduction of velocity and activity due to the nanoparticle-coated PMMA, reveals an effect of either the amphiphilic surface properties of the sol-gel coating (as suggested for the antiadhesive coating), the surface structure/porosity with incorporated $CeO_2$ nanoparticles (NPs), the oxidative properties of the nanoparticles, or some combination thereof. The effects of $CeO_2$ nanoparticles have not been previously tested on corals; however, recent research suggests that other nanoparticles used in cosmetics can have negative effects. For example, Tang et al. (2017) found ZnO nanoparticles (common in sunscreens) to affect lipid profiles in *Seriatopora caliendrum* through glycerophosphocholine (GPC) profiling and concluded a mechanical disturbance due to the presence of ZnO nanoparticles. Corinaldesi et al. (2018) reported that uncoated ZnO nanoparticles induced severe coral bleaching, while two coated forms of $TiO_2$ nanoparticles had no negative effect on *Acropora* spp. over a 48h exposure. Another study (Fel et al., 2019), found a negative impact of ZnO on the photosystem II of the algal symbionts (the functionality was reduced by 38% compared to the controls). However, as only a few studies are available, and methodologies differ, and assumptions and hypotheses need to be further evaluated, these results should be treated cautiously (Mitchelmore et al., 2021; Moeller et al., 2021; Miller et al., 2022).

We tested the catalytic activity of the NPs in their unconsolidated form and assumed their activity in the coating would still be present. Thus, the exact catalytic activity of the coating remains unclear and conclusions concerning its effect on larval motility require validation. We recommend testing the activity of NPs prior to incorporating them into the coating in future experiments to disentangle whether the chemical effect of the NPs plays a role. However, nothing is known of the effects or the mechanism of action of $CeO_2$ nanoparticles on corals. Our study also did not include an inert particle/surface control (for the encapsulated DCOIT

particles and $CeO_2$ nanoparticles) and observed effects are therefore difficult to attribute to either physical coating effects or chemical effects.

In addition to our identification of two efficient antifouling coatings with robust levels of coral settlement in Roepke et al. (2022), we propose future studies on settlement, survival and growth on these antifouling coatings, as well as behavioral studies and measures of biochemical markers in response to these coatings. Approaches to settle larvae directly onto restoration deployment substrates adjacent to, or surrounded by these coatings, may offer protection against overgrowth by algae.

## 4.2. The application of EthoVision for coral larval tracking

Compared with past studies of coral larval swimming behavior (Faimali et al., 2017), EthoVision XT provides useful and user-friendly tools to quantify behavior. An important consideration in adopting this software package, however, is the license cost, and alternative freeware applications, such as trackR (Garnier), pathtrackr in R (Harmer and Thomas, 2019) or idtracker.ai in Python (Romero-Ferrero et al., 2019) may also be suitable and warrant testing. A comparison of these methodologies could identify the most affordable and promising video-tracking methodology for standardization with coral larvae. EthoVision is able to process longer videos, without the need to subsample files or investigate still images, providing a more holistic representation of the observed behavior. Here, "session" as a random factor was found to improve model performance, which suggests that diurnal patterns of the larvae could have affected the measurements. Therefore, we recommend several recording setups in parallel to cover high replicate measurements during small time intervals. While it requires time to troubleshoot and correct the tracking parameters for each video file, the program allows for high throughput, complex data collection and reproducibility. Therefore, EthoVision XT and other similar programs should be considered to complement existing physiological studies and expand the field of behavioral ecotoxicology in marine organisms. With software options that allow diverse experimental setups for different species, automated tracking could represent a powerful tool to detect early signs of stress, providing scientists with standardized techniques for application across taxa to identify "universal responses" to environmental challenges. We recommend the use of cameras with fast loading rechargeable batteries to ensure a steady, smooth recording process. Also, cameras with AC energy supplies and parallel recording mode could be even more suitable than those used here. Finally, tethered recordings that feed to direct computer storage could also speed-up recording and analysis processes.

## 5. Conclusions and future considerations

Results from our behavioral ecotoxicological study of *Acropora millepora* larvae show that all antifoulant treatments significantly affected the swimming velocity and activity of larvae, albeit to a different degree. By reducing the swimming velocity and activity of the larvae to almost zero, the DCOIT treatment showed the strongest effect. The swimming velocities and activities of larvae exposed to the antiadhesive- and nanoparticle-coated tiles were similar, and were clearly reduced compared to the control. The results suggest three alternative interpretations of the coatings' effect on larval motility: the physical surface topographies of the coatings could have caused the larvae to move more slowly, the antifouling treatments interacted biochemically with the larvae, or the coatings had a potentially toxic effect on the larvae, or some combination of the effects. Before these coatings are applied in coral aquaculture or restoration, further information on their antifouling efficacy and effects on settlement (Roepke et al., 2022), survival and growth are necessary. Moreover, it is suggested to test the chemical stability and AF activity duration of the coatings on different materials over different time scales, under *ex situ* and *in situ* conditions, and on different coral species and developmental stages (gametes, early and late larvae, spat, recruits, adults).

The sensitivity of automated behavioral data collection was demonstrated with this movement tracking method and setup and we recommend its application in future studies. Our study encompasses a guided manual for the use of the software EthoVision with coral larvae, providing scientists with a powerful tool to detect the first indication of stress in early coral life stages. The method can be used to provide a benchmark for larval behavior under normal conditions, and to rapidly and reliably quantify deviations in swimming behavior due to chemical or physical challenges. Moreover, swimming velocity and activity represent ecologically relevant parameters to assess effects of contaminants at environmental concentrations that do not cause mortality. The results should be verified by more studies on the same antifouling coatings with particle controls, as well as other environmentally relevant toxic compounds, and across coral species.

## Data availability statement

The track analysis manual, a RMarkdown (.Rmd) script of the track data, a knitted HTML version ofthe RMarkdown including all results and figures, and supplementary tables can be found on GitHub (https://github.com/drefeld/CoralLarvaeTracking.git). The raw data supporting the conclusions of this article will be made available by the authors, without undue reservation.

## Author contributions

LR conceptualized and coordinated the study, with guidance provided by DB, US, CR, AN, and AK; LR and DB performed the experiments, analyzed the data and prepared figures/tables; LR wrote the manuscript; CR and AN substantively revised the manuscript. All authors contributed to the article and approved the submitted version.

## Acknowledgements

The authors would like to thank Constanze von Waldthausen for her technical support at ZMT, and Florita Flores and Peter Thomas-Hall for their guidance and lab support at AIMS. The authors also thank the staff at the National Sea Simulator at AIMS for assistance with experimental setup and field collections. We acknowledge the Bindal People as the Traditional Owners where this work took place. We pay our respects to their Elders past, present and emerging and we acknowledge their continuing spiritual connection to their land and sea country.

## References

Antonio-Martínez, F., Henaut, Y., Vega-Zepeda, A., Cerón-Flores, A. I., Raigoza-Figueras, R., Cetz-Navarro, N. P., et al. (2020). Leachate effects of pelagic *Sargassum* spp. on larval swimming behavior of the coral *Acropora palmata*. *Sci. Rep.* 10, 1–13. doi:10.1038/s41598-020-60864-z.

Bertram, M. G., Martin, J. M., McCallum, E. S., Alton, L. A., Brand, J. A., Brooks, B. W., et al. (2022). Frontiers in quantifying wildlife behavioural responses to chemical pollution. *Biol. Rev.* 46, 1346–1364. doi:10.1111/brv.12844.

Box, Steve, J., and Mumby, Peter, J. (2007). Effect of macroalgal competition on growth and survival of juvenile Caribbean corals. *Mar. Ecol. Prog. Ser.* 342, 139–149.

Bridges, C. M. (1997). Tadpole swimming performance and activity affected by acute exposure to sublethal levels of carbaryl. *Environ. Toxicol. Chem.* 16, 1935–1939.

Bruno, J. F., and Selig, E. R. (2007). Regional decline of coral cover in the Indo-Pacific: Timing, extent, and subregional comparisons. *PLoS One* 2, e711. doi:10.1371/journal.pone.0000711.

Campos, B. G. de, do Prado e Silva, M. B. M., Avelelas, F., Maia, F., Loureiro, S., Perina, F., et al. (2022a). Toxicity of innovative antifouling additives on an early life stage of the oyster Crassostrea gigas: short- and long-term exposure effects. *Environ. Sci. Pollut. Res.* 29, 27534–27547. doi:10.1007/s11356-021-17842-3.

Campos, B. G. de, Fontes, M. K., Gusso-Choueri, P. K., Marinsek, G. P., Nobre, C. R., Moreno, B. B., et al. (2022b). A preliminary study on multi-level biomarkers response of the tropical oyster Crassostrea brasiliana to exposure to the antifouling biocide DCOIT. *Mar. Pollut. Bull.* 174, 113241. doi:10.1016/j.marpolbul.2021.113241.

Carpenter, R. C., and Edmunds, P. J. (2006). Local and regional scale recovery of *Diadema* promotes recruitment of scleractinian corals. *Ecol. Lett.* 9, 268–277. doi:10.1111/j.1461-0248.2005.00866.x.

Cima, F., Ferrari, G., Ferreira, N. G. C., Rocha, R. J. M., Serôdio, J., Loureiro, S., et al. (2013). Preliminary evaluation of the toxic effects of the antifouling biocide Sea-Nine 211™ in the soft coral *Sarcophyton cf. glaucum* (Octocorallia, Alcyonacea) based on PAM fluorometry and biomarkers. *Mar. Environ. Res.* 83, 16–22. doi:10.1016/j.marenvres.2012.10.004.

Corinaldesi, C., Marcellini, F., Nepote, E., Damiani, E., and Danovaro, R. (2018). Impact of inorganic UV filters contained in sunscreen products on tropical stony corals (*Acropora* spp.). *Sci. Total Environ.* 637–638, 1279–1285. doi:10.1016/j.scitotenv.2018.05.108.

Cornwall, C. E., Comeau, S., Kornder, N. A., Perry, C. T., van Hooidonk, R., DeCarlo, T. M., et al. (2021). Global declines in coral reef calcium carbonate production under ocean acidification and warming. *Proc. Natl. Acad. Sci. U. S. A.* 118, e2015265118. doi:10.1073/pnas.2015265118.

Cunning, R., and Baker, A. C. (2013). Excess algal symbionts increase the susceptibility of reef corals to bleaching. *Nat. Clim. Chang.* 3, 259–262. doi:10.1038/nclimate1711.

da Silva, A. R., Guerreiro, A. da S., Martins, S. E., and Sandrini, J. Z. (2021). DCOIT unbalances the antioxidant defense system in juvenile and adults of the marine bivalve Amarilladesma mactroides (Mollusca: Bivalvia). *Comp. Biochem. Physiol. Part - C Toxicol. Pharmacol.* 250, 109169. doi:10.1016/j.cbpc.2021.109169.

Dafforn, K. A., Lewis, J. A., and Johnston, E. L. (2011). Antifouling strategies: History and regulation, ecological impacts and mitigation. *Mar. Pollut. Bull.* 62, 453–465. doi:10.1016/j.marpolbul.2011.01.012.

De'Ath, G., Fabricius, K. E., Sweatman, H., and Puotinen, M. (2012). The 27-year decline of coral cover on the Great Barrier Reef and its causes. *Proc. Natl. Acad. Sci. U. S. A.* 109, 17995–17999. doi:10.1073/pnas.1208909109.

Detty, M. R., Ciriminna, R., Bright, F. V., and Pagliaro, M. (2014). Environmentally Benign Sol-Gel Antifouling and Foul-Releasing Coatings. *Acc. Chem. Res.* 47, 678–687. doi:10.1021/ar400240n.

Dörfler, S. (2019). XMedia Recode 3.4.8.3. Available at: https://www.xmedia-recode.de/en/version.php.

Dos Santos, J. V. N., Martins, R., Fontes, M. K., Galv, B., Bruni, M., and Maia, F. (2020). Can Encapsulation of the Biocide DCOIT Affect the Anti-Fouling Efficacy and Toxicity on Tropical Bivalves? *Appl. Sci.* 10, 1–12. doi:8579; doi:10.3390/app10238579.

Eom, H. J., Haque, M. N., Nam, S. E., Lee, D. H., and Rhee, J. S. (2019). Effects of sublethal concentrations of the antifouling biocide Sea-Nine on biochemical parameters of the marine polychaete *Perinereis aibuhitensis*. *Comp. Biochem. Physiol. Part - C Toxicol. Pharmacol.* 222, 125–134. doi:10.1016/j.cbpc.2019.05.001.

Faimali, M., Gambardella, C., Costa, E., Piazza, V., Morgana, S., Estévez-Calvar, N., et al. (2017). Old model organisms and new behavioral end-points: Swimming alteration as an ecotoxicological response. *Mar. Environ. Res.* 128, 36–45. doi:10.1016/j.marenvres.2016.05.006.

Fel, J. P., Lacherez, C., Bensetra, A., Mezzache, S., Béraud, E., Léonard, M., et al. (2019).

Photochemical response of the scleractinian coral *Stylophora pistillata* to some sunscreen ingredients. *Coral Reefs* 38, 109–122. doi:10.1007/s00338-018-01759-4.

Ferreira, V., Pavlaki, M. D., Martins, R., Monteiro, M. S., Maia, F., Tedim, J., et al. (2021). Effects of nanostructure antifouling biocides towards a coral species in the context of global changes. *Sci. Total Environ.* 799, 149324. doi:10.1016/j.scitotenv.2021.149324.

Figueiredo, J., Loureiro, S., and Martins, R. (2020). Hazard of novel anti-fouling nanomaterials and biocides DCOIT and silver to marine organisms. *Environ. Sci. Nano* 7, 1670–1680. doi:10.1039/d0en00023j.

Finlay, J. A., Bennett, S. M., Brewer, L. H., Sokolova, A., Clay, G., Gunari, N., et al. (2010). Barnacle settlement and the adhesion of protein and diatom microfouling to xerogel films with varying surface energy and water wettability. *Biofouling* 26, 657–666. doi:10.1080/08927014.2010.506242.

Fonseca, V. B., Guerreiro, A. da S., Vargas, M. A., and Sandrini, J. Z. (2020). Effects of DCOIT (4,5-dichloro-2-octyl-4-isothiazolin-3-one) to the haemocytes of mussels Perna perna. *Comp. Biochem. Physiol. Part - C Toxicol. Pharmacol.* 232, 108737. doi:10.1016/j.cbpc.2020.108737.

Fox, J., and Weisberg, S. (2019). *An R Companion to Applied Regression*. Third Edit. Sage Publications Available at: https://socialsciences.mcmaster.ca/jfox/Books/Companion/.

Gardner, T. A., Côté, I. M., Gill, J. A., Grant, A., and Watkinson, A. R. (2003). Long-term region-wide declines in Caribbean corals. *Science* 301, 958–960. doi:10.1126/science.1086050.

Garnier, S. trackR - Multi-object tracking with R. Available at: https://swarm-lab.github.io/trackR/.

Gerhardt, A. (2007). Aquatic behavioral ecotoxicology - Prospects and limitations. *Hum. Ecol. Risk Assess.* 13, 481–491. doi:10.1080/10807030701340839.

Groneberg, A. H., Herget, U., Ryu, S., and De Marco, R. J. (2015). Positive taxis and sustained responsiveness to water motions in larval zebrafish. *Front. Neural Circuits* 9, 1–12. doi:10.3389/fncir.2015.00009.

Gutner-Hoch, E., Martins, R., Oliveira, T., Maia, F., Soares, A., Loureiro, S., et al. (2018). Antimacrofouling Efficacy of Innovative Inorganic Nanomaterials Loaded with Booster Biocides. *J. Mar. Sci. Eng.* 6, 6. doi:10.3390/jmse6010006.

Harayashiki, C. A. Y., Reichelt-Brushett, A., Cowden, K., and Benkendorff, K. (2018). Effects of oral exposure to inorganic mercury on the feeding behaviour and biochemical markers in yellowfin bream (*Acanthopagrus australis*). *Mar. Environ. Res.* 134, 1–15. doi:10.1016/j.marenvres.2017.12.018.

Harayashiki, C. A. Y., Reichelt-Brushett, A. J., Liu, L., and Butcher, P. (2016). Behavioural and biochemical alterations in *Penaeus monodon* post-larvae diet-exposed to inorganic mercury. *Chemosphere* 164, 241–247. doi:10.1016/j.chemosphere.2016.08.085.

Harmer, A. M. T., and Thomas, D. B. (2019). pathtrackr: An r package for video tracking and analysing animal movement. *Methods Ecol. Evol.* 10, 1196–1202. doi:10.1111/2041-210X.13200.

Harrison, P. L., and Wallace, C. C. (1990). "Reproduction, dispersal and recruitment of scleractinian corals," in *Coral Reefs (Ecosystems of the World; 25)*, ed. Z. Dubinsky (New York: Elsevier Science Publishing Company), 133–207.

Herget, K., Frerichs, H., Pfitzner, F., Tahir, M. N., and Tremel, W. (2018). Functional Enzyme Mimics for Oxidative Halogenation Reactions that Combat Biofilm Formation. *Adv. Mater.* 30, 1–28. doi:10.1002/adma.201707073.

Herget, K., Hubach, P., Pusch, S., Deglmann, P., Götz, H., Gorelik, T. E., et al. (2017a). Haloperoxidase Mimicry by CeO2-x Nanorods Combats Biofouling. *Adv. Mater.* 29, 1–8. doi:10.1002/adma.201603823.

Herget, K., Hubach, P., Pusch, S., Deglmann, P., Götz, H., Gorelik, T. E., et al. (2017b). Supporting Information: Haloperoxidase Mimicry by CeO2-x Nanorods Combats Biofouling. *Adv. Mater.* 29, 1603823. doi:10.1002/adma.201603823.

Hughes, T. P., Graham, N. A. J., Jackson, J. B. C., Mumby, P. J., and Steneck, R. S. (2010). Rising to the challenge of sustaining coral reef resilience. *Trends Ecol. Evol.* 25, 633–642. doi:10.1016/j.tree.2010.07.011.

Hughes, T. P., Kerry, J. T., Álvarez-Noriega, M., Álvarez-Romero, J. G., Anderson, K. D., Baird, A. H., et al. (2017). Global warming and recurrent mass bleaching of corals. *Nature* 543, 373–377. doi:10.1038/nature21707.

Hughes, T. P., Rodrigues, M. J., Bellwood, D. R., Ceccarelli, D., Hoegh-Guldberg, O., McCook, L., et al. (2007). Phase Shifts, Herbivory, and the Resilience of Coral Reefs to Climate Change. *Curr. Biol.* 17, 360–365. doi:10.1016/j.cub.2006.12.049.

Ianna, M. L., Reichelt-Brushett, A., Howe, P. L., and Brushett, D. (2020). Application of a behavioural and biochemical endpoint in ecotoxicity testing with *Exaiptasia pallida*. *Chemosphere* 257, 127240. doi:10.1016/j.chemosphere.2020.127240.

Ishibashi, H., Minamide, S., and Takeuchi, I. (2018). Identification and characterization of heat shock protein 90 (HSP90) in the hard coral *Acropora tenuis* in response to Irgarol 1051. *Mar. Pollut. Bull.* 133, 773–780. doi:10.1016/j.marpolbul.2018.06.014.

Ji, Z., Wang, X., Zhang, H., Lin, S., Meng, H., Sun, B., et al. (2012). Designed synthesis of CeO2 nanorods and nanowires for studying toxicological effects of high aspect ratio nanomaterials. *ACS Nano* 6, 5366–5380. doi:10.1021/nn3012114.

Kane, A. S., Salierno, J. D., and Brewer, S. K. (2005). "Fish models in behavioral toxicology: Automated techniques, updates and perspectives," in *Methods in Aquatic Toxicology* (Lewis Publishers, Boca Raton, Florida), 559–590. Available at: http://aquaticpath.phhp.ufl.edu/pubs/images/AqToxMethods-Ch32.pdf.

Karcher, D. B., Roth, F., Carvalho, S., El-Khaled, Y. C., Tilstra, A., Kürten, B., et al. (2020). Nitrogen eutrophication particularly promotes turf algae in coral reefs of the central Red Sea. *PeerJ* 2020, 1–25. doi:10.7717/peerj.8737.

Korschelt, K., Schwidetzky, R., Pfitzner, F., Strugatchi, J., Schilling, C., Von Der Au, M., et al. (2018a). CeO2-: X nanorods with intrinsic urease-like activity. *Nanoscale* 10, 13074–13082. doi:10.1039/c8nr03556c.

Korschelt, K., Tahir, M. N., and Tremel, W. (2018b). A Step into the Future: Applications of Nanoparticle Enzyme Mimics. *Chem. - A Eur. J.* 24, 9703–9713. doi:10.1002/chem.201800384.

Kwok, C. K., and Ang, P. O. (2013). Inhibition of larval swimming activity of the coral (*Platygyra acuta*) by interactive thermal and chemical stresses. *Mar. Pollut. Bull.* 74, 264–273. doi:10.1016/j.marpolbul.2013.06.048.

Kwok, C. K., Lam, K. Y., Leung, S. M., Chui, A. P. Y., and Ang, P. O. (2016). Copper and

thermal perturbations on the early life processes of the hard coral *Platygyra acuta*. *Coral Reefs* 35, 827–838. doi:10.1007/s00338-016-1432-1.

Lenth, R. V. (2021). Emmeans: estimated marginal means. Available at: https://cran.r-project.org/package=emmeans.

Linares, C., Cebrian, E., and Coma, R. (2012). Effects of turf algae on recruitment and juvenile survival of gorgonian corals. *Mar. Ecol. Prog. Ser.* 452, 81–88. doi:10.3354/meps09586.

Louis, Y. D., Bhagooli, R., Kenkel, C. D., Baker, A. C., and Dyall, S. D. (2017). Gene expression biomarkers of heat stress in scleractinian corals: Promises and limitations. *Comp. Biochem. Physiol. Part - C Toxicol. Pharmacol.* 191, 63–77. doi:10.1016/j.cbpc.2016.08.007.

Maia, F., Silva, A. P., Fernandes, S., Cunha, A., Almeida, A., Tedim, J., et al. (2015). Incorporation of biocides in nanocapsules for protective coatings used in maritime applications. *Chem. Eng. J.* 270, 150–157. doi:10.1016/j.cej.2015.01.076.

Maia, F., Tedim, J., Lisenkov, A. D., Salak, A. N., Zheludkevich, M. L., and Ferreira, M. G. S. (2012). Silica nanocontainers for active corrosion protection. *Nanoscale* 4, 1287–1298. doi:10.1039/c2nr11536k.

Marangoni, L. F. de B., Dalmolin, C., Marques, J. A., Klein, R. D., Abrantes, D. P., Pereira, C. M., et al. (2019). Oxidative stress biomarkers as potential tools in reef degradation monitoring: A study case in a South Atlantic reef under influence of the 2015–2016 El Niño/Southern Oscillation (ENSO). *Ecol. Indic.* 106, 105533. doi:10.1016/j.ecolind.2019.105533.

Martínez-Quintana, A., Bramanti, L., Viladrich, N., Rossi, S., and Guizien, K. (2015). Quantification of larval traits driving connectivity: the case of *Corallium rubrum* (L. 1758). *Mar. Biol.* 162, 309–318. doi:10.1007/s00227-014-2599-z.

Martins, R., Oliveira, T., Santos, C., Kuznetsova, A., Ferreira, V., Avelelas, F., et al. (2017). Effects of a novel anticorrosion engineered nanomaterial on the bivalve: *Ruditapes philippinarum*. *Environ. Sci. Nano* 4, 1064–1076. doi:10.1039/c6en00630b.

Miller, I. B., Moeller, M., Kellermann, M. Y., Nietzer, S., Di Mauro, V., Kamyab, E., et al. (2022). Towards the Development of Standardized Bioassays for Corals: Acute Toxicity of the UV Filter Benzophenone-3 to Scleractinian Coral Larvae. *Toxics* 10, 244. doi:10.3390/toxics10050244.

Miller, I. B., Pawlowski, S., Kellermann, M. Y., Petersen-Thiery, M., Moeller, M., Nietzer, S., et al. (2021). Toxic effects of UV filters from sunscreens on coral reefs revisited: regulatory aspects for "reef safe" products. *Environ. Sci. Eur.* 33, 74. doi:10.1186/s12302-021-00515-w.

Mitchelmore, C. L., Burns, E. E., Conway, A., Heyes, A., and Davies, I. A. (2021). A Critical Review of Organic Ultraviolet Filter Exposure, Hazard, and Risk to Corals. *Environ. Toxicol. Chem.* 40, 967–988. doi:10.1002/etc.4948.

Moeller, M., Pawlowski, S., Petersen-Thiery, M., Miller, I. B., Nietzer, S., Heisel-Sure, Y., et al. (2021). Challenges in Current Coral Reef Protection – Possible Impacts of UV Filters Used in Sunscreens, a Critical Review. *Front. Mar. Sci.* 8, 1–16. doi:10.3389/fmars.2021.665548.

Negri, A. P., and Heyward, A. J. (2000). Inhibition of Fertilization and Larval Metamorphosis of the Coral *Acropora millepora* (Ehrenberg, 1834) by Petroleum Products. *Mar. Pollut.*

*Bull*. 41, 420–427.

Negri, A. P., and Heyward, A. J. (2001). Inhibition of coral fertilisation and larval metamorphosis by tributyltin and copper. *Mar. Environ. Res.* 51, 17–27. doi:10.1016/S0141-1136(00)00029-5.

Negri, A. P., Smith, L. D., Webster, N. S., and Heyward, A. J. (2002). Understanding ship-grounding impacts on a coral reef: Potential effects of anti-foulant paint contamination on coral recruitment. *Mar. Pollut. Bull.* 44, 111–117. doi:10.1016/S0025-326X(01)00128-X.

Nordborg, F. M., Flores, F., Brinkman, D. L., Agustí, S., and Negri, A. P. (2018). Phototoxic effects of two common marine fuels on the settlement success of the coral *Acropora tenuis*. *Sci. Rep.* 8, 1–12. doi:10.1038/s41598-018-26972-7.

Olsen, K., Ritson-Williams, R., Ochrietor, J. D., Paul, V. J., and Ross, C. (2013). Detecting hyperthermal stress in larvae of the hermatypic coral *Porites astreoides*: The suitability of using biomarkers of oxidative stress versus heat-shock protein transcriptional expression. *Mar. Biol.* 160, 2609–2618. doi:10.1007/s00227-013-2255-z.

Overmans, S., Nordborg, M., Díaz-Rúa, R., Brinkman, D. L., Negri, A. P., and Agustí, S. (2018). Phototoxic effects of PAH and UVA exposure on molecular responses and developmental success in coral larvae. *Aquat. Toxicol.* 198, 165–174. doi:10.1016/j.aquatox.2018.03.008.

Pandolfi, J. M., Connolly, S. R., Marshall, D. J., and Cohen, A. L. (2011). Projecting coral reef futures under global warming and ocean acidification. *Science* 333, 418–422. doi:10.1126/science.1204794.

Parkinson, J. E., Baker, A. C., Baums, I. B., Davies, S. W., Grottoli, A. G., Kitchen, S. A., et al. (2019). Molecular tools for coral reef restoration: Beyond biomarker discovery. *Conserv. Lett.*, 1–12. doi:10.1111/conl.12687.

Pawlowski, S., Moeller, M., Miller, I. B., Kellermann, M. Y., Schupp, P. J., and Petersen-Thiery, M. (2021). UV filters used in sunscreens—A lack in current coral protection? *Integr. Environ. Assess. Manag.* 17, 926–939. doi:10.1002/ieam.4454.

Pinheiro, J., Bates, D., Debroy, S., Sarkar, D., and R Core Team (2021). Linear and Nonlinear Mixed Effects Models Contact. *Linear nonlinear Mix. Eff. Model.* 3, 103–135. Available at: https://cran.r-project.org/package=nlme.

R Core Team (2021). R: A Language and Environment for Statistical Computing. Available at: https://www.r-project.org/.

Randall, C. J., Negri, A. P., Quigley, K. M., Foster, T., Ricardo, G. F., Webster, N. S., et al. (2020). Sexual production of corals for reef restoration in the Anthropocene. *Mar. Ecol. Prog. Ser.* 635, 203–232. doi:10.3354/MEPS13206.

Reichelt-Brushett, A. J., and Harrison, P. L. (2000). The effect of copper on the settlement success of larvae from the scleractinian coral *Acropora tenuis*. *Mar. Pollut. Bull.* 41, 385–391. doi:10.1016/S0025-326X(00)00131-4.

Reichelt-Brushett, A. J., and Harrison, P. L. (2004). Development of a sublethal test to determine the effects of copper and lead on scleractinian coral larvae. *Arch. Environ. Contam. Toxicol.* 47, 40–55. doi:10.1007/s00244-004-3080-7.

Roepke, L. K., Brefeld, D., Soltmann, U., Randall, C. J., Negri, A. P., and Kunzmann, A. (2022). Antifouling coatings can reduce algal growth while preserving coral settlement. *Sci. Rep.* 12, 15935. doi:10.1038/s41598-022-19997-6.

Romero-Ferrero, F., Bergomi, M. G., Hinz, R. C., Heras, F. J. H., and de Polavieja, G. G. (2019). Idtracker.Ai: Tracking All Individuals in Small or Large Collectives of Unmarked Animals. *Nat. Methods* 16, 179–182. doi:10.1038/s41592-018-0295-5.

Ross, C., Olsen, K., Henry, M., and Pierce, R. (2015). Mosquito control pesticides and sea surface temperatures have differential effects on the survival and oxidative stress response of coral larvae. *Ecotoxicology* 24, 540–552. doi:10.1007/s10646-014-1402-8.

Siebeck, U. E., Marshall, N. J., Klüter, A., and Hoegh-Guldberg, O. (2006). Monitoring coral bleaching using a colour reference card. *Coral Reefs* 25, 453–460. doi:10.1007/s00338-006-0123-8.

Sokolova, A., Bailey, J. J., Waltz, G. T., Brewer, L. H., Finlay, J. A., Fornalik, J., et al. (2012). Spontaneous multiscale phase separation within fluorinated xerogel coatings for fouling-release surfaces. *Biofouling* 28, 143–157. doi:10.1080/08927014.2012.659244.

Spink, A. J., Tegelenbosch, R. A. J., Buma, M. O. S., and Noldus, L. P. J. J. (2001). The EthoVision video tracking system - A tool for behavioral phenotyping of transgenic mice. *Physiol. Behav.* 73, 731–744. doi:10.1016/S0031-9384(01)00530-3.

Tang, C. H., Lin, C. Y., Lee, S. H., and Wang, W. H. (2017). Membrane lipid profiles of coral responded to zinc oxide nanoparticle-induced perturbations on the cellular membrane. *Aquat. Toxicol.* 187, 72–81. doi:10.1016/j.aquatox.2017.03.021.

Tebben, J., Guest, J. R., Sin, T. M., Steinberg, P. D., and Harder, T. (2014). Corals like it waxed: Paraffin-based antifouling technology enhances coral spat survival. *PLoS One* 9, 1–8. doi:10.1371/journal.pone.0087545.

Thia, E., Chou, P. H., and Chen, P. J. (2020). In vitro and in vivo screening for environmentally friendly benzophenone-type UV filters with beneficial tyrosinase inhibition activity. *Water Res.* 185, 116208. doi:10.1016/j.watres.2020.116208.

Tudorache, C., Ter Braake, A., Tromp, M., Slabbekoorn, H., and Schaaf, M. J. M. (2015). Behavioral and physiological indicators of stress coping styles in larval zebrafish. *Stress* 18, 121–128. doi:10.3109/10253890.2014.989205.

Vermeij, M. J. A., and Sandin, S. A. (2008). Density-dependent settlement and mortality structure the earliest life phases of a coral population. *Ecology* 89, 1994–2004. doi:10.1890/07-1296.1.

Vermeij, M. J. A., Smith, J. E., Smith, C. M., Vega Thurber, R., and Sandin, S. A. (2009). Survival and settlement success of coral planulae: Independent and synergistic effects of macroalgae and microbes. *Oecologia* 159, 325–336. doi:10.1007/s00442-008-1223-7.

Wickham, H., Averick, M., Bryan, J., Chang, W., McGowan, L., François, R., et al. (2019). Welcome to the Tidyverse. *J. Open Source Softw.* 4, 1686; 10.21105/joss.01686. doi:10.21105/joss.01686.

Wijgerde, T., van Ballegooijen, M., Nijland, R., van der Loos, L., Kwadijk, C., Osinga, R., et al. (2020). Adding insult to injury: Effects of chronic oxybenzone exposure and elevated temperature on two reef-building corals. *Sci. Total Environ.* 733, 139030. doi:10.1016/j.scitotenv.2020.139030.

# Supplementary material (SM)

## Supplementary Manual

The track analysis of *Acropora millepora* coral larvae across antifouling (AF) coated surfaces encompassed two steps:

1. Post-processing of videos to enhance the contrast between larvae and background using XMedia Recode (version 3.4.8.3) (Dörfler, 2019).
2. Analysis of larvae tracks using the video tracking software EthoVision® XT (version 10.1.856) (Noldus, Wageningen, Netherlands), hereafter "EthoVision XT".

## XMedia Recode Settings

Videos were converted from the original format (.mov) to .avi video-container-format for further application in EthoVision XT. In the video tab, MPEG-4 was chosen as video codec and a constant bitrate of 3000 bit/sec was assigned. The framerate was lowered from the original 25 FPS to 10 FPS. Other settings remained default (**Supplementary Figure S4.1**).

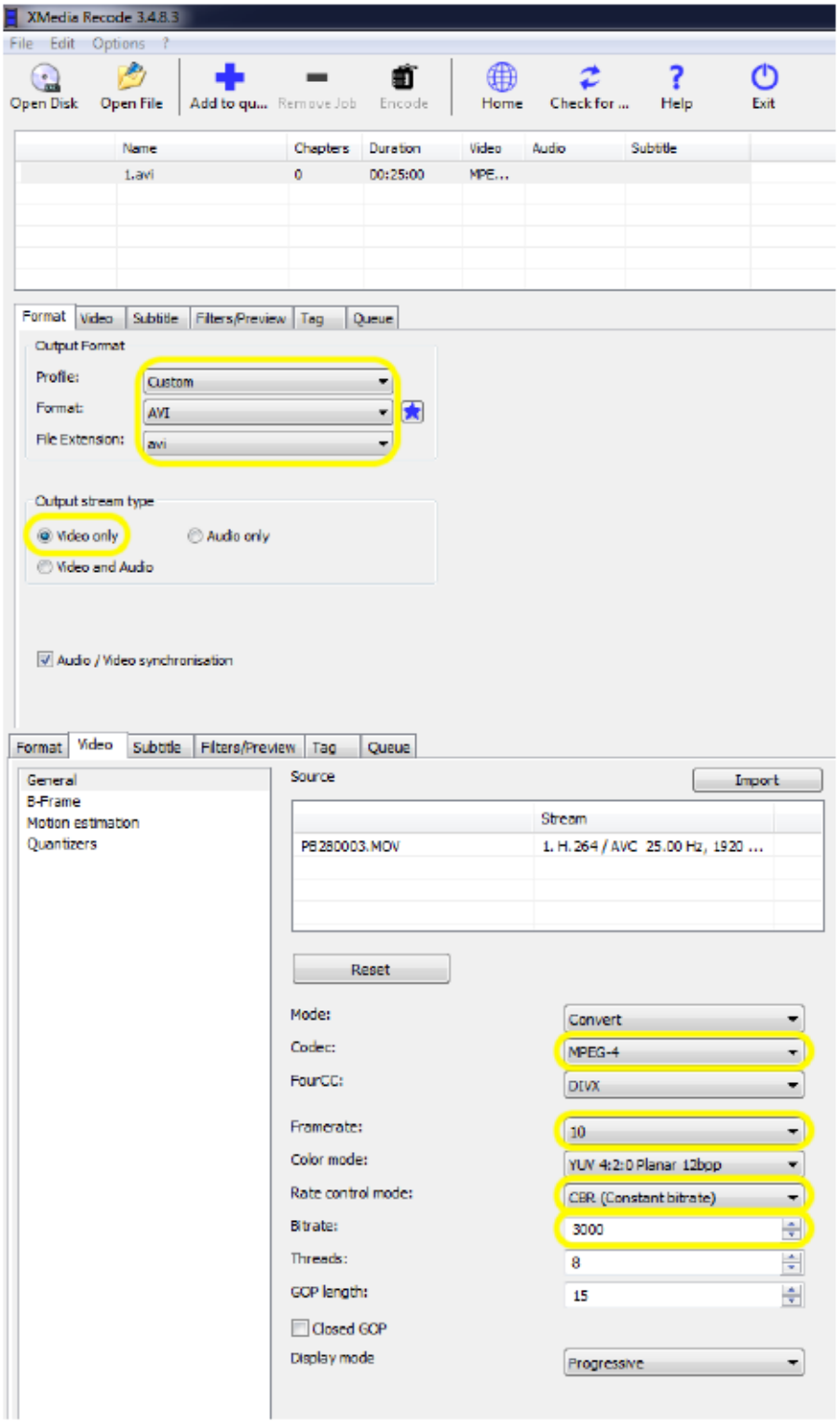


**Figure S4.1**: Format and video options in XMedia Recode. Yellow rectangles highlight settings changed from default.

Filters to enhance the contrast between larvae and background were adjusted to the following:

a. "*Color correction*" (+12 *Brightness*, +50 *Contrast*, +100 *Saturation*, -1 *Gamma Blue*)
b. "*Denoise*" (default settings)

c. "*Color Curves*" (preset: strong contrast)

d. "*Hue/Saturation*" (+12 *Saturation*) **(Supplementary Figure S4.2, Figure S4.3)**

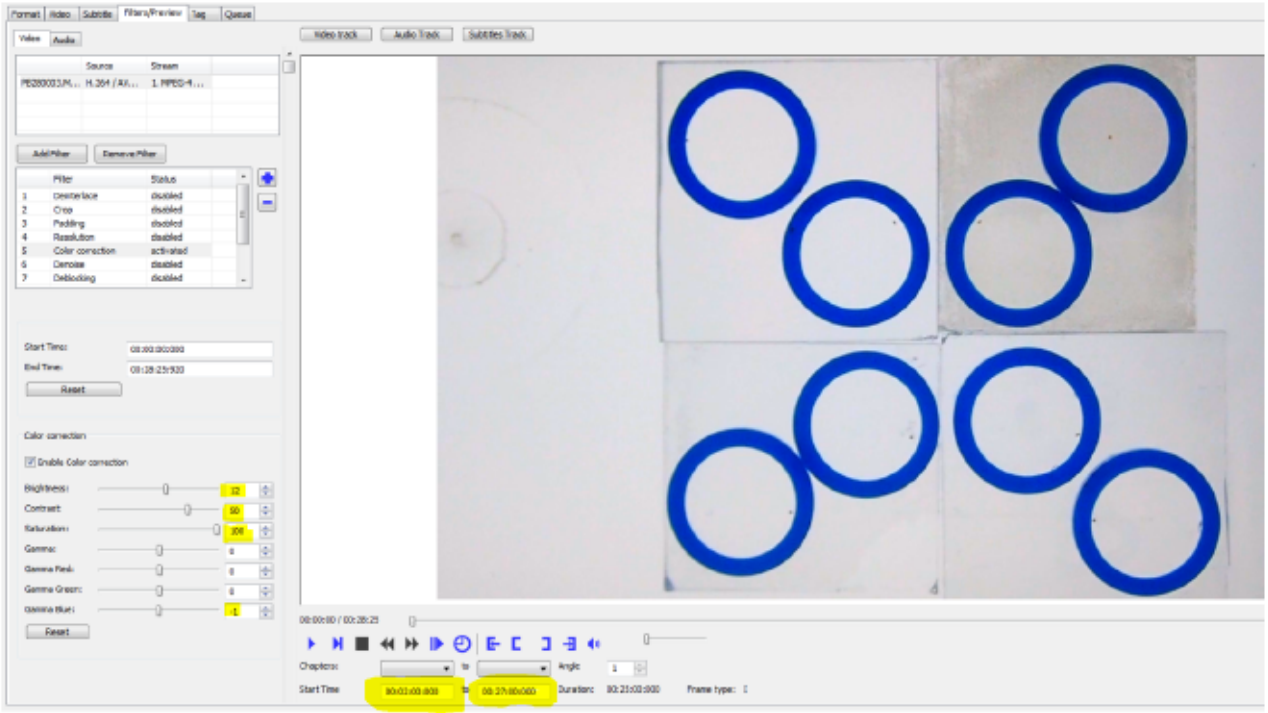

**Figure S4.2:** XMedia Recode *filters/preview* options. The *Color correction* filter was activated and its settings are shown here (yellow markings).

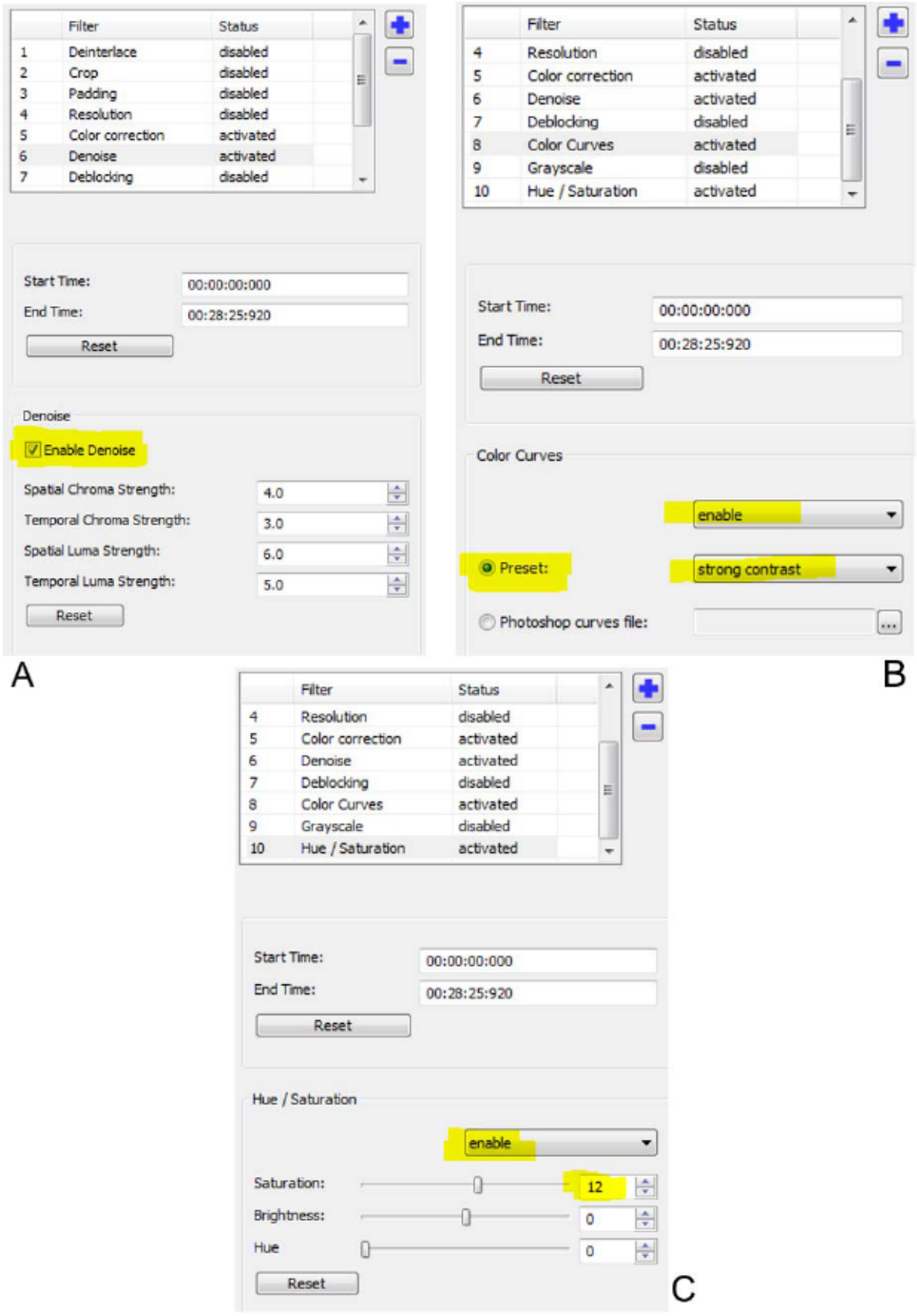


**Figure S4.3:** XMedia Recode filters/preview options. The *Denoise* filter (**A**), the *Color Curves* filter (**B**), and the *Hue/Saturation* filter (**C**) were activated. Yellow markings indicate settings.

## Track analysis in EthoVision XT

EthoVision XT was used to analyze the tracks of the recorded *A. millepora* coral larvae. This section shows which settings of the software were set for the analysis.

By using silicone rings, the larvae were contained in small "pools" filled with filtered seawater on top of PMMA tiles on uncoated controls and 3 different antifouling coatings: $CeO_2$ nanoparticle coating, DCOIT coating and antiadhesive coating. Each tile contained 2 silicone rings, each with one larva. 4 tiles were filmed (one tile from each treatment incl. control) with one of two identical camera settings, resulting in 8 larvae recordings per video session. The movements of the larvae in the "pools" on the coatings and control were recorded for 28 minutes (file size of four gigabytes: limit of FAT32 formatted SD cards). The first two and the last one minute of each video were cut to acquire clips with a duration of 25 minutes. This procedure ensured a steady video quality without any effects from camera handling and the start. In total, 32 larvae per treatment and control were recorded, resulting in 16 videos to be analyzed.

### Experiment Settings

The basic settings were adjusted to the following parameters (**Supplementary Figure S4.4**):

a. An experimental design with two arenas (= inner diameter of silicone rings) on one tile and one subject (= larva) per arena was chosen. Hereby, the clear separation of treatments was ensured and detection settings were easier to find within one treatment.
b. Center-point detection was used as tracking method.
c. "mm" was chosen as unit of distance and "min" as unit of time.

### Arena Settings

Each video contained recordings of 8 open-field arenas, with two arenas belonging to one treatment/control (and PMMA tile), respectively. Each arena contained one subject (= one larva). Detection parameters were set on a per treatment basis. Hence, each video was analyzed in 4 separate trials (3 treatments and control), in which each trial contained 2 arenas of the same treatment. The arenas were drawn slightly larger than the inside area of the silicone ring to avoid missed larval recordings by minimal shading effects of the silicone rings. The arenas were calibrated by setting the inner diameter of all arenas (= inner diameter of silicone rings) to the inside diameter of the silicone rings (15 mm) at two points (**Supplementary Figure S4.5**).

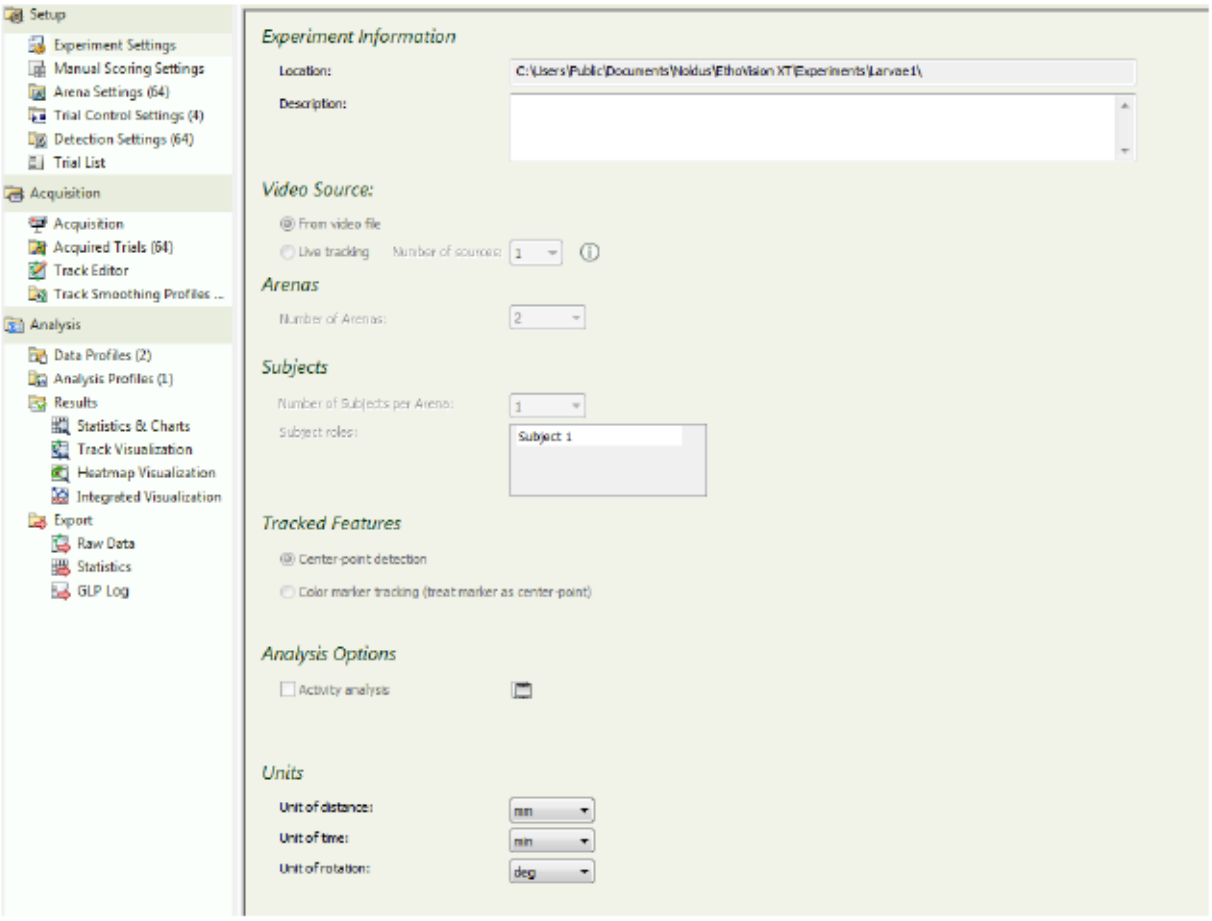


**Figure S4.4**: Basic experimental settings in EthoVision XT.

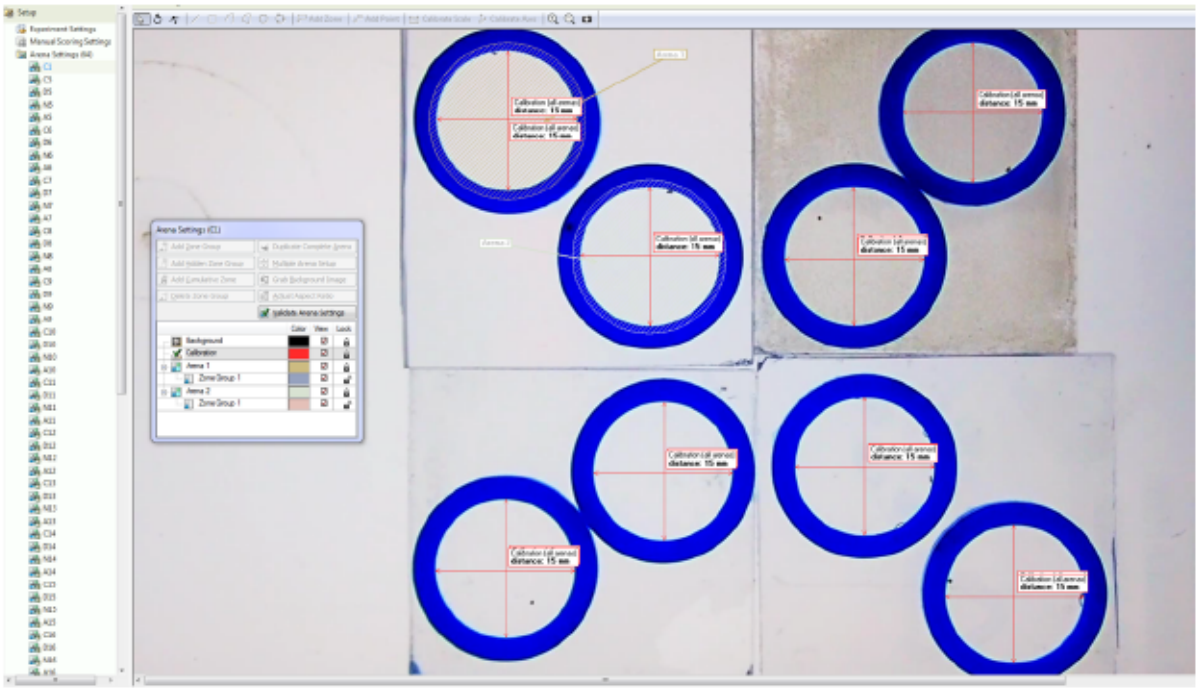

**Figure S4.5**: *Arena settings* in EthoVision XT. Arenas for tracking were drawn to be slightly larger than the area of the water surface. Arenas were calibrated by drawing two calibration lines in each arena (silicone rings had an inner diameter of 15 mm).

### Detection Settings

In the *detection settings* tab, the parameters used to track subjects inside the arena can be manipulated to ensure good detection and low noise. The following points demonstrate how the *detection settings* were manipulated to track the larvae (**Supplementary Figure 6**):

a. A new *detection setting* was produced for each two arenas on one tile (64 in total).
b. "*Differencing*" was used as detection method for all videos.
c. Under "*smoothing*", "*Track noise reduction*" was activated for all videos to eliminate noise in the detection.
d. A reference image was produced by averaging the videos using the "*start learning*" option in the reference image settings. If ghosts remained in the automatically acquired images, they were removed using Gimp (Version 2.10.14)(The GIMP Development, 2020) and the corrected images were imported using the "*grab from other*" button. "*Use the saved reference image*" was chosen upon track acquisition under the *acquisition settings* (**Supplementary Figure S4.7**).
e. "*Subject color compared to background*" was defined as darker.
f. "*Background changes*" was set to different values ranging from very slow to very fast, depending on detection.
g. "*Sensitivity*" was adjusted for each arena setting separately to ensure good detection.
h. "*Minimum subject size*" was defined as 35 and "*maximum subject size*" as 135.
i. "*Erosion* and *dilation*" were usually set to 1 and 2, respectively. However, *erosion* was sometimes set to 0 or *dilation* was set to 1 or 3 if continuous detection would fail.

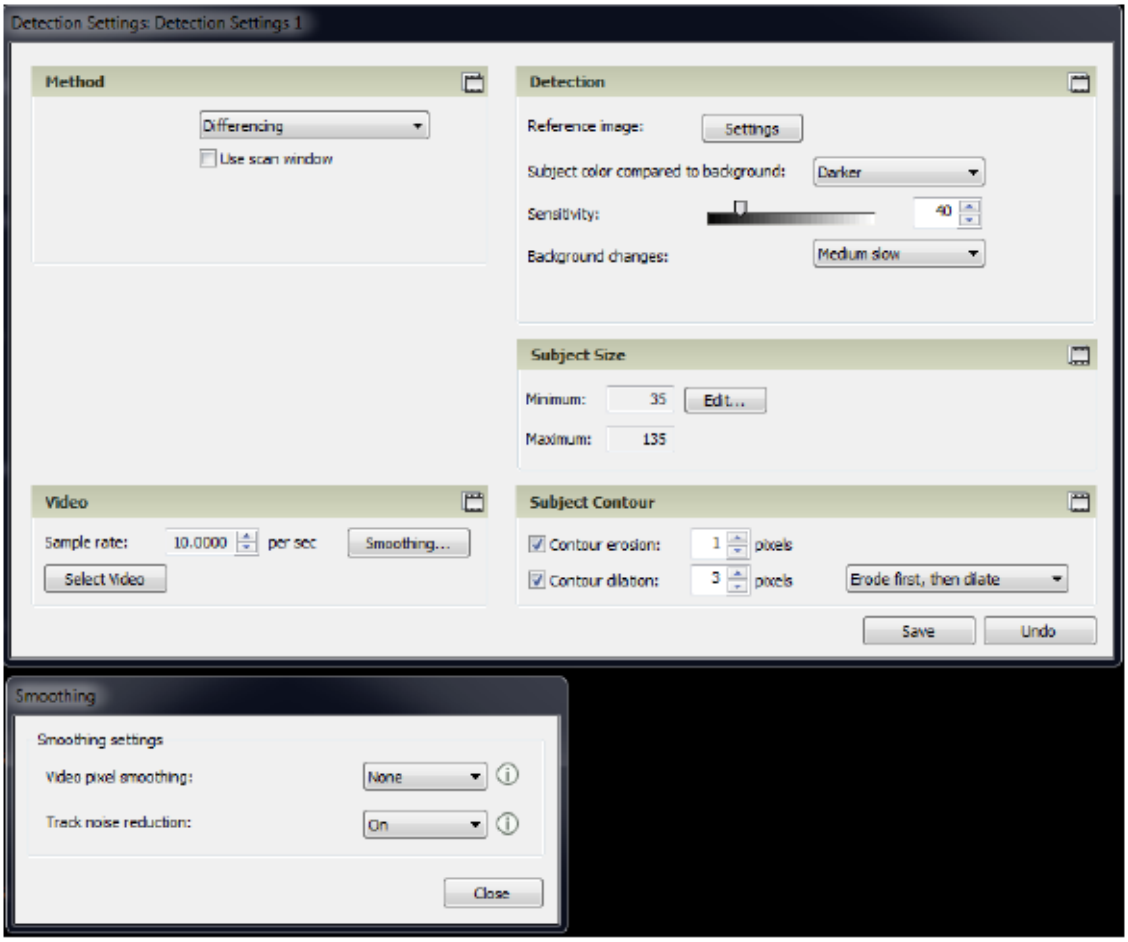


**Figure S4.6**: Detection settings in EthoVision XT.

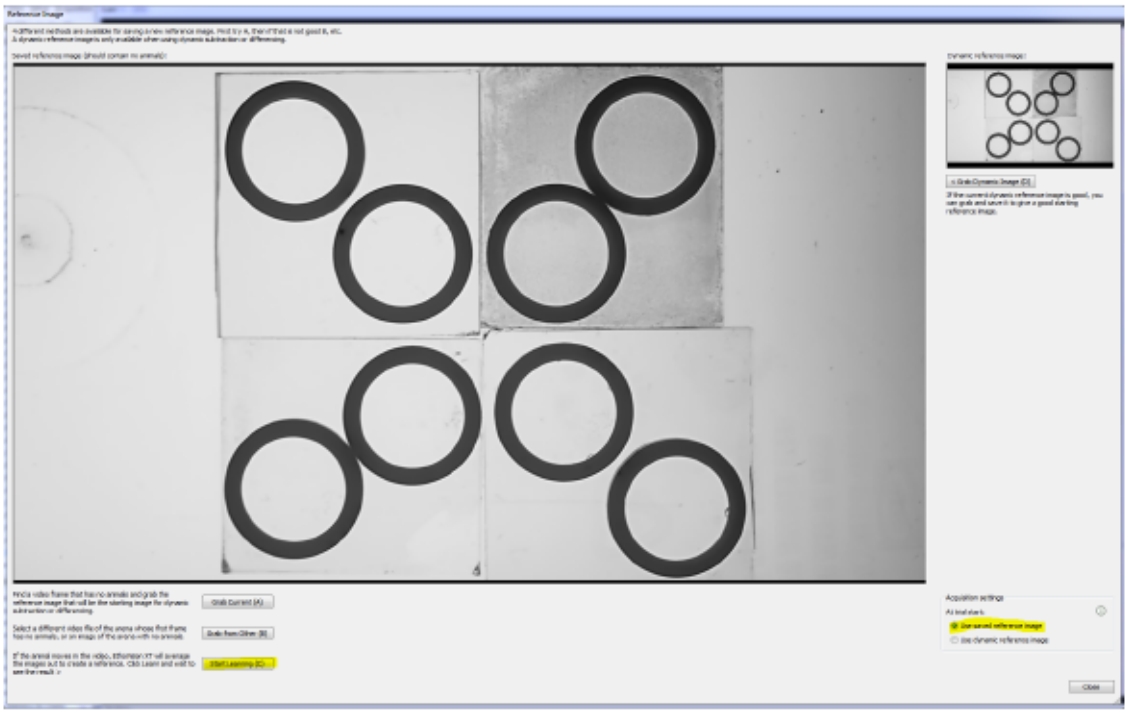

**Figure S4.7**: *Reference image* window in EthoVision XT. Chosen settings are marked in yellow.

## Trial Control Settings

In the *trial control settings* tab, the sequence of each trial can be adjusted. Each of our trials was set identically. Each trial was terminated after exact 1480 seconds (**Supplementary Figure S4.8**). 64 trials (128 acquired tracks) were set up, one for every tile (with 2 arenas each) of each treatment and control. The video files, *arena settings*, *detection settings* and the treatment/control were set herein for each trial to enable each track acquisition run.

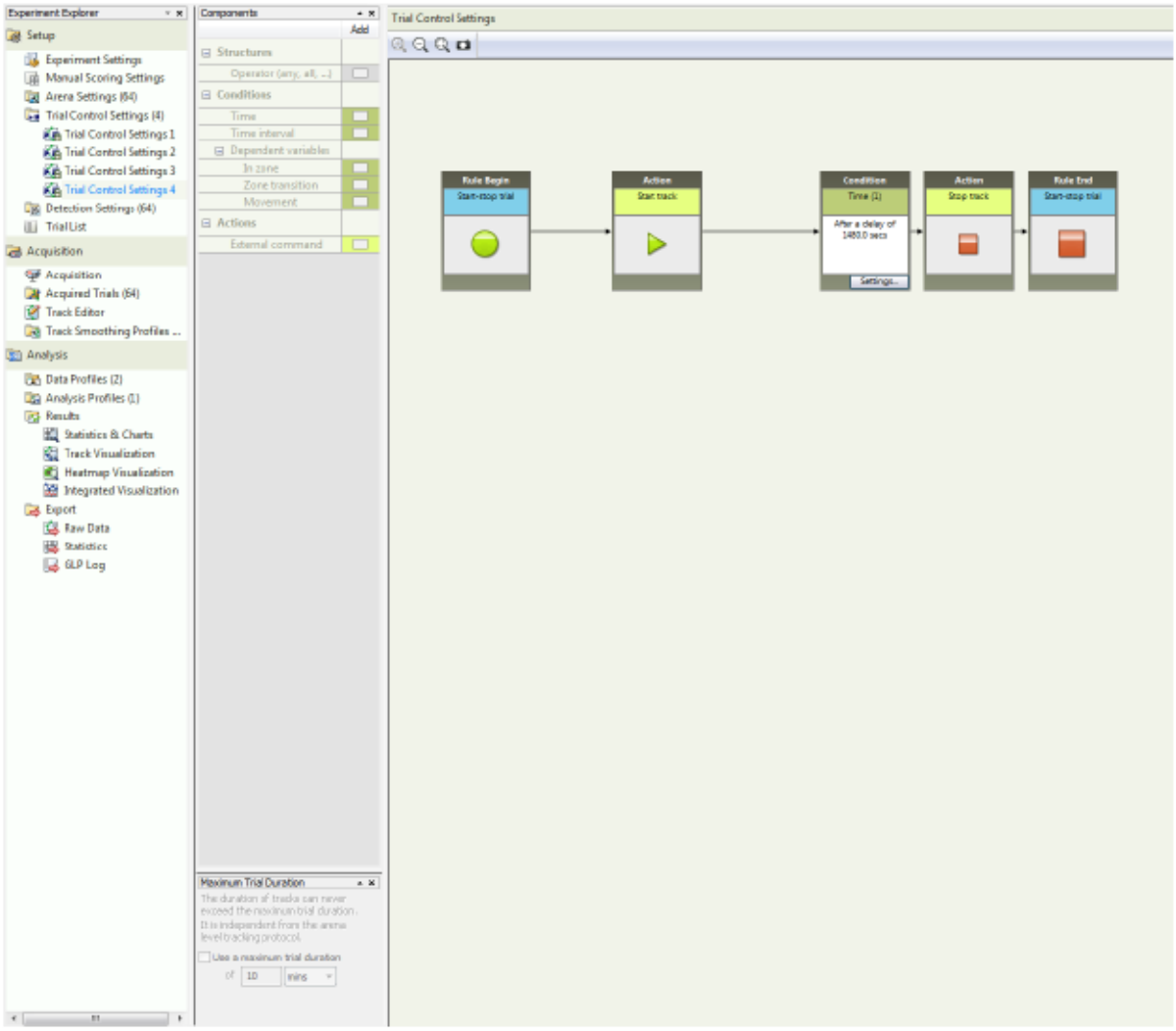


**Figure S4.8**: *Trial Control settings*.

## Track Smoothing Profile

*Track smoothing* can be enabled to get rid of detection noise, or the undesired detection of small movements (**Supplementary Figure S4.9**):

a. "*Lowess smoothing*" was set to smooth the track by taking 5 samples before and after each detection point into consideration.

b. "*Minimal distance moved*" was set to record track changes only when the larvae moved more than 0.25 mm (direct distance).

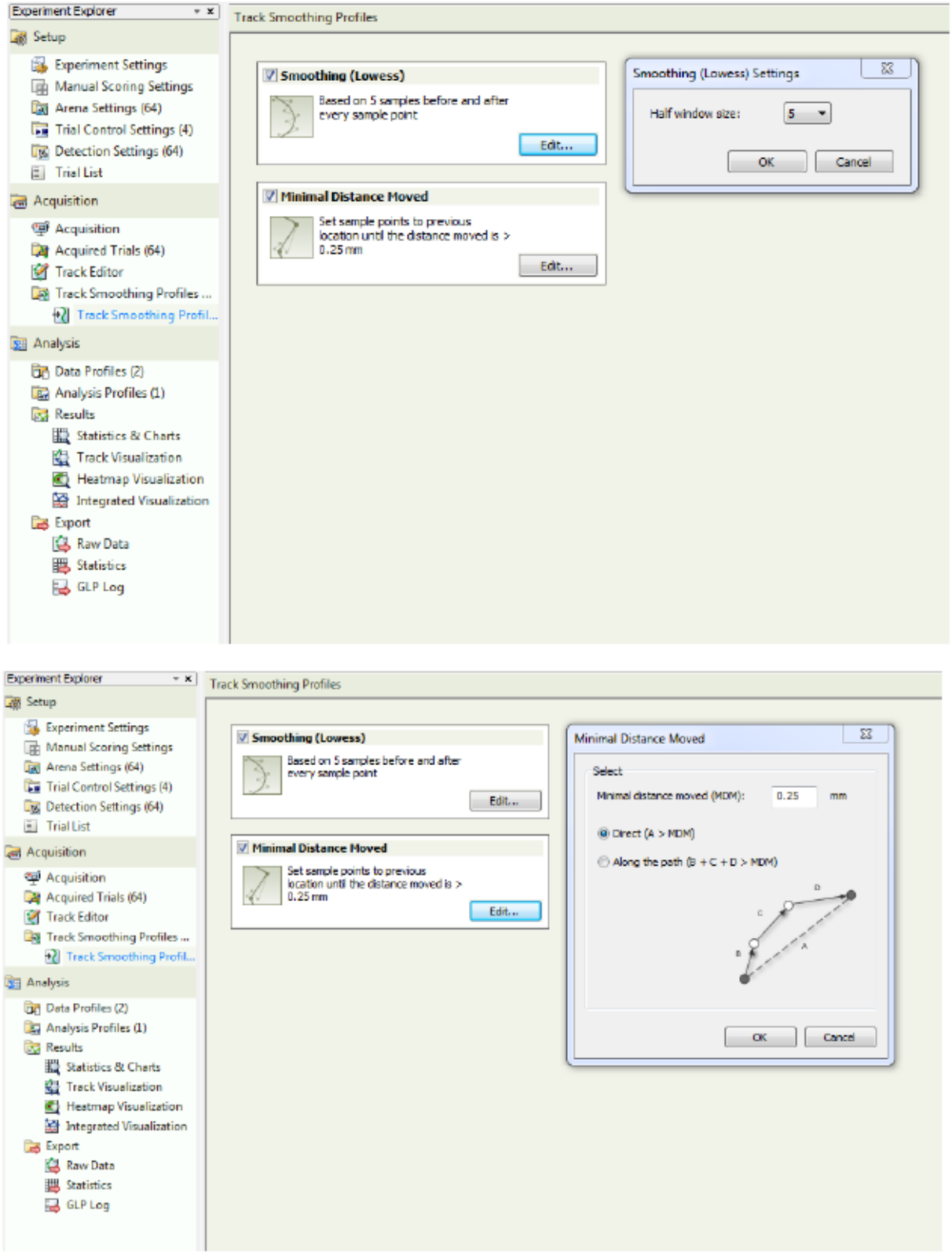


**Figure S4.9**: *Track smoothing profile* window in EthoVision XT.

## Data Profile

The *data profile* can be used to group trials by treatment and to determine how they should be analyzed after track acquisition. Here, the *data profile* was set for statistics to be calculated per treatment (**Supplementary Figure S4.10**).

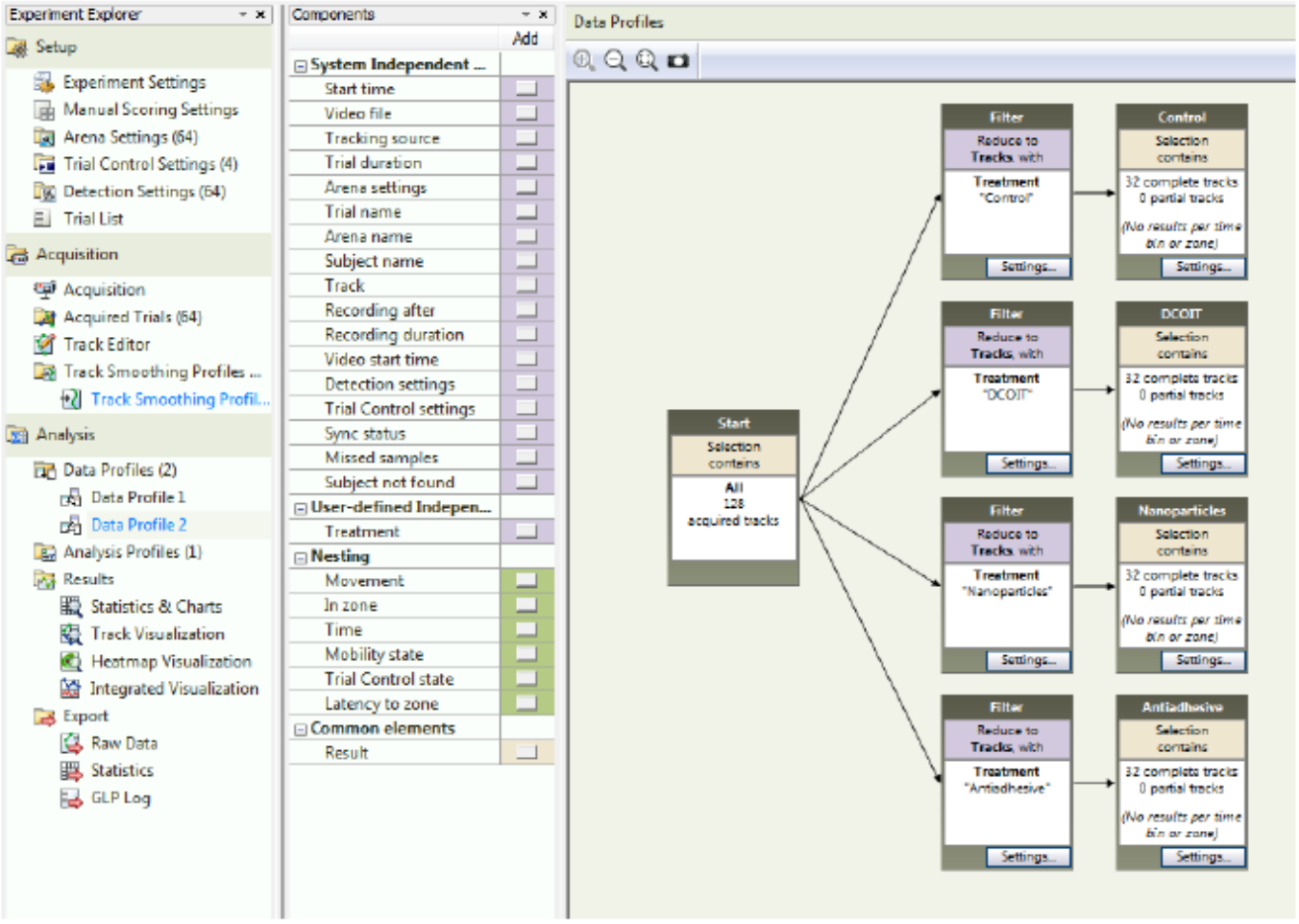


**Figure S4.10:** *Data profile* window in EthoVision XT with filters set for each treatment.

## Analysis Profile

The *analysis profile* can be used to set the parameters to be estimated from the acquired tracks (**Supplementary Figure S4.11**).

The Analysis Profile was set to calculate:

a. Total distance moved.

b. Mean velocity.

c. Activity time (moving/not moving).

d. The threshold velocity of the larvae considered "moving" was set to 0.033 mm $s^{-1}$ (~1.98 mm $min^{-1}$), the threshold for "not moving" was linked to a velocity below 0.02 mm $s^{-1}$ (~1.21 mm $min^{-1}$). If a larva travelled more than 1.98 mm $min^{-1}$ initially, but lost speed

below this threshold, "moving" was still detected. Below 1.21 mm $min^{-1}$, however, no movement was measured. These settings suppressed noise by ensuring recordings of actual larval movements and no "jitter of detail" video effects, that could have biased the behavior (**Supplementary Figure S4.12**).

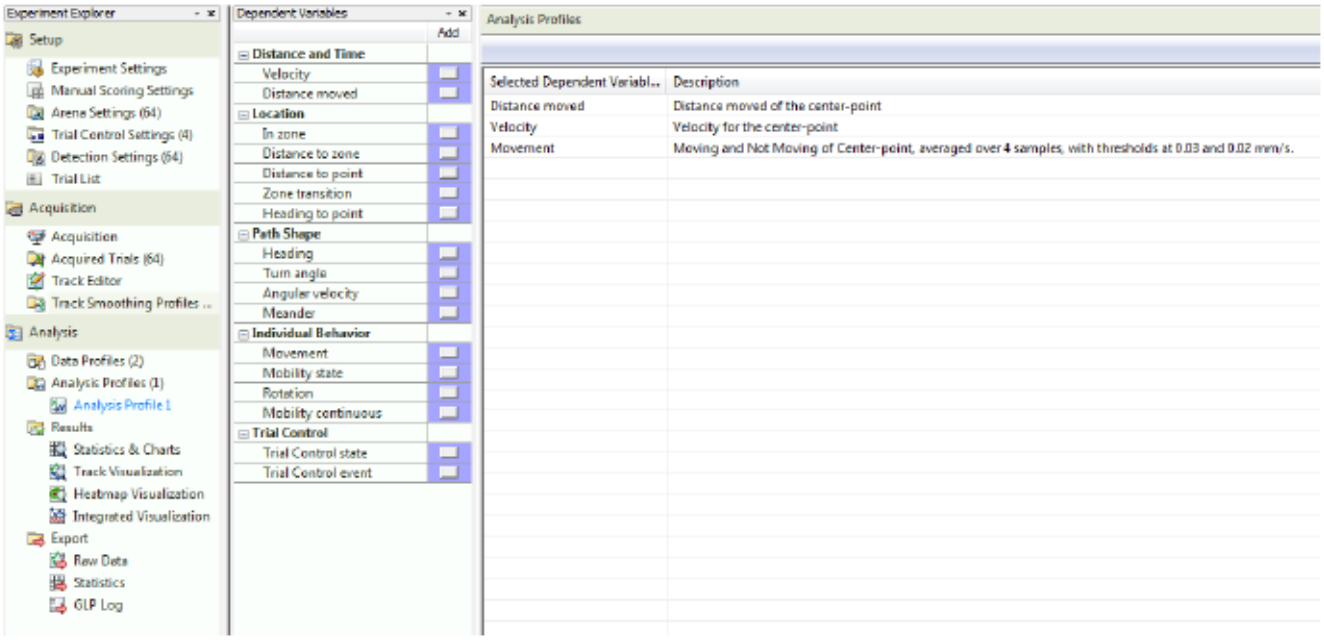


**Figure S4.11:** *Analysis profile* window in EthoVision XT. The total *distance moved*, the *velocity*, and the *activity* were chosen as parameters of interest.

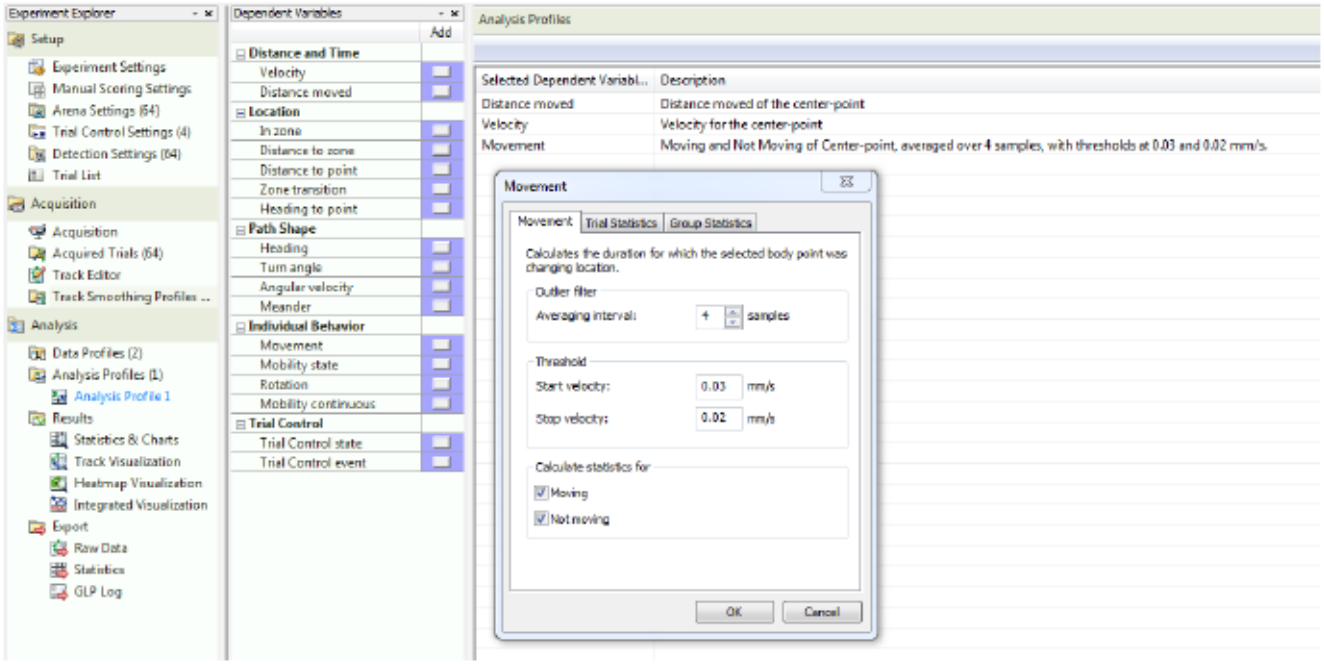


**Figure S4.12:** *Movement* settings in the analysis profile window.

## Acquisition of Tracks

The *acquisition* tab can be used to acquire tracks from subjects in video recordings using the previously determined *arena, trial control and detection settings* (**Supplementary Figure S4.13**):

a. The *acquisition* settings were set to the previously determined *arena, trial and detection settings* for the corresponding trial. Tracks were acquired one after another.
b. Successful detection was monitored throughout the analysis.
c. If detection of tracks was not continuous, the *detection settings* were altered to improve detection.
d. Speed of acquisition was determined by detection.

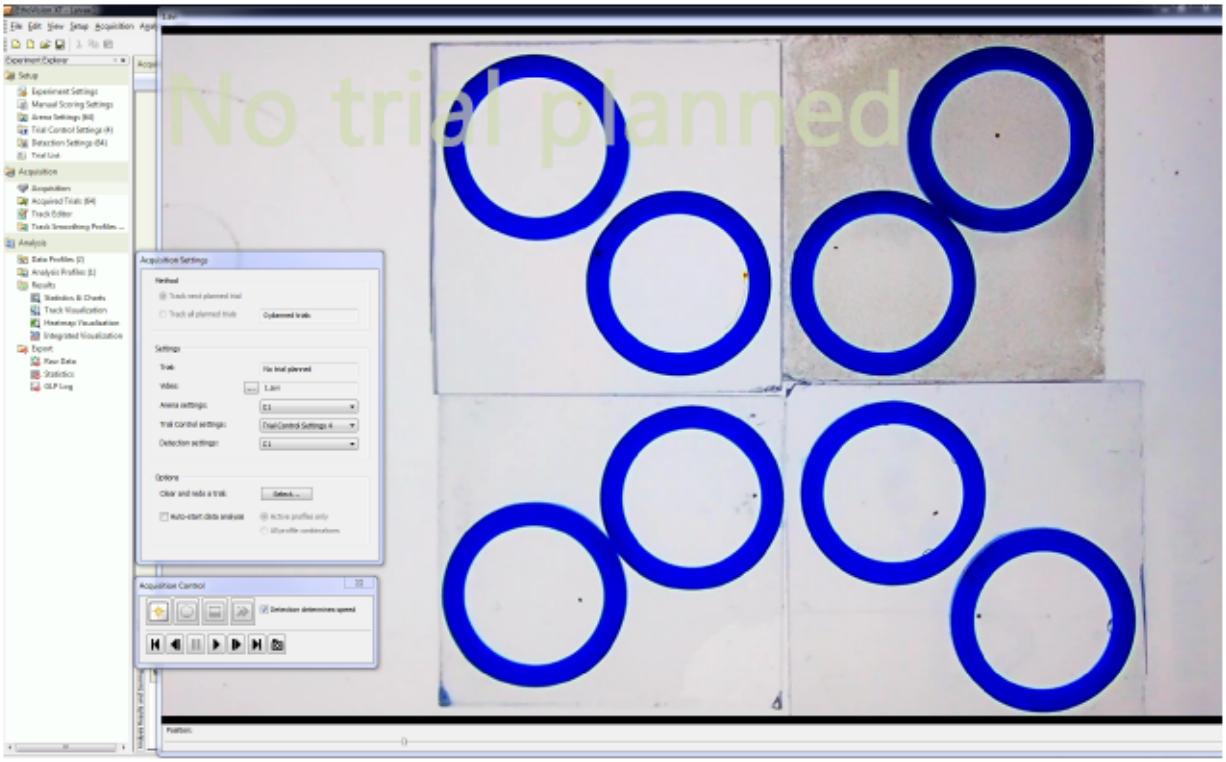


**Figure S4.13:** *Acquisition* window in EthoVision XT. Each recording was processed individually.

## Track Editor

The *track editor* can be used to correct acquired tracks, if detection briefly failed (**Supplementary Figure S4.14**):

a. Successful detection of tracks was analyzed in the trial editor by watching the detected tracks at higher speed (up to 16x, depending on the activity of the larvae).
b. Errors in acquisition were corrected.
c. Missing points were interpolated.

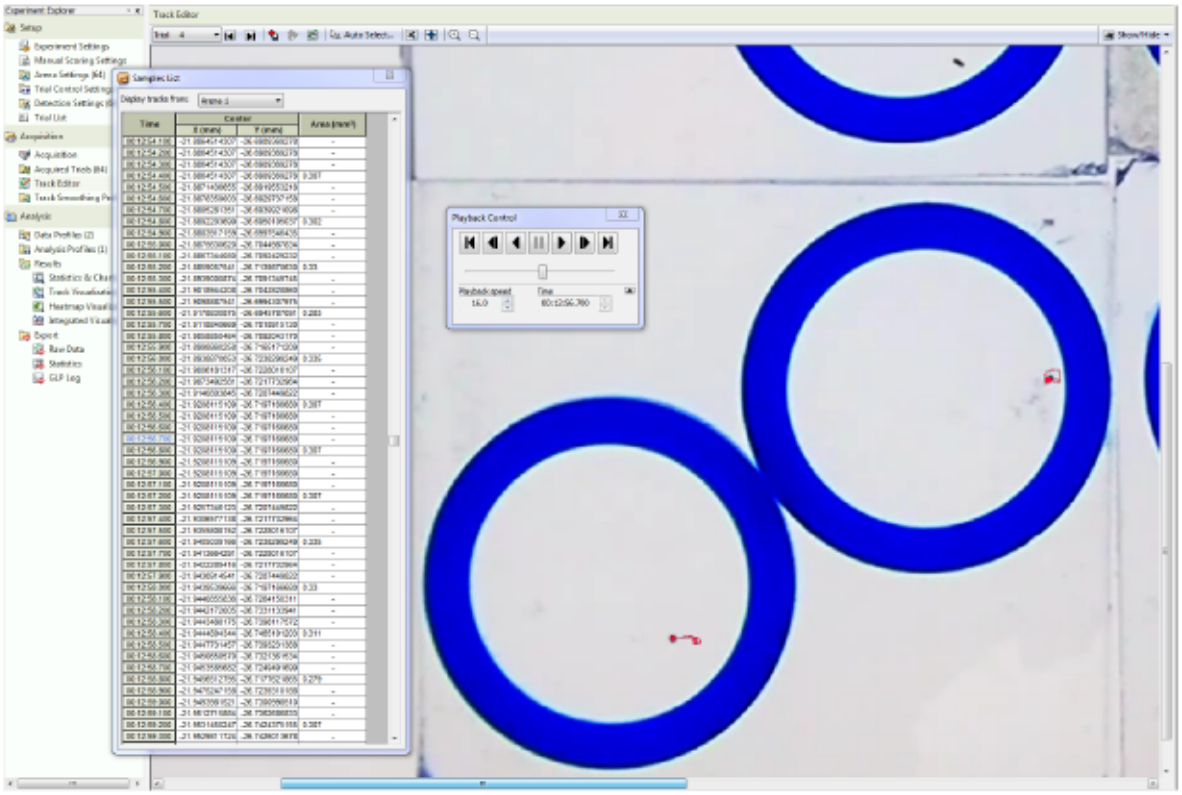

**Figure S4.14**: *Track editor* window in EthoVision XT with each trial sighted and corrected.

## Statistics

Trial statistics and group statistics were calculated per treatment group. Statistics were exported to Microsoft Excel 2019 for later analysis in R version 4.1.1 (R Core Team, 2021) **(Supplementary Figure S4.15)**.

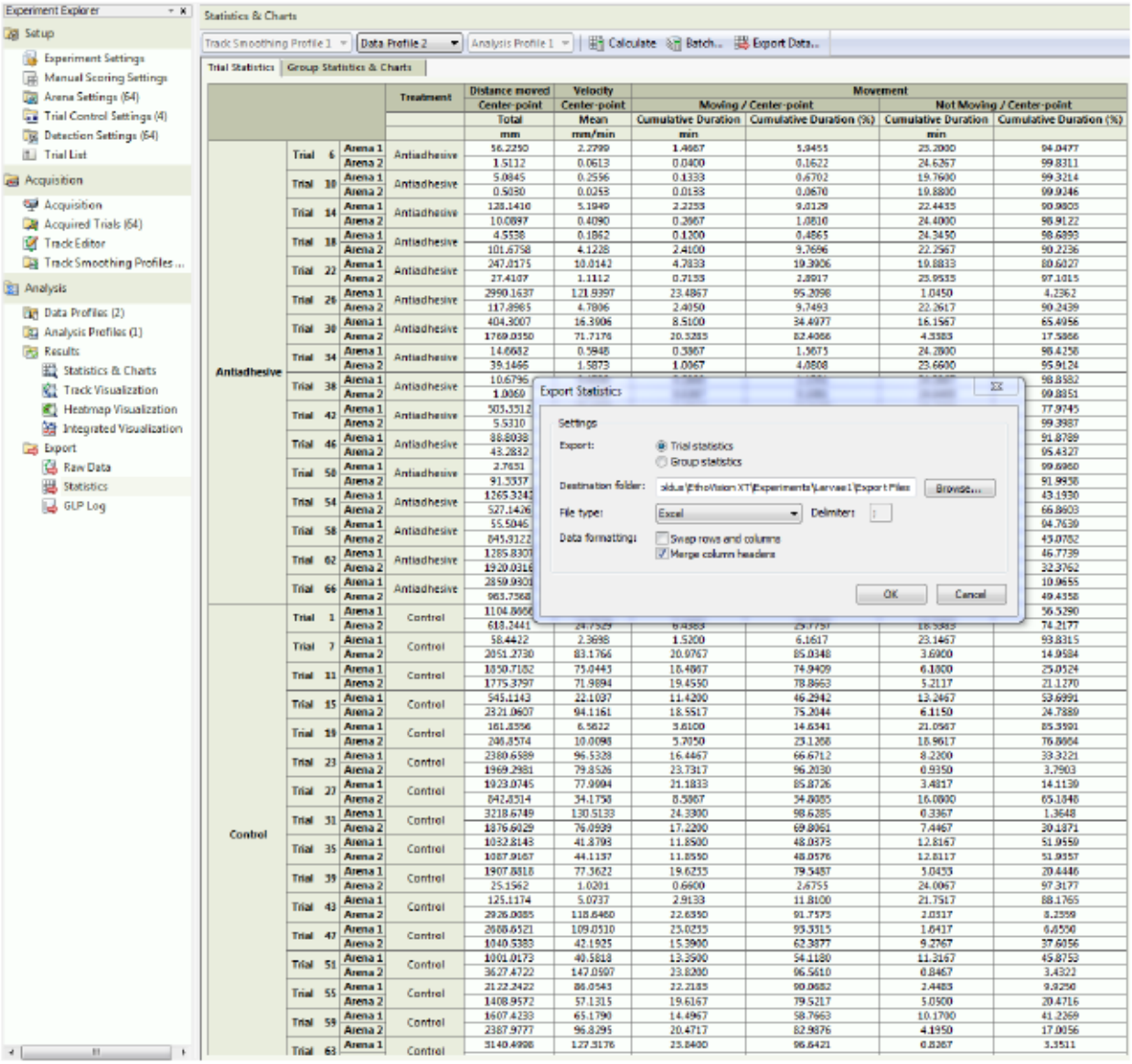


**Figure S4.15**: Export *statistics* window in EthoVision XT with export settings visible.

## SM References (Manual)

Dörfler, S. (2019). XMedia Recode 3.4.8.3. Available at: https://www.xmedia-recode.de/en/version.php.

R Core Team (2021). R: A Language and Environment for Statistical Computing. Available at: https://www.r-project.org/.

The GIMP Development (2020). GIMP (GNU Image Manipulation Programm). Available at: https://www.gimp.org.

## Supplementary Tables

**Table S4.1**: Estimated marginal means (EMM), standard error (SE), degrees of freedom (df) and upper and lower confidence levels (CL; 95%) of the swimming velocity in each treatment (Control, Nanoparticles, Antiadhesive, DCOIT) on the coated PMMA tiles. Intervals (EMM, SE, CL) were back-transformed from the sqrt-scale.

| Treatment | EMM | Standard error | df | Lower CL | Upper CL |
|---|---|---|---|---|---|
| Control | 89.8 | 6.3 | 8 | 75.9 | 104.9 |
| Antiadhesive | 55 | 4.6 | 8 | 44.9 | 66.2 |
| Nanoparticles | 46.4 | 3.4 | 8 | 39 | 54.5 |
| DCOIT | 36.2 | 3.1 | 8 | 29.3 | 43.7 |

**Table S4.2**: Estimated marginal means (EMM), standard error (SE), degrees of freedom (df) and upper and lower confidence levels (CL; 95%) of the swimming activity in each treatment (Control, Nanoparticles, Antiadhesive, DCOIT) on the coated PMMA tiles. Intervals (EMM, SE, CL) were back-transformed from the log-scale.

| Treatment | EMM | Standard error | df | Lower CL | Upper CL |
|---|---|---|---|---|---|
| Control | 49.6 | 9.4 | 8 | 32 | 77 |
| Antiadhesive | 6.2 | 2.2 | 8 | 2.7 | 13.9 |
| Nanoparticles | 5.8 | 1.6 | 8 | 3 | 11 |
| DCOIT | 0.7 | 0.2 | 8 | 0.4 | 1.3 |

**Table S4.3**: Pairwise statistical results of swimming velocity data on the coated PMMA tiles based on estimated marginal means. Tests were performed on the sqrt-scale. Note that the estimated contrasts are still on the sqrt-scale. The p-value was adjusted for multiple comparisons (family of 4 estimates) with the Tukey method. Significant codes indicate: * < 0.05, ** < 0.01, *** < 0.001. All statistical analyses were performed in R version 4.1.1 (R Core Team, 2021) using the 'tidyverse' (Wickham et al., 2019), 'nlme' (Pinheiro et al., 2021), 'car' (Fox and Weisberg, 2019) and 'emmeans' (Lenth, 2021) package.

| Compared treatment pair | Estimated contrast | Standard error | df | t ratio | p-value |
|---|---|---|---|---|---|
| Control / Antiadhesive | 2.1 | 0.4 | 116 | 5.13231 | < 0.001 *** |
| Control / Nanoparticles | 2.7 | 0.4 | 116 | 7.49747 | < 0.001 *** |
| Control / DCOIT | 3.5 | 0.4 | 116 | 9.534846 | < 0.001 *** |
| Antiadhesive / Nanoparticles | 0.6 | 0.3 | 116 | 1.800691 | 0.278 |
| Antiadhesive / DCOIT | 1.4 | 0.3 | 116 | 4.07811 | < 0.001 *** |
| Nanoparticles / DCOIT | 0.8 | 0.3 | 116 | 2.759482 | 0.034 * |

**Table S4.4**: Pairwise statistical results of swimming activity data (based on "moving") on the coated PMMA tiles based on estimated marginal means. Tests were performed on the log-scale. Note that the estimated contrasts are back-transformed from the log-scale. The p-value was adjusted for multiple comparisons (family of 4 estimates) with the Tukey method. Significant codes indicate: * < 0.05, ** < 0.01, *** < 0.001. All statistical analyses were performed in R version 4.1.1 (R Core Team, 2021) using the 'tidyverse' (Wickham et al., 2019), 'nlme' (Pinheiro et al., 2021), 'car' (Fox and Weisberg, 2019) and 'emmeans' (Lenth, 2021) package.

| Compared treatment pair | Estimated contrast | Standard error | df | t ratio | p-value |
|---|---|---|---|---|---|
| Control / Antiadhesive | 7.9 | 2.8 | 116 | 5.812 | < 0.001 *** |
| Control / Nanoparticles | 8.5 | 2.4 | 116 | 7.418 | < 0.001 *** |
| Control / DCOIT | 61.4 | 15.2 | 116 | 16.624 | < 0.001 *** |
| Antiadhesive / Nanoparticles | 1.1 | 0.4 | 116 | 0.177 | 0.998 |
| Antiadhesive / DCOIT | 7.8 | 3 | 116 | 5.396 | < 0.001 *** |
| Nanoparticles / DCOIT | 7.3 | 2.3 | 116 | 6.211 | < 0.001 *** |

## SM References (Tables)


Fox, J., and Weisberg, S. (2019). *An R Companion to Applied Regression*. Third Edit. Sage Publications Available at: https://socialsciences.mcmaster.ca/jfox/Books/Companion/.

Lenth, R. V. (2021). Emmeans: estimated marginal means. Available at: https://cran.r-project.org/package=emmeans.

Pinheiro, J., Bates, D., Debroy, S., Sarkar, D., and R Core Team (2021). Linear and Nonlinear Mixed Effects Models Contact. *Linear nonlinear Mix. Eff. Model.* 3, 103–135. Available at: https://cran.r-project.org/package=nlme.

R Core Team (2021). R: A Language and Environment for Statistical Computing. Available at: https://www.r-project.org/.

Wickham, H., Averick, M., Bryan, J., Chang, W., McGowan, L., François, R., et al. (2019). Welcome to the Tidyverse. *J. Open Source Softw.* 4, 1686; 10.21105/joss.01686. doi:10.21105/joss.01686.

# Chapter 5: Discussion

## 5.1 Key findings and significance

The overall objective of this thesis was to fill current knowledge gaps and develop methodologies to assess environmentally-benign antifouling (AF) coatings, including their efficacy to inhibit fouling, their potential toxicity towards coral juveniles, and their ability to improve spat survival in reef restoration efforts. To achieve this, innovative AF coatings including new chemical formulae were manufactured together with our project partner GMBU (Gesellschaft zur Förderung von Medizin-, Bio- und Umwelttechnologien e.V.), and tested for the first time in natural filtered SW tanks at the Australian Institute of Marine Science (AIMS) in Townsville, Australia. The coatings were tested for their efficacy to inhibit fouling, and a protocol for subsequent fouling analysis using photo monitoring was developed with the machine-learning Trainable Weka Segmentation (TWS) plugin in the Fiji distribution of the image processing program ImageJ (Arganda-Carreras et al., 2017). Furthermore, the swimming behavior of coral larvae was investigated for the first time with an automatic and quantitative measurement software EthoVision XT (Noldus Information Technology). The manual developed for the utilization of this software with coral larvae is included in this thesis and can be downloaded from: https://github.com/LisaKRoepke/CoralLarvaeTracking.

The chapters presented in this thesis provide a valuable contribution towards the development of effective and potential low-toxicity AF coatings for application in two different sectors: maritime industries (incl. shipping and aquaculture) and coral reef restoration. These sectors share a common objective of inhibiting macrofouling on submerged surfaces. Questions of fine-scale and selective antifouling (allowing and/or decreasing designated fouling species) become evident by the findings and boundaries of the studies conducted herein and could be addressed by future research into more functionalized coating systems, which match specific needs for a desired application. The three studies combined present the potential opportunities and limitations of the investigated coatings for future coral aquaculture and reef restoration applications.

## 5.2 Antifouling efficacy and fouling community structure

Two of the three herein tested AF coatings, the encapsulated DCOIT and antiadhesive coating, showed effective and localized antifouling action, while the $CeO_{2-x}$ coating formulation was ineffective (***Chapter 2***).

### 5.2.1 Ineffective $CeO_{2-x}$ nanoparticle coating

The $CeO_{2-x}$ nanoparticle (NP) coating did not decrease the fouling intensity or change the fouling community composition compared with the uncoated control. This contrasted with

Herget *et al*. (2017) and Wu *et al*. (2021) who demonstrated effective antifouling on stainless-steel plates coated with $CeO_{2-x}$ NP in freshwater and seawater environments. However, as mentioned in the previous studies, the coatings differed in their molecular entities. The herein investigated $CeO_{2-x}$ coating was hydrophilic, whereas the commercially available base-paints in Herget *et al*. (2017) and Wu *et al*. (2021) were hydrophobic. Moreover, the $CeO_{2-x}$ coating, in contrast to both other coatings in this work, was the only coating with a hydrophilic top layer, which could be one reason for ineffective fouling reduction. Whether hydrophobic or hydrophilic surfaces are preferred for bioadhesion, e.g. algal fouling or coral settlement, depends on the particular organism (Kang et al., 2006). For instance, diatoms adhere via hydrophilic proteins, whereas barnacles attach using hydrophobic adhesive proteins (Finlay et al., 2010). The attachment process of coral larvae is not well understood, and the potential proteins involved have not been described yet (as discussed in ***Chapter 3***). This knowledge gap offers further research potential, in order to identify molecular surface entities beneficial or at least not adverse for coral larval settlement and disadvantageous for competing fouling organisms.

Another difference between the $CeO_{2-x}$ coatings in previous studies and the coating tested in this work offers opportunities for further research. Herget *et al*. (2017) and Wu *et al*. (2021) applied a relatively low concentration of NPs in the coatings (2 wt% and 5 wt% of dry weight), as compared to 35.7 wt% $CeO_{2-x}$ dry weight in this work. The coating investigated here was ineffective in inhibiting fouling, indicating a high concentration of NPs might not necessarily result in high catalytic activity and antibacterial efficacy, as only the NPs on the surface of the coating can be activated, and particles in deeper layers of the coating are unlikely to encounter bromide ($Br^-$) and hydrogen peroxide ($H_2O_2$). A combination of lower $CeO_{2-x}$ content with a smoother and hydrophobic (as used for the antiadhesive and DCOIT coating), instead of hydrophilic coating, might have proven more effective. This hypothesis should be further investigated with different concentrations of NPs in the coating.

The $CeO_{2-x}$ nanoparticle's antifouling property is created by the biomimetic enzymatic activity of the NPs (as found in haloperoxidases), which catalyze the oxidation of halides in presence of $H_2O_2$ to hypobromous acid (HOBr) according to: $Br^- + H_2O_2 \rightarrow HOBr + H_2O$ (**Figure 5.1**). Therefore, constant availability of $H_2O_2$ and $Br^-$ must be provided for a dynamic antibacterial activity (HOBr formation). We assumed these would be present, as $H_2O_2$ is formed in natural water exposed to sunlight (Weller and Schrems, 1993), and $Br^-$ is a natural constituent of all waters (Stumm and Morgan, 1981). However, future studies should verify available $H_2O_2$ and $Br^-$ concentrations in the tested water body.

As the catalytic activity of the NPs was tested in solution, in their unconsolidated form (***Chapter 2***), it is recommendable to test their activity against isolated bacterial strains prior to integration in a coating (Hartog et al., 2012; Herget et al., 2017), and in actual filtered seawater conditions.

Furthermore, to our knowledge, no protocol has been developed in order to test for the catalytic activity of the NPs integrated in a coating. These steps could help to identify promising NPs with antibacterial properties and their effective concentrations in the coating.

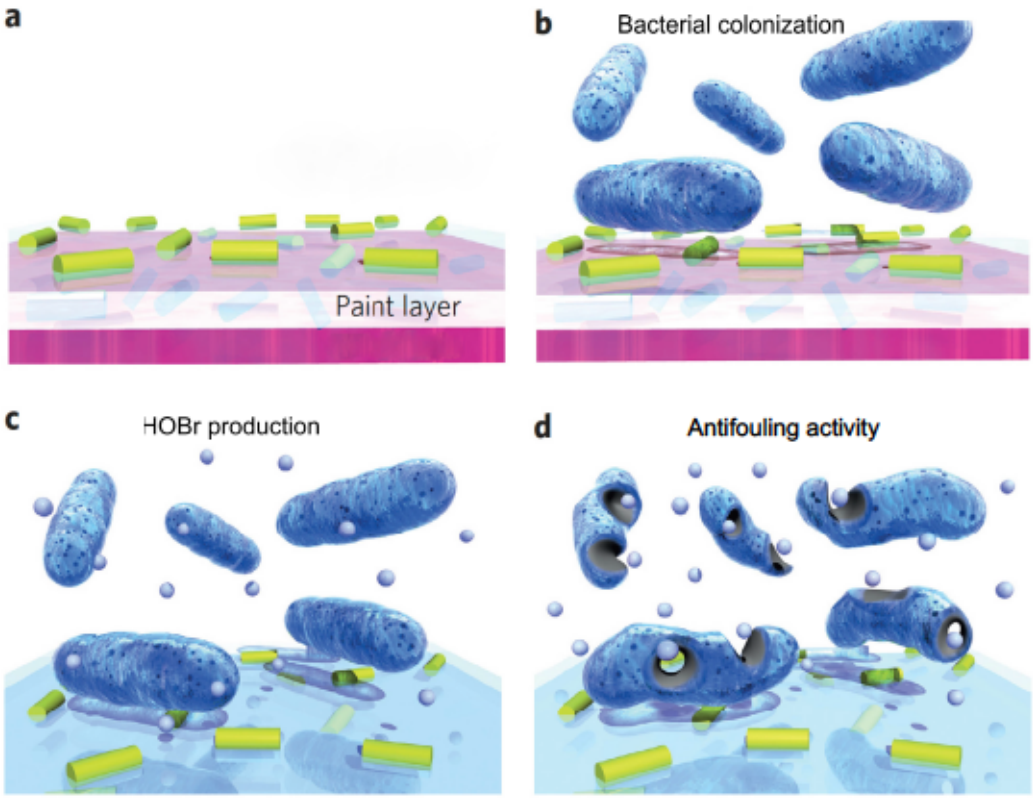


**Figure 5.1:** Schematic showing the bactericidal properties of $CeO_{2-x}$ nanoparticles (NPs). **a**, NPs (yellow-green rods) are embedded in a matrix (coating) and applied onto a surface. **b**, bacterial colonization of surface. **c**, The NP/coating displays an intrinsic biomimetic catalytic activity, as found in haloperoxidases; that is, in the presence of substrates such as $H_2O_2$ and $Br^-$, small amounts of hypobromous acid (HOBr, small light blue spheres) are produced continuously. **d**, The released HOBr interferes with the quorum sensing system of bacteria, preventing adhesion of bacteria and biofilm formation (taken and adapted from Hartog et al., 2012).

The concentration of NPs in the coating can also directly influence the roughness or structure of the coated surface and needs to be considered carefully. More particles generate a higher surface roughness. This might ultimately facilitate the adhesion of organisms and create microhabitats functioning as traps for e.g. organic molecules, as shear forces are weakened and anchorage appears to become easier for fouling organisms (Kerr and Cowling, 2003). The so-called surface roughness value (SRV) or roughness average (Ra) could help guide the manufacture and identify, and compare coating performances in future studies, as surface structure is an important parameter determining not only bacterial bioadhesion, but also coral larval settlement (Whalan et al., 2015). As a result of the observations here (***Chapter 2***), the roughness of the surface could have promoted fouling, irrespective of the high concentration of NPs in the coating. In addition and worth hypothesizing, non-lethal $CeO_{2-x}$ NP concentrations have been reported to facilitate the generation of reactive oxygen species (ROS), which in turn

accelerate quorum sensing molecules and activate inherent resistance capacities in bacteria, thus promote fouling (Xu et al., 2018, 2019).

### 5.2.2 Effective antiadhesive coating with CCA growth

The antiadhesive coating showed significant AF efficacy, although it was much lower than that of the DCOIT coating (***Chapter 2***). The hydrophobic antiadhesive surface of the coating worked well in suppressing green and brown algae on the fully-coated plugs, and created more free space (bare substrate), as compared to the uncoated control. These results are in agreement with literature discussing fouling-release observations in different organisms on similar coatings (e.g., algae and barnacles; see ***Chapter 2***).

Interestingly, CCA growth was unaffected by this type of coating and showed the highest amount of CCA in general, although not significantly different from the control plugs or uncoated areas on the partially-coated plugs. This finding raises questions regarding the mechanisms underlying differential reactions of fouling species or classes to specific coating types. In this particular case, with a focus on coral aquaculture, CCA observations are extremely relevant, as some CCA's compounds and/or associated bacteria induce larval settlement in many coral species (Morse et al., 1996; Heyward and Negri, 1999; Abdul Wahab et al., 2023). However, not every CCA species is a promoter of larval settlement, which underlines the importance of identifying specific CCA (and other fouling) species in order to create or manipulate a coral-thriving environment, possibly with AF applications. Potentially, this or a similar antiadhesive sol-gel coating could create a favorable environment that promotes CCA growth, advantageous for larval settlement in coral propagation programs.

### 5.2.3 Effective encapsulated DCOIT coating creating bare space

DCOIT is well known for its efficacy and applied in a range of AF products. The coating investigated herein provides new insights by incorporating DCOIT through attachment to silicic acid powder in order to decrease the effective concentration needed and extend the period of AF performance. The work within this thesis has demonstrated high AF efficacy of encapsulated DCOIT with a very local area of impact. The fouling analysis showed clear differences in fouling occurrences between coated and uncoated areas on the partially-coated plugs, indicating that antifouling activity was isolated to the coating's surface with negligible leaching of DCOIT onto adjacent uncoated areas (1-3 mm away; ***Chapter 2***). As the monitoring for antifouling efficacy was terminated after 37 days, the maximum time of efficacy remains unclear and should be further investigated (applies to antiadhesive coating as well).

The DCOIT coating (hydrophobic top surface layer and hydrophilic bottom layer) worked particularly well to suppress green and brown algae, as well as CCA. With 1% CCA coverage on the fully-coated plugs and 5% on the coated areas of the partially-coated plugs, CCA growth was strongly inhibited as compared to the control plugs with 31% CCA, and the uncoated areas

of the partially-coated plugs with 23% CCA after 37 days (***Chapter 2***). This finding could indicate a high toxicity of DCOIT towards CCA, which should be addressed in future research, as CCA-free surfaces might prove beneficial in some maritime sectors, including the control of inhibitor CCA species for coral aquaculture. In addition to the observations and assumptions above it should be mentioned, that the fouling class "bare substrate" was assessed and classified with photographs and visually, by which the machine-learning model was trained. Hence, an invisible microcosm of organisms may be present on the bare substrate and could be a relevant subject for more research. This applies to all surfaces and dominant fouling classes within this work, and could be addressed with e.g., smear tests and subsequent genetic analyses.

## 5.3 Target and non-target species: "competitor" and "promoter" CCA highlight importance of selective antifouling as a tool for application-oriented future solutions

The work of this thesis intends to pave the way towards applied research into the effective application of antifouling treated substrates for benefits in coral restoration. Over decades of research, specific algae have shown significant negative effects on corals' survival and growth, ultimately disturbing the lifecycle and the natural recruitment of coral reefs. Therefore, the AF coatings in this thesis were developed to reduce algal biomass, not knowing which algae would be affected by the coatings (***Chapter 2***). Careful monitoring assessed whether the antifouling coatings would affect beneficial or harmful algae, while also not directly affecting coral larvae or spat. In other words, it is selective antifouling vs. ecotoxicology, that is identified and discussed within this thesis. Some species are antifouling targets and others non-targets, which makes this approach highly complex. Also, information on the harmful and beneficial algae including their microbial communities are still scarce and, their classification in this way also depends on which organism is intended for protection (i.e., coral).

CCA's interactions with corals are diverse, ranging from settlement cues and facilitation by "promoter" CCA species to settlement inhibition and preemptive competition for space, and overgrowth of smaller coral colonies by "competitor" CCA species (**Figure 5.2** and **Figure 5.3**; Buenau et al., 2012). The latter was observed in ***Chapter 3***, in which competitive CCA overgrew vast numbers of coral spat, which in turn made growth measurements of individual coral settlers impossible and lead to a high mortality of coral spat.

In a competitive space between algae and coral spat, where each requires substrate, light, and nutrition and survival depends on size (Buenau et al., 2011), relative growth rates of competitors appear more important for the outcome than other mechanisms determining the fate of individual settlers (e.g., facilitation by CCA, high settlement/survival/aggregation). It is

important to note that while protected microhabitats are crucial for coral settlement and early growth, additional mechanisms are required for coral persistence in the long term, particularly when expanding into less protected areas. These mechanisms include competitive reversals (where coral populations outcompete algae for space over time) and patchy mortality of coralline algae, which can create open space for new coral settlement (Buenau et al., 2012).

Habitat complexity, combined with limitations on the growth of dominant CCA to retain space, as found for the herein investigated DCOIT coating (***Chapter 2***), could help to improve a reef's recruitment potential (Arnold et al., 2010; Arnold and Steneck, 2011; Buenau et al., 2012; Elmer et al., 2018). A previous modeling study by Buenau et al. (2011) suggests that if CCA only overgrow coral colonies smaller than a threshold size, coral persistence can improve considerably if the coral is competitive enough to reach this critical size. However, long-term coexistence remains highly unlikely if the coral cannot compete for space occupied by CCA.

Previous studies and the work within this thesis emphasize the importance to understand the details and links between competitive interactions with less-studied taxa such as CCA. Tebben et al. (2015a) point out, that while the sources of CCA settlement cues are well known, the links between their biological activity, chemical identity, presence and quantification *in situ* are largely unknown. However, only this knowledge will help to understand the functional importance and how to define the starting points in selecting the target organisms for antifouling. In this sense, (coral) aquaculture must adopt scientific research on intra- and interspecific fouling interactions in order to manipulate them effectively, thus taking advantage of the diverse biological capacities of aquatic micro- and macro-organisms, and taking antifouling systems to another level of knowledge and application (Garibay-Valdez et al., 2022).

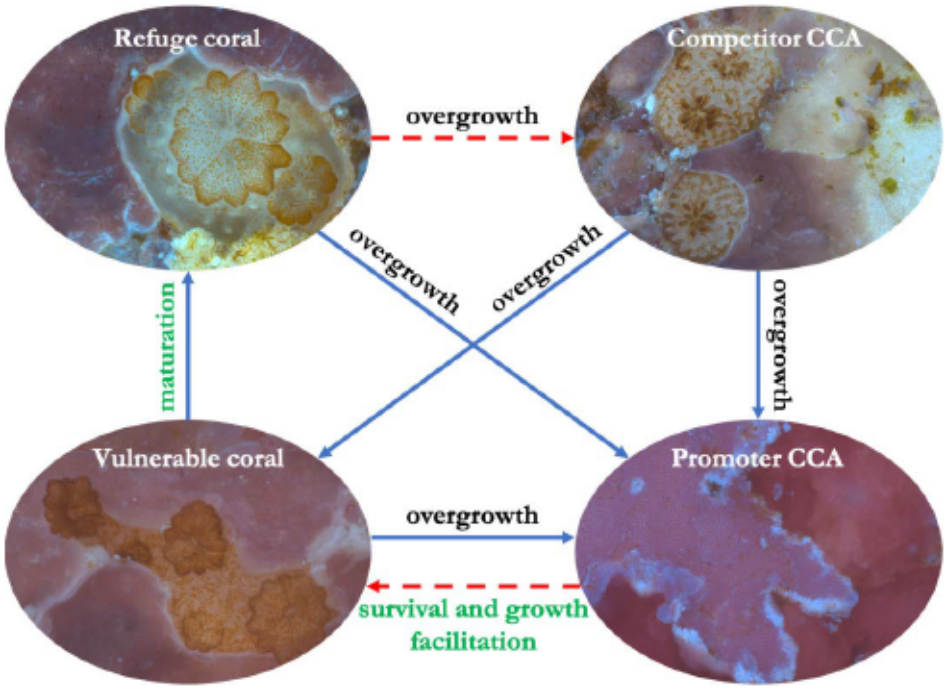


**Figure 5.2:** Schematic modified after Buenau et al. (2012) showing the proposed interactions between model groups: refuge coral, vulnerable coral, competitor CCA, promoter CCA. The solid blue lines indicate interactions that are always included, the dashed red lines indicate interactions that are included when specified in the coral persistence model.

The intricate network of cellular communication within a fouling community, spanning multiple biological languages and involving cross-linking, necessitates novel approaches for their investigation. It is important to recognize that biofilms in their natural environment are composed of diverse taxonomic groups from different kingdoms (i.e., prokaryotes, micro and macroalgae), whereas most biofouling studies focus solely on members of the same kingdom. It is not surprising that studying cellular communication among members of the same species is challenging and investigating real-time communication among taxonomic groups from different kingdoms, each with representatives of multiple species, poses an even greater difficulty. Nevertheless, the resemblance between the biofouling processes of bacteria and microalgae suggests a possible explanation for the coexistence of different taxonomic groups in the same biofilm.

Aquatic ecology and aquaculture face a significant challenge to comprehend the molecular communication systems among various taxonomic groups. Quorum sensing represents one of the most investigated of these communication systems. Recent research suggests that quorum sensing signals mediate interactions not only between prokaryotes, but also between prokaryotes and eukaryotes (Dow, 2021; Garibay-Valdez et al., 2022). CCA have been observed to suppress the growth and recruitment of other macroalgae and thrive under nutrient-rich conditions (Vermeij et al., 2011). As a strategy to compete for space and keep surfaces clean, CCA use allelopathy and microbial inhibition, in addition to epithelial tissue sloughing, against the settlement of epiphytic algae (Harrington et al., 2004; Gómez-Lemos and Diaz-

Pulido, 2017). Moreover, cell wall-associated compounds in CCA have been described to mediate coral larval settlement (Morse et al., 1994; Tebben et al., 2015; Gómez-Lemos et al., 2018).

Methodologies of the latter studies combined with findings of a more recent study by Abdul Wahab et al. (2023), who identified settlement patterns of 15 CCA species in a hierarchical matrix with 15 coral species, could help to identify the optimal CCA associations for coral settlement and recruitment success. By combining promoting CCA-coral pairs, and identifying the responsible compounds of interaction in CCA and corals, intimate mechanistic pathways for promoting coral larval settlement could be progressed for application in reef restoration (Abdul Wahab et al., 2023). In addition, antifouling coatings as the ones in this study or similar, could potentially strengthen suitable CCA-coral pairs by promoting or preventing specific CCA growth. The relatively high proportion of CCA on the antiadhesive coated, and low proportion on the DCOIT coated plugs show an effect of the coatings onto CCA abundance (***Chapter 2***). Further studies should investigate the diversity and abundances of specific CCA species affected. Some CCA species and their associated bacteria could potentially be manipulated, so that certain CCA-coral pairs would benefit with higher coral survival and growth rates (**Figure 5.3**). Unfortunately, these questions could not be answered by the experiments in this thesis, as the investigation timeframe was too short and would require at least six months to several years in order to identify long-term effects of the coatings onto CCA-coral pairs.

In addition to the already suggested future research, as a range of CCA are very successful in inhibiting undesirable algal growth, the chemical compounds and/or mechanical mechanisms driving this competition success could be further identified and isolated, and potentially applied to antifouling applications with antifoulants of natural origin for reef restoration (Figueiredo et al., 1997; Gómez-Lemos and Diaz-Pulido, 2017). Many marine organisms have developed a variety of different antifouling strategies to resist biofouling, mechanically through micro-textured surfaces, such as shark skin, mussel shells, or mangrove leaves, and chemically through compounds found in sponges, macroalgae, and corals (Niemann et al., 2015; Kacou et al., 2019; Sánchez-Lozano et al., 2019; Tian et al., 2020). Antifouling coatings inspired by these organisms could provide protection for different maritime sectors within an underwater environment. It is recommended, however, to define the desired outcome and field of application first, because one compound or coating will most probably not fit all strategies in need of antifouling solutions.

## 5.4 Coral juvenile performance on antifouling coatings

The findings of the studies conducted herein reveal differential performances (larval swimming velocity/activity and settlement and spat survival and growth) of *Acropora millepora* and

*Acropora tenuis* in response to the three tested antifouling coatings (***Chapters 2-4***). These results are separately reviewed and discussed in each coating type section below.

### 5.4.1 $CeO_{2-x}$ nanoparticle coating: ambiguous performance with many unknowns

Changes in coral larval and spat performance in relation to the $CeO_{2-x}$ nanoparticle (NP) coating raised many questions and it remains unclear as to whether this coating type was potentially beneficial or not. As demonstrated in ***Chapter 2*** and discussed in **section 5.2.1**, the coating showed no effect in suppressing visible algal growth. However, it remains unclear if the NPs affected larval performance, either directly through chemical mediation, or indirectly through physical or biological surface alteration.

In ***Chapter 2***, the highest **settlement** of *A. tenuis* larvae was found on the fully-coated (FC) NP plugs, although not statistically significant. Settlement on both the coated and uncoated areas of the partially-coated (PC) plugs was equally high. Among the coated areas of the PC treatments, settlement on the NP-coated plugs was the highest (statistically significant). **Survival** of *A. millepora* spat after 69 days on the FC plugs and coated areas of the PC plugs was higher than on the Control plugs, although not significantly. **Growth** of spat after 14 days was the lowest among all treatments (***Chapter 3***). However, the growth data should be treated with some caution: As the age from which to determine actual growth in early coral settlers remains subject to discussion, the period of 14 days to measure growth is relatively short (given the slow growth rates). This rather short period should be questioned as adequate for growth measurements, especially at the very beginning during which metamorphosis into a fully-developed settler is completed and the early skeletal development starts. **Swimming velocity and activity** on the NP-coated PMMA tiles was significantly below the activity measured on the uncoated Control tiles (***Chapter 4***). However, the interpretation of the results from this chapter cannot be construed negatively for the larvae, as other factors (e.g., unmeasured surface roughness controls for each coating type) could have confounded the results. Moreover, as only limited literature is available, "normal" swimming velocity of coral larvae still has to be investigated and evaluated, although efforts and methodologies in this scientific field have developed in recent years (Hata et al., 2017; Sakai et al., 2020; Geertsma et al., 2023). Therefore, ***Chapter 4***, through its innovative measurements of swimming velocity, should be understood as a methodological contribution to the field of coral toxicology, rather than an assessment of the coating's potential toxicity towards coral larvae.

The list of previously reported (antifouling) properties of $CeO_{2-x}$ NPs (Herget et al., 2017) can be extended with properties mentioned more recently in literature. Nanotechnology has been put forward as a new set of methodological instruments to help and protect coral reefs under pressure (Roger et al., 2023a, 2023b). Coral bleaching, induced by heat stress, is a very complex process, which has not yet been understood completely; however, high concentrations of free radicals, such as reactive oxygen species (ROS) are co-responsible for the breakdown of

symbiosis between cnidarian hosts and dinoflagellate algae partners through damage to cellular membranes, lipids, proteins, and DNA (Lesser, 2011; Szabó et al., 2020). ROS-scavenging NPs, termed redox nanoparticles (RNP$^{o}$) are designed (diameter of approx. 40 nm) not to internalize in cells and mitochondria, so do not interfere with normal redox reactions such as the electron transport chain (Vong et al., 2015). Motone et al. (2018) found a significantly increased survival rate of *A. tenuis* coral larvae in a 33 °C thermal stress treatment in which larvae were treated with RNP$^{o}$. These results indicate that RNP$^{o}$ can reduce ROS in aposymbiotic coral larvae and are therefore under consideration for delivery to corals as heterotrophic feed particles in order to protect corals from thermal stress (Motone et al., 2018).

A recent study by Roger et al. (2022) investigated the antioxidant effects of engineered poly(acrylic acid)-coated $CeO_{2-x}$ NPs (diameter of ~4 nm) on free-living Symbiodiniaceae (*Breviolum minutum*). These NPs were internalized by the dinoflagellates and did not show any interferences with cell growth over a 25-day exposure period. The NP treated 34 °C heat stress treatment showed a clear ROS-scavenging effect. Furthermore, aposymbiotic anemones (*Exaiptasia diaphana*, ex *Aiptasia pallida*) were successfully infected with NP-loaded *B. minutum*. These findings highlight potential positive effects of $CeO_{2-x}$ NPs on corals. However, opposite findings in literature report negative effects of $CeO_{2-x}$ NP-induced oxidative stress in organisms and enhancement effects of NP-selected resistant bacteria (Zhang et al., 2011; Gagnon et al., 2018; Xu et al., 2018, 2019; ***Chapter 2***). As the chemical formulas, manufacturing methods, concentrations, etc. of the NPs differ between studies, special attention needs to be paid to comparisons, and discussions need to clarify the prerequisites first in order to validate findings.

Given the developments in nanotechnology fields such as human medicine (drug delivery), and agriculture (protection against infections and parasites), transfer and adaptation for application in marine ecosystems will be a priority topic in the following decades. The studies provided in this thesis were unable to confirm the antifouling properties of the cerium dioxide nanoparticles, nor a substantially positive effect for coral juvenile performance. The reasons can be manifold, including the potential loss of catalytic activity of NPs in their consolidated form, the need to further optimize the effective concentration of particles in the coating, and the unknown influence of the coating's surface characteristics (e.g., roughness/porosity, amphiphily, light reflection, etc.) potentially influencing coral larva and spat performance (see more ***in Chapters 2-4***). However, future studies could address all these parameters in the search for effective antifouling properties, ROS-scavenging, or a combination thereof. In general, our data show that any positive influences of the NP-coating on early life stages of corals might be masked by the as yet understudied factors as described above.

### 5.4.2 Antiadhesive coating: efficacy without harm

In contrast to the nanoparticle coating, the antiadhesive coating did show efficacious antifouling action by creating more bare space without fouling (***Chapter 2***). However, the direct interactions of the coating with the coral spat and/or the effects of the coating on the fouling community, which in turn can affect the corals, remain subject to further research.

**Settlement** of *A. tenuis* on the coated antiadhesive areas and plugs was lower as compared to the uncoated Control areas (PC) and plugs (FC), although not significantly (***Chapter 2***). **Survival** of *A. millepora* spat after 69 days on the FC plugs was the highest among all treatments (noting that DCOIT was excluded from the analysis due to insufficient settlement). On the PC plugs, the highest survival was found on the uncoated areas of the DCOIT treatment, followed by the coated antiadhesive treatment. In addition, settlers on the antiadhesive coating showed the highest **growth** measurements. These results were not statistically confirmed; however, and require further replication and validation (***Chapter 3***). As for the other treatments, **swimming velocity and activity** on the antiadhesive-coated PMMA tiles was significantly below the activity measured on the uncoated Control tiles (***Chapter 4***). The interpretation limitations and cautions were addressed in **section 5.4.1**.

As mentioned in **section 5.2.2** and ***Chapter 3***, the hydrophobic surface layer of the antiadhesive coating could be the reason why fouling organisms (green and brown algae in this study) and coral larvae showed less surface attachment. However, the surface was attractive for CCA anchorage and growth (***Chapter 2***). The positive (however, not significant) coral spat survival and growth results of both, the antiadhesive and DCOIT (uncoated) treatment, support the hypothesis that the general reduction of fouling pressure from algae could have benefitted the coral's survival (***Chapter 3***). Although ***Chapter 2*** and *3* were conducted with different coral species under different experimental settings, it became clear that the antiadhesive coating alone without biological cues (i.e., CCA) was not attractive for larval settlement. The antiadhesive coating does not contain any toxic compounds of potential concern for coral settlement; however, coatings such as the one investigated in this study should be further investigated for their attractiveness and any potential negative impacts on coral larvae and spat. A recent study by Levenstein et al. (2022) identified settlement preferences for coral larvae on calcium carbonate substrates, with larvae reported to sense and positively respond to soluble inorganic minerals such as silica ($SiO_2$) and strontianite ($SrCO_3$), possibly by the release of ions into the water column.

As uncoated Control plugs become progressively overgrown by algae, antiadhesive-coated plugs could potentially supply more free space with less competition from fouling organisms for coral spat. Their benefit in reducing fouling pressure by brown/green algae, while not negatively affecting the coral's fitness could prove to be a useful tool to create habitat with coral dominance and space for recovery from disturbances. The reduction in speed and activity

of coral larvae measured on the antiadhesive coating in comparison to the Control does not allow for any realistic interpretation, as "normal" swimming speed and activity have not been defined for different materials in the presence and absence of settlement cues (***Chapter 4***).

### 5.4.3 Encapsulated DCOIT coating: promising and controllable?

The encapsulated DCOIT coating was highly efficacious in reducing overall fouling, incl. CCA and brown/green algae (***Chapter 2***). The studies conducted herein found differential effects of coral larval settlement onto this coating depending on its age of pre-conditioning in aquaria (***Chapter 2***, ***3***). Moreover, the AF area of impact was visibly linked to the coating surface with neglectable AF action on uncoated areas (***Chapter 2***). In general, the results show promising insights for future potential handling mechanisms with this coating type.

*A. tenuis* coral larval **settlement** on the fully-coated DCOIT plugs was lower as compared to the Control plugs, however, not significantly. Settlement on the uncoated Control areas of the partially-coated plugs was also consistently higher, although again not significantly different from the coated areas (***Chapter 2***). In contrast, **survival and growth** of *A. millepora* coral spat on the fully-coated plugs and coated areas of the partially-coated plugs could not be measured, as these coatings were not pre-conditioned as in ***Chapter 2*** and more strongly inhibited larval settlement (***Chapter 3***). However, **survival** on the uncoated areas of the partially-coated DCOIT plugs was the highest found among all treatments and differed significantly from the uncoated Control plugs. Also, **growth** performance of *A. millepora* after 14 days was higher than on the Control plugs, although not significantly (***Chapter 3***). **Swimming velocity and activity** was significantly lower as compared to the Control and other two antifouling treatments. As for the other two antifouling coatings, the reasons can be manifold and are discussed in ***Chapter 4***.
Although DCOIT's toxicity on marine organisms has been reported in a wide range of studies (Wendt et al., 2016; Fonseca et al., 2020; Campos et al., 2022b), still little is known about any effects in corals (Cima et al., 2013; Ferreira et al., 2021). As DCOIT is a dominant biocide used in antifouling paints, recent research has investigated alternative coating designs with DCOIT encapsulated in silica nanocapsules to ensure a lower long-term toxicity towards fouling organisms (Maia et al., 2015; Dos Santos et al., 2020; Campos et al., 2022a).

The results presented in ***Chapters 2-4*** show, that the toxicity of DCOIT can be moderated by pre-handling strategies before being offered for coral larval settlement. In ***Chapter 3***, larvae were not willing to settle directly on the coating. However, settlement only millimeters away from the coating resulted in the highest survival of spat among all treatments. Moreover, the seeding unit (SU) yield, a measure of success to compare the effectiveness of different restoration approaches, assuming that a single, large, coral colony can theoretically grow to adulthood per outplanted SU (Chamberland et al., 2017a; Randall et al., 2020), was evaluated. The highest SU yield, representing the highest number of tiles with at least one living settler

after 69 days, was registered for the partially-coated DCOIT plugs, albeit not significantly different from the control (**Table 5.1** ***Chapter 3***).

**Table 5.1**: Seeding unit (SU) yield per treatment in absolute (numbers) and relative (%) abundances. N (= 45) corresponds to the number of plugs in each treatment after 69 days (end of experiment). Note that no settlement/survival was measured on the fully-coated DCOIT plugs and therefore the treatment was excluded.

| *Treatment* | *SU's (number)* | *SU's (%)* |
|---|---|---|
| *Control* | 19 | 42.2 |
| *Partially-coated Nanoparticles* | 16 | 35.6 |
| *Fully-coated Nanoparticles* | 22 | 48.9 |
| *Partially-coated Antiadhesive* | 23 | 51.1 |
| *Fully-coated Antiadhesive* | 24 | 53.3 |
| *Partially-coated DCOIT* | 25 | 55.6 |

In addition to these findings, ***Chapter 2*** demonstrated high settlement on the uncoated areas and moderate settlement (not different from control) on the coated areas of the partially-coated plugs and fully-coated plugs. However, these plugs were pre-conditioned in filtered natural seawater tanks for 37 days and had developed a certain biofouling community, clearly visible on the uncoated areas and plugs. In general, fouling was reduced by DCOIT, but did not prevent all fouling. Positive "fouling" cues on these conditioned plugs created attractiveness for coral larvae and allowed for settlement (***Chapter 2***). Throughout the experiment and as time progressed the plugs became heavily fouled. However, the DCOIT treated areas performed best in delaying fouling pressure and growth of macroalgae. As spat survival was significantly higher on the uncoated areas of the partially-coated DCOIT plugs in comparison to the uncoated control plugs (***Chapter 3***), it can be hypothesized that an established but controlled (by antifouling) biofilm might cause less negative fouling impacts (competition by overgrowth, allelochemicals, etc.) on coral spat than an untreated control surface on which the fouling community starts to compete for space with the corals at the same time. Given that some algae grow much more rapidly than coral spat, fouling is a limiting factor for coral's survival and growth, particularly in the first months (Ceccarelli et al., 2018; Evensen et al., 2019; Rölfer et al., 2021). As more coral reefs switch to algae-dominated states by phase-shifts following eutrophication, overfishing, and heat-exposure (Hughes, 1994; Hughes et al., 2007; Norström et al., 2009; Karcher et al., 2020), encapsulated DCOIT or other low-toxicity biocidal antifouling coating designs might be worthy of further investigation in order to boost coral's health by creating space to occupy algae-controlled substrate. If the potential toxicity of encapsulated DCOIT immobilized in a coating is controllable, it would be worthwhile to invest in restoration substrate designs and test these in the field (**section 5.5**).

Similar to the rapidly-developing fields in nanotechnology (**section 5.4.1**), 3D-printing has gained much interest in recent years as manufacturing of different materials and shapes in different sizes can be accomplished. A recent study by Shimeta et al. (2023) has successfully investigated 3D-printed thermoplastics with embedded DCOIT. These thermoplastics were equally resistant to macrofouling as three commercial antifouling coatings. Such alterations of the biofilm community may not only influence biofilm growth, but also the microbial dynamics and settlement cues to which fouling organisms or coral larvae respond. Similar substrates (e.g., DCOIT-infused limestone or aragonite) with inherent antifouling properties could prove useful for marine applications in different sectors, including reef restoration.

## 5.5 Potential strategies to use antifouling coatings in coral restoration

The long-term survival of tropical coral reef ecosystems relies on a multifaceted approach encompassing three crucial levels of action: mitigating stressors that have led to coral mortality, maintaining and rebuilding remnant coral populations until stressor abatement is achieved, and researching and implementing methods to help corals adapt to a changing ocean (Duarte et al., 2020; Hein et al., 2020).

### 5.5.1 Coral restoration methods

Given the pressures tropical coral reefs are facing, and insufficient management of coral reefs to control ongoing global threats (***Chapter 1***), these ecosystems are unlikely to persist naturally (Pollock et al., 2017; van Oppen et al., 2017; Boström-Einarsson et al., 2020; Vardi et al., 2021; Banaszak et al., 2023). The loss of coral populations is so severe that larval supply is limited or even insufficient to re-establish a coral community. Consequently, researchers and reef managers are carefully approaching solutions in active coral restoration (Rinkevich, 2014; Barton et al., 2017; Cruz and Harrison, 2017). Current coral restoration methods include asexual and sexual propagation, as well as substratum enhancement methodologies (**Table 5.2**).

**Table 5.2**: Restoration methods, their definitions, and other common terms. Categories are not mutually exclusive as some methods are often combined. Red shaded box indicates potential for antifouling coating applications. Table taken and adapted from Boström-Einarsson et al. (2020).

| Method | Definition | Other common terms |
|---|---|---|
| ***Asexual Propagation Methods*** | | |
| Direct transplantation | Transplanting coral colonies of fragments without intermediate nursery phase | Coral tipping, post-disturbance repair |
| Coral gardening | Transplanting coral fragments after an intermediate nursery phase | Population enhancement, asexual propagation, * |
| Coral gardening - Nursery phase | Transplanting coral fragments with an intermediate nursery phase (used to describe case studies that only detail the nursery phase). Nurseries can be *in situ* (on the reef) or *ex situ* (flow | |

| | | |
|---|---|---|
| | through aquaria). Note that following the above definition of restoration, a coral nursery does not constitute restoration, until outplanting has occurred. | |
| Coral gardening - Transplantation phase | Transplanting coral fragments with an intermediate nursery phase, including outplanting juveniles raised in the nursery (used to describe case studies that only detail the transplantation phase) | Outplanting |
| Coral gardening - Micro-fragmentation | Transplanting micro-fragments from corals, with an intermediate nursery phase | Re-skinning |
| ***Sexual Propagation Methods*** | | |
| Larval enhancement | Using sexually derived coral larvae to release or outplant at restoration site, after intermediate holding phase which can be *in-* or *ex- situ* | Larval propagation, sexual propagation, larval seeding, assisted breeding |
| ***Substratum Enhancement Methods*** | | |
| Substratum addition - Artificial reef | Adding artificial structures for purpose of coral reef restoration | Engineered/artificial structures, various brand names (e.g., BioRock, EcoReef, ReefBall, Mars Spiders) |
| Substratum stabilization | Stabilising substratum to facilitate coral recruitment or recovery (often combined with artificial reefs and transplantation of coral fragments) | |
| Substratum enhancement - electric | Enhancing artificial substrata with an electrical field or direct current | Electrochemically formed structures, mineral accretion, BioRock |
| Substratum enhancement - Algae removal | Enhancing substrata by removing macroalgae (e.g., by cultivation of grazing sea urchins or selective antifouling coatings | |
| * In some geographic locations (primarily Caribbean, due to focus on endangered species recovery) coral restoration is synonymous to coral gardening | | |

Worldwide, a large majority of coral reef restoration projects employ asexual propagation techniques whereby fragmented colonies are grown in either an ocean-based or land-based nursery and then transplanted (or "outplanted") onto the reef (Boström-Einarsson et al., 2020). These techniques will not (nor are they intended to) save the world's coral reefs alone. However, various aspects (e.g., nursery rearing, outplanting) are important restoration components regardless of whether coral colonies are multiplied asexually or sexually, from natural populations or from genetically assisted strains. Larval-based coral restoration (sexually propagated coral larvae) generates large numbers of genetically unique individuals created from gametes collected during spawning events. This approach promotes genetic variability within restored populations, thereby increasing the adaptability of restored populations to a rapidly changing ocean. Advances in assisted fertilization and husbandry techniques (Chamberland et al., 2017b; Randall et al., 2020), alongside the development of mass-rearing and outplanting technologies (Chamberland et al., 2017a; Cruz and Harrison, 2017; Miller et al., 2021) have made this approach increasingly attractive to restoration practitioners. However, the scale and effectiveness of larval-based coral propagation efforts remains limited by naturally low survivorship rates of outplanted recruits, as well as the often complex, time-consuming, and costly operations required for mass larval rearing and outplanting. Like asexual-based efforts, larval- based efforts are often too small (<1 ha) to address reef decline at relevant ecological scales (Boström-Einarsson et al., 2020); however, they hold great potential to be scaled up based on sheer numbers of individuals produced during spawning events (Banaszak et al., 2023).

### 5.5.2 Bottlenecks in larval-based restoration and potential for antifouling

As reported by Boström-Einarsson et al. (2020) and supported by others (Pollock et al., 2017; Hughes et al., 2023), the most scalable methods (i.e. beyond 1 ha in a single project) appear to be techniques that use sexually derived propagules as a source for restored coral populations and communities. In order to increase the effectiveness and scale of coral breeding in restoration, Banaszak et al. (2023) highlight four priority areas for research and cooperative innovation:

1. Expanding the number of restoration sites and species
2. Improving broodstock selection to maximize genetic diversity and adaptive capacity
3. Enhancing culture conditions to improve offspring health
4. Scaling up infrastructure and technologies for large-scale breeding & restoration

Priority area no. 3. includes the design and conditioning of substrates for successful larval settlement and outplanting, as well as the reduction of algal fouling by beneficial grazers (Toh et al., 2013; Craggs et al., 2019). Other studies and reports support the strategy to reduce fouling in order to increase coral survivorship (Ceccarelli et al., 2018; Boström-Einarsson et al., 2020; Hein et al., 2020; Suggett and Van Oppen, 2022). As the idea to reduce fouling with antifouling coatings is relatively new and has first been investigated by Tebben et al. in 2014, and meanwhile supported by van Oppen et al. (2017), the work of this thesis presents a promising starting point for this strategy by creating knowledge and suggestions for applied approaches leading towards antifouling-oriented applications in reef restoration.

Following ***Chapter 1*** and **section 5.3**, the coral's development from a settled polyp (spat) to a juvenile recruit is often terminated early by competitive algal species. Antifouling-treated settlement substrates as the ones in this study could offer attractive settlement space while preventing growth of aggressive competitors (see **Figure 5.3**). Once larvae have settled, early spat could find protection from overgrowing or manipulating fouling species by antifouling-mediated coatings, and even after one year of development, these coatings could potentially increase the likelihood of coral survival to size-escape thresholds. Therefore, it is recommended to test for the long-term efficiency and effects of the coatings towards target and non-target organisms.

| Spawning adult colony | Fertilization | Developing embryos | Swimming larva (2 days) | Settled polyp (1 week) | Settled polyp (6 weeks) | Juvenile (up to 6 months) | Juvenile (up to 1 year) | Mature colony (4+ years) |
|---|---|---|---|---|---|---|---|---|
| Collecting high genetic diversity from multiple reef habitats | Achieving high fertilization in rare/gonochoric species | Maintaining high water quality and culture health | Providing effective settlement cues and substrates | Managing and eliminating fouling species and pests | Preventing algal overgrowth and trampling by invertebrates | Timing outplanting to avoid bleaching/ hurricanes | Preventing direct predation by fish/ invertebrates | Preserving genetic diversity in F2 crosses/ gene banking |
| Capturing/ fertilizing gametes from gonochores | Successfully cryopreserving and fertilizing with post-thaw sperm | Preventing genetic bottlenecks/ dominant genotypes | Preventing substrate fouling by aggressive competitors | Facilitating symbiont and microbiome establishment | Promoting rapid growth toward escape size | Selecting suitable outplanting habitats and densities | Managing fouling and overgrowth by benthic competitors | Maintaining accurate records on parentage and phenotype |
| Capturing gametes at aquaculture scales | Achieving high gamete concentrations in large-scale batches | Facilitating embryo development at aquaculture scales | Successfully mass-settling/ direct-seeding larvae | Maintaining stable aquarium systems and conditions for *ex situ* rearing | Determining effective feeding protocols for *ex situ* rearing | Outplanting at large scales/ reducing per-unit cost and handling time | Tracking survival/ growth/genotype on large spatial scales | Maintaining funding and capacity for long-term monitoring |

**Figure 5.3:** Current challenges and stage-specific bottlenecks in applying coral larval propagation to reef restoration. Red boxes indicate potential for antifouling coating applications. Schematic taken and adapted from Banaszak et al. (2023).

### 5.5.3 Coral restoration substrate specificity

Artificial reefs (Shin et al., 2014) and coral settlement substrates (Chamberland et al., 2017a; Randall et al., 2022) are frequently advocated as possible strategies to counteract the loss of tropical coral reefs worldwide. Despite increasing availability of novel materials, there is limited understanding of how different materials and their physical and chemical properties can influence coral recruitment success and early benthic community development (Leonard et al., 2022). As reported by Boström-Einarsson et al. (2020), a majority of artificial reefs and structures are made from concrete, and 10% of studies which attach corals to the substrate used cement and concrete. The production of cement is responsible for 5–7% of global carbon emissions, mainly due to $CO_2$ emissions during the calcination process of limestone, from combustion of fuels in the kiln, as well as from power generation (Worrell et al., 2001). Certainly, the contribution of coral restoration to the overall carbon footprint of concrete is negligible; however, there is considerable irony in using a technique for restoration that directly contributes to climate change. Further, a substantial number of projects (~60%) use plastics to attach coral fragments to the substrate, primarily in the form of epoxy putty or cable ties (Boström-Einarsson et al., 2020). There are marine grade versions of both materials, although they are also likely to break down in the shallow, warm and high-UV environments of corals reefs. Other manufactured materials such as steel are also commonly used in coral restoration (Rinkevich, 2005; Kotb, 2016). All these materials can accumulate on reefs, potentially with unforeseen longer-term consequences. However, while the growing problem of microplastics in the marine environment has been demonstrated to be detrimental to corals (Allen et al., 2017; Lamb et al., 2018) it pales in comparison to the primary threat of climate change. As the field of coral restoration grows and spreads to more coral reefs around the world, practitioners are urged to use biologically sustainable and biodegradable alternatives.

Recent research has investigated a variety of potential substrates for coral larval settlement, in order to increase the attractiveness for larvae to settle and improve post-settlement survival and growth. Leonard et al. (2022) compared the coral settlement efficacy between eight materials and two common (control) materials during major coral spawning events on the forereef of Mo'orea, French Polynesia. Six of these materials, including 3D printed concrete, polyvinyl chloride (PVC) with chitosan coating, fiber- glass polymer, and flax-based polylactic acid, produced similar coral recruitment to control materials (Portland concrete and PVC). Two materials (porous concrete and ceramic foam) produced lower recruitment. The results suggest that the structural micro-complexity and durability of an artificial material and the composition of the benthic communities colonizing it can strongly influence coral recruitment. These findings are in line with the outcome of this thesis.

Another study by Levenstein et al. (2022) investigated custom settlement substrates made from calcium carbonate, modified with additives including sands, glasses, and alkaline earth carbonates. Interestingly, they found additive-specific settlement preferences independent of mean surface roughness or wettability. Coral larvae were able to detect localized topographical features more than an order of magnitude smaller than their body width and positively responded to soluble inorganic minerals such as silica ($SiO_2$) and strontianite ($SrCO_3$). The authors of the study suggest that the settlement stimulation in coral larvae is triggered by the release of ions into the water column which navigate toward the substrates. This hypothesis should be further addressed in future research, as the research in this thesis also applied $SiO_2$ capsules in combination with DCOIT and $CeO_{2-x}$ nanoparticles. Any effects of these potential inorganic cues should be identified and classified as either advantageous or disadvantageous for coral larvae.

Decades of research and ongoing investigations show that coral settlement behavior is a very complex process which depends on a catalogue full of factors. In order to identify the most suitable and promising cues, intensive focus should be paid to this topic that includes diverse coral species and considers a variety of reef habitats. A network, or even an application trained by sufficient scientific knowledge could potentially help reef restoration practitioners to choose the suitable substrate-coral species combination including inorganic and organic based materials.

### 5.5.4 Golden rules for coral reef restoration

Reef ecosystem management is at a historical turning point in which active interventions such as restoration are being increasingly adopted to assist existing protection strategies to slow reef declines under climate change. A number of peer-reviewed articles by leading experts in the field of coral ecology, adaptation and restoration have brought together a suite of golden rules for coral reef restoration (Boström-Einarsson et al., 2020; Vardi et al., 2021; Quigley et al.,

2022; Suggett and Van Oppen, 2022; Banaszak et al., 2023; Hughes et al., 2023; Madin et al., 2023):

1. **Protect existing reefs:** There is no substitute for the protection of natural ecosystems. Therefore, $CO_2$ emissions must be reduced.
2. **Work together with all relevant stakeholders:** Collective action across practitioners and disciplines is required to build scalable solutions.
3. **Maximize coral biodiversity:** Biodiversity, incl. genetic diversity of individual species is a key factor positively affecting reef resilience.
4. **Select appropriate reef areas:** Not every reef area is one to be restored. The decision framework involves consideration of ecological, economic and cultural values. The future of coral reef restoration is likely to diverge towards two different scales; a. small-scale local projects with socio-economic objectives led by tourism-industry and citizen scientists using existing technologies (dominantly asexual propagation measures) to increase coral cover at high value sites, and b. large-scale ecosystem interventions with innovative and automatized multidisciplinary solutions and highly coordinated elements (dominantly sexual propagation measures).
5. **Support natural regeneration:** Adopt nature-based solutions, identify and remove negative local impacts (such as e.g., eutrophication, sedimentation, pollution, overharvesting).
6. **Select functional coral species:** Adopt a species priority framework relative to ecosystem service recovery goals.
7. **Use resilient coral material:** The "reefs of tomorrow" should be more tolerant to anthropogenic stressors (climate change, poor water quality, etc.).
8. **Plan ahead for infrastructure, capacity, and coral supply:** Access to sufficient and appropriate material, as well as longevity of monitoring out-planting is needed to gauge ecological and economic success over time.
9. **Learn by doing restoration:** practices require "fast-fail" exercises to develop tailored context-specific solutions.
10. **Make coral restoration pay:** Unlike terrestrial forests or mangroves, seagrasses, and kelp forests, coral reefs are not effective carbon sinks and therefore do not fall under blue carbon market economies. However, their economic value for e.g., flood risk reduction, marine biodiversity, health and population growth, tourism, etc. need to be incorporated into funding schemes to generate long-term investment.

In order to develop more standardized practice, as well as catalyze innovative tools, restoration activities need to network via regional and global bodies (e.g., Coral Restoration Consortium) to systematically and collectively build knowledge. It is also important to consider and adapt knowledge from more established terrestrial (Quigley et al., 2022) and coastal (Bertolini and da Mosto, 2021) restoration fields. A transformation in scale, feasibility, and cost-effectiveness

needs to solidify reef restoration as a tangible management action. The before mentioned golden rules for coral reef restoration can be integrated into rapidly advancing propagation and outplanting methods, so that efforts to rebuild coral biomass also equip reefs with enhanced resilience to stress.

### 5.5.6 Proposed antifouling strategy following golden rules

This study investigated and further developed an antifouling approach as a tool to support and accelerate the transformation process towards scale, feasibility, and cost-effectiveness of coral reef restoration with deployed coral spat: Antifouling coating development and testing requires knowledge and expertise from different disciplines (e.g., material sciences, chemistry, physics, and biological sciences: microbiology, ecology, biochemistry, ecophysiology including neurobiology), and needs to be readily prepared to adapt new findings to innovative testing in a "fast-fail" approach. Established testing environments (and standardized protocols) from each discipline can be used to inform the suitable adaptation of protocols to identify the most promising and sustainable antifouling coatings for use in coral restoration. The ASTM (American Society for Testing and Materials), as well as guidelines by ISO (International Organization for Standardization) could offer additional strategies for test environments which are aligned with standardized methodologies and could therefore ensure higher comparability among assessments. Once successfully and sufficiently tested and verified as sustainable and environmentally-benign (positive impact outweighs potential negative impact), antifouling treated substrates could find wide application in reef areas suffering from algal overgrowth. The success of enhanced sexual coral propagation measures (e.g., heat tolerant and/or functional species) could be further improved by deployment on antifouling-treated settlement surfaces. The ecological and economic success of this method could be monitored *in situ* over an adequate period (several years) and coral offspring deployed in this way could be financially supported by philanthropic sources. Similar to tree planting, outplanted corals could be treated as an offset to corals lost from heatwaves caused by increasing anthropogenic carbon emissions. The above mentioned strategy could transform reef restoration action supported and complemented by the application of antifouling treatments.

## 5.6 Concluding remarks

Competition with benthic algae, often triggered by excess nutrients associated with runoff is recognized as a key threat to coral settlement and the survival and growth of coral recruits. Therefore, control of algal overgrowth should be considered as an innovative methodology to improve the survival of coral spat in parallel with decreasing anthropogenically driven nutrient discharges that foster algal growth. However, only a few previous studies address this problem. This thesis clearly demonstrates the potential of the antifouling strategy to be applied in future test and coral restoration scenarios. Two innovative coatings (antiadhesive and encapsulated

DCOIT) demonstrated effective antifouling action, while settlement on pre-conditioned plugs was not disturbed by the presence of the coatings. Interestingly, the encapsulated DCOIT strongly reduced CCA growth. This finding might prove beneficial for coral spat, especially under future climate change scenarios that might promote higher CCA growth, resulting in more coral overgrowth. Also, this thesis demonstrates handling- and design-specific effects of DCOIT towards early coral spat. Fresh unconditioned plugs coated with DCOIT were not readily settled by coral larvae; however, uncoated areas close to coated DCOIT areas on the partially-coated plugs showed the highest survival of coral spat. These results indicate indirect positive effects of the DCOIT coating on coral spat, potentially by creating more algal-free space for coral spat to develop. This thesis covers the development of innovative toxicity testing techniques for the investigated organisms (coral and fouling species). One such method advanced for future standardized coral toxicity tests is the automatic and quantitative measurement of swimming behavior using the software Noldus EthoVisionXT. The guide for video-processing and track-analysis that was developed is included. Also highlighted by this work are limitations in the understanding of the complex intra- and inter-specific interactions between organisms in their biotic and with their abiotic environment. It became evident that by applying antifouling coatings, the existing inter-species interactions were changed and this could only be assessed experimentally. The question of "target" or "non-target" organisms, i.e., selective antifouling, can only be fully answered and successfully applied, once this network with all neutral, beneficial and disadvantageous interactions is understood. The UN Ocean Decade emphasizes the urgent need for innovative actions to restore marine ecosystems, creating an imperative for interdisciplinary research. The work of this thesis provides a valuable contribution (and advice for further research) to the development of innovative and sensitive techniques to assess the ability of AF coatings to reduce competition from biofouling and increase coral survival to size-escape thresholds.

## 5.7 References

Abdul Wahab, M. A., Ferguson, S., Snekkevik, V. K., McCutchan, G., Jeong, S., Severati, A., et al. (2023). Hierarchical settlement behaviours of coral larvae to common coralline algae. *Sci. Rep.* 13, 5795. doi:10.1038/s41598-023-32676-4.

Allen, A. S., Seymour, A. C., and Rittschof, D. (2017). Chemoreception drives plastic consumption in a hard coral. *Mar. Pollut. Bull.* 124, 198–205. doi:10.1016/j.marpolbul.2017.07.030.

Arganda-Carreras, I., Kaynig, V., Rueden, C., Eliceiri, K. W., Schindelin, J., Cardona, A., et al. (2017). Trainable Weka Segmentation: A machine learning tool for microscopy pixel classification. *Bioinformatics* 33, 2424–2426. doi:10.1093/bioinformatics/btx180.

Arnold, S. N., and Steneck, R. S. (2011). Settling into an increasingly hostile world: The rapidly closing "recruitment window" for corals. *PLoS One* 6. doi:10.1371/journal.pone.0028681.

Arnold, S. N., Steneck, R. S., and Mumby, P. J. (2010). Running the gauntlet: Inhibitory effects of algal turfs on the processes of coral recruitment. *Mar. Ecol. Prog. Ser.* 414, 91–105.

doi:10.3354/meps08724.

Banaszak, A. T., Marhaver, K. L., Miller, M. W., Hartmann, A. C., Albright, R., Hagedorn, M., et al. (2023). Applying coral breeding to reef restoration: best practices, knowledge gaps, and priority actions in a rapidly-evolving field. *Restor. Ecol.*, 1–17. doi:10.1111/rec.13913.

Barton, J. A., Willis, B. L., and Hutson, K. S. (2017). Coral propagation: a review of techniques for ornamental trade and reef restoration. *Rev. Aquac.* 9, 238–256. doi:10.1111/raq.12135.

Bertolini, C., and da Mosto, J. (2021). Restoring for the climate: a review of coastal wetland restoration research in the last 30 years. *Restor. Ecol.* 29, 0–3. doi:10.1111/rec.13438.

Boström-Einarsson, L., Babcock, R. C., Bayraktarov, E., Ceccarelli, D., Cook, N., Ferse, S. C. A., et al. (2020). Coral restoration – A systematic review of current methods, successes, failures and future directions. *PLoS One* 15, 1–24. doi:10.1371/journal.pone.0226631.

Buenau, K. E., Price, N. N., and Nisbet, R. M. (2011). Local interactions drive size dependent space competition between coral and crustose coralline algae. *Oikos* 120, 941–949. doi:10.1111/j.1600-0706.2010.18972.x.

Buenau, K. E., Price, N. N., and Nisbet, R. M. (2012). Size dependence, facilitation, and microhabitats mediate space competition between coral and crustose coralline algae in a spatially explicit model. *Ecol. Modell.* 237–238, 23–33. doi:10.1016/j.ecolmodel.2012.04.013.

Campos, B. G. de, do Prado e Silva, M. B. M., Avelelas, F., Maia, F., Loureiro, S., Perina, F., et al. (2022a). Toxicity of innovative antifouling additives on an early life stage of the oyster *Crassostrea gigas*: short- and long-term exposure effects. *Environ. Sci. Pollut. Res.* 29, 27534–27547. doi:10.1007/s11356-021-17842-3.

Campos, B. G. de, Fontes, M. K., Gusso-Choueri, P. K., Marinsek, G. P., Nobre, C. R., Moreno, B. B., et al. (2022b). A preliminary study on multi-level biomarkers response of the tropical oy ster *Crassostrea brasiliana* to exposure to the antifouling biocide DCOIT. *Mar. Pollut. Bull.* 174, 113241. doi:10.1016/j.marpolbul.2021.113241.

Ceccarelli, D. M., Loffler, Z., Bourne, D. G., Al Moajil-Cole, G. S., Boström-Einarsson, L., Evans-Illidge, E., et al. (2018). Rehabilitation of coral reefs through removal of macroalgae: state of knowledge and considerations for management and implementation. *Restor. Ecol.* 26, 827–838. doi:10.1111/rec.12852.

Chamberland, V. F., Petersen, D., Guest, J. R., Petersen, U., Brittsan, M., and Vermeij, M. J. A. (2017a). New Seeding Approach Reduces Costs and Time to Outplant Sexually Propagated Corals for Reef Restoration. *Sci. Rep.* 7, 1–12. doi:10.1038/s41598-017-17555-z.

Chamberland, V. F., Snowden, S., Marhaver, K. L., Petersen, D., and Vermeij, M. J. A. (2017b). The reproductive biology and early life ecology of a common Caribbean brain coral, *Diploria labyrinthiformis* (Scleractinia: Faviinae). *Coral Reefs* 36, 83–94. doi:10.1007/s00338-016-1504-2.

Cima, F., Ferrari, G., Ferreira, N. G. C., Rocha, R. J. M., Serôdio, J., Loureiro, S., et al. (2013). Preliminary evaluation of the toxic effects of the antifouling biocide Sea-Nine 211™ in the soft coral *Sarcophyton cf. glaucum* (Octocorallia, Alcyonacea) based on PAM fluorometry and biomarkers. *Mar. Environ. Res.* 83, 16–22. doi:10.1016/j.marenvres.2012.10.004.

Craggs, J., Guest, J., Bulling, M., and Sweet, M. (2019). Ex situ co culturing of the sea urchin, Mespilia globulus and the coral *Acropora millepora* enhances early post-settlement survivorship. *Sci. Rep.* 9, 1–12. doi:10.1038/s41598-019-49447-9.

Cruz, D. W. D., and Harrison, P. L. (2017). Enhanced larval supply and recruitment can replenish reef corals on degraded reefs. *Sci. Rep.* 7, 1–13. doi:10.1038/s41598-017-14546-y.

Dos Santos, J. V. N., Martins, R., Fontes, M. K., Galv, B., Bruni, M., and Maia, F. (2020). Can Encapsulation of the Biocide DCOIT Affect the Anti-Fouling Efficacy and Toxicity on Tropical Bivalves? *Appl. Sci.* 10, 1–12. doi:8579; doi:10.3390/app10238579.

Dow, L. (2021). How do quorum-sensing signals mediate algae–bacteria interactions? *Microorganisms* 9. doi:10.3390/microorganisms9071391.

Duarte, C. M., Agusti, S., Barbier, E., Britten, G. L., Castilla, J. C., Gattuso, J. P., et al. (2020). Rebuilding marine life. *Nature* 580, 39–51. doi:10.1038/s41586-020-2146-7.

Elmer, F., Bell, J. J., and Gardner, J. P. A. (2018). Coral larvae change their settlement preference for crustose coralline algae dependent on availability of bare space. *Coral Reefs* 37, 397–407. doi:10.1007/s00338-018-1665-2.

Evensen, N. R., Doropoulos, C., Morrow, K. M., Motti, C. A., and Mumby, P. J. (2019). Inhibition of coral settlement at multiple spatial scales by a pervasive algal competitor. *Mar. Ecol. Prog. Ser.* 612, 29–42. doi:10.3354/meps12879.

Ferreira, V., Pavlaki, M. D., Martins, R., Monteiro, M. S., Maia, F., Tedim, J., et al. (2021). Effects of nanostructure antifouling biocides towards a coral species in the context of global changes. *Sci. Total Environ.* 799, 149324. doi:10.1016/j.scitotenv.2021.149324.

Figueiredo, M. A. D. O., Norton, T. A., and Kain, J. M. (1997). Settlement and survival of epiphytes on two intertidal crustose coralline alga. *J. Exp. Mar. Bio. Ecol.* 213, 247–260. doi:10.1016/S0022-0981(96)02766-9.

Finlay, J. A., Bennett, S. M., Brewer, L. H., Sokolova, A., Clay, G., Gunari, N., et al. (2010). Barnacle settlement and the adhesion of protein and diatom microfouling to xerogel films with varying surface energy and water wettability. *Biofouling* 26, 657–666. doi:10.1080/08927014.2010.506242.

Fonseca, V. B., Guerreiro, A. da S., Vargas, M. A., and Sandrini, J. Z. (2020). Effects of DCOIT (4,5-dichloro-2-octyl-4-isothiazolin-3-one) to the haemocytes of mussels *Perna perna*. *Comp. Biochem. Physiol. Part - C Toxicol. Pharmacol.* 232, 108737. doi:10.1016/j.cbpc.2020.108737.

Gagnon, C., A, B., P, T., M, P., and F, G. (2018). Fate of Cerium Oxide Nanoparticles in Natural Waters and Immunotoxicity in Exposed Rainbow Trout. *J. Nanomed. Nanotechnol.* 09. doi:10.4172/2157-7439.1000489.

Garibay-Valdez, E., Martínez-Córdova, L. R., Vargas-Albores, F., Emerenciano, M. G. C., Miranda-Baeza, A., Cortés-Jacinto, E., et al. (2022). The biofouling process: The science behind a valuable phenomenon for aquaculture. *Rev. Aquac.*, 1–15. doi:10.1111/raq.12770.

Geertsma, R. C., Kamermans, P., Murk, A. J., and Wijgerde, T. (2023). Real-time high resolution tracking of coral and oyster larvae. *J. Exp. Mar. Bio. Ecol.* 565, 151910. doi:10.1016/j.jembe.2023.151910.

Gómez-Lemos, L. A., and Diaz-Pulido, G. (2017). Crustose coralline algae and associated microbial biofilms deter seaweed settlement on coral reefs. *Coral Reefs* 36, 453–462. doi:10.1007/s00338-017-1549-x.

Gómez-Lemos, L. A., Doropoulos, C., Bayraktarov, E., and Diaz-Pulido, G. (2018). Coralline algal metabolites induce settlement and mediate the inductive effect of epiphytic microbes on coral larvae. *Sci. Rep.* 8, 1–11. doi:10.1038/s41598-018-35206-9.

Harrington, L., Fabricius, K., De'ath, G., and Negri, A. (2004). Recognition and Selection of Settlement Substrata Determine Post-Settlement Survival in Corals. *Ecology* 85, 3428–3437. Available at: https://pdfs.semanticscholar.org/b6b9/8971ac0350e1f014c5fb251f5c111529c662.pdf.

Hartog, A. F., Stoll, B., Jochum, K. P., Wever, R., Natalio, F., Andre, R., et al. (2012). Vanadium pentoxide nanoparticles mimic vanadium haloperoxidases and thwart biofilm formation. *Nat. Nanotechnol.*, 1–6. doi:10.1038/nnano.2012.91.

Hata, T., Madin, J. S., Cumbo, V. R., Denny, M., Figueiredo, J., Harii, S., et al. (2017). Coral larvae are poor swimmers and require fine-scale reef structure to settle. *Sci. Rep.* 7, 1–9. doi:10.1038/s41598-017-02402-y.

Hein, M., McLeod, I. M., Shaver, E., Vardi, T., Pioch, S., Boström-Einarsson, L., et al. (2020). *Coral reef restoration as a strategy to improve ecosystem services - A guide to coral restoration methods*. UNEP - UN Environment Programme.

Herget, K., Hubach, P., Pusch, S., Deglmann, P., Götz, H., Gorelik, T. E., et al. (2017). Haloperoxidase Mimicry by CeO2-x Nanorods Combats Biofouling. *Adv. Mater.* 29, 1–8. doi:10.1002/adma.201603823.

Heyward, A. J., and Negri, A. P. (1999). Natural inducers for coral larval metamorphosis. *Coral Reefs* 18, 273–279. doi:10.1007/s003380050193.

Hughes, T. P. (1994). Catastrophes, Phase Shifts, and large-scale reef degradation in the Caribbean. *Science* 265, 1547–1551.

Hughes, T. P., Baird, A. H., Morrison, T. H., and Torda, G. (2023). Principles for coral reef restoration in the anthropocene. *One Earth* 6, 656–665. doi:10.1016/j.oneear.2023.04.008.

Hughes, T. P., Rodrigues, M. J., Bellwood, D. R., Ceccarelli, D., Hoegh-Guldberg, O., McCook, L., et al. (2007). Phase Shifts, Herbivory, and the Resilience of Coral Reefs to Climate Change. *Curr. Biol.* 17, 360–365. doi:10.1016/j.cub.2006.12.049.

Kacou, A., Ouvrard, A., Jamet, D., Jamet, J. L., and Blache, Y. (2019). Towards eco-friendly biocides: preparation, antibiofilm activity of hemibastadin analogues. *Lett. Appl. Microbiol.* 68, 360–368. doi:10.1111/lam.13150.

Kang, S., Hoek, E. M. V., Choi, H., and Shin, H. (2006). Effect of membrane surface properties during the fast evaluation of cell attachment. *Sep. Sci. Technol.* 41, 1475–1487. doi:10.1080/01496390600634673.

Karcher, D. B., Roth, F., Carvalho, S., El-Khaled, Y. C., Tilstra, A., Kürten, B., et al. (2020). Nitrogen eutrophication particularly promotes turf algae in coral reefs of the central Red Sea. *PeerJ* 2020, 1–25. doi:10.7717/peerj.8737.

Kerr, A., and Cowling, M. J. (2003). The effects of surface topography on the accumulation of biofouling. *Philos. Mag.* 83, 2779–2795. doi:10.1080/1478643031000148451.

Kotb, M. M. A. (2016). Coral translocation and farming as mitigation and conservation measures for coastal development in the Red Sea: Aqaba case study, Jordan. *Environ. Earth Sci.* 75, 1–8. doi:10.1007/s12665-016-5304-3.

Lamb, J. B., Willis, B. L., Fiorenza, E. A., Couch, C. S., Howard, R., Rader, D. N., et al. (2018). Plastic waste associated with disease on coral reefs. *Sci. Am. Assoc. Adv. Sci.* 359, 460–462. doi:10.1126/science.aar3320.

Leonard, C., Hédouin, L., Lacorne, M. C., Dalle, J., Lapinski, M., Blanc, P., et al. (2022). Performance of innovative materials as recruitment substrates for coral restoration. *Restor. Ecol.* 30, 1–14. doi:10.1111/rec.13625.

Lesser, M. P. (2011). "Coral Bleaching: Causes and Mechanisms," in *Coral Reefs: An Ecosystem in Transition*, eds. Z. Dubinsky and N. Stambler (Springer, Dordrecht), 1–552. doi:10.1007/978-94-007-0114-4.

Levenstein, M. A., Marhaver, K. L., Quinlan, Z. A., Tholen, H. M., Tichy, L., Yus, J., et al. (2022). Composite Substrates Reveal Inorganic Material Cues for Coral Larval Settlement. *ACS Sustain. Chem. Eng.* 10, 3960–3971. doi:10.1021/acssuschemeng.1c08313.

Madin, J. S., McWilliam, M., Quigley, K., Bay, L. K., Bellwood, D., Doropoulos, C., et al. (2023). Selecting coral species for reef restoration. *J. Appl. Ecol.*, 1537–1544. doi:10.1111/1365-2664.14447.

Maia, F., Silva, A. P., Fernandes, S., Cunha, A., Almeida, A., Tedim, J., et al. (2015). Incorporation of biocides in nanocapsules for protective coatings used in maritime applications. *Chem. Eng. J.* 270, 150–157. doi:10.1016/j.cej.2015.01.076.

Miller, M. W., Latijnhouwers, K. R. W., Bickel, A., Mendoza-Quiroz, S., Schick, M., Burton, K., et al. (2021). Settlement yields in large-scale in situ culture of Caribbean coral larvae for restoration. *Restor. Ecol.* doi:10.1111/rec.13512.

Morse, A. N. C., Iwao, K., Baba, M., Shimoike, K., Hayashibara, T., and Omori, M. (1996). An ancient chemosensory mechanism brings new life to coral reefs. *Biol. Bull.* 191, 149–154. doi:10.2307/1542917.

Morse, D. E., Morse, A. N. C., Raimondi, P. T., and Hooker, N. (1994). Morphogen-based chemical flypaper for *Agaricia humilis* coral larvae. *Biol. Bull.* 186, 172–181. doi:10.2307/1542051.

Motone, K., Takagi, T., Aburaya, S., Aoki, W., Miura, N., Minakuchi, H., et al. (2018). Protection of Coral Larvae from Thermally Induced Oxidative Stress by Redox Nanoparticles. *Mar. Biotechnol.* 20, 542–548. doi:10.1007/s10126-018-9825-5.

Niemann, H., Hagenow, J., Chung, M.-Y., Hellio, C., Weber, H., and Proksch, P. (2015). SAR of Sponge-Inspired Hemibastadin Congeners Inhibiting Blue Mussel PhenolOxidase. *Mar. Drugs* 13, 3061–3071. doi:10.3390/md13053061.

Norström, A. V., Nyström, M., Lokrantz, J., and Folke, C. (2009). Alternative states on coral reefs: Beyond coral-macroalgal phase shifts. *Mar. Ecol. Prog. Ser.* 376, 293–306. doi:10.3354/meps07815.

Pollock, F. J., Katz, S. M., van de Water, J. A. J. M., Davies, S. W., Hein, M., Torda, G., et al. (2017). Coral larvae for restoration and research: a large-scale method for rearing *Acropora millepora* larvae, inducing settlement, and establishing symbiosis. *PeerJ* 5, e3732. doi:10.7717/peerj.3732.

Quigley, K. M., Hein, M., and Suggett, D. J. (2022). Translating the 10 golden rules of reforestation for coral reef restoration. *Conserv. Biol.* 36, 1–8. doi:10.1111/cobi.13890.

Randall, C. J., Giuliano, C., Allen, K., Bickel, A., Miller, M., and Negri, A. P. (2022). Site mediates performance in a coral-seeding trial. *Restor. Ecol.* 31, 1–9. doi:10.1111/rec.13745.

Randall, C. J., Negri, A. P., Quigley, K. M., Foster, T., Ricardo, G. F., Webster, N. S., et al. (2020). Sexual production of corals for reef restoration in the Anthropocene. *Mar. Ecol. Prog. Ser.* 635, 203–232. doi:10.3354/MEPS13206.

Rinkevich, B. (2005). Conservation of coral reefs through active restoration measures: Recent approaches and last decade progress. *Environ. Sci. Technol.* 39, 4333–4342. doi:10.1021/es0482583.

Rinkevich, B. (2014). Rebuilding coral reefs: Does active reef restoration lead to sustainable reefs? *Curr. Opin. Environ. Sustain.* 7, 28–36. doi:10.1016/j.cosust.2013.11.018.

Roger, L., Lewinski, N., Putnam, H., Chen, S., Roxbury, D., Tresguerres, M., et al. (2023a). Nanotechnology for coral reef conservation , restoration and rehabilitation. *Nat. Nanotechnol.*, 10–12. doi:10.1038/s41565-023-01402-6.

Roger, L. M., Lewinski, N. A., Putnam, H. M., Roxbury, D., Tresguerres, M., and Wangpraseurt, D. (2023b). Nanobiotech engineering for future coral reefs. *One Earth*. doi:10.1016/j.oneear.2023.05.008.

Roger, L. M., Russo, J. A., Jinkerson, R. E., Giraldo, J. P., and Lewinski, N. A. (2022). Engineered nanoceria alleviates thermally induced oxidative stress in free-living *Breviolum minutum* (Symbiodiniaceae, formerly Clade B). *Front. Mar. Sci.* 9, 1–14. doi:10.3389/fmars.2022.960173.

Rölfer, L., Reuter, H., Ferse, S. C. A., Kubicek, A., Dove, S., Hoegh-Guldberg, O., et al. (2021). Coral-macroalgal competition under ocean warming and acidification. *J. Exp. Mar. Bio. Ecol.* 534. doi:10.1016/j.jembe.2020.151477.

Sakai, Y., Kato, K., Koyama, H., Kuba, A., Takahashi, H., Fujimori, T., et al. (2020). A step-down photophobic response in coral larvae: implications for the light-dependent

distribution of the common reef coral, *Acropora tenuis*. *Sci. Rep.* 10, 1–11. doi:10.1038/s41598-020-74649-x.

Sánchez-Lozano, I., Hernández-Guerrero, C. J., Muñoz-Ochoa, M., and Hellio, C. (2019). Biomimetic approaches for the development of new antifouling solutions: Study of incorporation of macroalgae and sponge extracts for the development of new environmentally-friendly coatings. *Int. J. Mol. Sci.* 20, 1–18. doi:10.3390/ijms20194863.

Shimeta, J., Wilding-Mcbride, G., Bott, N. J., Piola, R., Santander, R., Leary, M., et al. (2023). Growth of marine biofilms and macrofouling organisms on biocide-infused, 3D-printed thermoplastics. 1–15. doi:10.3389/fmars.2023.1172942.

Shin, P. K. S., Cheung, S. G., Tsang, T. Y., and Wai, H. Y. (2014). *Ecology of artificial reefs in the subtropics*. 1st ed. Elsevier Ltd. doi:10.1016/B978-0-12-800169-1.00001-X.

Stumm, W., and Morgan, J. J. (1981). *Aquatic Chemistry: An Introduction Emphasizing Chemical Equilibria in Natural Waters*. 2nd ed. New York: John Wiley & Sons Ltd.

Suggett, D. J., and Van Oppen, M. J. H. (2022). Horizon scan of rapidly advancing coral restoration approaches for 21st century reef management. *Emerg. Top. Life Sci.* 6, 125–136. doi:10.1042/ETLS20210240.

Szabó, M., Larkum, A. W. D., and Vass, I. (2020). "Photosynthesis in Algae: Biochemical and Physiological Mechanisms," in *Advances in Photosynthesis and Respiration*, eds. A. W. D. Larkum, A. R. Grossmann, and J. A. Raven (Springer, Cham), 532.

Tebben, J., Guest, J. R., Sin, T. M., Steinberg, P. D., and Harder, T. (2014). Corals like it waxed: Paraffin-based antifouling technology enhances coral spat survival. *PLoS One* 9, 1–8. doi:10.1371/journal.pone.0087545.

Tebben, J., Motti, C. A., Siboni, N., Tapiolas, D. M., Negri, A. P., Schupp, P. J., et al. (2015). Chemical mediation of coral larval settlement by crustose coralline algae. *Sci. Rep.* 5, 1–11. doi:10.1038/srep10803.

Tian, L., Yin, Y., Jin, H., Bing, W., Jin, E., Zhao, J., et al. (2020). Novel marine antifouling coatings inspired by corals. *Mater. Today Chem.* 17, 100294. doi:10.1016/j.mtchem.2020.100294.

Toh, T. C., Ng, C. S. L., Guest, J., and Chou, L. M. (2013). Grazers improve health of coral juveniles in ex situ mariculture. *Aquaculture* 414–415, 288–293. doi:10.1016/j.aquaculture.2013.08.025.

van Oppen, M. J. H., Gates, R. D., Blackall, L. L., Cantin, N., Chakravarti, L. J., Chan, W. Y., et al. (2017). Shifting paradigms in restoration of the world's coral reefs. *Glob. Chang. Biol.* 23. doi:10.1111/gcb.13647.

Vardi, T., Hoot, W. C., Levy, J., Shaver, E., Winters, R. S., Banaszak, A. T., et al. (2021). Six priorities to advance the science and practice of coral reef restoration worldwide. *Restor. Ecol.* 29, 1–7. doi:10.1111/rec.13498.

Vermeij, M. J. A., Dailer, M. L., and Smith, C. M. (2011). Crustose coralline algae can suppress macroalgal growth and recruitment on hawaiian coral reefs. *Mar. Ecol. Prog. Ser.* 422, 1–7. doi:10.3354/meps08964.

Vong, L. B., Yoshitomi, T., Matsui, H., and Nagasaki, Y. (2015). Development of an oral nanotherapeutics using redox nanoparticles for treatment of colitis-associated colon cancer. *Biomaterials* 55, 54–63. doi:10.1016/j.biomaterials.2015.03.037.

Weller, R., and Schrems, O. (1993). H2O2 in the marine troposphere and seawater of the Atlantic Ocean (48°N – 63°S). *Geophys. Res. Lett.* 20, 125–128. doi:10.1029/93GL00065.

Wendt, I., Backhaus, T., Blanck, H., and Arrhenius, Å. (2016). The toxicity of the three antifouling biocides DCOIT, TPBP and medetomidine to the marine pelagic copepod *Acartia tonsa*. *Ecotoxicology* 25, 871–879. doi:10.1007/s10646-016-1644-8.

Whalan, S., Abdul Wahab, M. A., Sprungala, S., Poole, A. J., and De Nys, R. (2015). Larval settlement: The role of surface topography for sessile coral reef invertebrates. *PLoS One*

10, 1–17. doi:10.1371/journal.pone.0117675.

Worrell, E., Price, L., Martin, N., Hendriks, C., and Meida, L. O. (2001). Carbon Dioxide Emissions from the Global Cement Industry. *Annu. Rev. Energy Environ.* 26, 303–329. Available at: http://www.annualreviews.org/doi/abs/10.1146/annurev.energy.26.1.303.

Wu, R., Wang, W., Luo, Q., Zeng, X., Li, J., Li, Y., et al. (2021). Room temperature synthesis of defective cerium oxide for efficient marine anti-biofouling. *Adv. Compos. Hybrid Mater.* Available at: https://doi.org/10.1007/s42114-021-00256-7.

Xu, Y., Wang, C., Hou, J., Wang, P., You, G., and Miao, L. (2018). Mechanistic understanding of cerium oxide nanoparticle-mediated biofilm formation in *Pseudomonas aeruginosa*. *Environ. Sci. Pollut. Res.* 25, 34765–34776. doi:10.1007/s11356-018-3418-8.

Xu, Y., Wang, C., Hou, J., Wang, P., You, G., and Miao, L. (2019). Effects of cerium oxide nanoparticles on bacterial growth and behaviors: induction of biofilm formation and stress response. *Environ. Sci. Pollut. Res.* 26, 9293–9304. doi:10.1007/s11356-019-04340-w.

Zhang, H., He, X., Zhang, Z., Zhang, P., Li, Y., Ma, Y., et al. (2011). Nano-CeO2 exhibits adverse effects at environmental relevant concentrations. *Environ. Sci. Technol.* 45, 3725–3730. doi:10.1021/es103309n.

# Affidavit - Eidesstattliche Versicherung

Ich, Lisa K. Röpke, wohnhaft in der Verdener Straße 35, 28205 Bremen, versichere an Eides Statt gem. § 65 Abs. 5 BremHG durch meine Unterschrift, dass ich die vorstehende Arbeit mit dem Titel „The application and potential toxicity of innovative antifouling coatings for coral reef restoration“ selbstständig und ohne unerlaubte fremde Hilfe angefertigt und alle Stellen, die ich wörtlich dem Sinne nach aus Veröffentlichungen entnommen habe, als solche kenntlich gemacht habe, mich auch keiner anderen als der angegebenen Literatur oder sonstiger Hilfsmittel bedient habe.

Ich versichere an Eides Statt, dass die zu Prüfungszwecken beigelegte elektronische Version der Dissertation identisch ist mit der abgegebenen gedruckten Version.

Ich versichere an Eides Statt, dass ich die vorgenannten Angaben nach bestem Wissen und Gewissen gemacht habe und dass die Angaben der Wahrheit entsprechen und ich nichts verschwiegen habe.

Die Strafbarkeit einer falschen eidesstattlichen Versicherung ist mir bekannt, namentlich die Strafandrohung gemäß § 156 StGB bis zu drei Jahren Freiheitsstrafe oder Geldstrafe bei vorsätzlicher Begehung der Tat bzw. gemäß § 161 Abs. 1 StGB bis zu einem Jahr Freiheitsstrafe oder Geldstrafe bei fahrlässiger Begehung.

Bremen, 29.09.2023